IMPROVING DELIVERY OF THERAPEUTICS TO TARGETED TISSUES IN LYSOSOMAL DISEASES

A DISSERTATION

SUBMITTED TO THE FACULTY OF THE

UNIVERSITY OF MINNESOTA

BY

Sarah Kim

IN PARTIAL FULFILLMENT OF THE REQUIREMENTS

FOR THE DEGREE OF

DOCTOR OF PHILOSOPHY

Jeanine Jarnes, PharmD, Advisor

James Cloyd III, PharmD, Co-Advisor

December 2021

ACKNOWLEDGEMENTS

I want to thank everyone who supported me during my graduate education.

Thank you to my advisor, Dr. Jeanine Jarnes, who introduced me to the field of lysosomal diseases. Your altruism, openness to ideas, and strength in times of adversity are characteristics I strive for daily. I want to thank my co-advisor, Dr. James Cloyd III, who has provided countless professional advice and career opportunities. You also remind me to think of the bigger picture.

Thank you, Dr. Chester Whitley, one of the most influential mentors during my education. Your endless optimism pushes me to question the impossible and think creatively. I thank Dr. Li Ou and Dr. Michael Przybilla for their scientific guidance in pre-clinical studies and professional advice. I also want to thank other members of the Whitley lab, the Lysosomal Disease Network, and Dr. McIvor's lab.

I thank my other committee members, Dr. Lisa Coles and Dr. Mahmoud Al-Kofahi, for their scientific insight in pharmacokinetics/pharmacodynamics modeling, neurological diseases, and biological therapies. I want to thank other members of the Experimental and Clinical Pharmacology Department at the University of Minnesota College of Pharmacy for their knowledge in pharmacokinetics/pharmacodynamics and administrative support.

I would like to thank the National Institute of Health, Frieda Kunze Endowed Fellowship, and Ted Rowell Graduate Fellowship for their financial support.

Finally, I want to thank my friends and family for their support and patience.

ABSTRACT

Lysosomal diseases are a group of over 70 diseases with a combined incidence of approximately 1 in 7,700 live births. Most lysosomal diseases are caused by mutations in enzymes normally present in the lysosome. Lysosomal diseases are multi-systemic and progressive diseases. Currently, only 12 lysosomal diseases have treatments. A challenge in drug development is the lack of biomarkers that reflect disease progression or show response to therapy. Furthermore, current therapies have difficulty reaching certain tissues that are major contributors to morbidity and mortality, such as the central nervous system (CNS) and cardiac valves.

The overall objective of this dissertation is to improve the delivery of therapeutics to targeted tissues in lysosomal diseases. To accomplish this objective, three main studies were performed.

1) Validation of Chitotriosidase as a CNS Biomarker for Gangliosidoses. Chitotriosidase was investigated as a probable surrogate endpoint for clinical trials with gene therapy. The first objective was to validate chitotriosidase levels for important clinical outcomes in patients with lysosomal diseases. The second objective was to assess chitotriosidase's ability to detect effective gene therapy in murine models of lysosomal diseases. In patients with gangliosidoses, the most severe infantile phenotype had higher chitotriosidase levels in the cerebrospinal fluid (CSF) and a different pattern over time than the more attenuated juvenile and late-onset forms. Chitotriosidase levels were also significantly associated with neurocognitive impairment. In mice with mucopolysaccharidosis type I (MPS I), there were significant differences among the untreated, gene-therapy treated, and mice heterozygous for a mutation in the *IDUA* gene. These results support the use of CSF chitotriosidase levels to diagnose different disease phenotypes and to monitor disease progression in

patients. As a potential biomarker of neurological improvement, CSF chitotriosidase can aid in the development of therapies that target the CNS.

2) Investigation of Iduronidase Enzymes Linked to Pepcan to Improve Delivery to Targeted Tissues. The objective of this study was to determine if pepcan-12 can increase the uptake of iduronidase into the brain of MPS I mice. Pepcan-12 is a ligand for the cannabinoid receptor type 1 (CB1), a highly expressed receptor in the CNS. The hypothesis was that a fusion iduronidase containing pepcan-12 would have higher activity levels than iduronidase in the brain. Sequences of one of two linkers, Linker S or Linker T, were inserted between pepcan-12 and *IDUA* to conjugate the ligand and iduronidase. MPS I mice were injected with plasmids encoding either the native iduronidase or one of four fusion iduronidase enzymes containing: pepcan-12 + Linker S, pepcan-12 + Linker T, Linker S, or Linker T. The fusion enzymes and iduronidase had similar activity levels in the brain. Unexpectedly, the fusion enzymes had higher activity levels than iduronidase in the heart and plasma, which appears to be caused by the linkers. Therefore, these fusion enzymes may improve cardiovascular outcomes in MPS I. In several MPS disorders, the cardiac valves continue to worsen despite enzyme replacement therapies (ERT) and hematopoietic cell transplants. The small size of these linkers facilitates their use as fusion enzymes encoded in gene therapy or administered directly as ERT. Therefore, these linkers may aid in therapeutic development for other lysosomal diseases.

3) Pharmacokinetic Analysis of Iduronidase and a Fusion Iduronidase Enzyme Encoded in Gene Therapy. In the previous study, an iduronidase enzyme containing Linker T, termed Linker T iduronidase, had higher activity levels than iduronidase in the plasma and heart. This study sought to investigate the mechanism of Linker T iduronidase, but a gap between the fields of lysosomal diseases/gene therapy and pharmacokinetics (PK)/ pharmacodynamics (PD) became apparent. In the field of lysosomal diseases, the activity level of an enzyme is an important measurement of efficacy, because an enzyme's activity levels are more predictive of efficacy than its physical levels.

However, pre-clinical studies in lysosomal diseases lack well-described methods to quantify changes in enzyme activity levels over time. In contrast, the pharmacokinetic field has rigorous and reproducible methods to quantify changes in a therapy over time in the body. However, traditional pharmacokinetic methods face challenges in gene therapy because of the need for uniform or convertible units. Furthermore, absorption, distribution, metabolism, and elimination processes are well-characterized for small molecule drugs but not yet adapted for biological therapies. To bridge the fields of lysosomal diseases/gene therapy and PK/PD, I aimed to develop an approach incorporating values with greater prediction of efficacy from the field of lysosomal diseases and the quantitative methods from the field of pharmacokinetics. The objective of this study was to perform a pharmacokinetic analysis of iduronidase and Linker T iduronidase administered as gene therapies. The hypothesis was that Linker T iduronidase would have a higher area under the curve (AUC) or half-life, estimated with enzyme activity levels, than iduronidase in the plasma. MPS I mice were injected with plasmids encoding either iduronidase or Linker T iduronidase. At ten time points, ranging from 0.5 to 168 hours post-injection, the enzymes' physical levels in the liver, activity levels in the liver, and activity levels in the plasma were measured. In the liver, both the physical and activity levels over time were similar between the native iduronidase and Linker T iduronidase. In contrast, enzyme activity levels over time in the plasma showed differences between the native iduronidase and Linker T iduronidase. The time curves of activity in the plasma showed biphasic profiles for both enzymes. Iduronidase had a sharper decline between 24 and 48 hours, and both enzymes had approximately parallel slopes between 96 and 168 hours. The Linker T iduronidase had a two-fold higher AUC of activity than the normal iduronidase in the plasma. The AUC of plasma activity and other PK parameters were contextualized in gene therapy, and experimental data were used to deduce the mechanism of Linker T. These results suggest that Linker T iduronidase may have a distinct property that protects the enzyme from degradation or inactivation in the plasma. The enzymes were estimated to have a

half-life of activity in the plasma under noncompartmental analysis. Future studies with compartmental analysis would better characterize half-lives of activity in biphasic profiles. This study performs a novel approach of conducting a formal pharmacokinetics analysis on enzyme activity levels, a traditionally pharmacodynamic outcome. The resulting PK parameters can be interpreted and used to gain mechanistic insight on gene therapy, by integrating concepts from pharmacokinetics and gene therapy

In summary, these findings improve the therapeutic delivery in lysosomal disease through the validation of a CNS biomarker for lysosomal diseases, creation of a fusion enzyme with improved activity in the heart and plasma, and a novel approach and interpretation of pharmacokinetics to gain mechanistic insight on gene therapy.

TABLE OF CONTENTS

LIST OF TABLES

LIST OF FIGURES

LIST OF ABBREVIATIONS

Abbreviation	Meaning
%FVC	Percentage predicted forced vital capacity
6MWT	6-minute walk test
AAV	Adeno-associated virus
AE	Adverse events
AT1	Angiotensin II type 1
AUC	Area under the curve
Bayley-III®	Bayley Scales of Infant and Toddler Development®, Third Edition
BBB	Blood-brain barrier
BQL	Below quantification limit
CB1	Cannabinoid receptor type 1
CB2	Cannabinoid receptor type 2
CGT	Cellular and gene therapy
CHITO	Chitotriosidase
CHO	Chinese hamster ovary
CMV	Cytomegalovirus
CNS	Central nervous system
CRISPR	Clustered regularly interspaced short palindromic repeats
CSF	Cerebrospinal fluid
CV	Cardiovascular
DAMP	Damage-associated molecular pattern
DQ	Developmental quotient
ELISA	Enzyme-linked immunosorbent assay
EMA	European Medicines Agency
ER	Endoplasmic reticulum

ERT	Enzyme replacement therapy
FDA	Food and Drug Administration
GAG	Glycosaminoglycan
GPCR	G-protein coupled receptor
GPR55	G-protein coupled receptor 55
GTD	Gene Therapy and Diagnostics
hAAT	Human α1-antitrypsin
HCR-apoE	Hepatic control region of human apolipoprotein E
HCT	Hematopoietic cell transplant
HRP	Horseradish peroxidase
IACUC	Institutional Animal Use and Care
IQ	Intelligence quotient
IRB	Institutional Review Board
LLOQ	Lower limit of quantification
LR	Lactated Ringer's
LVH	Left ventricular hypertrophy
MEC	Minimum effective concentration
MPS	Mucopolysaccharidosis (followed by type I, II, III, IV, VI, VII, and IX)
M6P	Mannose 6-phosphate
MR	Mannose receptor
MRI	Magnetic resonance imaging
MSD	Multiple sulfatase deficiency
NCA	Noncompartmental analysis
NCATS	National Center for Advancing Translational Sciences
NCBI	National Center for Biotechnology Information
NIDDK	National Institute of Diabetes and Digestive and Kidney Diseases
NIH	National Institute of Health

NINDS	National Institute of Neurological Disorders and Stroke
ORDR	Office of Rare Diseases Research
PBS	Phosphate-buffered saline
PCR	Polymerase chain reaction
PD	Pharmacodynamics
PDUFA	Prescription Drug User Fee Act
PK	Pharmacokinetics
QGRS	Quadruplex forming G-rich sequence
qPCR	Quantitative polymerase chain reaction
RDCRN	Rare Diseases Clinical Research Network
rpm	Revolutions per minute
SD	Standard deviation
SRT	Substrate reduction therapy
Tat	Transactivator of transcription
TRPV1	Transient receptor potential cation channel subfamily V member 1
TMB	3,3',5,5'-tetramethylbenzidine
TMDD	target-mediated drug disposition
USP	United States Pharmacopeia

CHAPTER 1: INTRODUCTION

1.1 Purpose and Significance of Dissertation

Lysosomal diseases are a group of over 70 diseases with a combined incidence of approximately 1 in 7,700 live births (1). Lysosomal diseases are caused by mutations in an enzyme or protein normally present in the lysosome. They are multi-systemic and progressive diseases. Current therapies have difficulty reaching certain tissues that are major contributors to morbidity and mortality, such as the central nervous system (CNS) and cardiac valves. Currently, only 12 lysosomal diseases have treatments. One challenge of drug development is the lack of biomarkers that reflect disease progression or show response to therapy.

The **overall objective** of this dissertation is to improve delivery of therapeutics to targeted tissues in lysosomal diseases. To accomplish this objective, three main studies were performed.

1) Validation of Chitotriosidase as a CNS Biomarker for Gangliosidoses
2) Investigation of Iduronidase Enzymes Linked to Pepcan to Improve Delivery to Targeted Tissues
3) Pharmacokinetic Analysis of Iduronidase and a Fusion Iduronidase Enzyme Encoded in Gene Therapy

The remainder of Chapter 1 provides an overview of lysosomal diseases. Chapter 2 reviews currently existing therapies in lysosomal diseases, drug development in rare diseases, and unmet needs in lysosomal diseases. Chapter 3 discusses the validation of chitotriosidase as a biomarker for gangliosidoses. Chapter 4 details the investigation of plasmids encoding pepcans linked to lysosomal enzymes. Chapter 5 discusses the pharmacokinetic analysis of a novel fusion iduronidase enzyme encoded in gene therapy. Chapter 6 summarizes each study's results and potential impact.

1.2 Overview of Lysosomal Diseases

Lysosomal diseases are a group of over 70 diseases with a combined incidence of approximately 1 in 7,700 live births (1). Most lysosomal diseases are autosomal recessive disorders, with four exceptions: Mucopolysaccharidosis type II (MPS II) and Fabry disease are X-linked recessive diseases; Danon disease is an X-linked dominant disease; Neuronal ceroid lipofuscinosis 4B, one of the adult-onset forms of neuronal ceroid lipofuscinosis, can be inherited in an autosomal dominant pattern (2).

Most lysosomal diseases are monogenic, i.e., caused by a mutation in one gene. However, some lysosomal diseases are caused by a biallelic mutation in one of several genes. For example, GM2-gangliosidosis is caused by mutations in either *HEXA* or *HEXB* (3). *HEXA* and *HEXB* encode for the α and β subunit of the β-hexosaminidase isozyme A, respectively (3). Both the α and β subunits are needed for the proper function of β-hexosaminidase isozyme A (3). In another example, mucopolysaccharidosis type III (MPS III) can be caused by mutations in one of four genes that each encode an enzyme that degrades heparan sulfate.

Lysosomes are membrane-bound, cellular organelles that metabolize macromolecules and are present in most cell types (4). The lysosome carries out its metabolic function through 60 different hydrolases (4). Lysosomal enzymes include glycosidases, lipases, nucleases, phospholipases, and proteases (4). The metabolic function of these enzymes is why lysosomal diseases are sometimes classified as inborn errors of metabolism, inherited metabolic diseases, or metabolic diseases. Lysosomal diseases account for approximately 14% of all inherited metabolic diseases (5, 6). In addition to metabolism, lysosomes play roles in phagocytosis, autophagy, apoptosis, signal transduction, exocytosis, and inflammatory responses (5).

In most lysosomal diseases, there is a mutation in a gene encoding for a lysosomal enzyme, resulting in enzyme deficiency. Some diseases are caused by a mutation in a protein that stabilizes a lysosomal enzyme, ultimately resulting

in a deficiency of the lysosomal enzyme. For example, galatosialidosis is caused by a mutation in the protein protective protein/cathepsin A, which stabilizes the lysosomal enzyme β-galactosidase. Some lysosomal diseases are caused by a mutation in proteins that transport macromolecules. For example, impairment of cystinosin, a transporter in the lysosomal membrane, causes the accumulation of cysteine and the disease cystinosis (7). Additionally, some diseases are caused by mutations that affect posttranslational modification of lysosomal enzymes. For example, multiple sulfatase deficiency is caused by mutations in *SUMF1*, which encodes for the formylglycine-generating enzyme that normally performs post-translational modifications on sulfatase enzymes. The lack of formylglycine-generating enzyme prevents the activation of all sulfatase enzymes, leading to the accumulation of storage material (4).

Lysosomal diseases can be categorized based on the affected enzyme or the primary storage material (8). The primary storage material is usually a substrate of the impaired enzyme or transporter. These storage materials include sphingolipids, glycosaminoglycans (GAG) or mucopolysaccharides, oligosaccharides, glycoproteins, and glycogens (8). The accumulation of storage compounds occurs within a cell only if that cell synthesizes or ingests those materials (9). For example, glucocerebrosides accumulate in macrophages due to macrophages phagocytosing cells and cellular debris (9). Some lysosomal diseases can have multiple stored compounds. For example, GAGs and gangliosides can accumulate in certain MPS diseases (8).

The storage of compounds in these diseases is reflected by their historical name of “lysosomal storage diseases.” However, contemporary views in the field have shifted to the term “lysosomal diseases” because storage of material does not encompass the full spectrum of pathophysiology (9, 10). Other pathogenic cascades in lysosomal diseases include defective intracellular calcium signaling, oxidative stress, impaired autophagy, and chronic inflammation (11).

The mannose 6-phosphate (M6P) receptor plays an important role in targeting enzymes to the lysosome and cellular uptake of lysosomal enzymes.

Enzymes are synthesized in the rough endoplasmic reticulum (ER) and translocate into the ER lumen using their signal sequence (4). In the ER lumen, enzymes are N-glycosylated, and the signal sequence is removed (4). A recognition marker for the M6P receptor is attached to the enzymes in the Golgi (4). The enzymes can then undergo one of two pathways. In the first pathway, enzymes bind to the M6P receptor in the Golgi and are trafficked to the late endosome, where the low pH causes dissociation from the M6P receptor (4). These enzymes undergo partial proteolysis, folding, and aggregation, further maturing in the late endosome (4). The second pathway occurs in a variable portion of newly synthesized enzymes that do not bind to the M6P receptor in the Golgi (12). Instead, these enzymes are secreted into the circulatory system, bind to extracellular M6P receptors on cells, and endocytosed into lysosomes, where they carry out their functions (12). This phenomenom of lysosomal enzymes being secreted and taken up into neighboring cells is termed cross-correction (13)

Cross-correction and metabolic correction are the underlying mechanisms for enzyme replacement therapy (ERT) and hematopoietic cell transplant (HCT) in lysosomal diseases. Cross-correction was first described in a seminal study by the Neufeld group (13). They discovered that mixing fibroblasts from patients with MPS I and MPS II corrected the GAG accumulation in both cell types, and this correction was mediated by the secretion of lysosomal enzymes from fibroblasts (13). Metabolic correction, the reversal of accumulation of storage material and the disappearance of corresponding pathophysiologic correlations, was first described in a study by Whitley et al. (14). This pivotal study proposed four mechanisms of metabolic correction in the context of HCT (14). One, degradation of GAG by the enzyme circulating in the plasma (14). This mechanism was noted to be unlikely due to diminished enzyme activity in the blood's relatively high pH (14). Two, transplantation of normal stem cells for marrow-derived cell populations (14). Three, receptor-mediated replacement of enzymes in lysosomes (14). Four, filtration of substrates by donor cells of the marrow (14).

Multi-organ manifestations are common in lysosomal diseases. Disorders in the CNS and cardiovascular (CV) system will be detailed in later sections, due to their relevance to the diseases and experiments in this dissertation. However, the lungs, skeletal tissue, and kidneys are also significant contributors to morbidity and mortality in lysosomal diseases (9).

The clinical progression of a lysosomal disease can vary widely, creating a spectrum of disease severity. The onset or severity of the disease may be attributed to the residual activity of the enzyme (9). However, correlations between genotypes and phenotypes are not always well defined (9). The terms “form of disease” or “phenotype” generally refer to different clinical presentations within a lysosomal disease. In general, a disease can have two or three forms. The terms “infantile” or “severe” generally refer to the earliest onset and most rapidly progressive form of the disease. The terms “juvenile” or “intermediate” generally refer to the disease form with an intermediate onset and disease progression. “Adult,” “late-onset,” or “attenuated” refers to the latest onset and slowest progressing form of the disease.

Within the 70 different lysosomal diseases, Table 1 provides information on diseases that are either part of the dissertation’s experiments or have relatively high incidences. More background information will be provided on GM1-gangliosidosis, GM2-gangliosidosis, and MPS I, because these diseases are the most impacted by this dissertation.

Table 1: An Overview of Selected Lysosomal Diseases

Disease	Gene	Enzyme Affected	Primary Storage Material	Disease Forms	Included in Dissertation Studies
GM1-gangliosidosis	*GLB1*	β-galactosidase	GM1 ganglioside	Infantile, juvenile, late-onset	Y
GM2-gangliosidosis (Tay-Sachs disease)	*HEXA*	β-hexosaminidase isozyme A (α subunit impaired)	GM2 ganglioside	Infantile, juvenile, late-onset	Y
GM2-gangliosidosis (Sandhoff disease)	*HEXB*	β-hexosaminidase isozyme A (β subunit impaired)	GM2 ganglioside	Infantile, juvenile, late-onset	Y
MPS I	*IDUA*	α-L-iduronidase	Dermatan sulfate, heparan sulfate	Severe (Hurler), intermediate (Hurler-Scheie), attenuated (Scheie)	Y
MPS II (Hunter syndrome)	*IDS*	Iduronate 2-sulphatase	Dermatan sulfate, heparan sulfate	Neuronopathic, non-neuronopathic	Y
MPS III (Sanfilippo syndrome	Type A: *SGSH*	N-sulfoglucosamine sulfohydrolase	Heparan sulfate	Type A, type B, type C, type D (depending on gene)	Y
	Type B: *NAGLU*	N-Acetyl-α-glucosaminidase			
	Type C: *HGSNAT*	Heparan-α-glucosaminide N-acetyltransferase			
	Type D: *GNS*	N-acetylglucosamine-6-sulfatase			
MPS IV (Morquio syndrome)	Type A: *GALNS*	N-acetylgalactosamine-6-sulfatase	Keratan sulfate, chondroitin sulfate	Severe, attenuated	Y
	Type B: *GLB1*	β-galactosidase	Keratan sulfate	Severe, attenuated	N
MPS VI (Maroteaux-Lamy disease)	*ARSB*	Arylsulphatase B	Dermatan sulfate, chondroitin sulfate	Severe, attenuated	N
MPS VII (Sly syndrome)	*GUSB*	β-glucuronidase	Dermatan sulfate, heparan sulfate, chondroitin sulfate	Severe, attenuated	N

MPS IX	*HYAL1*	Hyaluronidase 1	Hyaluronan		N
Multiple sulfatase deficiency	*SUMF1*	Formylglycine-generating enzyme	Sulfatides	Neonatal, late-infantile, juvenile	Y
Gaucher disease	*GBA*	Glucocerebrosidase	Glucocerebroside	Type I (non-neuronopathic), type II (acute or infantile neuronopathic), type III (chronic or juvenile neuronopathic)	Y
Anderson-Fabry disease	*GLA*	α-galactosidase A	Globotriaosylceramide	Type 1 (classic), type II (late-onset)	N
Glycogen storage disease type II (Pompe disease)	*GAA*	α-glucosidase	Glycogens	Infantile (classic), Late-onset (nonclassic)	N

This table includes the diseases that are part of this dissertation's studies or have the highest incidences. Mucopolysaccharidoses are abbreviated as MPS following the type (e.g., MPS I, MPS II, MPS III, MPS IV, MPS VI, MPS VII, MPS IX). References (4, 15-17)

1.2.1 Overview of Gangliosidoses

This section will first discuss information specific to GM1-gangliosidosis, then GM2-gangliosidosis, and conclude with a review of the clinical presentation of GM1- and GM2-gangliosidosis.

1.2.1.1 GM1-Gangliosidosis

GM1-gangliosidosis is an autosomal recessive disease with an incidence of 1 in 100,000 to 200,000 (18, 19). It is caused by a mutation in the gene *GLB1,* which encodes for the enzyme β-galactosidase. *GLB1* is located in chromosome 3p22.3 and has 19 exons (20).

A mutation in *GLB1* can lead to two different lysosomal diseases, either GM1-gangliosidosis or mucopolysaccharidosis type IVB (MPS IVB). Both diseases result in a deficiency in β-galactosidase. GM1-gangliosidosis primarily involves the CNS, whereas MPS IVB primarily involves the skeletal system (18). In the lysosomal disease, galactosialidosis, a deficiency in β-galactosidase is caused by a mutation in the *CTSA* gene. The *CTSA* gene encodes for protective protein/cathepsin A, which stabilizes β-galactosidase and N-acetyl-α-neuraminidase (18). Patients with galactosialidosis have a partial deficiency in β-galactosidase and severe deficiency in N-acetyl-α-neuraminidase, and the clinical presentation is attributed to the severe deficiency in N-acetyl-α-neuraminidase (18).

There are two isoforms of β-galactosidase. β-galactosidase isoform 1 catalyzes the β-linked terminal galactosyl residues in gangliosides, glycoproteins, and GAG (21, 22). β-galactosidase isoform 2 plays a role in the formation of elastic fibers and connective tissue and lacks the catalytic activity seen in isoform 1 (23, 24). The remainder of the discussion will focus on β-galactosidase isoform 1. β-galactosidase contains a signal peptide, a triose phosphate isomerase barrel domain, β domain 1, and β domain 2 (25). The exact locations of these domains

vary among publications, because many forms of β-galactosidase are generated during protein processing. β-galactosidase is synthesized as an 85 kDa or 88 kDa precursor, which is then N-glycosylated, transferred to the lysosome, and becomes enzymatically active (26). In the lysosome, β-galactosidase is processed into the 64 kDa mature enzyme by cleavage at the N- and C-terminal, possibly through proteolytic processing (25, 27, 28). The C-terminal fragment is thought to remain associated with the N-terminal and required for enzymatic activity (28). The mature 64 kDa β-galactosidase complexes with a 32 kDa protective protein/cathepsin A, N-acetyl-α-neuraminidase, and the 20 kDa C-terminal end of β-galactosidase (27, 28). The protective protein/cathepsin A protects β-galactosidase from proteolytic degradation (26, 28). β-galactosidase can also form a complex with N-acetylgalactosamine-6-sulfatase (28).

In GM1-gangliosidosis, the primary storage material is GM1 gangliosides, and the secondary storage materials are oligosaccharides and keratans (4). Because gangliosides are categorized as sphingolipids, GM1-gangliosidosis can be classified as sphingolipidoses disorders (4). Other sphingolipidoses disorders include GM2-gangliosidosis, Gaucher disease, Fabry disease, and metachromatic leukodystrophy (4).

1.2.1.2 GM2-Gangliosidosis

GM2-gangliosidosis has an incidence of 1 in 222,000 and 1 in 422,000 births for Tay-Sachs and Sandhoff disease, respectively (6). It is an autosomal recessive disease. GM2-gangliosidosis is caused by mutations in either the *HEXA* or *HEXB* gene. *HEXA* is located in chromosome 1q23 and has 14 exons (29). *HEXB* is located in chromosome 15q13.3 and has 15 exons (30). In rare cases, GM2-gangliosidosis can be caused by a mutation in *GM2A,* which is located in chromosome 5q33.1 and has four exons (31).

GM2-gangliosidosis can have one of two names, depending on the affected gene. Tay-Sachs disease is caused by mutations in *HEXA* that encodes for the α subunit of the β-hexosaminidase isozyme A. Sandhoff disease is caused by mutations in *HEXB* that encodes for the β subunit of the β-hexosaminidase isozyme A. Both the α and β subunits are needed for the proper function of β-hexosaminidase isozyme A (31). The gene *GM2A* encodes for the protein GM2 ganglioside activator (31). GM2 ganglioside activator is required for the proper catalytic activity of β-hexosaminidase isozyme A (31). Mutations in *GM2A* are called the AB variant of Tay-Sachs disease.

There are three isoforms of β-hexosaminidase: isozyme A, isozyme B, and isozyme S. β-hexosaminidase isozyme A catalyzes the non-reducing end N-acetyl-D-hexosamine of glycoconjugates or sulfated N-acetyl-D-hexosamine of conjugates (32, 33). Isozyme B and isozyme S have been detected in humans but have unknown physiological significance (32, 33). Isozyme B is composed of two β subunits, and isozyme S is composed of two α subunits (32, 33). The rest of the discussion will focus on β-hexosaminidase isozyme A, also called β-hexosaminidase A. The α and β subunits each have an active site (34). The α subunit hydrolyzes GM2 gangliosides, and the β subunit catalyzes neutral substrates (34). The α subunit has a flexible loop that interacts with the GM2 activator protein (34).

The primary storage material is GM2 gangliosides, although the accumulation of oligosaccharides has been reported in Sandhoff disease (4). Because GM2 gangliosides are categorized as sphingolipids, GM2-gangliosidosis can be characterized as sphingolipidoses disorders (4). Other sphingolipidoses disorders include GM1-gangliosidosis, Gaucher disease, Fabry disease, and metachromatic leukodystrophy (4).

1.2.1.3 Clinical Presentation of Gangliosidoses

There are three forms of GM1-gangliosidosis: infantile, juvenile, and late-onset. Similarly, there are three forms of GM2-gangliosidosis with the same names. Clinical presentation is similar between GM1- and GM2-gangliosidosis, although GM1-gangliosidosis has greater skeletal involvement. The infantile phenotype has the earliest onset and most rapid disease progression. The juvenile phenotype has an intermediate onset and disease progression. The late-onset form has the latest onset and the slowest disease progression.

In the infantile form, symptoms occur by six months of age, and death occurs between two to five years of age (3, 35, 36). Hypotonia and developmental delays occur by six months of age (3). Motor skills are severely impaired within the first year of life (3). By 18 months of age, patients exhibit dysphagia and have feeding tubes placed (3). Seizures are another common clinical presentation, although the onset of seizures varies between seven to 18 months of age (3). Between 18 and 28 months of age, cognitive skills rapidly decline and reach the floor of the scales in neurocognitive tests (3). The leading cause of death is respiratory complications, most commonly aspiration pneumonia (3). One notable difference between infantile GM1 and GM2-gangliosidosis is skeletal abnormalities (3). Vertebral beaking and kyphosis are present in patients with infantile GM1-gangliosidosis but not infantile GM2-gangliosidosis (3). The higher prevalence of skeletal abnormalities in GM1-gangliosidosis is likely due to β-galactosidase's role in degrading keratan sulfate.

Compared to the infantile form, the juvenile form has a later onset, slower disease progression, and a more heterogeneous clinical presentation (37). Furthermore, a sub-classification of the juvenile form, called late-infantile, has clinical characteristics similar to the infantile and juvenile forms (37). In late-infantile gangliosidoses, symptoms first occur between one to three years of age, and death occurs between five and ten years of age (36-38). In the classic juvenile gangliosidoses, symptoms first occur between three to five years of age,

and the age of death varies widely, ranging between late childhood to the third decade of life (36, 37, 39, 40). The most common initial symptoms in the late-infantile and classic juvenile forms are gait abnormalities, balancing difficulties, frequent falling, and speech difficulties (37). Patients also exhibit ataxia, dysarthria, dysphagia, and hypotonia (36, 37, 39, 40). The cause of death can vary, although one frequent cause is aspiration pneumonia (37).

The late-onset form has the latest onset and the slowest progression. The late-onset phenotype is also called the “adult” or “chronic” form of the disease (3). Symptoms first occur in early to mid-adulthood, and lifespan varies widely (36, 38, 40-43). Limb-girdle weakness is usually the first symptom, and patients develop ataxia, progressive neuromuscular weakness, and loss of ambulation (36, 38, 40-43). Difficulties with speech and psychiatric changes may also occur (36, 38, 40-43).

1.2.2 Overview of MPS

In this section, information specific to MPS I, including molecular biology, will be discussed first. The molecular biology in the other MPS disorders is summarized in Table 1. The clinical presentation of MPS disorders will then follow.

1.2.2.1 MPS I

The incidence of MPS I is 1 in 100,000 births (6, 44). MPS I is an autosomal recessive disease caused by mutations in *IDUA*, which encodes for the enzyme α-L-iduronidase. *IDUA* is located in chromosome 4p16.3 and has 16 exons (45). An A300T mutation in the *IDUA* gene has been reported to cause pseudodeficiency (46, 47).

The α-L-iduronidase catalyzes the hydrolysis of the terminal α-L-iduronic acid in dermatan sulfate and heparan sulfate (45). The isoform A of the enzyme is 653 amino acids long (48). A signal sequence is located in amino acids 1-19, a conserved domain in the glycosyl hydrolase family 1 in amino acids 30-543, and a fibronectin type 3 domain in amino acids 544-636 (48).

In MPS I, the primary storage materials are heparan sulfate and dermatan sulfate. MPS diseases can be categorized as glycosidoses, which are diseases caused by the accumulation of complex carbohydrates or carbohydrate-containing compounds (4). In most glycosidoses, a glycosidase enzyme is deficient, but a sulfatase can be deficient in some diseases (4). Deficiency in some sulfatases retains the sulfate resides on the ends of carbohydrate chains of glycol-conjugates, blocking downstream enzymes from detaching monosaccharide units from the non-reducing ends of glycan chains, ultimately resulting in GAG accumulation (4).

1.2.2.2 Clinical Presentation of MPS

There are three forms of MPS I: Hurler (MPS IH), Hurler-Scheie (MPS I HS), and Scheie (MPS IS). The Hurler form has the earliest onset and the most rapidly progressing form of the disease. Approximately 50 to 80% of patients have this severe form of MPS I (49). Scheie form has the latest onset and the slowest progressing form of the disease. The heart, bones, joints, and respiratory system are commonly affected among MPS disorders. MPS I, II, and VII have similar clinical manifestations (15).

In the Hurler or severe for MPS I, symptoms occur by 12 months of age, and, if untreated, death occurs within the first decade (17). Patients with the severe forms of MPS I, II, and VII have similar somatic and cognitive involvement (15). Cardiac involvement will be discussed in detail in Section 1.2.4. Respiratory involvements include decreased pulmonary function, recurrent upper and lower respiratory tract infections, obstructive sleep apnea, and persistent nasal

discharge (17). Skeletal and joint symptoms include vertebral dysplasia, kyphosis, hip dysplasia, restricted joint mobility, short stature, carpal tunnel syndrome, and osteopenia or osteoporosis (17). Other symptoms include coarse facial features, hearing loss, vision loss, corneal clouding, and open-angle glaucoma (15, 17). Extensive cognitive impairment occurs in the severe forms of MPS I, II, and VII but not in the attenuated forms of these MPS diseases (15). Extensive cognitive impairment is exhibited first as a delay in developmental skills, then a plateau and regression (15, 50).

Hurler-Scheie is the intermediate form of MPS I, and Scheie is the attenuated form of MPS I (17). Patients with the attenuated form of MPS I have a normal life expectancy (17). Unlike the severe forms, there is little to no cognitive impairment in the intermediate or attenuated forms of MPS I, II, and VII. Patients with the intermediate or attenuated forms otherwise have somatic symptoms similar to the severe form. Typically, there are mild symptoms in multiple organ systems with or without severe symptoms in one or two organ systems (15). Cervical cord compression occurs in intermediate and attenuated forms (17). Progressive airway obstruction and cardiac disease can cause premature death (15). Airway obstruction in MPS I is caused by macroglossia, narrowed nasal airway, enlarged adenoids and tonsils, and thick secretions (14).

MPS III primarily has CNS involvement (15). There are four types of MPS III: type A, type B, type C, and type D. Each type corresponds to one of the four genes that encode for a different enzyme that degrades heparan sulfate (Table 1). In the severe form of MPS III, symptoms occur in childhood, and death occurs in the second to third decade of life (15). Patients exhibit severe developmental delays, behavioral difficulties, sleep disturbances, and dementia (15). There may be mild or moderate neurocognitive impairment in some patients (15).

MPS IV primarily has skeletal or joint involvement (15). Of note, joint hypermobility is unique in this disease (15). Although cognition is minimally affected, cervical spine instability and communicating hydrocephalus are

common (15). MPS IVB is caused by a mutation in the same gene as GM1-gangliosidosis.

MPS VI has similar manifestations as MPS I, II, and VII, except there is little cognitive impairment (15). In the severe form, symptoms occur before two or three years of age, and death occurs in the second or third decade of life (15). In attenuated forms of the disease, symptoms may occur in the teenage years or early adulthood (15).

The few reports of MPS IX describe skeletal and joint manifestations and frequent otitis media (15).

1.2.3 Central Nervous System Dysfunction

Two-thirds of lysosomal diseases have some CNS involvement (51). The clinical manifestations of CNS vary widely and include deficits in cognition, motor, and verbal skills, as well as seizures and psychological disorders (3, 52). In the infantile forms of GM1- and GM2-gangliosidosis, neurological deficits can severely limit motor function (3). In infantile GM1-gangliosidosis, 100% of patients could not support their head, 100% of patients could not sit independently, and 88% of patients never gained the ability to crawl (3). Patients with infantile GM2-gangliosidosis were also unable to reach motor milestones or retain motor skills: 93% of patients lost the ability to support their head, 62% of patients never gained the ability to sit independently, and 100% of patients never gained the ability to crawl (3).

Lysosomal diseases can affect multiple areas of the brain. The affected brain region can vary both between diseases and within a disease. In GM1- and GM2-gangliosidosis, there is decreased myelination and abnormalities in cerebellar white matter, corpus callosum, basal ganglia, and thalamus. These CNS involvements are discussed below.

Abnormalities in brain white matter have been reported in several lysosomal diseases. White matter abnormalities may be due to the loss of glial

cells that synthesize myelin or interruption of the normal recycling of gangliosides and oligosaccharides, causing a shortage of substrates needed to synthesize myelin (4). In patients with the infantile or juvenile forms of GM1- and GM2-gangliosidosis, there was decreased volume of cerebellar white matter over time, whereas the volume increased over time in the healthy, age-matched group (53). The low cerebellar white matter may explain the impairment of cognition and language skills in GM1- and GM2-gangliosidosis (54, 55). In patients with MPS IH, MPS II, MPS III, and MPS VII, multifocal or diffuse lesions in the white matter are commonly reported (56-58). Abnormalities in the brain's white matter were also detected in pediatric patients with Gaucher disease type I and type III using diffusion tensor imaging (59). Diffusion tensor imaging has also detected early microstructural changes in the cerebral white matter in pediatric patients with cystinosis (60). In cystinosis, changes in the white matter may be due to cystine crystal formation in myelin precursors (60, 61). In a 4-month-old patient with fucosidosis, a severe global hypomyelination of supra- and infratentorial white matter was seen after cranial magnetic resonance imaging (MRI) (62). When the patient was 16 months of age, these neuroradiological abnormalities progressed and showed involvement of the basal ganglia and thalami (62). Severe hypomyelination was also reported in a patient with Salla disease (63).

Delayed myelination or dysmyelination, more specific abnormalities involving white matter in the brain, have been reported in GM1- and GM2-gangliosidosis. White matter myelination indicates functional brain maturation, and delayed myelination has been reported in children with developmental delays not caused by lysosomal diseases (64). Delayed myelination has been observed in patients with infantile and juvenile GM1-gangliosidosis (67). An autopsy of two patients with infantile GM1-gangliosidosis revealed delayed myelination in the corpus callosum, cingulum, posterior frontal, occipital pole, and anterior limb of internal capsule (65). In contrast, the brainstem and cerebellar sites had a normal onset of myelination (65). A different study saw a persistent delay in the myelination of the cerebrum's white matter, except the splenium of

corpus callosum, in a patient with late-infantile GM1-gangliosidosis (66). Delayed myelination has also been reported in an MRI study of a feline model of Sandhoff disease (67).

Several studies in GM1- and GM2-gangliosidosis have reported thinning of the corpus callosum. The corpus callosum's volume decreases over time in patients with infantile and juvenile GM1- and GM2-gangliosidosis (53). A thin corpus callosum has been found in patients with Sandhoff and infantile GM1-gangliosidosis (65, 68). A thin corpus callosum has also been detected in canine and feline models of GM1- and GM2-gangliosidosis (69). The thin corpus callosum in gangliosidoses is likely due to a disruption in the formation of myelin. A disruption in myelin formation may also explain the presence of corpus callosum abnormalities in other lysosomal diseases, such as mucolipidosis type IV and metachromatic leukodystrophy (70).

Several areas of the basal ganglia are affected in GM1- and GM2-gangliosidosis, which may explain the motor impairment in these diseases (55, 71). The caudate nuclei and putamen showed progressively decreasing volumes in patients with infantile and juvenile GM1- and GM2-gangliosidosis (55). Abnormal signal intensities in the caudate and putamen have also been reported in patients with Sandhoff disease (68). Hyperintensities in the putamen were reported in two patients with late-infantile GM1-gangliosidosis (71). Another part of the basal ganglia, the globus pallidum, had abnormal signal intensities in patients with Sandhoff disease (68). T2 scans of the globus pallidum had non-homogenous high signal intensities in patients with infantile and juvenile GM1-gangliosidosis (72). One study reported paramagnetic ion accumulation in the globus pallidum in late-infantile GM1-gangliosidosis (71). Additionally, storage of GM1 gangliosides were found in the basal ganglia in an autopsy of infantile, juvenile, and late-onset patients with GM1-gangliosidosis (73).

The thalamus has a wide range of functions involving memory, emotions, executive function, processing of sensory information, and relaying sensory

information to the cortex (74). Patients in the early stages of Krabbe disease have hypointense thalamic signals on both T1- and T2-weighted imaging, whereas later stages of Krabbe disease have hyperintense signals on these sequences (74). Interestingly, the opposite pattern is observed in patients with gangliosidoses (74). That is, patients with gangliosidoses have hyperintense thalamic lesions in T1-weighted imaging and hypointense thalamic lesions in T2-weighted imaging (74). This pattern has been reported in patients infantile GM1-gangliosidosis and one 11-month-old patient with late-infantile GM1-gangliosidosis (66, 75). In patients with Sandhoff disease, neuroimages show bilateral symmetric thalamic hyperdensity (68). These findings may be due to calcification and vascular malformations in the thalamus, and these patterns may be associated with leukoencephalopathy and cerebellar atrophy (74).

In addition to neuroimaging, the CNS pathology in lysosomal diseases can be seen at the cellular level. Neurons have abnormal morphologies, most commonly meganeurites, ectopic dendritogenesis, and axonal spheroids (9). Meganeurites are enlarged axon hillocks that contain storage material related to the deficient enzyme (9). Meganeurites have been reported in the cerebral cortex, diencephalon, and brainstem in several MPS diseases (58, 76-83). Another abnormal neuronal morphology is ectopic dendritogenesis in cortical pyramidal neurons (9). Ectopic dendritogenesis is the abnormal sprouting of new dendrites at the axon hillock (9, 84). The accumulation of GM2 gangliosides initiates ectopic dendritogenesis in cortical pyramidal neurons (85). One supporting evidence is the presence of ectopic dendritogenesis in the cerebral cortex of animal models of diseases that accumulate GM2 gangliosides, specifically GM2-gangliosidosis, GM1-gangliosidosis, MPS I, Niemann-Pick disease type C, and juvenile-onset form of α-mannosidosis (86). Correspondingly, ectopic dendritogenesis was not detected in animal models of lysosomal diseases that do not accumulate GM2 gangliosides, specifically fucosidosis, neuronal ceroid lipofuscinosis, and adult-onset form of α-

mannosidosis (86). Another common neuronal abnormal morphology in lysosomal diseases are axonal spheroids (9). Axonal spheroids are focal granular enlargements, and these enlargements contain storage materials that are unrelated to the deficient lysosomal enzyme (9, 87). Spheroids are commonly found on GABAergic neurons and have been reported in Niemann-Pick disease type A and type C, as well as α-mannosidosis (9, 87).

The exact mechanisms of neuropathy in lysosomal diseases are unclear, but one mechanism may involve the accumulation of storage materials in neurons. Several studies in MPS have reported the accumulation of GAG and other metabolites within neurons. A patient with MPS I had meganeurites in several neurons in the cerebral cortex (80). Patients with MPS IH, MPS II, and MPS III had focal dendritic swellings in Purkinje cells, which appeared to accumulate gangliosides (81). Purkinje cells are a type of neuron located in the cerebellar cortex. Patients with MPS IH, MPS II, and MPS IIIA had four to sixfold higher total GAG levels in neurons than people without a neurological disease (82). Notably, a patient with the attenuated form of MPS I had normal GAG levels in neurons (82). While it may be evident that there is an accumulation of storage materials in the CNS, the development of neuropathy could occur through one of the many different pathogenic cascades in lysosomal diseases, such as defective intracellular calcium signaling, oxidative stress, impaired autophagy, and chronic inflammation (9, 11).

In addition to neurons, microglial cells are another cell type commonly affected in lysosomal diseases. Microglia play a critical role in neuroinflammation, including in lysosomal diseases (5). Microglia are the resident macrophages in the brain and play important roles in immune responses and CNS maintenance (88). It is not clear how neuroinflammation is initiated in lysosomal diseases. One possibility is that the excess storage material distends the lysosomes and disrupts the integrity of lysosomal membranes (5, 89). The lysosomal contents may then be released into the cytosol and subsequently presented extracellularly

as damage-associated molecular patterns (DAMPs) (5, 89). Microglia can sense DAMP signals from damaged or dying neurons, using toll-like receptors and other pattern recognition receptors (5, 90). Microglia may then secrete chemokines and cytokines to recruit and activate local microglia, astrocytes, neurons, and oligodendrocytes (5). Astrocytes, the most abundant cell type in the brain, may also participate in neuroinflammation by secreting chemokines (5). A chronic state of neuroinflammation could perpetuate the death of neurons, accelerating neurodegeneration.

1.2.3.1 Neuroinflammation

While the exact mechanism of neuroinflammation is unclear, neuroinflammation is widely becoming accepted as a key contributor to the pathology and symptoms in lysosomal diseases (5, 11, 51). Patients with neurodegenerative lysosomal diseases had elevated levels of inflammatory mediators in the cerebrospinal fluid (CSF) (91). Neuroinflammation appears to be the cause of neuropathological processes in lysosomal diseases rather than a byproduct. Neuroinflammation has been shown to precede the death of neurons and the onset of symptoms in several animal models of lysosomal diseases, including GM2-gangliosidosis, Gaucher disease type I, Niemann-Pick disease type C, and neuronal ceroid lipofuscinoses (92-95). Investigations of anti-inflammatory drugs in pre-clinical studies provide further evidence of the importance of neuroinflammation in lysosomal diseases. Mice with Niemann-Pick disease type C1 that were administered a triple combination of ibuprofen, curcumin, and miglustat had better motor function than a dual combination of curcumin and miglustat (96). However, ibuprofen alone did not improve disease progression (96). In a different study, MPS IIIB mice treated with prednisolone had better performance on behavioral tests than untreated mice (97).

Activation of microglial cells is a critical component of neuroinflammation in lysosomal diseases (5, 92, 98). Microglial activation preceded the death of neurons in a murine model of Gaucher disease type I (94). Similarly, activation of microglia and astrocytes preceded neuronal death in affected brain regions in murine models of juvenile neuronal ceroid lipofuscinoses (95). Microglial activation preceded the onset of symptoms in murine models of GM1-gangliosidosis, Tay-Sachs disease, and Sandhoff disease (92). Similar findings were reported in Niemann-Pick disease type C and Gaucher disease type I (93, 94).

Importantly, neuroinflammation may reflect the disease severity and disease progression. There are higher levels of neuroinflammatory mediators in the severe forms of GM1- and GM2-gangliosidosis compared to the attenuated forms (91, 92). Furthermore, neuroinflammation has increased during disease progression (92, 99). For example, the activation of microglia and astrocytes was higher at nine months than at four months in murine models of MPS I, MPS IIIA, and MPS IIIB (99). These findings suggest that a biomarker for neuroinflammation may be valuable for distinguishing among different forms of a lysosomal disease and monitoring disease progression.

1.2.4 Cardiovascular Manifestations

This section discusses cardiovascular manifestations in lysosomal diseases, particularly in MPS. The most common CV manifestations in MPS are cardiac valve abnormalities, ventricular hypertrophy, and coronary narrowing or occlusion (100). These CV manifestations in MPS are detailed in the next following paragraphs. The remainder of this paragraph briefly describes the CV manifestations in other lysosomal diseases. There is extensive cardiac involvement in Fabry disease, including cardiac hypertrophy, atrial fibrillation, heart failure, and cardiac fibrosis (101). In Pompe disease, massive left

ventricular hypertrophy (LVH) and cardiac failure can occur (102). Patients with Gaucher disease can have pulmonary hypertension, pericardial effusion, and valvular abnormalities (102). In Danon disease, hypertrophic cardiomyopathy and progressive conduction abnormalities have been reported (102).

Approximately 60 to 100% of patients with MPS exhibit CV disease (100, 103-109). CV disease has been reported in all the MPS diseases but is more common in MPS disorders that store dermatan sulfate, specifically MPS I, II, and VI (100, 103-107). Storage of dermatan sulfate also occurs in MPS VII, but cardiac findings are less commonly reported in MPS VII because this disease is rarer than others (105). The most common cardiac manifestations in MPS are cardiac valve abnormalities, ventricular hypertrophy, and coronary narrowing or occlusion (100).

Abnormalities in cardiac valves are the most common cardiac manifestation in MPS, occurring in approximately 60 to 90% of patients (100, 105, 107). Mitral regurgitation is the most common cardiac lesion in MPS (105). Cardiac valve abnormalities are more common in MPS diseases with impaired degradation of dermatan sulfate, more specifically, MPS I, II, and VI (100, 103-107). MPS VII also stores dermatan sulfate, but there are few reports of cardiac valvular in MPS VII because this disease is rarer than others (105). Valvular dysfunction is classified as regurgitation (leaky valves) or stenosis (obstructive to flow). Valvular regurgitation is more common than stenosis in MPS (100, 104, 105, 110-112). Left-sided valves (mitral and aortic) are more severely affected than right-sided valves (tricuspid and pulmonary) in patients (100, 104, 105, 110-112). Mice with MPS I can model some of the valvular dysfunction seen in patients. MPS I mice exhibit aortic insufficiency but not mitral insufficiency (113, 114). In patients, mitral and aortic valves have thick leaflets, short chordae tendinae, and thick papillary muscles, limiting the mobility in leaflets (100, 115-117). Accumulation of GAG occurs in valvular interstitial cells in patients with MPS IH (118). The accumulation of GAG causes morphological changes in the cells, altering the structural properties of the valves.

Regurgitation in the mitral valve is usually the first sign of cardiac involvement in MPS I, II, III, IV, and VI (105). Valvular dysfunction can lead to volume overload in the left atrium and left ventricle, as well as left ventricular hypertrophy (100). LVH and diastolic dysfunction occur early in the disease (100, 106). In the later stages of the disease, left ventricular dilation and systolic dysfunction occurs (100, 106). Valvular dysfunction can contribute to systolic and diastolic dysfunction (100). Heart failure, arrhythmias, and coronary occlusion are cardiac causes of death in MPS (100, 108, 119, 120).

Hypertrophy is another common cardiac manifestation in MPS (100). Hypertrophy may be due to valvular dysfunction and/or accumulation of GAG (100). High levels of GAG were detected in fibroblasts and macrophages located in the myocardial interstitium of a patient with MPS IH (118). Mice with MPS I do not reliably reflect LVH assessed by echocardiography, as LVH was detected in one study with MPS I mice but not in another study (113, 114). However, MPS I mice did have higher GAG levels in the myocardium than healthy mice, and GAG levels in the myocardium increased over time in MPS I mice (113).

Coronary narrowing or coronary occlusion is a serious cardiac manifestation of MPS (100). Coronary narrowing and occlusion have been reported in all MPS diseases but are more common in MPS I and MPS II (100). In patients with MPS, the narrowing in coronary arteries is caused by myointimal proliferation from GAG accumulation (100, 121). This diffuse involvement of the coronary arteries poses challenges in evaluating coronary artery disease with the traditional methods of electrocardiograms and angiograms (100). Additionally, MPS I mice do not exhibit myointimal proliferation in the epicardial coronary arteries (113, 114).

The cardiovascular pathophysiology of MPS is not well understood but is assumed to be initiated by the accumulation of GAG (100). Sulfated heparan, dermatan, chondroitin, and keratan are normal components of cardiac tissue (100, 122-124). Dermatan sulfate is a component of normal cardiac valves, likely explaining the higher prevalence of valvular abnormalities in MPS I, II, and VI

(100, 103-107). Cells that accumulate GAG have been detected in the cardiac valve, endocardium, myocardial walls, coronary arteries, aorta, and conduction system (100, 125). Cells that accumulate GAG are described as large cells with clear cytoplasm or vacuolated cells with enlarged cytoplasm (100). These cells have been called Hurler cells, gargoyle cells, clear cells, or balloon cells. The accumulation of GAG can distend cells, leading to structural abnormalities in the heart (100). The storage of GAG in valvular interstitial cells may initiate structural changes in the valves that propagate other cardiac manifestations such as hypertrophy and heart failure.

Cardiac valve abnormalities in MPS are inadequately treated by current therapies. HCT is routinely performed for patients with MPS IH (50). HCT preserves systolic ventricular function, regresses cardiac hypertrophy, and may prevent narrowing and occlusion in the coronary arteries in MPS I (100, 126-131). However, HCT does not improve valvular dysfunction, and left-sided valvular dysfunction continues to progress in patients (100, 126, 132). Similarly, ERT preserves systolic ventricular function and resolves ventricular hypertrophy in MPS I and MPS II (100, 133-136). However, patients on ERT still exhibit progressive thickening and dysfunction of left-sided valves (100). Although initiating ERT at four years of age or younger may prevent the development of valvular abnormalities, this benefit has only been reported in two patients so far (100, 137, 138). HCT's and ERT's limited benefits on cardiac valves have been attributed to the poor vascularization of cardiac valves (100). Cardiac valvular abnormalities in MPS are surgically treated, and these procedures are one of the most frequent procedures performed in patients with MPS (100, 139).

CHAPTER 2: OVERVIEW OF CURRENTLY AVAILABLE THERAPIES FOR LYSOSOMAL DISEASES, DRUG DEVELOPMENT IN RARE DISEASES, AND UNMET NEEDS IN LYSOSOMAL DISEASES

In this chapter, currently available therapies for lysosomal diseases will be discussed first, followed by an overview of drug development in rare diseases. I will then discuss unmet needs in lysosomal diseases that are relevant to this dissertation's studies.

2.1 Overview of Currently Available Therapies for Lysosomal Diseases

The main classes of therapies for lysosomal disease are intravenous enzyme replacement therapy (ERT), oral substrate reduction therapy (SRT), oral pharmacological chaperones, and HCT. There are currently 22 therapies for lysosomal diseases approved by the Food and Drug Administration (FDA) (Table 2). Alglucerase (Ceredase®), a placentally-derived ERT for Gaucher disease, was withdrawn from the market and replaced with imiglucerase (Cerezyme®) that is manufactured using a safer technique with genetically engineered Chinese hamster ovary (CHO) cells (140). Additionally, there are two therapies for lysosomal diseases that are approved by the European Medicines Agency (EMA). Agalsidase alfa (Replagal®) is an ERT for Fabry disease, and velmanase alfa (Lamzede®) is an ERT for alpha-mannosidosis. In 2021, pabinafusp alfa (IZCARGO®), an ERT for MPS II, was approved in Japan (141). In addition to FDA-approved treatments, HCTs are also performed for certain lysosomal diseases. The underlying mechanism for ERT and HCT relies on cross-correction and metabolic correction, which are described in Section 1.2.

2.1.1 Enzyme Replacement Therapy

Thirteen of the 22 FDA-approved therapies are ERT. ERT is typically administered as an intravenous infusion. One exception is cerliponase alfa which is administered intracerebroventricularly. In ERT, a functional enzyme is produced in cell cultures and then administered to patients. In general, infusion

reactions are a notable adverse effect. Infusion reactions can be managed with antihistamines, corticosteroids, and decreasing the infusion rate (142). Patients can also develop antibodies to ERT, which may impact efficacy of treatment (143). The main advantage of ERT is the target specificity. By only replacing the deficient enzyme, there are minimal off-target effects. However, currently approved ERTs have the disadvantages of not reaching the CNS or poorly vascularized sites such as cardiac valves and bones. Other disadvantages of ERTs include infusion reactions, complex manufacturing, high cost, and inconvenience to patients.

Table 2: List of FDA-Approved Therapies for Lysosomal Diseases

Drug/Therapy Name	Indication	Mechanism of Action
laronidase (Aldurazyme®)	MPS I	ERT
idursulfase (Elaprase®)	MPS II	ERT
elosulfase alfa (Vimizim®)	MPS IVA	ERT
N-acetylgalactosamine 4-sulfatase/galsulfase (Naglzyme®)	MPS VI	ERT
vestronidsae alfa (MEPSEVII®)	MPS VII	ERT
imiglucerase (Cerezyme®)	Gaucher disease	ERT
velaglucerase alfa (VPRIV®)	Gaucher disease	ERT
taliglucerase alfa (Elelyso®)	Gaucher disease	ERT
eliglustat (Cerdelga®)	Gaucher disease	SRT
miglustat (Zavesca®)	Gaucher disease, type I (mild to moderate)	SRT
alglucosidase alfa (Lumizyme® in US/ Myozyme® outside US)	Pompe disease	ERT
alglucosidase alfa-ngpt (Nexviazyme ®)	Pompe disease-late-onset, 1 year of age or older	ERT
agalsidase beta (Fabrazyme®)	Fabry disease	ERT
migalastat (Galafold®)	Fabry disease	Chaperone therapy
sebelipase alfa (Kanuma®)	Lysosomal acid lipase deficiency	ERT
cerliponase alfa (Brineura®)	Ceroid lipofuscinosis type 2	ERT (intracerebroventricular route)
cysteamine bitartrate (Cystagon®)	Cystinosis	SRT

cysteamine delayed-release (Procysbi®)	Cystinosis	SRT
cysteamine ophthalmic solution 0.44% (Cystaran®)	Cystinosis	corneal cystine crystal accumulation
cysteamine ophthalmic solution 0.37% (Cystadrop®)	Cystinosis	corneal cystine crystal accumulation

2.1.1.1 Review of Selected Clinical Trials with Enzyme Replacement Therapies in MPS I and II

This section will discuss the safety and efficacy results from the clinical trials of laronidase, valanafusp, idursulfase, and pabinafusp ERTs. Laronidase is discussed because it is an ERT approved for MPS I. Valanfusp is still being investigated for MPS I, but its clinical trials are discussed because the fusion iduronidase enzyme uses receptor-mediated uptake, a mechanism that is relevant for my study in Chapter 4. Pabinafusp is an ERT that also uses receptor-mediated uptake and is approved in Japan for MPS II. Idursulfase, an ERT approved MPS II, is discussed to help frame pabinafusp's results and because of the clinical similarities between MPS I and MPS II.

In an open-labeled, phase III extension study of laronidase ERT, 45 patients with attenuated MPS I were followed for four years (144). Patients were intravenously infused a dose of 100 U/kg body weight (0.58 mg/kg) of iduronidase once weekly (144). In the original phase III study, the coprimary endpoints were median changes from baseline to 26 weeks in the 6-minute walk test (6MWT) and the percentage predicted forced vital capacity (%FVC) (145). In the extension study, the change in distance walked from baseline was 23.1 meters after one year, 31.7 meters after two years, and 17.7 meters after three and a half years of treatment. The %FVC declined by 0.78% each year and was approximately -2.73% %FVC at 3.5 years. Adverse events (AE) related to treatment were reported in 67% of patients, and infusion-associated reactions occurred in 53% of patients (144). Antibodies to laronidase were detected in 93% of patients during the study, and only 29% of patients were seronegative at their last assessment (144). Neutralizing antibodies were not reported (144). This phase III extension provided valuable information on how different efficacy parameters respond to treatment over time. Changes in urinary GAG, liver volume, and sleep apnea occurred within months after initiating laronidase (144). In contrast, changes in respiratory function, physical endurance, mobility, and

daily living activities took several years to detect, although this may be dependent on the therapy. laronidase appeared to stabilize rather than improve clinical parameters. This may be due to initiating therapy after irreversible damage from the disease has occurred.

Valanafusp has not been approved but is discussed in this section because it uses a receptor-mediated transport mechanism. An overview of receptor-mediated transport is in Section 2.3.2.4. Briefly, valanafusp is a fusion iduronidase enzyme in which iduronidase is conjugated to an antibody for the human insulin receptor to mediate uptake into the CNS. Valanafusp has been studied in a phase I/II trial in MPS I (146). In the phase I trial, six adults with the attenuated MPS IS were intravenously infused a dose of either 0.3 mg/kg, 1 mg/kg, and 3 mg/kg (146). In the phase II trial, 11 pediatric patients with MPS IH or MPS IHS were intravenously infused a dose of either 1 mg/kg, 3 mg/kg, or 6 mg/kg once weekly for 52 weeks (146). In the phase II trial, the mean age was 7.6 years, and nine patients had previously been treated with laronidase ERT (146). The incidence of hypoglycemia was 6.4% and was resolved within 20 minutes of a snack or glucose sachet. Hypoglycemia appeared to be dose-dependent, as 67% of hypoglycemia occurred at the 6 mg/kg (146). Cognition was assessed as the developmental quotient from the cognitive domain of the Bayley Scales of Infant and Toddler Development®, Third Edition (146).

In the valanafusp phase I/II trial, the mean change in developmental quotient (DQ) from baseline to 52 weeks was -1.2±2.8 (mean and standard error of mean) (146). There was no control group, so cognitive scores were informally compared to a previously published study by Shapiro et al. (147). The valanafusp publication states “if untreated, patients suffer from a severe neurocognitive decline starting at the age of one year, and the median DQ declines 14-17 points per year” (146, 147). However, this statement may be misconstrued. In the study by Shapiro et al., patients exhibited a decline of 14-17 DQ per year between one to three years of age (147). In contrast, the patients in the phase II clinical trial had a mean age of 7.6 years. The DQ trajectory for untreated MPS I patients

between seven and eight years of age in Shapiro et al. may be closer to a decline of 5 points a year, although there was only one patient in the age range, so this is difficult to compare (147). Furthermore, the cognitive improvement from valanafusp should be compared to the standard of care in MPS IH. Two studies in MPS I patients treated with HCT have reported similar changes in DQ as the one seen in the valanafusp phase I/II trial (148, 149). These studies may not have been discussed in the valanafusp publication, because of the difficulty in finding studies that use the same method of assessing cognition, more specifically, DQ from the cognitive domain of Bayley Scales of Infant and Toddler Development®, Third Edition.

In an open-labeled, phase III extension study of idursulfase ERT, 94 patients with MPS II were followed for two years (150). Patients were intravenously infused a dose of 0.5 mg/kg idursulfase once weekly. In the phase II/III clinical trial, the primary endpoint was a combination of the change from baseline in 6MWT and % FVC (151). In the extension study, the primary measures of clinical efficacy were changes in FVC and 6MWT distance (150). In the extension study, a positive trend in %FVC was seen between 0 to 16 months and a decline was seen between 16 to 36 months. At 36 months, there was a -2% change in FVC from baseline (150). For the 6MWT, the improvement in distance walked from baseline was sustained and was approximately 25% at 36 months (150). Treatment-related AE occurred in 59.6% of patients, and infusion-related AE occurred in 53% of patients (150). Antibodies to idursulfase were detected in 50% of patients during the study, and 27.1% of patients were seropositive at the end of the study (150). Neutralizing antibodies were present in 22.3% of patients at the end of the study, and neutralizing antibodies attenuated the improvements in absolute FVC (150).

Pabinafusp is a fusion idursulfase enzyme that is conjugated to an antibody for the human transferrin receptor (152). In a phase II/III trial, 28 Japanese patients with MPS II were intravenously infused pabinafusp at a dose of 2 mg/kg once weekly for 52 weeks (152). The primary efficacy endpoint was a

change in the heparan sulfate concentrations in the CSF (152). The heparan sulfate level in the CSF at baseline was 5856 ± 2614 ng/mL and decreased to 2124 ± 882.6 ng/mL at week 52, which was statistically significantly different ($p<0.001$) (152). A decrease in CSF heparan sulfate levels was also seen separately for the patients with the severe phenotype (152). However, changes in neurocognitive development, a secondary endpoint, were more difficult to ascertain (152). Analysis of neurocognition was complicated by different disease phenotypes (e.g., attenuated vs severe), clinical stage within a disease (e.g., the initial, middle, or late phase of the severe phenotype), and different neurocognitive scores between phenotypes (e.g., developmental quotient vs age-equivalent scores) (152). These challenges are unfortunately common in clinical trials with rare diseases. In the 20 patients with the severe phenotype, 11 patients maintained neurocognitive scores (age-equivalent scores ± 3 months), and two patients had improved neurocognitive scores (age-equivalent scores > 3 months) (152). There was no comparator arm, either placebo or with idursulfase, due to ethical concerns (152). One reason why a clear neurocognitive benefit was not seen was that 52 weeks was too short to see an improvement (152). Serum levels of heparan and dermatan sulfate, the other secondary endpoints, decreased from baseline (152). The 6MWT appeared to stabilize and improve in both idursulfase-naïve and idursulfase-treated patients (152). There were no significant changes in cardiac function (152). Over the study's 52 weeks, fourteen patients developed an antibody to the pabinafusp, but these were not associated with infusion-associated reactions or serum heparan sulfate concentrations (152).

2.1.2 Substrate Reduction Therapy

SRTs are another class of therapies for lysosomal diseases. SRTs reduce the synthesis of the storage material. By doing so, a poorly functioning lysosomal enzyme can maintain normal levels of the storage material. SRTs are small

molecules and have the advantage of more easily crossing the blood-brain barrier (BBB) than ERT. Miglustat has been shown to cross the BBB in rats (153). However, eliglustat is not able to achieve therapeutic levels in the CNS, because it is a substrate for the p-glycoprotein 1, an efflux transporter located on the BBB (154). Another advantage is that one SRT could be used for multiple diseases if those diseases share a biochemical pathway. The ability to treat multiple diseases with one therapy is particularly attractive in orphan/rare diseases. However, targeting multiple biochemical pathways also increases the potential for off-target effects.

Miglustat is an FDA-approved SRT for Gaucher disease type I (the non-neuronopathic form) but has been studied extensively in other lysosomal diseases (3, 155-158). Miglustat is an imino sugar and a reversible inhibitor of glucosylceramide synthase, which catalyzes the first committed step of glycosphingolipid synthesis (158). Miglustat has been studied in multiple lysosomal diseases because of its ability to decrease ganglioside levels and cross the BBB in rodents. However, clinical studies with miglustat have shown inconsistent improvements in neurocognition, which may be due to subtherapeutic levels of the drug in the CNS. In a phase IIb to phase III study in MPS III, miglustat crossed the BBB but did not cause a significant reduction in gangliosides (158). Furthermore, miglustat did not improve or stabilize behavioral problems in patients with MPS III (158). Miglustat did not improve neurocognition in other lysosomal diseases, including infantile GM1-gangliosidosis, infantile Tay-Sachs, late-onset Tay-Sachs disease, Niemann-Pick disease type C, and Gaucher disease type 3 (3, 155-157). One possible reason why miglustat did not improve neurocognition is that patients were not administered the target dose because of the gastrointestinal side effects (3). However, even when patients reached the target dose, miglustat did not have significant neurocognitive improvements in patients with the infantile forms of GM1- and GM2-gangliosidosis (3).

2.1.3 Chaperone Therapy

Chaperone therapies improve the affected enzyme's function. Chaperones can change the conformation of an improperly folded enzyme to restore its function partially. One advantage of chaperone therapies is that they are small molecules, allowing for easier manufacturing. One disadvantage of chaperones is that they are specific for mutations. For example, they do not benefit patients with early nonsense mutations because no enzymes are produced.

2.1.4 Hematopoietic Cell Transplant

In addition to FDA-approved therapies, HCT is another option for certain lysosomal diseases. In HCT, cells that can produce the enzyme are transplanted into patients. One advantage of HCT is that there is a potentially life-long and temporally continuous source of enzyme for patients. A disadvantage of HCT is reaching the CNS and poorly vascularized sites such as cardiac valves and bones (14). Other disadvantages of HCT include the need for myeloablative conditioning regimens and immunosuppressive regimens to avoid rejection (159). The use of HCT in clinical practice can range from investigational to standard of care, depending on the disease phenotype, age of diagnosis, and disease progression (115).

HCT is the standard of care for patients with MPS IH, because HCT can preserve intellectual development in MPS IH if transplant occurs before the onset of neurologic damage, and the first HCT was described in a publication by Hobbs et al. (159, 160). In a study by Whitley et al., MPS IH patients with normal developmental quotient/intelligence quotient (DQ/IQ) scores (DQ/IQ >80) before transplantation were able to maintain normal DQ/IQ scores several years after transplantation had occurred (159). In contrast, patients with DQ/IQ scores <80 prior to transplant had DQ/IQ scores that decreased by -10 to -61 several years after transplant (159). Possible mechanisms for the neurological improvement

seen in HCT may be due to HCT's ability to reverse or prevent hydrocephalus and metabolic correction within the brain parenchyma in MPS IH (159). While HCT has been effective in preventing cognitive decline in MPS IH and MPS II, this effect has not been demonstrated in other lysosomal diseases (15).

2.2. Drug Development in Rare Diseases

The majority of lysosomal diseases do not have treatments that address the underlying pathology. Out of the 70 different lysosomal diseases, there are only 12 diseases with a treatment. HCT and off-label treatments have improved underlying pathology in some diseases. Yet, a high number of lysosomal diseases lack therapies that can improve or even stabilize clinical conditions. There are multiple challenges in developing therapies for rare diseases: lack of natural history studies, small sample sizes, heterogeneity within groups, difficulty discerning between disease phenotypes, and uncertainty in choosing efficacy endpoints (161). Section 2.1.1.1 discusses some of these challenges in clinical trials with lysosomal diseases, such as the phase II/III clinical trial with pabinafusp (152).

Despite the numerous challenges, developing therapies for rare diseases is a rapidly expanding field. In 2019, 44% of novel drugs approved by the FDA were to treat rare or orphan diseases (162). Rare diseases are also called orphan diseases because they have traditionally been neglected in drug development (163). Orphan drugs are drugs that are used to treat rare diseases. An orphan designation is given to drugs if it meets one of the three criteria: 1) The condition affects less than 200,000 people in the United States; 2) If the drug is a vaccine, diagnostic drug, or preventive drug, less than 200,000 people in the United States per year will be administered the drug; 3) the condition affects more than 200,000 people in the United States, but the sales of the drug cannot reasonably be expected to cover the cost of R&D (164).

Orphan drug development is a growing field because of the financial incentives to pharmaceutical companies. The Orphan Drug Act of 1983 introduced financial incentives to pharmaceutical companies to offset the risk of drug development in rare diseases. If the FDA designates a drug as an orphan product, the company receives the following benefits: a tax credit for 25% of qualified clinical trial costs, waived fees under the Prescription Drug User Fee Act (PDUFA), and market exclusivity for seven years following FDA approval (161). The reduced costs allow small biotech companies to compete with big pharmaceutical companies. For example, the PDUFA fee may be insignificant to a large pharmaceutical company, but this fee may be substantial to a smaller biotech company. By waiving the PDUFA fee, an orphan drug allows smaller biotech companies to allocate their funds elsewhere, encouraging the growth of smaller biotech companies and increasing the number of potential therapies. Unfortunately, pharmaceutical companies may also charge high prices for drugs to overcome the developmental costs.

Another incentive for developing therapies for rare diseases is that orphan drugs frequently qualify for FDA's Accelerated Approval tracks, which expedite the approval process. The Accelerated Approval program is used to approve drugs that offer a benefit over current treatments for a serious or life-threatening illness (162). Most rare diseases do not have a treatment (163). Therefore, an orphan drug may qualify for one of the Accelerated Approval programs if it is used for a rare disease that is serious or life-threatening.

The advantage of being the first to market is another incentive for therapy development in rare diseases. The advantage of a therapy being first to market is particularly pronounced in rare diseases. If there are only 100 people with the disease and 30 people are on an existing treatment, this leaves only 70 people that can enroll in a clinical trial. This does not take into account the strict exclusion criteria in clinical trials. There is even an advantage of being the first clinical trial in a disease, because a common exclusion criterion in clinical trials is if participants are enrolled in another clinical trial for an investigational therapy.

2.3 Review of Delivery of Therapies into the CNS: Challenges and Progress

This section will review strategies that are being investigated to deliver therapies into the CNS, focusing on biological therapies. Delivery into the CNS is a common challenge for therapies but is particularly difficult for biological therapies due to their polarity and large size compared to small molecule drugs. This section will begin with background information on the structure of the BBB to provide context on the challenges of delivering therapies into the CNS. Then this section will discuss the strategies used by molecules to enter the CNS, emphasizing adsorptive transport and receptor-mediated transport, given their use in biological therapies.

2.3.1 Structure of the Blood-Brain Barrier and Challenges to Therapeutic Delivery

The BBB's structure protects the CNS from xenobiotics and endogenous neurotoxic substances but presents a critical challenge when delivering therapies into the CNS (165). The first barrier is comprised of endothelial cells that line the lumen of brain capillaries (166). These endothelial cells have tight junctions, which restrict the paracellular transport of molecules, such as proteins (166, 167). Additionally, these endothelial cells exhibit polarization (166, 167). That is, the luminal and abluminal surfaces of endothelial cells have different expressions of transporters, receptors, and lipid composition (166, 167). The luminal surface is the side of the endothelial cell that is facing the blood, and the abluminal surface is the side that is facing the CNS (166, 167). If an endothelial cell expresses a transporter or receptor on its luminal surface but not the abluminal surface, the molecule does not transcytose, remains inside the endothelial cell and cannot reach the target cells such as neurons.

Another challenge is the presence of efflux transporters on endothelial cells. Endothelial cells can express an efflux transporter on the luminal, abluminal, or both surfaces. An efflux transporter expressed on the luminal surface can decrease the intracellular concentration of a molecule low enough to prevent transport across the abluminal surface. A well-known example of an efflux transporter is the p-glycoprotein, which is expressed on the luminal surface and pumps multiple lipophilic drugs into the lumen (165). The transporter p-glycoprotein 1 prevents the SRT eliglustat from crossing the BBB (154).

The endothelial cells' abluminal surface and a discontinuous layer of pericytes are enclosed by and are a part of a basal laminal layer (165). The close endfoot of astrocytes contributes to the neurovascular unit (165). The pericytes and astrocytes regulate the function and maintenance of the BBB (165). Neurons and microglia, which are both located relatively further away from the endothelial cells than the pericytes and astrocytes, also aid in the function and maintenance of the BBB (165).

If the target is a specific cell type in the CNS, e.g., neuron, there is the additional challenge of the enzyme of interest needing to be taken up intracellularly again. This is particularly challenging because the enzyme's mechanism of transport must be 1) non-specific enough to facilitate entry into two different cell types (e.g., endothelial cells and neurons) but 2) specific enough to limit entry into other cells present in the CNS (e.g., pericytes, astrocytes, microglia).

2.3.2 Transport Systems into the CNS

There are four transport systems into the CNS: passive diffusion, carrier-mediated transport, adsorptive transport, and receptor-mediated transport. Each of these transport systems and their feasibility in delivering biological therapies will be discussed below.

2.3.2.1 Passive Diffusion

One mechanism by which molecules can enter the CNS is through passive diffusion. In passive diffusion, molecules cross the lipid bilayer of cell membranes to travel down their concentration gradient. Transport into the CNS is limited by cerebral blood flow (168). A molecule's ability to utilize passive diffusion is dictated by its physiochemical properties. Molecules with octanol/water partition coefficients between 10:1 and 100:1, less than six hydrogen bonds, and molecular weights of less than 450 Da have a greater chance of entering the CNS (165, 166). Passive diffusion is utilized by water and gases such as O_2 and CO_2 (168). This mechanism is also utilized by lipophilic drugs such as ethanol, nicotine, and benzodiazepines (168). However, passive diffusion is challenging for biological therapies, because biological therapies typically have a polar nature and a high molecular mass.

2.3.2.2 Carrier-Mediated Transport

Small, polar molecules can enter the CNS if a transporter is present on the luminal and abluminal surfaces of endothelial cells. Molecules are transported across the cell membrane through their transporter. Carrier-mediated transport is utilized by glucose, amino acids, and small peptides (165). This mechanism has been investigated in ketoprofen by conjugating it to L-tyrosine, which can be transported by the LAT1 transporter (169). However, carrier-mediated transport is challenging for large biological therapies, because transporters are stereo- and size-selective (170).

2.3.2.3 Adsorptive Transport

In adsorptive transport, the enzyme of interest first induces endocytosis either through a net positive charge or a glycoprotein-glycoprotein interaction on

endothelial cells (166). Endocytosis may be mediated by clathrin, caveolin, or neither molecule (171). Adsorptive transport is utilized by cationized albumin, histones, and some viral pathogens (167). For example, the human immunodeficiency virus type 1 utilizes a transactivator of transcription (Tat) protein to induce adsorptive endocytosis (167). While Tat and other cell-penetrating peptides are the most common examples of molecules utilizing adsorptive endocytosis, cell-penetrating peptides can gain entry into cells through other mechanisms such as direct translocation (171).

One disadvantage of adsorptive transport is the unpredictability of intracellular vesicle trafficking (166). After endocytosis, the vesicle containing the enzyme becomes an early endosome, and this early endosome can be directed to various destinations (167). If there is exocytosis at the abluminal surface of the endothelial cells, the enzyme successfully enters the CNS (167). However, another possibility is that the early endosome is recycled back to the luminal surface, preventing the enzyme's transcytosis (167). Another possibility is the early endosome maturing into a late endosome, which can transfer the enzyme to a lysosome (167). Other limitations of cell-penetrating peptides include instability, immunogenicity, cellular toxicity, and low organ specificity (171).

Some studies have investigated the adsorptive transport of lysosomal enzymes into the CNS. The most common method is to conjugate the lysosomal enzyme to a cell-penetrating peptide. A study by Schwarze et al. examined organ uptake of a β-galactosidase enzyme that contained 11 amino acids from the protein transduction domain from the Tat protein (172). Mice were intraperitoneally injected with either the Tat-β-galactosidase or the control β-galactosidase, and an X-Gal staining was performed on the brain (172). Mice that were treated with the Tat-β-galactosidase showed greater staining on mid-hemispheric sagittal brain sections at four hours post dose and on coronal brain sections at eight hours post dose (172). These results suggest that Tat can enhance the uptake of β-galactosidase into the brain, at least short-term. The authors also reported "no signs of gross neurological problems or systemic

distress” when Tat-β-galactosidase was administered once daily for 14 days (172). A longer assessment of safety or efficacy was not reported.

2.3.2.4 Receptor-Mediated Transport

In receptor-mediated transport, the enzyme of interest is attached to a molecule that binds to the receptor of interest. Either a ligand or an antibody can be used to bind to the receptor of interest. Receptor-mediated transport differs from carrier-mediated transport in that receptor-mediated transport triggers endocytosis. After endocytosis, intracellular trafficking of vesicles occurs, similar to adsorptive transport. Receptor-mediated transport is utilized by endogenous substances such as transferrin, insulin, and lipoproteins (167).

Receptor-mediated transport has been investigated in several lysosomal enzymes. Pabinafusp, an idursulfase enzyme conjugated to a ligand for the transferrin receptor, is an ERT for MPS II approved in Japan (152). Valanafusp alpha, also called AGT-181, is an iduronidase enzyme conjugated to an antibody for the human insulin receptor (146). Valanfusp is currently in clinical trials for MPS I (146). The clinical trials for pabinafusp and valanafusp were discussed in Section 2.1.1.1.

One disadvantage of receptor-mediated transport is that the uptake of enzyme into cells is limited by the number of available receptors. Therefore, the target receptor should be highly expressed on the surface of cells. Another disadvantage of receptor-mediated transport is the unpredictability of intracellular vesicle trafficking after endocytosis.

2.3.2.5 Direct Administration into the CNS

Direct administration into the CNS allows the therapy to bypass the BBB. These routes include intraparenchymal, intracerebroventricular, and intrathecal. The intranasal route of delivery is also discussed, because it bypasses the BBB.

In the intraparenchymal route, therapy is directly injected into the brain tissue (173). The therapy remains within the injected area of the brain. This is advantageous for neurodegenerative diseases where the affected brain region is localized, such as Parkinson's disease (173). As such, studies in Parkinson's disease have administered gene therapy using the intraparenchymal route (173). However, this is problematic for lysosomal disease and other diseases in which multiple brain areas are affected. Neurodegenerative diseases with diffuse brain involvement require multiple burr holes and injection sites (173). The intraparenchymal route is highly invasive and poses a significant safety risk.

In the intracerebroventricular route, therapy is injected into the lateral ventricle through a catheter or reservoir (174). The therapy travels within the CSF to reach the ventricles. One advantage of intracerebroventricular route is that the therapy can reach multiple regions of the brain (175). One disadvantage of the intracerebroventricular route is that therapies are removed with the CSF, and the CSF can turn over 140 times a day (176). Cerliponase alfa, an ERT for the lysosomal disease neuronal ceroid lipofuscinosis type 2, is delivered intracerebroventricularly (175).

In the intrathecal route, therapy is injected into the lumbar spine (lumbar) or subarachnoid space at the cisterna magna (cisternal) (174). The therapy travels within the CSF to reach the ventricles. Similar to the intracerebroventricular route, therapy delivery to the brain is more widespread (173). One advantage of lumbar intrathecal delivery is that it is a more common route in clinical practice. For example, lumbar intrathecal delivery of baclofen is used to alleviate pain and spasticity (177, 178). Similar to the

intracerebroventricular route, intrathecal delivery has the disadvantage of a high turnover rate of the CSF (176).

In general, the advantages of direct administration into the CNS are that it employs a local route of administration. Compared to a systemic administration, there is a lower chance of adverse effects, and a lower dose is needed to achieve a therapeutic effect. The lower dose is a compelling advantage for biological therapies with complex manufacturing and high costs. The primary disadvantage of direct administration into the CNS is the safety risk (51). Furthermore, direct administration into the CNS may limit the therapy from reaching therapeutic levels in organs not in the CNS. This may limit the clinical benefit on multi-systemic diseases. Cerliponase alfa, is an intracerebroventricular ERT for neuronal ceroid lipofuscinosis type 2, a lysosomal disease with extensive clinical manifestations in the CNS (175). It is not yet known whether cerliponase alfa has benefits on the non-CNS organs in clinical practice settings.

Intranasal delivery is not a direct CNS administration but does allow drugs to bypass the BBB. Therapies can bypass the BBB using olfactory sensory neurons. Intracellular transport within olfactory sensory neurons allows therapies to travel from the epithelium and into the CSF in the subarachnoid space (179). Anti-seizure medications have been reformulated for an intranasal route of delivery (179). These medications include diazepam (Valtoco®) and midazolam (Nayzilam®) (180, 181). Additionally, intranasal delivery of a biological therapy, insulin (Afrezza®), is FDA-approved for type 1 and type 2 diabetes (182). Intranasal delivery of adeno-associated virus serotype 9 (AAV9) gene therapy for MPS I has also been investigated (183). The advantage of intranasal delivery is that it is considerably safer than direct administration into the CNS. The disadvantages of intranasal delivery are the requirements for a high concentration of therapies and a drug delivery device that enhances drug disposition in the olfactory area of the nose (184). Another disadvantage is that the amount of therapy reaching its target site can vary depending on anatomical differences and mucosal health (184).

2.4 Pharmacokinetics/Pharmacodynamics and Biological Therapies for Lysosomal Diseases

In this section, I will first discuss an alternative strategy that has been investigated in a lysosomal enzyme to increase its uptake into organs (185-187). This mechanism was supported by reports of “half-life,” a familiar term in pharmacokinetics. The use of other pharmacokinetic terms from the perspectives of lysosomal disease/gene therapy fields will be discussed. Then, the pharmacokinetic (PK) and pharmacodynamic (PD) approaches for biological therapies in lysosomal diseases will be described. This section collectively describes a gap between the fields of lysosomal diseases/gene therapy and pharmacokinetics/pharmacodynamics.

2.4.1 Importance of Enzyme Activity Levels in Lysosomal Diseases

Seminal studies by the Sly group suggested that a lysosomal enzyme with a longer “half-life” in the plasma can increase its uptake into the CNS (185). These studies were conducted with β-glucuronidase, the enzyme deficient in MPS VII, also called Sly syndrome. In the original study, a chemically modified β-glucuronidase with a longer “half-life” caused lower storage levels in the brain of MPS VII mice than the native enzyme (185). In this and other studies, $t_{1/2}$ was estimated using the activity levels of enzymes, not physical levels of enzymes (185-187). Other studies from the Sly group suggested that prolonging enzyme activity levels in the plasma could increase uptake into organs (185-187). In these studies, mice with MPS VII were infused or injected with β-glucuronidase in the enzyme form, not as gene therapy (185-187). Most graphs of time-enzyme activity levels had different slopes that would have corresponded to different $t_{1/2}$ of activities (185-187). However, it is unclear how $t_{1/2}$ were calculated using

enzyme activity levels, because there was no mention of conversion factors, equations, or PK software programs (185-187). One possibility is that the $t_{1/2}$ of activities may have been estimated directly from the graphs by determining the time the activity decreases by 50%. However, the $t_{1/2}$ of activities did not always reflect the graphs, and, in some cases, $t_{1/2}$ of activities were reported when the activity had not yet decreased by 50% (185-187); these may be due to changes in the graph's formatting during the publication process. Therefore, clearer methods are needed to characterize the $t_{1/2}$ of enzyme activity. One study also reports an area under the curve (AUC) using enzyme activity, but it does not describe the calculation (187). The unit of time for the AUC was reported in the denominator, that is, (unit of enzyme activity)/(time) (187). This error may reflect how time is expressed differently between lysosomal diseases and pharmacokinetics. The unit for enzyme activity has time in the denominator, such as nmol/hr/mL. However, because AUC is an integration over time, the AUC should be reported as (unit of enzyme activity)*(time). For example, (nmol/hr/mL)*(hr), where the time for the enzyme activity is in the denominator but the time for the AUC is in the numerator.

Another noteworthy study is from the Hackett group, one of the discoverers of the Sleeping Beauty transposon system, which revolutionized non-viral vectors for gene therapy (188). In one study, $t_{1/2}$ was calculated using enzyme activity levels from the Sleeping Beauty gene therapy system (188). Enzyme activities were measured in the plasma at multiple timepoints up to one year, and copies of transgenes in the liver were measured at one year (188). The $t_{1/2}$ of enzyme activity in the plasma were reported, but the method was unclear (188). There are no conversion factors, equations, or reference to a PK program, and the $t_{1/2}$ was reported when a 50% decrease in activity was not seen in graphs (188). Yet, one remarkable contribution of this paper was a mechanistic time profile that depicts a biphasic pattern (188). The authors suggested that the first decline in plasma enzyme activity, "initial decay" (reported as $t_{1/2}$ of activity

approximately 1 to 2 days), will occur within one week of administering gene therapy. The “initial decay” was proposed to be associated with silencing of the CAGG promoter in female mice (188, 189). Although promoter silencing in CAGG can certainly attribute to this initial decline, there may be other possible factors, because this initial decline was also seen with the human α1-antitrypsin promoter that does not have gender-specific silencing (188). After “initial decay,” one of three outcomes can occur: “rapid decay,” “gradual decay,” or “stable expression” (188). A sharp decline in plasma activity, termed “rapid decay” (defined as $t_{1/2}$ of activity <3 days), was suggested to be associated with loss of plasmids and transgenes from cells due to the adaptive immune response (188). A second possibility is a slower decline of plasma activity, termed “gradual decay” (reported as $t_{1/2}$ of activity around 90 days), which was suggested to occur from low levels of transgene expression from episomes but not from integrated chromosomes (188). The third outcome was “stable expression,” i.e., no decline in plasma activity, which would occur if the transgene was integrated into chromosomes (188). However, the terms “rapid decay,” “gradual decay,” and “stable expression” could be misconstrued because these terms do not appear to describe the changes in plasma activity over time (188). Instead, $t_{1/2}$ of plasma activity appears to be calculated from categorizing mice at a fixed timepoint (188). More specifically, whether 1) their plasma activity was 1000 nmol/hr/mL at one year and 2) a combination of detectable levels of transgene, excision products, and Sleeping Beauty transposase in the liver all assessed at one year (188). This post-hoc type of calculation of $t_{1/2}$ can be helpful to differentiate between groups, but the validity of the proposed mechanisms may rely more heavily on how $t_{1/2}$ of activity was determined, which was not clearly described (188). For example, it is not clear how mouse 21 was categorized as being a hybrid of “rapid decay” and “sustained expression” (188). Also, the plasma activity of mice varied considerably over time, even log-fold fluctuations, so mice categorized as “stable expression” at week 48 may not meet that criteria the following week (188).

These studies highlight some of the challenges and benefits when the fields of lysosomal diseases and pharmacokinetics intersect. These studies are noteworthy because they contextualized $t_{1/2}$ as biological processes to shed knowledge on lysosomal enzymes and gene therapy (185-188). In one study from the Sly group, changes in AUC of activity were used to interpret the effects of mannose receptors on cellular uptake of lysosomal enzymes (187). A study from the Hackett group proposed different biological processes occurring at different phases in a time profile (188). These biological processes also importantly considered the effects of gene therapy at the DNA level (188). Furthermore, their study showed greater variations in plasma activity levels when more complex gene therapy was used, which might be anticipated with gene-editing therapies (188).

There is a gap between the fields of lysosomal diseases/gene therapy and pharmacokinetics/pharmacodynamics. One clear example is how the term “enzyme levels” is interpreted. In lysosomal diseases, enzyme levels are synonymous with enzyme activity levels. From this field’s perspective, physical levels of enzymes do not hold as much value as an enzyme’s function because an enzyme’s function is more predictive of efficacy. The previously mentioned papers that used enzyme activity to calculate $t_{1/2}$ were authored by thought leaders in their fields of lysosomal diseases or gene therapy, demonstrating the importance of pharmacodynamics in these fields (185-188). In contrast, researchers from the field of pharmacokinetics may interpret the term “enzyme levels” with respect to the dosage form, which would be physical levels of enzymes in ERT. The next section will further discuss how ERT and gene therapy studies are analyzed in the fields of PK and PD.

2.4.2 Traditional Pharmacokinetic and Pharmacodynamic Approaches to ERT and Gene Therapy in Lysosomal Diseases

In the field of pharmacokinetics, therapies are assessed with respect to the dosage form. For example, physical levels of enzymes are used to calculate PK parameters for ERT. One reason is that the calculation of PK parameters requires matching or convertible units for dose and the PK analyte. PK studies have provided important information to guide dosing in small molecules and some biological therapies. The field of PK has rigorous, standardized, reproducible methods to quantify changes in a therapy over time in the body. However, assessing *only* the physical levels of enzymes may limit the scientific and clinical relevance of a PK model in ERT. The physical levels of an enzyme can be misleading because inactive enzyme can be included in the measurements. In contrast, measuring enzyme activity assesses the enzyme's actual function. For this reason, enzyme activity is used to predict efficacy in pre-clinical studies, clinical trials, and clinical practice. Therefore, physical levels of enzymes are rarely measured in lysosomal diseases outside of PK studies.

One way to account for enzyme activity in a PK model for ERT is to convert the activity levels to physical levels of enzymes using a standard curve. In some PK studies of ERT for lysosomal diseases, enzyme activities are measured, then the enzyme activity is converted to physical levels of enzymes using a standard curve, and the physical levels of enzymes are used for PK analysis (190-192). This approach provides a conversion factor between the ERT dose and enzyme activity needed to calculate some PK parameters. However, a conversion factor calculated from one timepoint may be unreliable, because the amount of active enzyme relative to the total number of an enzyme may vary among timepoints, for example, from protein folding.

One sophisticated method to account for enzyme activity would be to create PKPD models. Notably, there are even PKPD models linking physical

levels of enzymes to clinical parameters (e.g., urinary GAG, 6MWT) for two ERTs in lysosomal diseases (191, 193). In one paper, PKPD models used direct measurements of physical levels of the enzyme with enzyme-linked immunosorbent assay (ELISA) (193). In another paper, PKPD models used physical levels of the enzyme levels that were measured indirectly (i.e., converted enzyme activity) (191). However, one limitation of PKPD studies is that they are time- and resource-intensive.

In an FDA guidance on early-phase clinical trials of cellular and gene therapy (CGT), “traditional PK study designs are generally not feasible for CGT products” in pre-clinical studies (194). A traditional pharmacokinetic approach to gene therapy would assess vector levels (DNA levels). However, there are challenges in applying traditional PK analysis in gene therapy. One major challenge is that gene therapy studies use several different units, and PK analysis requires uniform or convertible units (195). Another major challenge is that the PK processes of absorption, distribution, metabolism, and elimination are well-characterized for small molecular drugs but have yet to be adapted for biological therapies (195). Additionally, analysis of *only* the levels of the DNA levels may limit the scientific and clinical relevance of the models in gene therapy. The purpose of AAV and other vectors is to deliver the enzyme. The enzyme is the effector molecule and catalyzes the reduction of substrates. In other words, the vector is a pro-drug, and the enzyme is the active metabolite. Dose-finding studies have been able to associate the doses of gene therapy with efficacy (194). Therefore, a comprehensive model of DNA levels and enzyme levels would strengthen the impact of PKPD in gene therapy. However, these PKPD studies require extensive knowledge of pharmacometrics, gene therapy, and disease of interest. Additionally, PKPD models can be time- and resource-intensive.

There are situations when enzyme activity levels should not be used for PK or PKPD analysis of gene therapy. First, there are gene therapy studies that

assess intracellular pharmacokinetics (196). Intracellular PK studies measure DNA levels to develop mathematical models for gene expression, and these studies have advanced knowledge of vectors in gene therapy (196). Second, DNA levels of a vector provide important information in toxicology studies of gene therapy. Third, some gene therapies do not encode for an enzyme. Some gene therapies encode for proteins, such as monoclonal antibodies, or can function as a nucleic acid, such as antisense oligonucleotides. Finally, some enzymes' activities are hard to quantify reliably.

A close interplay between PK and PD is exemplified in target-mediated drug disposition (TMDD). In TMDD, a drug binds with high affinity and high selectivity to its target, and the saturation of this drug-target binding causes nonlinear pharmacokinetics (197). The conventional view of pharmacokinetics affecting pharmacodynamics is reversed in TMDD, because TMDD can be seen as pharmacodynamics affecting pharmacokinetics (197). Interestingly, TMDD was originally described in a small-molecular drug in 1994, and the importance of TMDD emerged with the growing number of biopharmaceuticals (197, 198).

2.5 Unmet Needs in Lysosomal Diseases

In this section, the unmet needs in lysosomal diseases that will be addressed by the studies in this dissertation are summarized. First, there is a need for a biomarker that can reflect the neuropathology in lysosomal diseases. Ideally, a biomarker would have a biologically plausible association with the disease(s) of interest (199). For example, a biomarker involved in neuroinflammation in lysosomal diseases. Section 1.2.3.1 details the evidence supporting neuroinflammation as a critical pathological process in lysosomal diseases. Such biomarkers could benefit the clinical care and development of future therapies through the diagnosis of disease phenotypes, monitoring of disease progression, and serving as surrogate endpoints. Different phenotypes

of a lysosomal disease cause extreme variations in the disease's progression and degree of neurological involvement. There are challenges in predicting a patient's phenotype because the mutation has not been previously reported or different studies predict different phenotypes (200, 201). Therefore, a biomarker for disease phenotypes can provide essential information on therapeutic decisions and clinical trial enrichment. After diagnosis with a disease subtype, there is still uncertainty in monitoring the progression of a disease. So knowledge of a biomarker's fluctuations over time would allow clinicians and investigators to interpret changes in the biomarker's levels. Additionally, there are several clinical trials with gene therapy in lysosomal diseases, but no known biomarker is responsive to gene therapy for lysosomal diseases. A biomarker that can predict a long-term benefit from gene therapy can accelerate approval for gene therapy by serving as a surrogate endpoint.

A second unmet need in lysosomal diseases is better therapeutic delivery to the CNS and the cardiovascular system. The pathology and clinical features in the CNS and CV disorders are discussed in Section 1.2.3 and 1.2.4, respectively. In general, uptake of biological therapies into the CNS is hindered by the presence of the BBB. The challenges in therapeutic delivery to the CNS and current strategies being investigated were discussed in Section 2.3. There is still limited knowledge on potential mechanisms to deliver biological therapies into the CNS, such as targeting other highly expressed receptors in the CNS. Additionally, improved delivery to cardiac tissues could prevent the disease progression in cardiac valves, improving the lives of patients with MPS disorders. While 60 to 90% of patients with MPS have an abnormal cardiac valve, the current therapies of HCT and ERT do not adequately treat the valves, possibly due to the poor vascularization in valves (104, 107, 109). Therefore, discovering a novel strategy to enhance the delivery of therapies into organs such as heart tissues could aid several lysosomal diseases.

The final set of unmet needs addressed in this dissertation is better approaches to characterize and compare the functionality of biological therapies for lysosomal diseases. In lysosomal diseases, there is an emphasis on pharmacodynamic outcomes such as enzyme activity. However, the methods to reliably quantify pharmacodynamic outcomes require PKPD models that are data- and resource-intensive. A method that could capture the emphasis on biological activity with the rigorous, reproducible methods of PK could facilitate translation of pre-clinical to clinical studies in gene therapies. Such a method could also provide mechanistic information of therapies that could be applied to other rare diseases.

CHAPTER 3: VALIDATION OF CHITOTRIOSIDASE AS A CNS BIOMARKER IN GANGLIOSIDOSES

The majority of lysosomal diseases cause severe neurological deficits. Validated surrogate endpoints or biomarkers are critically important to accelerate approval of therapies by more rapidly detecting efficacy than clinical outcomes. However, there are currently no surrogate endpoints or biomarkers that can predict long-term clinical benefit from gene therapy for lysosomal diseases. In a natural history study of two lysosomal diseases, GM1-gangliosidosis and GM2-gangliosidosis, chitotriosidase enzyme activity was one of the few analytes out of approximately 200 screened that appeared to relate to the most severe phenotypes of gangliosidoses (91). However, no clinical laboratories were positioned to pursue a more rigorous evaluation. Moreover, chitotriosidase has never been evaluated as a biomarker of gene therapy efficacy.

To investigate chitotriosidase levels in the CSF as a probable surrogate endpoint for clinical trials with gene therapy, the **first objective** was to validate chitotriosidase for important clinical outcomes in patients with lysosomal diseases. This article was published in Molecular Genetics and Metabolism Reports, Vol 29, Sarah Kim, Chester B. Whitley, Jeanine R. Jarnes, Chitotriosidase as a biomarker for gangliosidoses, Page No 100803, Copyright Elsevier (2021), (202).

The **second objective** was to assess chitotriosidase's ability to detect effective gene therapy in murine models of lysosomal diseases.

In this chapter, an introduction, which is from the publication, will first be presented. Then the clinical study's methods, results, discussion, and acknowledgement will be presented. Afterward, the pre-clinical study's methods, results, and discussion will be presented.

3.1 Clinical Study of Chitotriosidase as a Biomarker in Lysosomal Diseases

3.1.1 Introduction

Chitotriosidase enzyme (CHITO) (EC: 3.2.1.14) is exclusively produced by activated macrophages in humans (203-205). It is considered part of the innate immunity's response to chitin-containing pathogens (203-205). CHITO is a marker of macrophage activation and has also been explored as a marker of inflammation in a number of disease states, including some lysosomal diseases (203, 206-210). For over a decade, plasma CHITO levels have been used by clinicians as a biomarker of inflammation in a lysosomal disease, Gaucher disease, including monitoring response to therapies in patients with Gaucher disease type I (211-215).

Progressive neurodegeneration and associated neuro-inflammation are becoming increasingly recognized as important contributors towards morbidity and mortality in several lysosomal diseases, including GM1-gangliosidosis, GM2-gangliosidosis, and mucopolysaccharidoses diseases (3, 91, 98, 216-219). The relation of CHITO levels to disease burden and disease-associated inflammation, however, has not been well-characterized in the majority of lysosomal diseases.

As part of an ongoing natural history study of the gangliosidoses and mucopolysaccharidoses, nearly 200 analytes in the cerebrospinal fluid and serum from patients with GM1-gangliosidosis, GM2-gangliosidosis, and MPS were screened and the results reported by Jarnes et al. (2014) (91). In this previous work, five inflammatory mediators (ENA-78, MCP-1, MIP-1α, MIP-1β, and TNFR2) were identified to be persistently elevated in the CSF in the most severe phenotypes of the gangliosidoses (91). CHITO was not assessed in the initial screening. Subsequent work by the same researchers yielded additional, albeit preliminary data, which suggested that levels of CHITO levels were persistently elevated in the CSF in the severe phenotypes of GM1- and GM2-

gangliosidosis. This was reported at WORLD*Symposium* annual meeting, Orlando, Florida, 2019 (220).

A biomarker that reliably reflects neuroinflammation would have the potential for being a valuable tool for diagnosing disease phenotypes and assessing response to lysosomal diseases therapies. The objectives of the study reported herein were to develop a validated chitotriosidase assay in a clinical laboratory and to determine if chitotriosidase levels in the serum or CSF were related to important clinical parameters in patients with lysosomal diseases. More specifically, this study aimed to determine if chitotriosidase levels could be diagnostic for different lysosomal diseases or phenotypes, useful in monitoring for disease progression, or associated with neurocognitive impairment in patients with lysosomal diseases.

3.1.2 Methods

3.1.2.1 Participant Specimens

This study was conducted under clinical trials (NCT00668187 and NCT02030015) of the Lysosomal Disease Network (U54NS065768) which is a part of the National Institutes of Health (NIH) Rare Diseases Clinical Research Network (RDCRN). This study was conducted with IRB approval and IRB-approved consent of the patients' parents or legal guardians.

CSF specimens were collected by lumbar puncture with a 22-gauge (1.5- or 3.5-inch) Quincke spinal tap needle while the patient was under general anesthesia for MRI imaging. CSF was collected in 1 mL aliquots directly into cryovials, immediately labeled, placed on dry ice, and then transported to a laboratory for distribution or stored in a freezer at -80°C. Blood specimens were obtained concurrently by phlebotomy and taken to a laboratory for centrifugation. Serum was aliquoted, frozen on dry ice, and then transported to the laboratory for distribution or stored in a freezer at -80°C.

3.1.2.2 Chitotriosidase Activity Assay

Chitotriosidase activity assays were performed at two different labs. The original lab eventually discontinued its services for CSF specimens. At that time, the Gene Therapy and Diagnostics (GTD) Laboratory then developed its own chitotriosidase activity assay for CSF and serum specimens. Both labs used an artificial substrate for chitotriosidase and measured the fluorescent product. At the GTD Lab, I performed the chitotriosidase assay for patient specimens as described with minor modifications (221). Briefly, 5 µL of CSF or serum specimens was mixed with 100 µL of 26 µM of 4-methylumbelliferyl-β-D-N,N',N''-triacetylchitotrioside (Sigma M5639) in 0.1 M/0.2 M citrate-phosphate buffer. This mixture was incubated at 37°C for 15 minutes. To stop the reaction, 210 µL of 0.5 M glycine-NaOH buffer, pH 10.6, was added. Fluorescence was measured at 360 nm excitation and 455 nm emission using a Biotek plate reader. The lower limit of detection at the GTD Lab was 1.0 nmol/h/mL. The reference ranges for serum specimens was <80 nmol/h/mL. The reference range for CSF specimens was 5 nmol/h/mL.

3.1.2.3 Statistics

I performed statistical analysis using R and GraphPad Prism 8. To compare chitotriosidase levels reported between labs, a Pearson's correlation test was performed. To compare the independent disease profiles by showing changes in chitotriosidase levels at different ages (and therefore different times in disease progression) in the CSF between different lysosomal diseases, a one-way ANOVA type III test was performed with disease as the independent variable and chitotriosidase levels in the CSF as the dependent variable. Chitotriosidase levels in the CSF were natural log transformed, and outliers were excluded

based on a pre-determined, studentized residual cut-off of $\geq$ 2.5. Multiple comparisons were adjusted using Tukey's method. These statistical steps were repeated for CSF specimens for different disease phenotypes, serum specimens for different diseases, and serum specimens for different disease phenotypes.

To analyze the relationship between chitotriosidase levels in the CSF and serum and neuropsychological testing done in patients, neuropsychological scores from the Bayley Scales of Infant and Toddler Development®, Third Edition (Bayley-III®) were used. All CSF and serum specimens were taken within one week of neuropsychological evaluations. A multiple linear regression was calculated to predict the raw score of the cognitive domain in the Bayley-IIII test based on the disease and chitotriosidase levels in the CSF. A Pearson's correlation test was performed with natural log transformed serum chitotriosidase levels and the raw score of the cognitive domain in the Bayley-III test. Chitotriosidase levels were natural log transformed, and outliers were excluded based on a pre-determined, studentized residual cut-off of $\geq$ 2.5.

3.1.3 Results

3.1.3.1 Validation of Gene Therapy and Diagnostics Lab's Chitotriosidase Activity Assay to the Original Lab's Assay

Since two different labs performed chitotriosidase assays for patient specimens, it was possible that chitotriosidase levels could differ between labs, which could confound further analysis. Therefore, a Pearson's correlation test was performed to see if there was a correlation in chitotriosidase levels obtained between the two labs. Twenty-eight specimens were processed at both labs. Of these specimens, eight were CSF specimens and 20 were serum specimens. Chitotriosidase levels between the two labs were highly correlated (R^2=0.91 for CSF and serum specimens) (Figure 1). Levels of chitotriosidase were highly

correlated between the two labs, regardless of the specimen type (R^2=0.95 for CSF specimens, R^2=0.90 for serum specimens) (Figure 1). Therefore, chitotriosidase levels reported by the two different labs were unlikely to confound analysis.

Figure 1: Comparison of Chitotriosidase Levels Between Labs

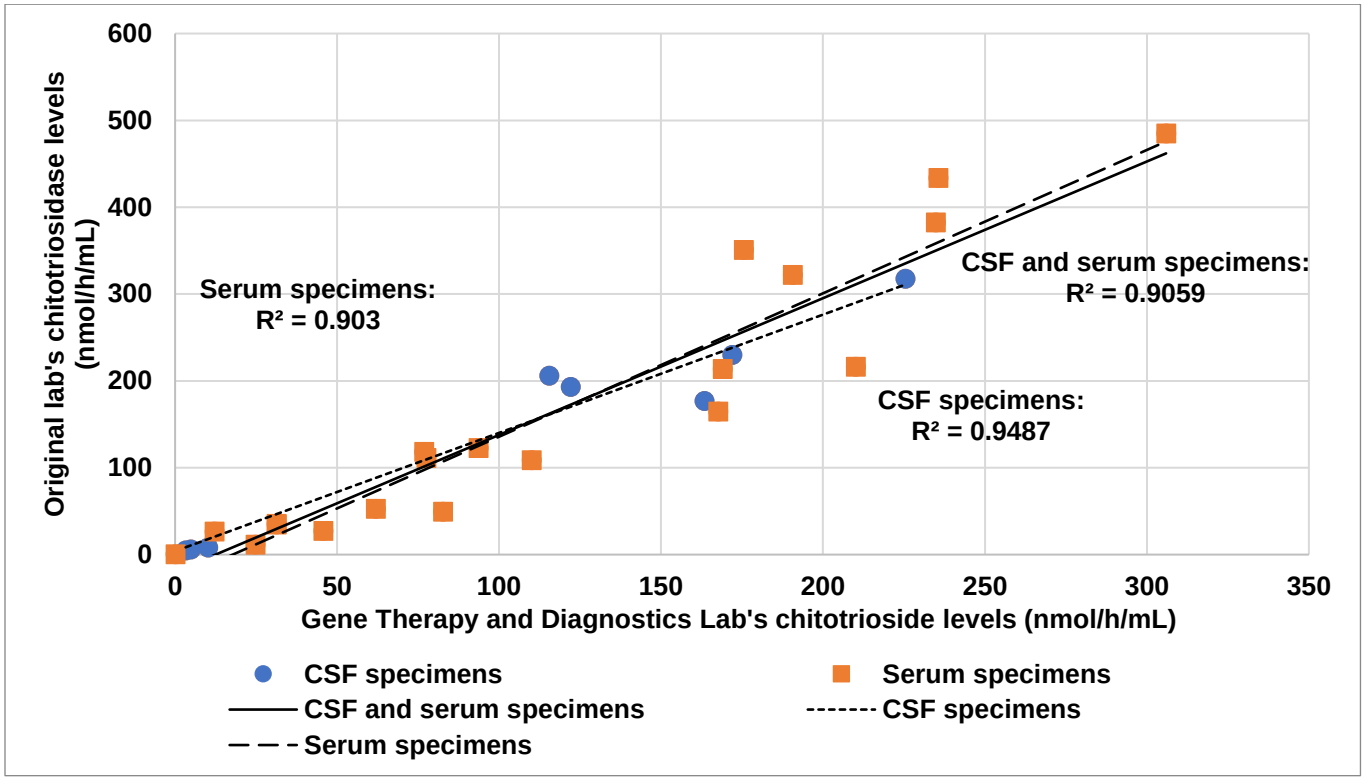

Eight cerebrospinal fluid (CSF) specimens and 20 serum specimens were assayed at both the Gene Therapy and Diagnostics Lab and the original lab. Three Pearson's correlation tests were performed to see if there was a correlation between chitotriosidase levels reported at the Gene Therapy and Diagnostics Lab and the original lab. Correlation tests were performed for serum specimens alone, CSF specimens alone, and CSF and serum specimens together.

3.1.3.2 Summary of Chitotriosidase Levels in the CSF and Serum Specimens from Patients

A total of 134 specimens from 34 patients were reported: 52 CSF specimens from 30 patients and 82 serum specimens from 33 patients. Patients with Gaucher disease, GM1-gangliosidosis, GM2-gangliosidosis, MPS, and multiple sulfatase deficiency (MSD) were included in this study.

3.1.3.3 Chitotriosidase Levels in the CSF from Patients

Patients with GM1- or GM2-gangliosidosis had higher levels of chitotriosidase and higher variations in levels than patients with Gaucher disease or MPS. To determine if there were significant differences in chitotriosidase levels in the CSF among diseases, a one-way ANOVA was performed. There was a statistically significant difference in chitotriosidase levels in the CSF between Gaucher disease and GM1-gangliosidosis ($p=0.0349$); GM1-gangliosidosis and MPS ($p<0.0001$); and GM2-gangliosidosis and MPS ($p<0.0001$).

Chitotriosidase levels in the CSF within each lysosomal disease are shown in Figure 2. In GM1-gangliosidosis, patients with infantile phenotype had increasing levels of chitotriosidase in the CSF over time (Figure 2A). One patient with late-infantile GM1 had eight sequential levels that showed a steady decrease over time, with exception of the last level (Figure 2B). CSF chitotriosidase appeared to be higher in the infantile and late-infantile phenotypes than the juvenile phenotype (Figure 2A through 2C).

In GM2-gangliosidosis, two patients with infantile Sandhoff disease had lower levels of chitotriosidase levels than patients with infantile Tay-Sachs disease (Figure 2D). Patients with infantile Tay-Sachs had higher chitotriosidase

levels in the CSF than patients with juvenile or late-onset Tay-Sachs (Figure 2D through 2F).

In patients with Gaucher disease, chitotriosidase levels decreased over time in the patient with Gaucher disease type I phenotype, which may have been a treatment effect (Figure 2G through 2H). It is unknown if these patients were receiving treatment for Gaucher disease.

In MPS, patients with MPS III type A (Sanfilippo syndrome type A, or MPS IIIA), an MPS condition associated with severe CNS disease, had higher chitotriosidase levels in the CSF than patients with MPS I Scheie, a phenotype not associated with severe CNS disease (Figure 2I through 2L). Chitotriosidase levels were similar among patients with MPS IS, attenuated MPS II, and multiple sulfatase deficiency.

To determine if there were significant differences in chitotriosidase levels in the CSF between among phenotypes, a one-way ANOVA was performed (Appendix Table 1). CSF chitotriosidase levels were significantly higher in most GM1-gangliosidosis phenotypes analyzed compared to Gaucher type I. Infantile GM1- and late-infantile GM1-gangliosidosis had significantly higher CSF chitotriosidase levels than nearly all MPS subtypes analyzed. Furthermore, infantile Tay-Sachs and juvenile Tay-Sachs had significantly higher CSF chitotriosidase levels compared to nearly all MPS subtypes analyzed. There was no significant difference between CSF chitotriosidase levels between the infantile and late-infantile GM1-gangliosidosis ($p=1$) (Appendix Table 1), between the infantile GM1- and juvenile GM1-gangliosidosis ($p=0.17$), and between the late-infantile GM1- and juvenile GM1-gangliosidosis ($p=0.19$).

Infantile Tay-Sachs had a statistically significantly higher CSF chitotriosidase levels than late-onset Tay-Sachs ($p<0.0001$). There was no significant difference between the infantile Tay-Sachs and juvenile Tay-Sachs

(p=0.16). However, juvenile Tay-Sachs had higher CSF chitotriosidase levels than late-onset Tay-Sachs, which was near statistical significance (p=0.06).

Figure 2: Chitotriosidase Levels in the CSF in Multiple Lysosomal Diseases

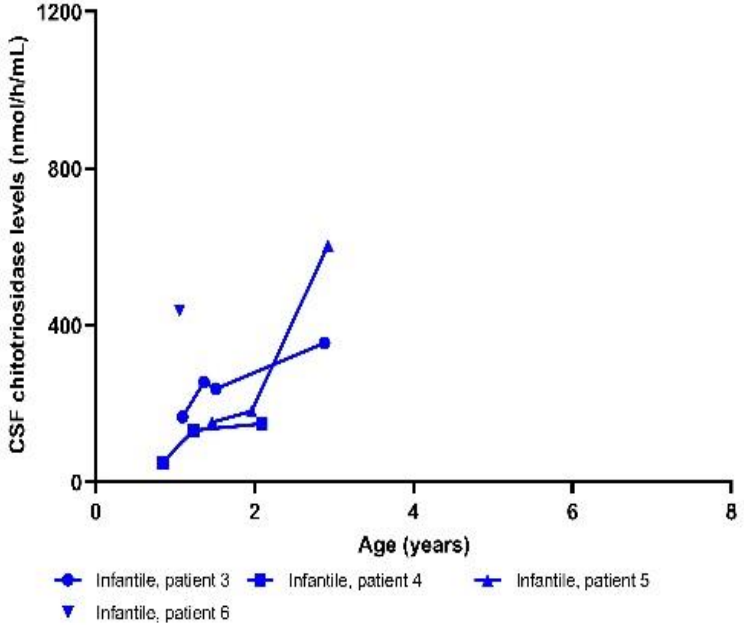

A)

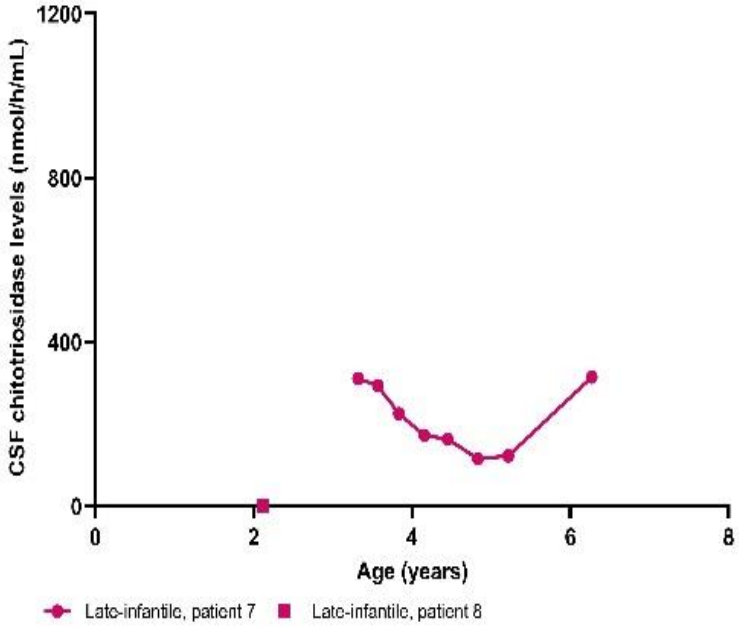

B)

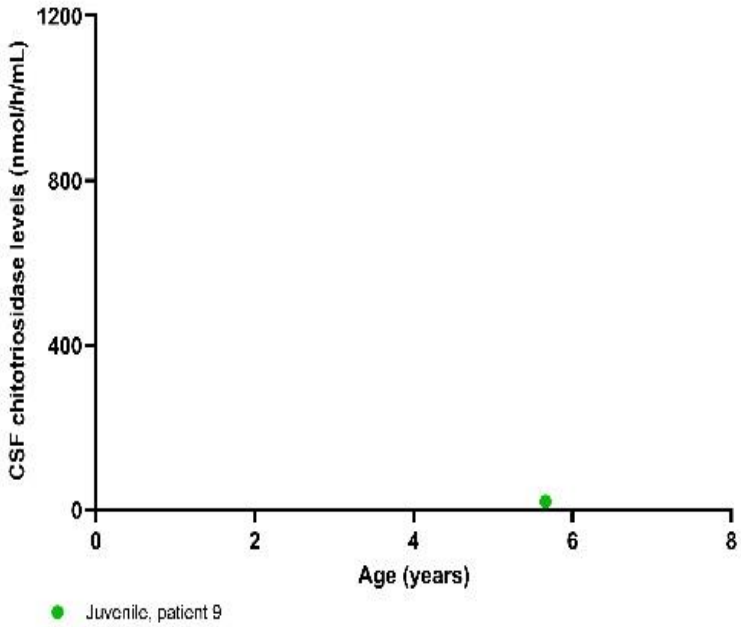
CSF chitotriosidase levels (nmol/h/mL)
1200
800
400
0
0
2
4
6
8
Age (years)
Juvenile, patient 9

C)

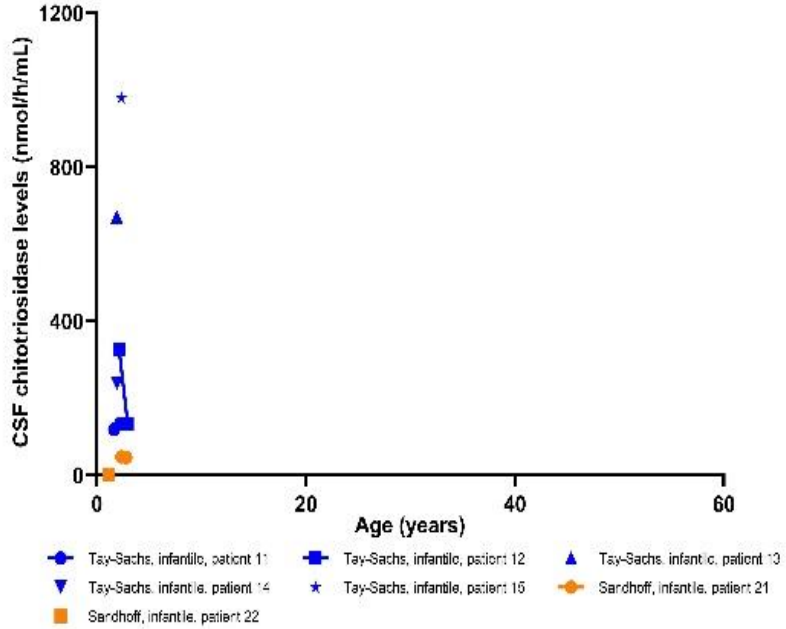
CSF chitotriosidase levels (nmol/h/mL)
1200
800
400
0
0
20
40
60
Age (years)
Tay-Sachs, infantile, patient 11
Tay-Sachs, infantile, patient 12
Tay-Sachs, infantile, patient 13
Tay-Sachs, infantile, patient 14
Tay-Sachs, infantile, patient 15
Sandhoff, infantile, patient 21
Sandhoff, infantile, patient 22

D)

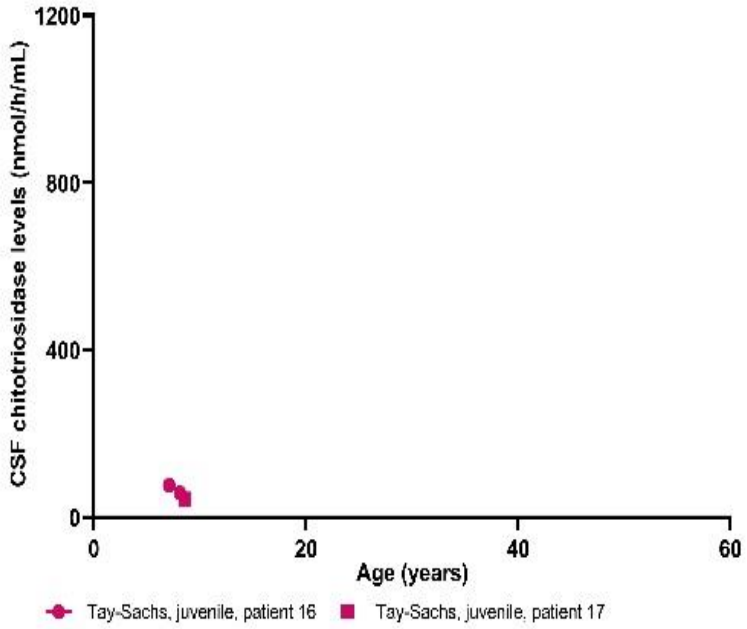
1200
800
400
0
CSF chitotriosidase levels (nmol/h/mL)
0
20
40
60
Age (years)
Tay-Sachs, juvenile, patient 16
Tay-Sachs, juvenile, patient 17

E)

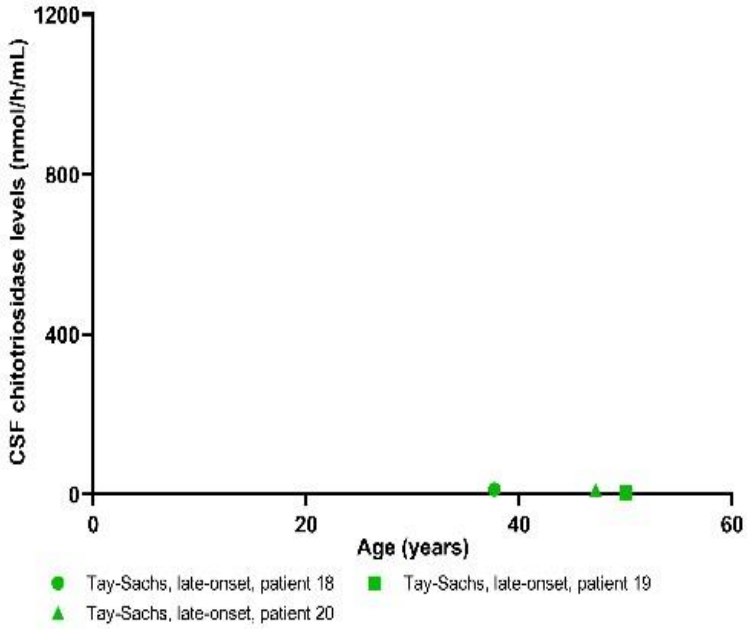
1200
800
400
0
CSF chitotriosidase levels (nmol/h/mL)
0
20
40
60
Age (years)
Tay-Sachs, late-onset, patient 18
Tay-Sachs, late-onset, patient 19
Tay-Sachs, late-onset, patient 20

F)

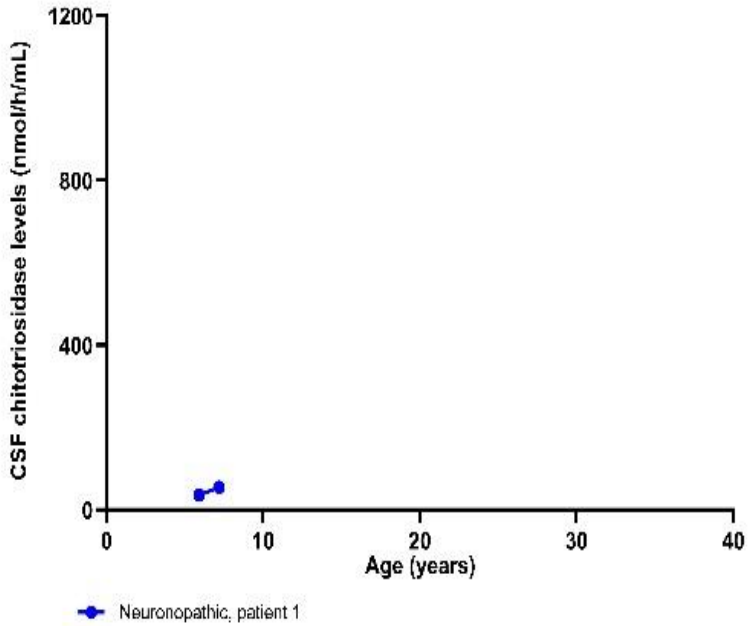
CSF chitotriosidase levels (nmol/h/mL)
1200
800
400
0
0
10
20
30
40
Age (years)
Neuronopathic, patient 1

G)

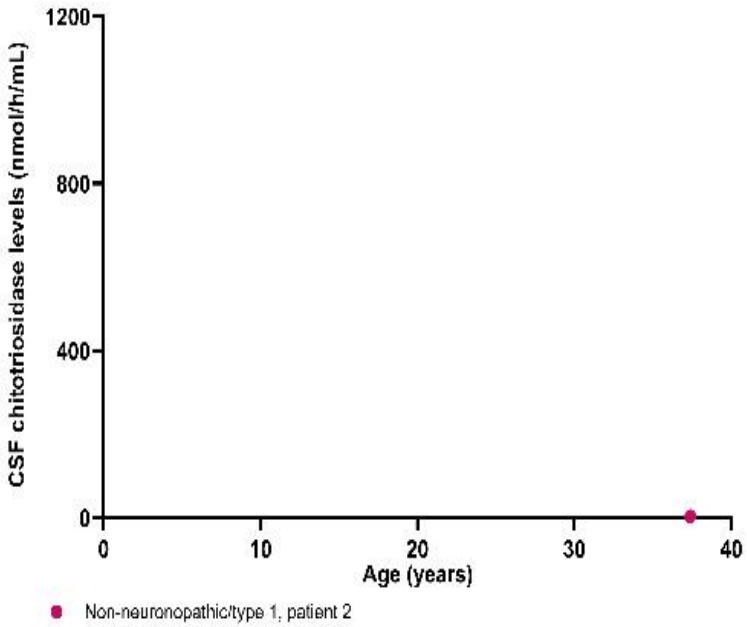
CSF chitotriosidase levels (nmol/h/mL)
1200
800
400
0
0
10
20
30
40
Age (years)
Non-neuronopathic/type 1, patient 2

H)

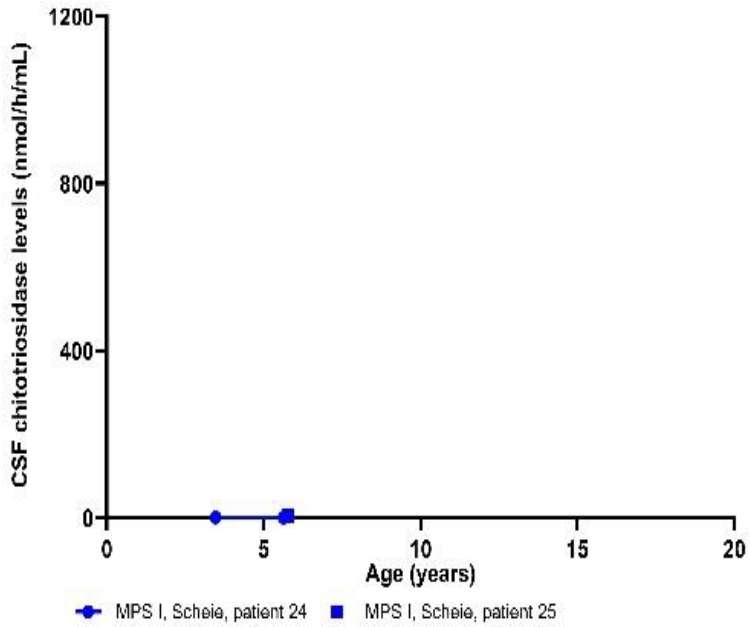
CSF chitotriosidase levels (nmol/h/mL)
1200
800
400
0
0
5
10
15
20
Age (years)
MPS I, Scheie, patient 24
MPS I, Scheie, patient 25

I)

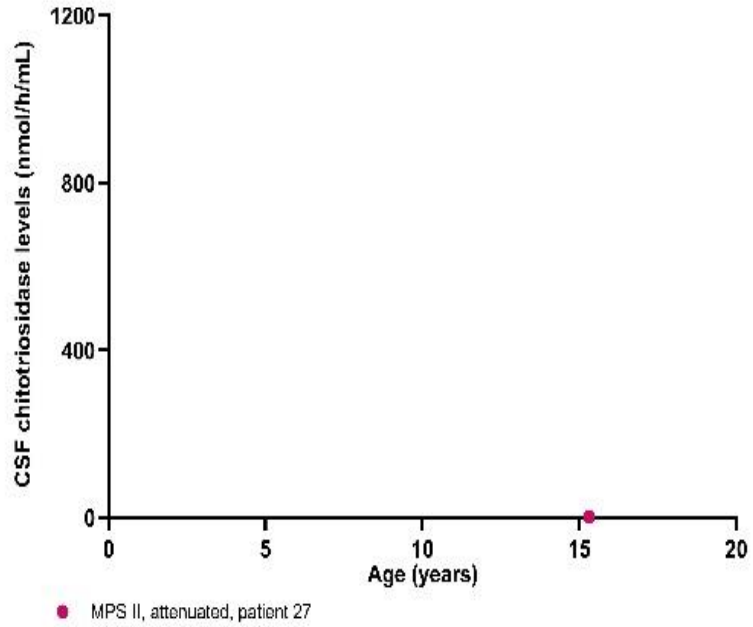
CSF chitotriosidase levels (nmol/h/mL)
1200
800
400
0
0
5
10
15
20
Age (years)
MPS II, attenuated, patient 27

J)

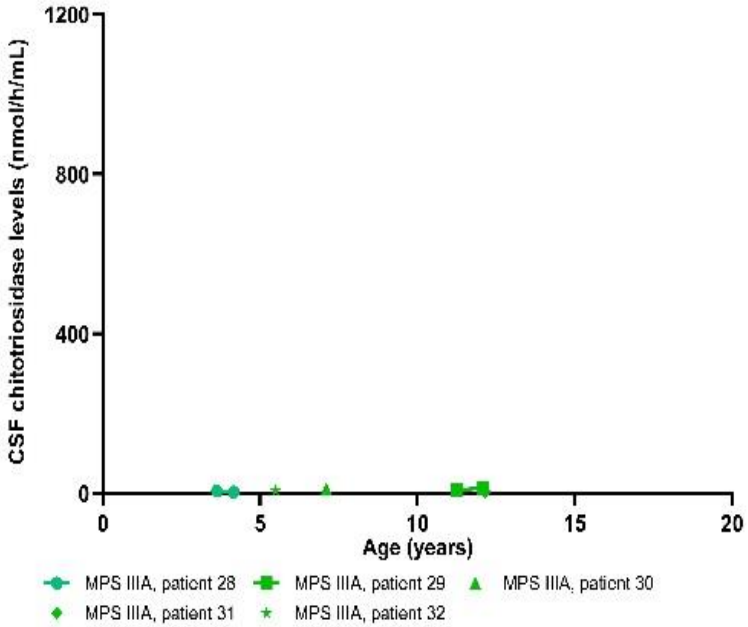

K)

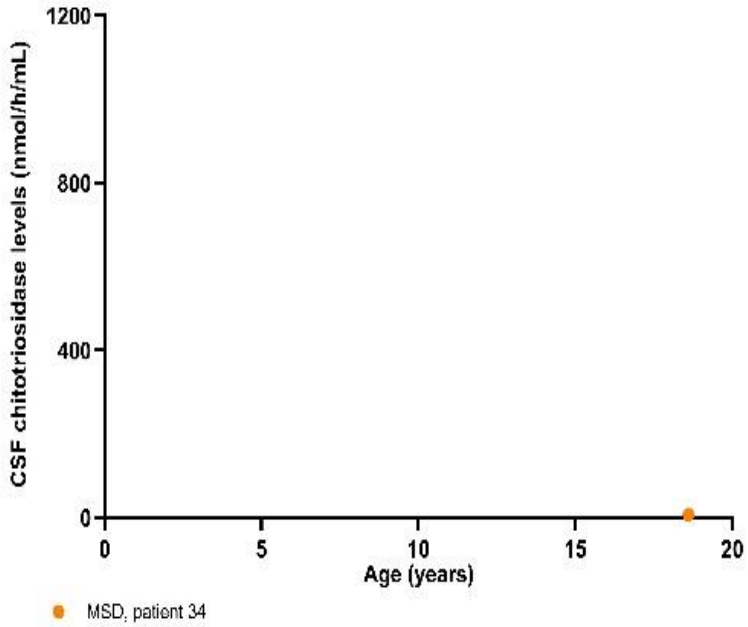

L)

Chitotriosidase levels in the cerebrospinal fluid (CSF) are shown for patients with lysosomal diseases. Sequential points from patients are connected by lines. A-C) GM1-gangliosidoses. Infantile: n=11 CSF specimens, late-infantile: n=9, juvenile: n=1. D-F) GM2-gangliosidoses. Tay-Sachs infantile: n=7 CSF specimens, Tay-Sachs juvenile: n=3, Tay-Sachs adult: n=3, and Sandhoff infantile: n=3. G-H) Gaucher disease. Non-neuronopathic/type 1: n=1 CSF specimen, neuronopathic phenotype: n=2. I-L) Mucopolysaccharidoses (MPS) and multiple sulfatase deficiency (MSD). MPS IS: n=3 CSF specimens, MPS II attenuated: n=1, MPS IIIA: n=7, and MSD: n=1.

3.1.3.4 Chitotriosidase Levels in the Serum from Patients

Patients with Gaucher disease or GM1-gangliosidosis had higher CHITO serum levels than patients with GM2-gangliosidosis or MPS. A one-way ANOVA determined a significant difference in CHITO levels in the serum among all diseases analyzed, except GM2-gangliosidosis and MPS, which was near statistical significance.

CHITO levels in the serum within each lysosomal disease group are shown in Figure 3. In GM1-gangliosidosis, chitotriosidase levels increased over time for patients with infantile and late-infantile phenotypes but remained stable for patients with the juvenile phenotype (Figure 3A through 3C). Serum chitotriosidase levels were the highest in the infantile, followed by the late-infantile, then juvenile phenotype.

In GM2-gangliosidosis, there were no apparent increases or decreases in serum CHITO over time across the GM2-gangliosidosis phenotypes (Figure 3D through 3F). Serum CHITO levels were similar among infantile Tay-Sachs, juvenile Tay-Sachs, and late-onset Tay-Sachs, suggesting that chitotriosidase levels in the serum may not reflect disease severity in Tay-Sachs.

Serum CHITO levels were elevated in patients with Gaucher disease, independent of age (Figure 3G through 3H). CHITO levels were similar between for the pediatric and adult patients, suggesting that serum CHITO is not influenced by age in Gaucher disease. The use of enzyme replacement therapy may have stabilized serum chitotriosidase levels among different age groups in Gaucher disease.

In MPS, patients with MPS IIIA had levels that increased over time, but one patient with MPS IS subtype had levels that decreased over time (Figure 3I through 3L), possibly a treatment effect. MPS IV type A (MPS IVA) had higher serum chitotriosidase levels than other MPS diseases, although more data is

needed to confirm this. Patients with MPS IIIA had slightly higher chitotriosidase levels than patients with MPS IH, MPS IS, or MPS II attenuated. There were no apparent differences between the Hurler and Scheie subtypes of MPS I.

There was a statistically significant difference in chitotriosidase levels among different phenotypes of lysosomal diseases (Appendix Table 2). Infantile GM1- and late-infantile GM1-gangliosidosis had significantly higher serum chitotriosidase levels than infantile GM2- and juvenile GM2-gangliosidosis, and most MPS subtypes analyzed. There were no significant differences between infantile Tay-Sachs or juvenile Tay-Sachs compared to the MPS subtypes.

There was no difference in serum CHITO levels among the infantile and late-infantile GM1-gangliosidosis ($p=0.97$) (Appendix Table 2), but infantile GM1-gangliosidosis had significantly higher serum CHITO levels than juvenile GM1-gangliosidosis ($p=0.03$).

Figure 3: Chitotriosidase Levels in the Serum in Multiple Lysosomal Diseases

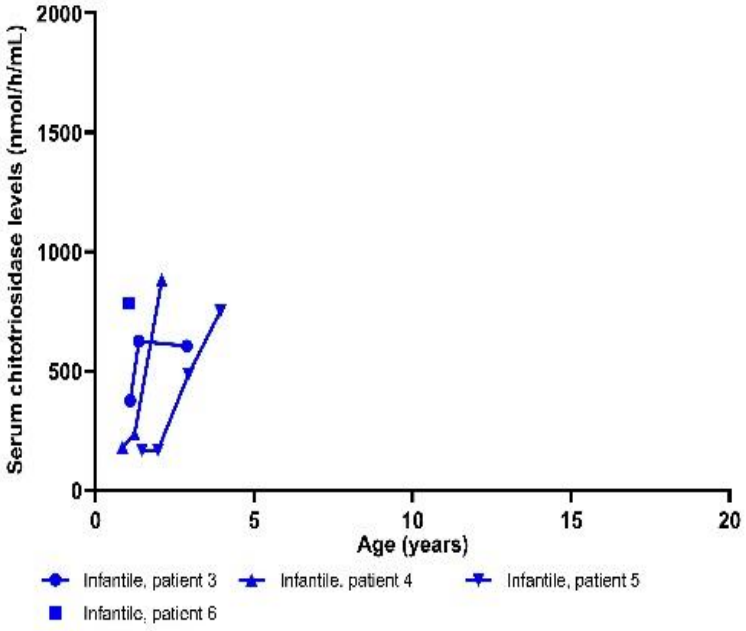

A)

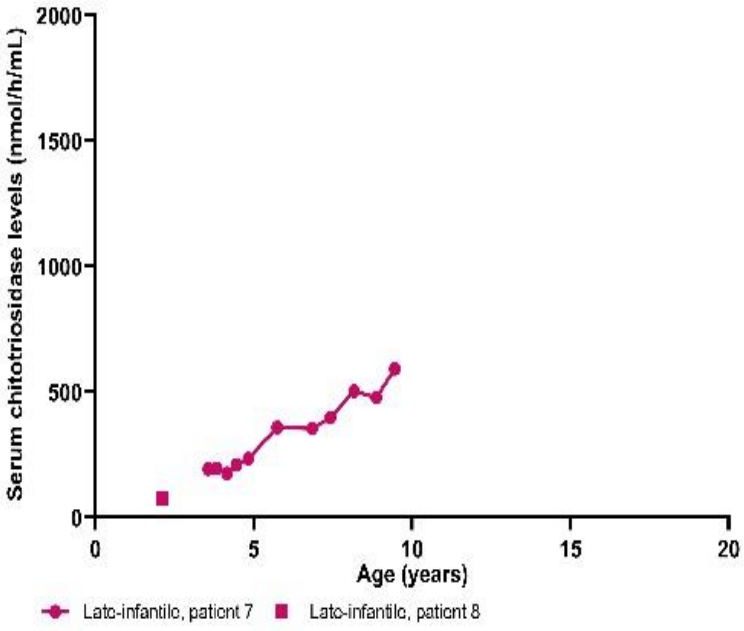

B)

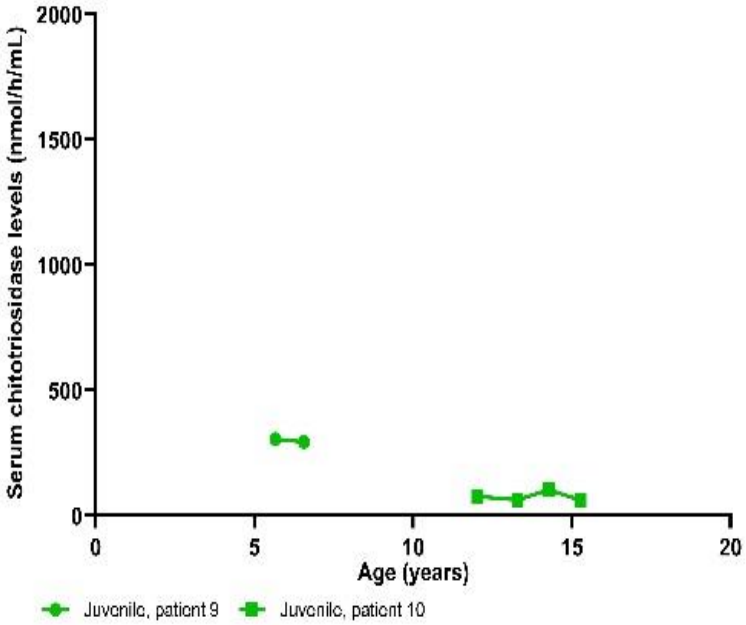
Serum chitotriosidase levels (nmol/h/mL)
2000
1500
1000
500
0
0
5
10
15
20
Age (years)
Juvenile, patient 9
Juvenile, patient 10

C)

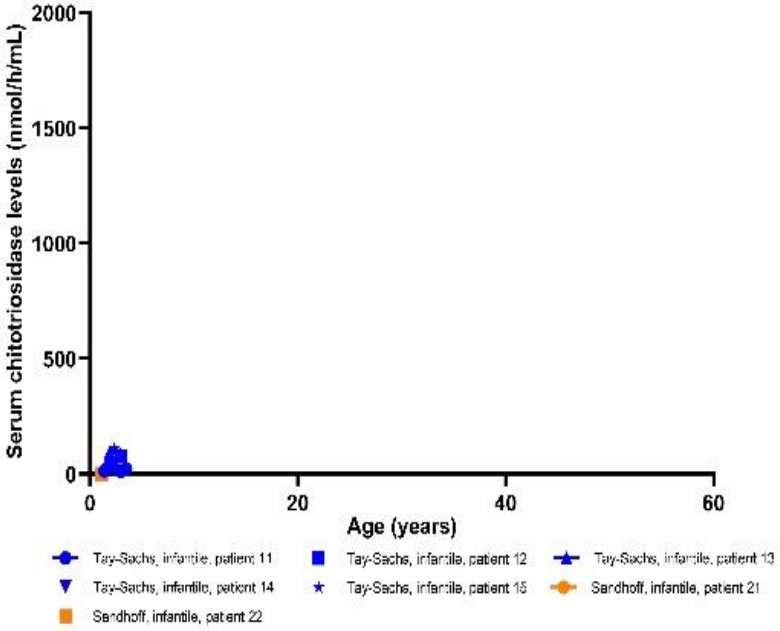
Serum chitotriosidase levels (nmol/h/mL)
2000
1500
1000
500
0
0
20
40
60
Age (years)
Tay-Sachs, infantile, patient 11
Tay-Sachs, infantile, patient 12
Tay-Sachs, infantile, patient 13
Tay-Sachs, infantile, patient 14
Tay-Sachs, infantile, patient 15
Sandhoff, infantile, patient 21
Sandhoff, infantile, patient 22

D)

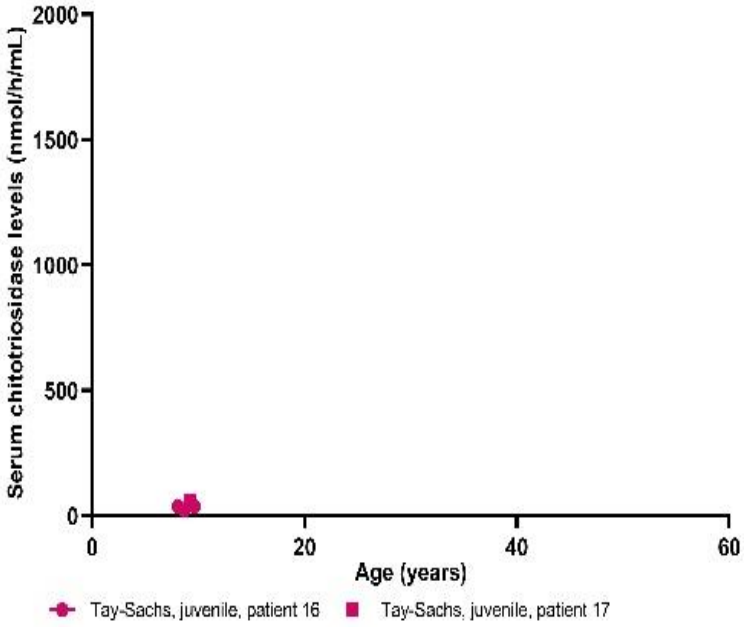
Serum chitotriosidase levels (nmol/h/mL)
2000
1500
1000
500
0
0
20
40
60
Age (years)
Tay-Sachs, juvenile, patient 16
Tay-Sachs, juvenile, patient 17

E)

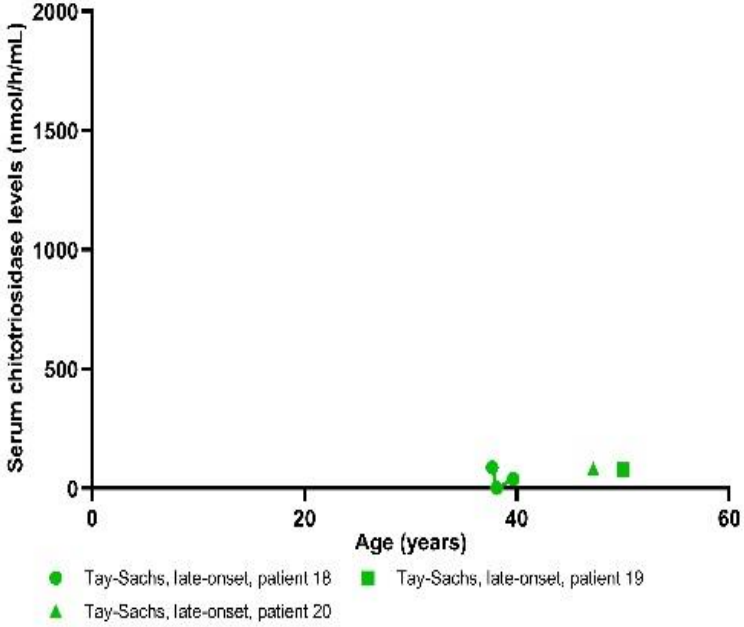
Serum chitotriosidase levels (nmol/h/mL)
2000
1500
1000
500
0
0
20
40
60
Age (years)
Tay-Sachs, late-onset, patient 18
Tay-Sachs, late-onset, patient 19
Tay-Sachs, late-onset, patient 20

F)

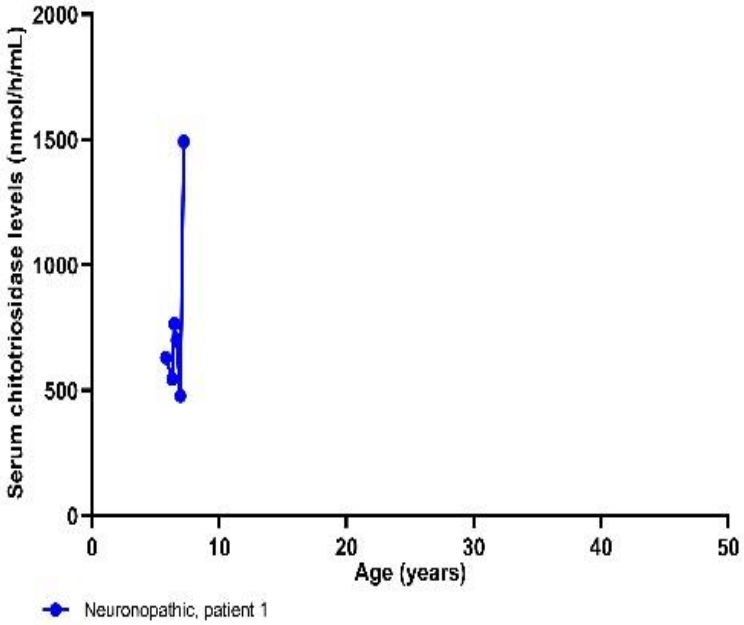
Serum chitotriosidase levels (nmol/h/mL)
2000
1500
1000
500
0
0
10
20
30
40
50
Age (years)
Neuronopathic, patient 1

G)

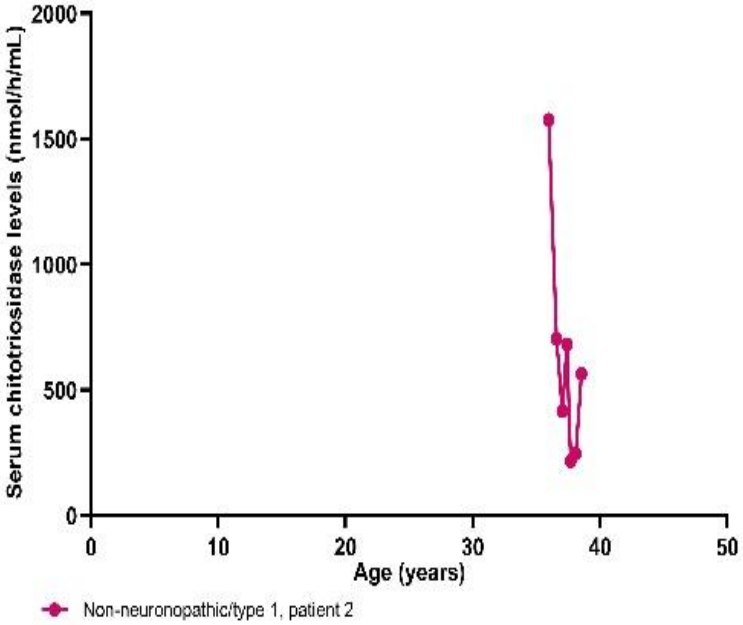
Serum chitotriosidase levels (nmol/h/mL)
2000
1500
1000
500
0
0
10
20
30
40
50
Age (years)
Non-neuronopathic/type 1, patient 2

H)

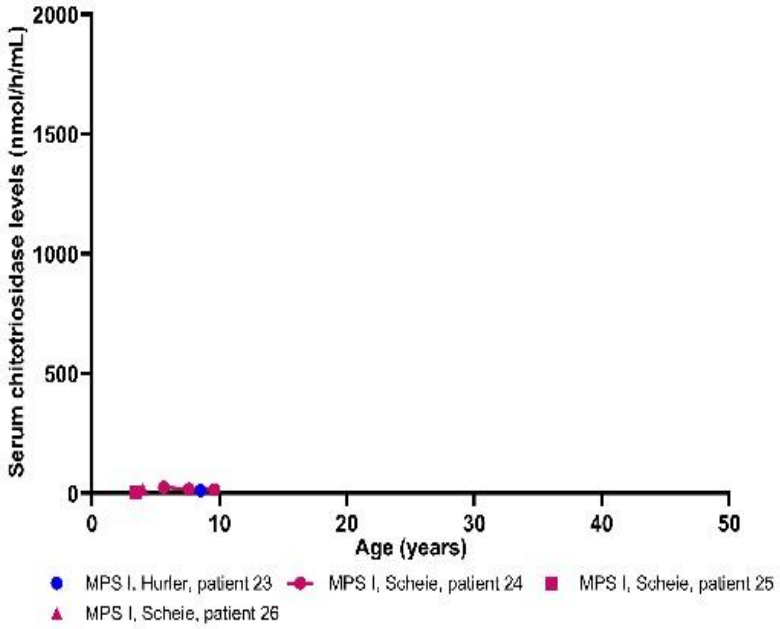
Serum chitotriosidase levels (nmol/h/mL)
2000
1500
1000
500
0
0
10
20
30
40
50
Age (years)
MPS I, Hurler, patient 23
MPS I, Scheie, patient 24
MPS I, Scheie, patient 25
MPS I, Scheie, patient 26

I)

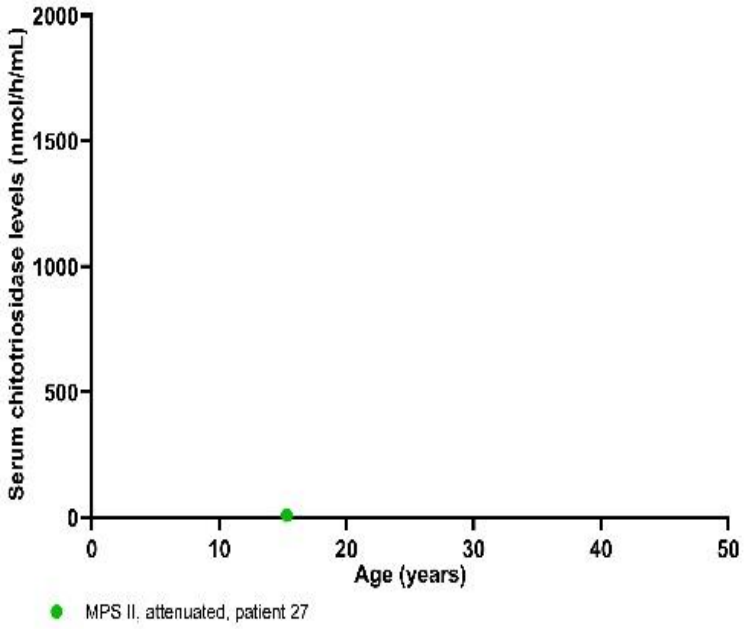
Serum chitotriosidase levels (nmol/h/mL)
2000
1500
1000
500
0
0
10
20
30
40
50
Age (years)
MPS II, attenuated, patient 27

J)

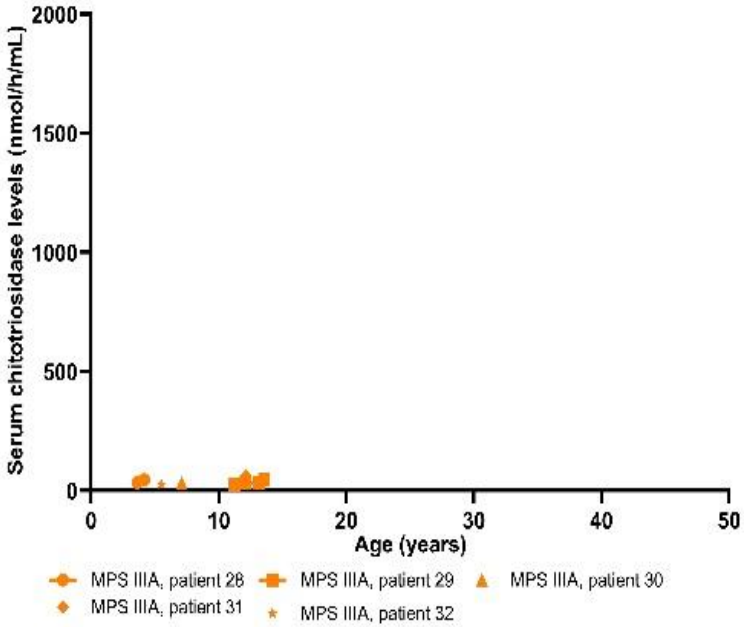

K)

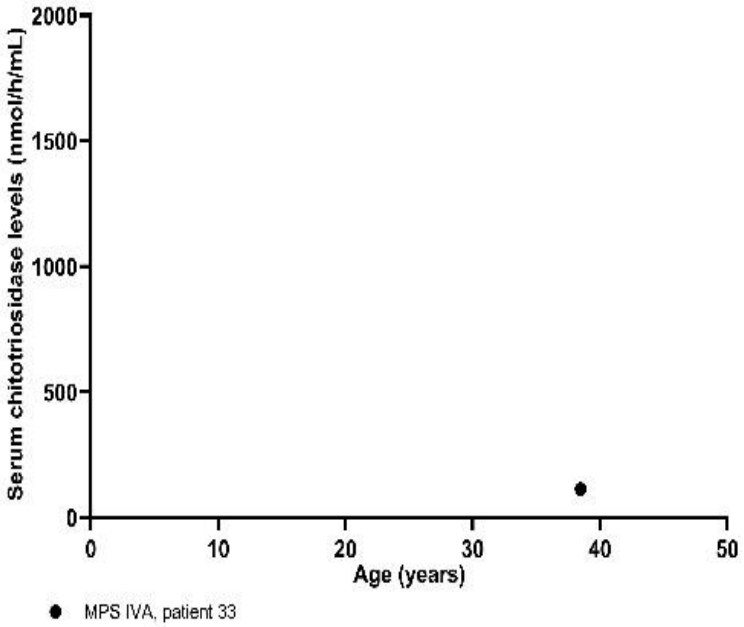

L)

Chitotriosidase levels in the serum are shown for patients with lysosomal diseases. Sequential points from patients are connected by lines. A-C) GM1-gangliosidoses. Infantile: n=11 serum specimens, late-infantile: n=12, juvenile: n=6. D-F) GM2-gangliosidoses. Tay-Sachs infantile: n=10 serum specimens, Tay-Sachs juvenile: n=4, Tay-Sachs adult: n=5, and Sandhoff infantile: n=3. G-H) Gaucher disease. Non-neuronopathic/type 1: n=7 serum specimens, neuronopathic phenotype: n=6. I-L) Mucopolysaccharidoses (MPS). MPS IH: n=1 serum specimen, MPS IS: n=5, MPS II attenuated: n=1, MPS IIIA: n=9, and MPS IVA: n=1.

3.1.3.5 Chitotriosidase Levels and Cognitive Performance in Patients

Bailey-III cognitive raw scores and age-equivalent scores were higher in patients with the lowest CHITO levels in the CSF (Figure 4). The majority of the patients with GM1- or GM2-gangliosidosis scored at the lowest possible score of age-equivalent scores, which was <16 days. Therefore, the age-equivalent scores could not capture changes in cognitive function for most patients with GM1- or GM2-gangliosidosis. Patients with different diseases were tested at different ages, making it difficult to compare them to each other. Therefore, a multiple linear regression model was created to determine if there was a significant relationship between CSF CHITO levels and the Bayley-III cognitive domain's raw score, accounting for disease. CHITO levels in the CSF were a significant predictor of Bayley-III cognitive raw scores ($p=1.12*10^{-5}$). A significant regression equation was found with an adjusted R^2 of 0.72 ($p=9.96*10^{-7}$). Bayley-III cognitive domain's raw scores were equal to 60.79-[9.92*ln(CHITO level in the CSF as nmol/h/mL)]-(7.17*disease), where disease was coded as 1 = GM1, 0 = GM2, and -1 = MPS. Moreover, every increase in the natural log of CSF CHITO levels was associated with a decrease of 9.92 in the raw scores from the Bayley-III cognitive domain, adjusting for disease.

Serum CHITO levels showed a strong association with raw scores from the Bayley-III cognitive domain for GM1-gangliosidosis but not for GM2-gangliosidosis or MPS (Figure 5). A Pearson's correlation test showed that there was a statistically significant relationship between serum CHITO levels and raw scores from the Bayley-III cognitive domain ($p=0.0002$, R^2 of 0.69).

Figure 4: Bayley Cognitive Domain and Chitotriosidase Levels in the CSF

A)

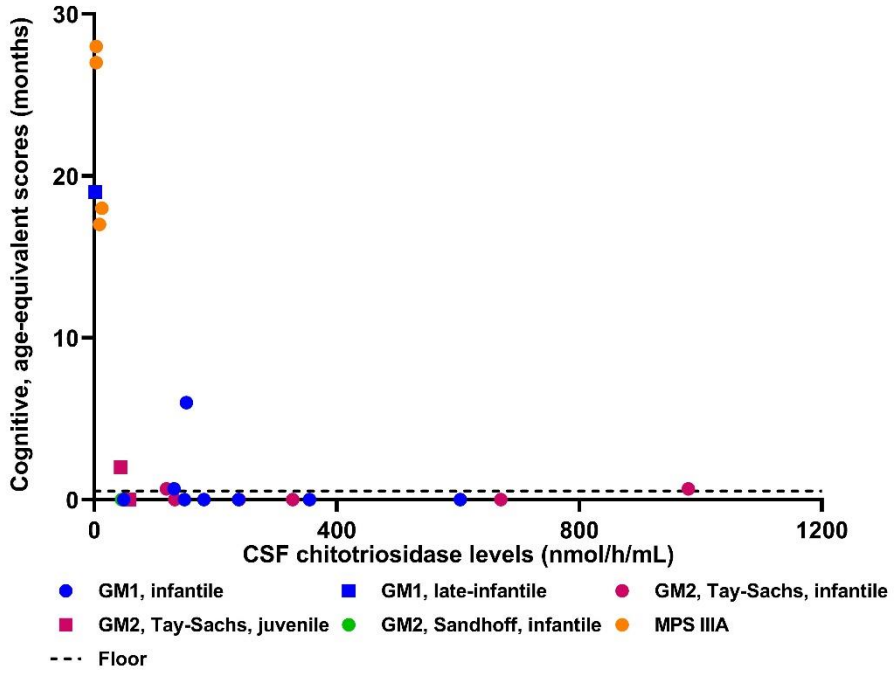

B)

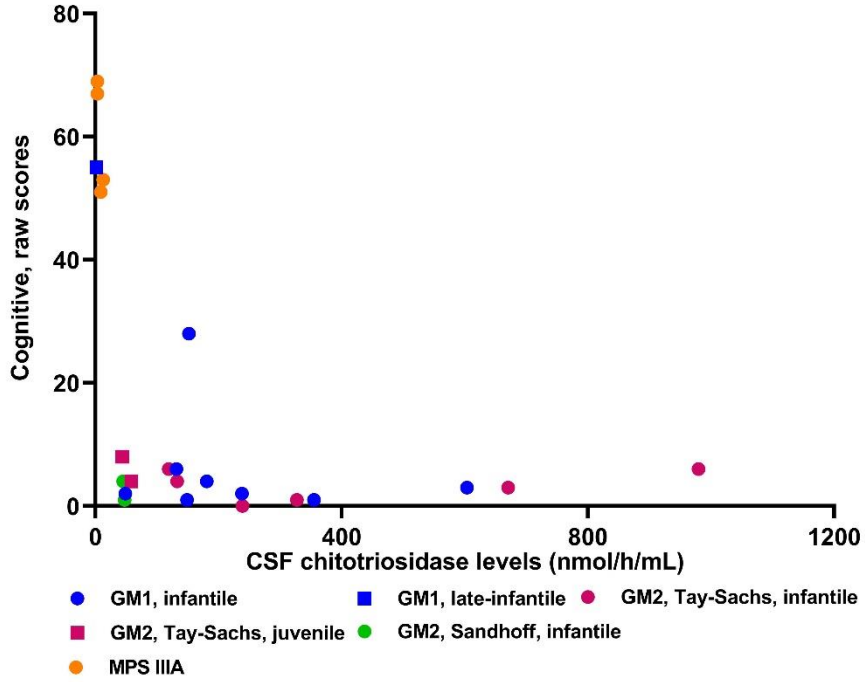

Chitotriosidase levels in the CSF were plotted against the cognitive domain in the Bayley-III test measured as either age-equivalent scores (3A) or raw scores (3B). A) The floor (dotted line) designates the lowest possible score of the age-equivalent score, which is <16 days or 0.53 month.

Figure 5: Bayley Cognitive Domain and Chitotriosidase Levels in the Serum

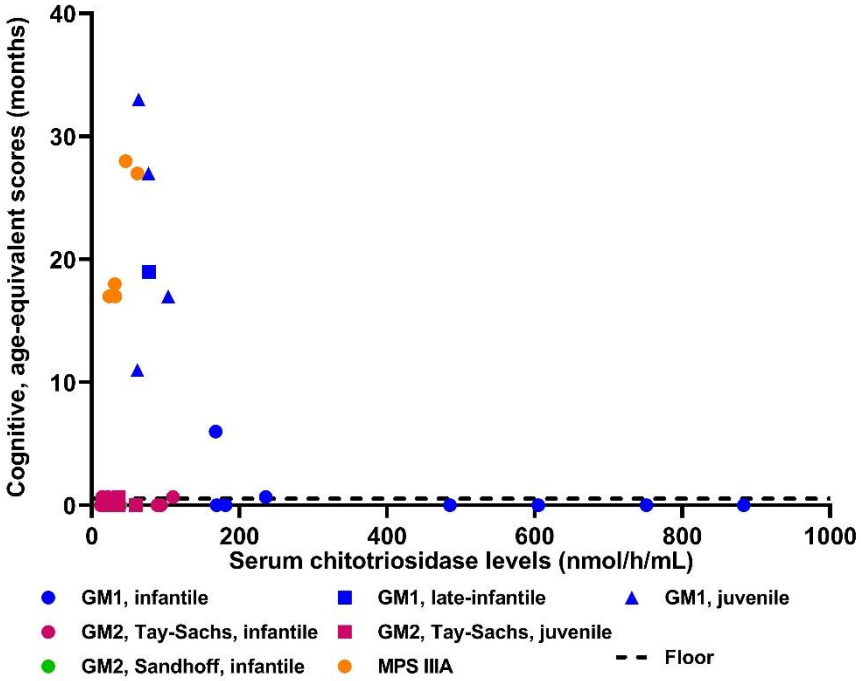

A)

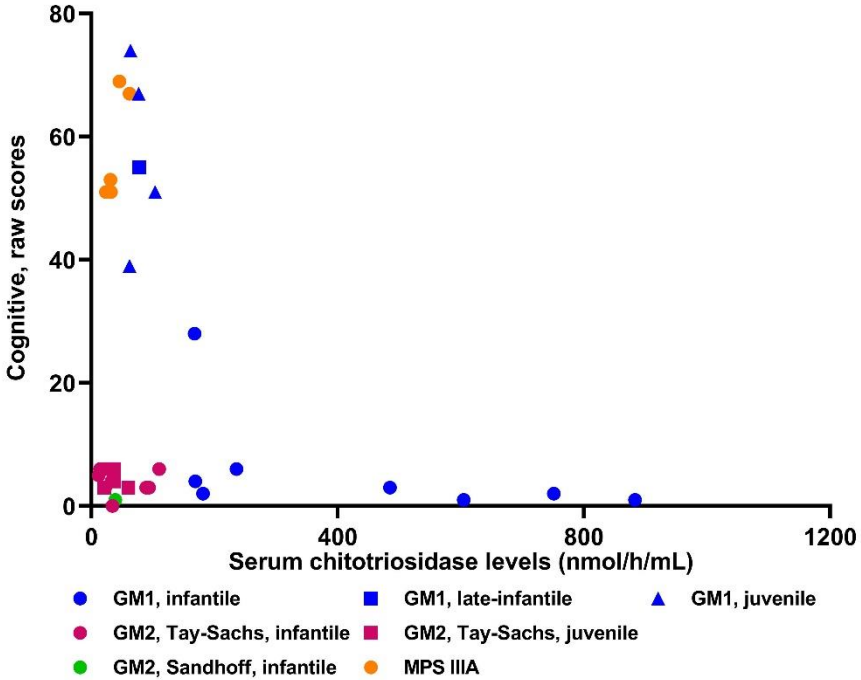

B)

Chitotriosidase levels in the serum were plotted against the cognitive domain in the Bayley-III test measured as either age-equivalent scores (4A) or raw scores (4B). A) The floor (dotted line) designates the lowest possible score of the age-equivalent score, which is <16 days or 0.53 month.

3.1.4 Discussion

This is the first study to report CHITO levels in the CSF of patients with lysosomal diseases. In this study, CSF CHITO levels were found to be elevated in several lysosomal diseases with a more rapidly progressing CNS pathology, suggesting CSF CHITO has potential as a biomarker in lysosomal diseases that affect the CNS, with important applications in the diagnosing of disease phenotypes and monitoring disease progression. Higher CHITO levels in the CSF were associated with worsened cognitive function for GM1-gangliosidosis, GM2-gangliosidosis, and MPS.

3.1.4.1 Diagnosing Disease Phenotypes

The ability to predict phenotype (e.g., infantile vs juvenile vs late-onset) is becoming increasingly important in the era of newborn screening and will be critical for making treatment decisions for newly diagnosed infants. Currently, diagnosis of phenotypes is based on onset of signs and symptoms. This poses a problem because symptoms begin after neurological damage has already occurred (3). Genotype-phenotype relationships have been helpful in predicting disease phenotypes of gangliosidoses but are not comprehensive, and there are discrepancies with some genotype-phenotype that have yet to be better understood (200, 201). In this study, average CHITO levels were higher in more severe phenotypes of GM1-gangliosidosis (infantile vs juvenile) in both CSF and serum specimens. These results are similar to a study by Arash-Kaps et al. which also saw elevated serum chitotriosidase levels in patients with the more severe phenotypes of GM1 gangliosidosis (222). CSF CHITO levels were higher in more severe phenotypes of GM2-gangliosidosis (infantile vs late-onset/adult onset). Thus, CHITO serum and CSF levels may aid in predicting gangliosidoses

disease phenotypes, and thereby help guide treatment decisions and lead to earlier treatment.

3.1.4.2 Changes in Chitotriosidase Levels Over Time

Measurement of serum CHITO levels in patients with Gaucher disease type I, is often used as an aid in determining response to therapy. In the untreated adult patient with Gaucher disease type I, CHITO levels are typically elevated, relatively stable. In contrast, CHITO levels in the blood and CSF showed marked increases over time in the severe infantile phenotype of GM1-gangliosidosis. Better understanding how a biomarker will fluctuate over time, if at all, as part of a disease natural history or assessment of response to therapy, will improve appropriate application and accurate interpretation of biomarker values.

Increases in the CHITO levels in the CSF over time were associated with progressive decreases in cognitive function. For every increase of the natural log CSF CHITO, there was a decrease of 9.92 raw scores in the cognitive domain of Bayley-III, adjusting for disease. CSF and serum chitotriosidase levels increased after the onset of seizures in one patient with infantile GM1-gangliosidosis and one patient with infantile Tay-Sachs disease. In this study, a broader comparison of CHITO levels before and after onset of initial seizures could not be performed as most of the initial chitotriosidase levels were drawn after the patients were experiencing seizures. Future studies could examine if CHITO is associated with other neurological outcomes in patients, such as seizures or changes in MRI.

3.1.4.3 Serum Chitotriosidase and Bone Health

In humans, CHITO is produced exclusively by activated macrophages. Osteoclasts are the resident macrophages in bones and play important roles in bone resorption. As such, increases in serum CHITO has been shown to be associated with increase bone resorption and is a biomarker in osteolytic diseases (223, 224). Elevated serum chitotriosidase is a known indicator of bone health in Gaucher disease type I (225, 226). This study demonstrated that serum CHITO is higher in MPS IVA than other MPS diseases, consistent with MPS IVA having more severe bone pathology and osteolytic pathology. In like fashion, serum CHITO was also elevated in GM1-gangliosidosis, a condition sharing numerous bone pathology with MPS conditions. Therefore, the elevated chitotriosidase levels in the serum may reflect the skeletal pathogenesis in numerous lysosomal diseases.

3.1.4.4 Additional Considerations

Approximately 5% of the general population have homozygous mutations in the *chit1* gene resulting in significantly reduced production or no production of CHITO (i.e., CHITO non-producers) (227). In this study, one patient with infantile Sandhoff (patient 22) was a CHITO nonproducer and was excluded from the analysis. It is unknown if the other subjects were heterozygotes in terms of their *chit1* genotype.

Recent studies have shown that chitotriosidase may induce pathogenic inflammation and tissue remodeling (228, 229). Evidence of microglial activation and elevated chitotriosidase levels were seen in the brain tissue of a patient with Sandhoff disease (230). Serum CHITO levels can be elevated from various non-lysosomal conditions or diseases. Elevations in serum CHITO levels has been reported in athlerosclerosis, brucellosis, and active tuberculosis (231-233).

Elevations in CHITO levels in the CSF has been reported in Alzheimer's disease and cerebral adrenoleukodystrophy (234, 235). The elevations in CHITO levels from such conditions, however, are not as high as the elevations typically seen in untreated Gaucher disease type I, which commonly exceed levels greater than 1000 nmol/h/mL. Likewise, serum CHITO elevations found in subjects in this study who had infantile GM1-gangliosidosis and MPS IVA, exceeded that reported in non-lysosomal conditions.

3.1.5 Conclusions

This study has shown that CSF and serum CHITO may serve as a candidate biomarker for select lysosomal diseases with CNS, as well as peripheral disease pathology. Specifically, CSF CHITO levels may distinguish the most severe infantile forms of the gangliosidoses from more attenuated juvenile and adult/late-onset forms and may be a marker of disease progression and for therapy outcomes.

3.1.6 Acknowledgement for Chitotriosidase's Clinical Portion

Dr. Sarah Kim is a fellow of the Lysosomal Disease Network. The Lysosomal Disease Network (2U54NS065768-06) is a part of the National Center for Advancing Translational Sciences (NCATS) Rare Diseases Clinical Research Network (RDCRN). RDCRN is an initiative of the Office of Rare Diseases Research (ORDR), NCATS, funded through a collaboration between the NCATS, the National Institute of Neurological Disorders and Stroke (NINDS) and the National Institute of Diabetes and Digestive and Kidney Diseases (NIDDK).

This article/chapter was published in Molecular Genetics and Metabolism Reports, Vol 29, Sarah Kim, Chester B. Whitley, Jeanine R. Jarnes,

Chitotriosidase as a biomarker for gangliosidoses, Page No 100803, Copyright Elsevier (2021), (202).

3.2 Pre-Clinical Study of Chitotriosidase as a Biomarker in Lysosomal Diseases

3.2.1 Methods

Three different murine models of lysosomal diseases were studied: GM1-gangliosidosis, GM2-gangliosidosis (Sandhoff disease), and MPS I. Mice for GM1-gangliosidosis and MPS I studies were C57Bl/6 strains, and the mice for Sandhoff studies were a mix of C57Bl/6 and 129S4 strains. For each lysosomal disease, there were three groups: untreated homozygous, gene-editing treated homozygous, and heterozygotes. There were three mice in each group for the GM1-gangliosidosis study (9 mice total) and the MPS I study (9 mice total). There were six mice in each group for the Sandhoff disease study (18 mice total).

Homogenized brain samples of untreated, treated, and heterozygous mice were provided courtesy of Dr. Li Ou and Dr. Michael Przybilla from the Whitley lab. The gene-editing therapies for MPS I and Sandhoff disease were developed by Dr. Li Ou (236, 237). The gene-editing therapy for GM1-gangliosidosis was developed by Dr. Michael Przybilla (238). The details of these gene-editing therapies are published elsewhere (236-238). Briefly, gene editing using a clustered regularly interspaced short palindromic repeats (CRISPR)-Cas9 system was used to insert a transgene encoding for a lysosomal gene into the albumin locus in hepatocytes. Mice were injected intravenously with gene editing therapy at one to two days post-birth. Mice with GM1-gangliosidosis received a total dose of 8 $x10^{10}$ vg/kg of the AAV8 vector, Sandhoff mice received $3.5x10^{13}$ vg/kg, and MPS I mice received $3.5x10^{14}$ vg/kg. Mice were sacrificed at eight months, four months, or 11 months post-birth for the GM1-gangliosidosis, Sandhoff, and MPS I studies, respectively. At the time of sacrifice, brain samples were isolated and homogenized.

I performed the chitotriosidase assays described in Section 3.1.2.2. The total protein levels in the brain tissues were quantified using a modified Bradford assay. The PierceTM protein assay was performed as described by the manufacturer (PierceTM 660-nm Protein Assay Reagent ThermoFisher 22660). Preformulated standards of Bovine Albumin Fraction V in 0.9% NaCl were used (ThermoFisher 23208). Absorbance was read on a clear 96-well plate (Sarstedt 82.1582) at 660 nm.

An ordinary one-way ANOVA followed by Tukey's multiple comparisons test was performed using GraphPad Prism version 8 for Windows, GraphPad Software, San Diego, California USA, www.graphpad.com.

3.2.2 Results

There was a statistically significant difference in chitotriosidase levels among untreated mice with GM1-gangliosidosis, Sandhoff disease, and MPS I ($F=238.4$, $p<0.0001$) (Figure 6). Mice with MPS I had the highest chitotriosidase levels in the brain, followed by GM1-gangliosidosis, then Sandhoff disease.

Figure 6: Chitotriosidase Levels in the Brain in Untreated Mice

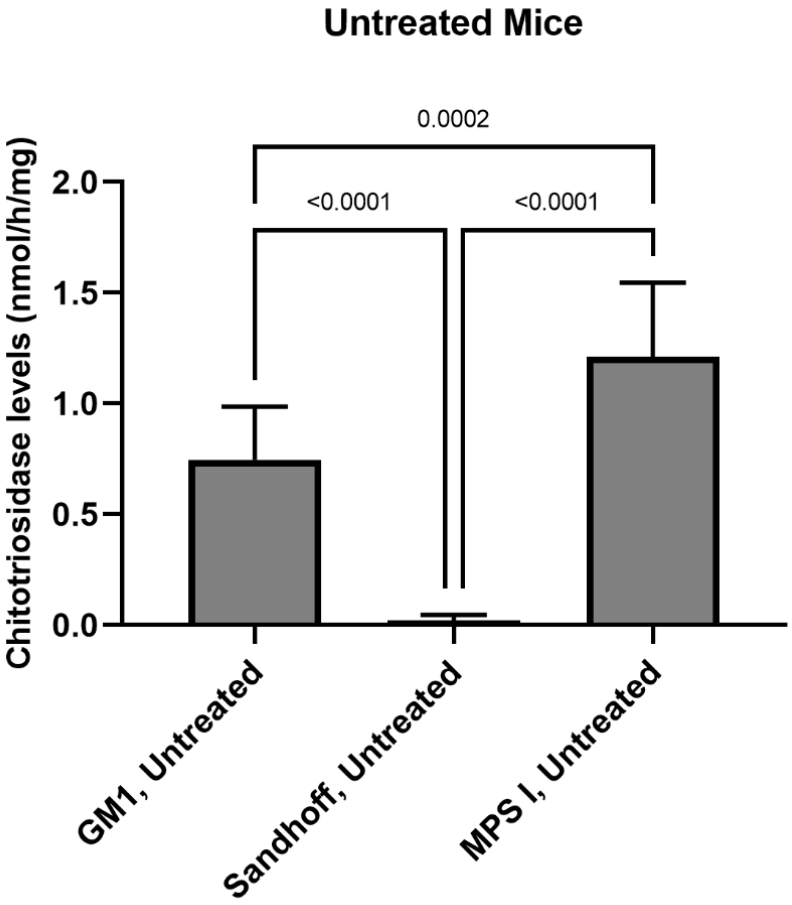

The mean and 95% confidence intervals for each group are shown (n=3 mice in GM1-gangliosidosis, 6 Sandhoff disease, 3 in MPS I).

In GM1-gangliosidosis, there was no statistically significant difference in chitotriosidase levels among untreated, treated, and heterozygous mice. (F=2.812, p=0.1375) (Figure 7).

Figure 7: Chitotriosidase Levels in the Brain from GM1-gangliosidosis Mice Treated with Gene Therapy

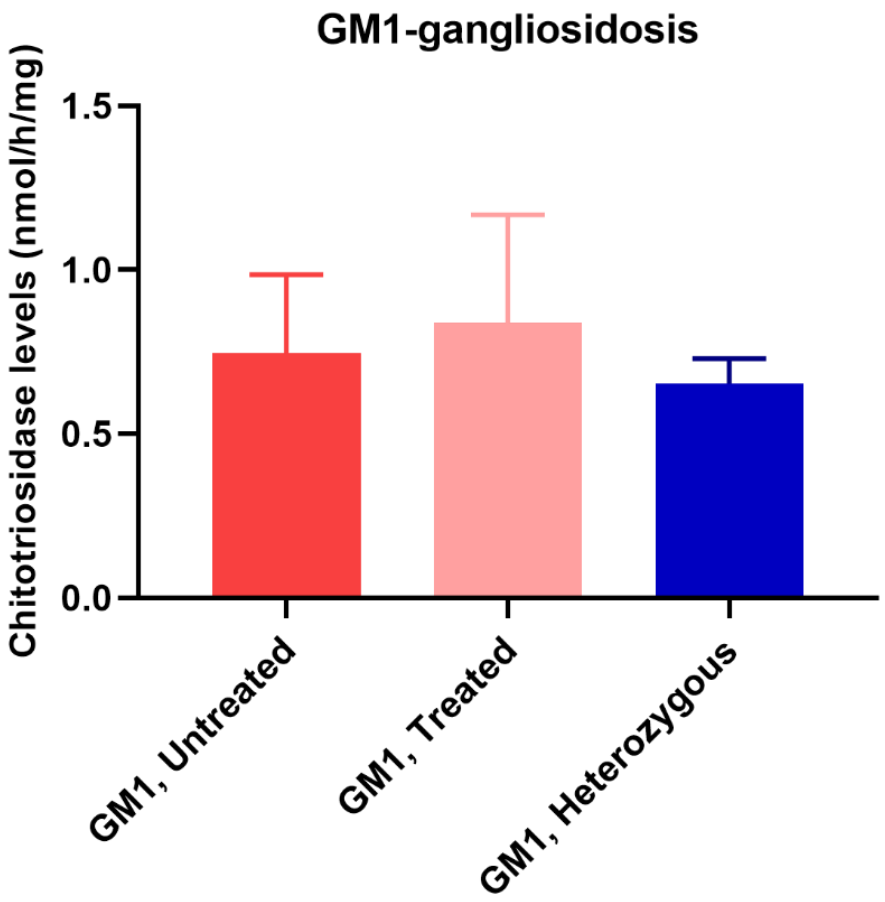

The mean and 95% confidence intervals for each group are shown (n=3 in each group).

In Sandhoff disease, there was no statistically significant difference in chitotriosidase levels among untreated, treated, and heterozygous mice. (F=0.7022, p=0.5111) (Figure 8).

Figure 8: Chitotriosidase Levels in the Brain from Sandhoff Mice Treated with Gene Therapy

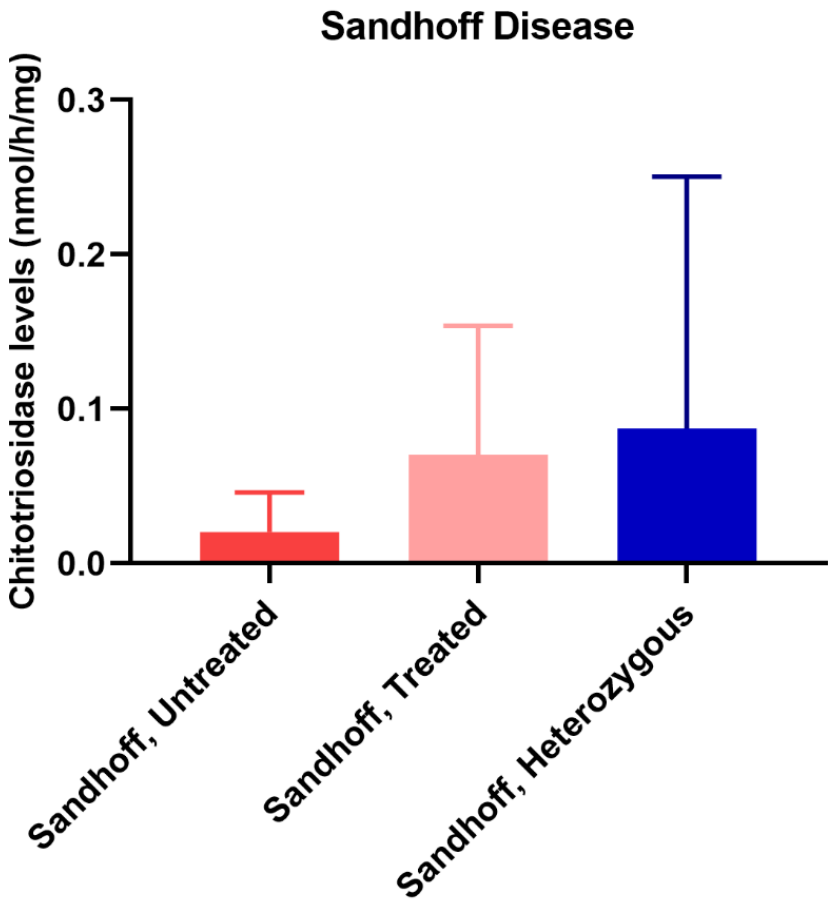

The mean and 95% confidence intervals for each group are shown (n=6 in each group).

In MPS I, there was a statistically significant difference in chitotriosidase levels among untreated, treated, and heterozygous mice. (F=34.17, p=0.0005) (Figure 9). Untreated mice had the highest chitotriosidase levels in the brain, followed by heterozygous, then treated mice.

Figure 9: Chitotriosidase Levels in the Brain from MPS I Mice Treated with Gene Therapy

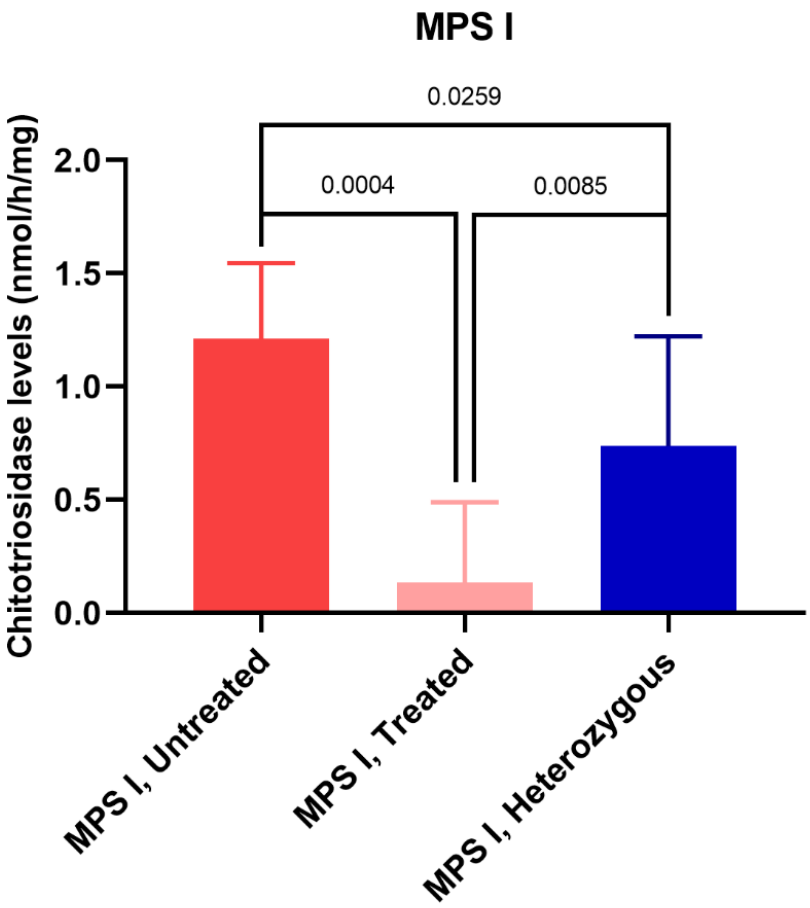

The mean and 95% confidence intervals for each group are shown (n=3 in each group).

3.2.3 Discussion

This study assessed chitotriosidase's ability to respond to effective gene therapy in murine models of lysosomal diseases. Chitotriosidase levels appear to be useful in murine models for MPS I, because there was a significant difference among these untreated, treated, and heterozygous mice. The efficacy of the gene-editing system is detailed in a publication by Ou et al. (236). The chitotriosidase levels reported in this dissertation were quantified from the high dose group in the study by Ou et al. (236). In that study, the high dose group had statistically significantly higher iduronidase activity levels in the brain than untreated mice ($p<0.0001$) and decreased vacuolization in Purkinje cells (236). Therefore, chitotriosidase levels in the brain may be a biomarker for gene therapy's efficacy.

The utility of chitotriosidase in murine models of GM1-gangliosidosis and Sandhoff disease is uncertain. In Section 3.1.3.3, patients with GM1-gangliosidosis had high elevations in chitotriosidase levels in the CSF. In contrast, mice with GM1-gangliosidosis had similar chitotriosidase levels in their brain compared to heterozygous mice. The lack of difference between the untreated and heterozygous mice may be due to a different disease progression or chitotriosidase's involvement in mice with GM1-gangliosidosis. In 3.1.3.3, patients with Sandhoff disease had lower chitotriosidase levels in the CSF than patients with other gangliosidoses. Similarly, untreated Sandhoff mice had lower chitotriosidase levels in the brain than untreated GM1-gangliosidosis mice. The low chitotriosidase levels in Sandhoff mice may also be due to differences in murine strains (239, 240).

A previous study reported that mice expressed chitotriosidase in the gastrointestinal tract, tongue, fore-stomach, and Paneth cells in the small intestine (239). In that study, mRNA levels for chitotriosidase were not detected in the brain, which may be due to the use of wildtype mice (239). The expression of chitotriosidase in mice may be disease-specific, similar to humans. In one

study, a murine model for Gaucher disease had a significantly higher chitotriosidase levels in the serum than wildtype mice (609 nmol/h/mg vs 167 nmol/h/mg) (241).

The strength of this study is that chitotriosidase levels in the brain were measured in multiple murine models of lysosomal diseases. Another strength of this study is that it assessed whether chitotriosidase levels could respond to gene therapy. While statistically significantly differences were seen, the absolute difference in chitotriosidase levels was small in the brain. Therefore, a sensitive method is needed to measure chitotriosidase levels in murine brain. Future studies with more mice and at various disease stages would further elucidate chitotriosidase's response to gene therapies.

CHAPTER 4: INVESTIGATION OF IDURONIDASE ENZYMES LINKED TO PEPCAN TO IMPROVE DELIVERY TO TARGETED TISSUES

4.1 Introduction

CNS disorders are a major contributor to morbidity and mortality in lysosomal diseases. Section 1.2.3 details these CNS disorders. Biological therapies, such as ERTs, have difficulty reaching the CNS due to their large molecular weight. One method to improve the delivery of enzymes is through receptor-mediated transport. In receptor-mediated transport, the enzyme of interest is physically attached to a ligand for a receptor expressed on the surface of the BBB. Section 2.3.2.4 discusses more details on receptor-mediated transport and examples from lysosomal diseases. There is still limited knowledge on potential mechanisms to deliver biological therapies into the CNS, such as targeting other highly expressed receptors.

The long-term goal of this study is to identify a strategy to increase the uptake of different lysosomal enzymes into targeted tissues. MPS I, which has a deficiency in the iduronidase enzyme, was chosen as the initial disease model. The **objective** of this study was to determine if pepcan-12 can increase the uptake of iduronidase in the brain of MPS I mice. Pepcan-12 is a ligand for the cannabinoid receptor type 1 (CB1) that is highly expressed in the CNS. The primary **hypothesis** was that the plasmid encoding pepcan-12 in tandem with *IDUA* will cause higher enzyme activity levels in the brain than the plasmid encoding *IDUA*. More specifically, mice treated with pepcan-12+Linker S+*IDUA* or pepcan-12+Linker T+*IDUA* were hypothesized to have higher enzyme activity levels in the brain than mice treated with *IDUA*. The secondary **hypothesis** was that the linkers would not affect the activity levels of iduronidase. More specifically, mice treated with Linker S+*IDUA* or Linker T+*IDUA* would have similar enzyme activity levels to mice treated with *IDUA* in the organs and plasma.

4.1.1 CB1 as the Target Receptor

A strategy using receptor-mediated transport was chosen over adsorptive transport because adsorptive transport using cell-penetrating peptides can cause non-specific uptake of enzymes into organs. Non-specific uptake into organs can limit the amount of enzyme entering the CNS because the CNS competes with organs for enzymes. Moreover, non-specific uptake into organs poses significant safety risks.

A target receptor with the following characteristics was desired:

- High homology between humans and mice
- High expression on the luminal surface of endothelial cells on BBB and target cells within the CNS
- Low risk of adverse effects from disrupting the receptor's function
- Known ligand or antibody that can be encoded as DNA

These considerations are discussed in this section. The characteristic of low risk of adverse effects from disrupting the receptor's function will be discussed in Section 4.1.2 when pepcans are discussed.

To increase the translatability of this dissertation's study, the scientific rationale for the study design was considered for both humans and murine models. Mice are common pre-clinical models due to their high genetic similarity to humans, accelerated lifespan, ease of breeding, and low cost. Thus, the scientific rationale for selecting the target receptor and ligand needed to be supported by data from both humans and mice. While mice and humans have 90% genome similarity, there are still translatability challenges (242). One relevant example is in the development of AGT-181 or valanafusp, which is an iduronidase enzyme conjugated to an antibody for the human insulin receptor. The initial antibody, MAb 83-14, was produced by mouse ascites cells, contained fragments of murine antibodies, but did not recognize the murine insulin receptor (243). Instead, MAb 83-14 antibody recognized the human insulin receptor, specifically the amino acids 469-592 of the α subunit, and thus studies with MAb

83-14 were performed in human cell cultures or rhesus monkeys (243-246). The authors state that there is no known antibody that cross-reacts to rodent and human insulin receptors (244, 245). Therefore, a surrogate way to study this mechanism in mice targeted a different receptor, more specifically, the transferrin receptor (245).

The CB1 and cannabinoid receptor type 2 (CB2) receptors are part of the endocannabinoid system (247). The endocannabinoid system plays a role in neuroprotection, memory, pain modulation, appetite, immune functions, cardiovascular disease, cancer, and fertility (247). CB1 is primarily expressed in the CNS, whereas CB2 is primarily expressed in the peripheral and immune cells (247).

In humans, CB1 is encoded by the *CNR1* gene, which is located on chromosome 6q15 (248). In mice, CB1 is encoded by the *Cnr1* gene located on chromosome 4 16.28 cM (249). The *CNR1* and *Cnr1* gene contain eight and 11 exons, respectively (248, 249). In humans, CB1 is 473 amino acids long and can exist as three protein isoforms (248, 250, 251). In mice, CB1 is 472 amino acids long and can exist as two protein isoforms (249, 252). CB1 is a G-protein coupled receptor (GPCR) and has the canonical seven transmembrane structure (248, 250). A Blast 2 sequence program identified a 97.04% amino acid similarity between the human and mice CB1, indicating high similarity between the two organisms (253).

The high expression of CB1 in the CNS makes it an attractive target for therapeutic delivery. The expression of receptors on the cell's extracellular surface is a rate-limiting step for receptor-mediated transport. CB1 is the highest expressed GPCR in the CNS (247). Since the test article was going to be administered intravenously, CB1 would need to be expressed extracellularly on the luminal surface of endothelial cells on BBB, as well as the target cells within the CNS.

CB1 is expressed on the extracellular surface of endothelial cells on the BBB, which is required for receptor-mediated transport into the CNS. One study

detected the CB1 protein on cultured human brain microvascular endothelial cells using fluorescein isothiocyanate staining or Western blot (254, 255). However, it was not reported whether CB1 was expressed at the luminal or abluminal surface of human cultured cells. One study detected CB1 proteins at both the luminal and abluminal surface of rat brain microvascular endothelial cells using immunostaining and electron microscopy (256). Thus, these studies suggest that a fusion enzyme has the potential to be taken up from the blood vessel's lumen and into endothelial cells.

CB1 is also expressed on neurons in humans and mice, which is important because neurons are one of the affected cells in MPS I and in other lysosomal diseases (257, 258). Section 1.2.3 discusses how neurons are affected in lysosomal diseases. Therefore, a fusion enzyme has the potential to be taken up into neurons using receptor-mediated transport mediated by CB1.

The expression of CB1 in other tissues is important for predicting off-target effects. CB1 has a preferential and ubiquitous expression in the CNS but also expressed in other tissues. RNA-seq of tissue samples from 95 humans detected *CNR1* in adipose tissues, adrenal gland, lung, and lymph nodes (248, 258). The mouse ENCODE transcriptome data reported expression of *Cnr1* expression in the adrenal glands of adult mice (249).

4.1.2 Pepcan as the Ligand for CB1

Pepcans, termed after pep<u>tide endocan</u>nabinoids, were first discovered in 2003 (259). The first pepcan discovered, pepcan-9, was found in the brain of rats (259). Pepcan-9's amino acid sequence in rats, PVNFK**F**LSH, corresponds to amino acid 96-104 in the α chain of hemoglobin (259). The human and murine homolog of pepcan-9 differs by a Phe to Leu change at position 6 (PVNFK**L**LSH) (260). Pepcan-9 is also called hemopressin due to its sequence similarity to hemoglobin and dose-dependent hypotensive effects in rats (259). Later studies demonstrated that pepcan-9 was a serendipitous artifact of the hot acid

extraction used in rat brains, which caused an Asp-Pro peptide bond cleavage (261). That is, pepcan-9 is not synthesized in vivo. Additional studies identified other pepcans such as pepcan-12, pepcan-23, and pepcan-14 (260, 262).

Pepcans, a class of peptides that bind to the CB1 receptor, were chosen as the ligand for the CB1 receptor because they can be encoded as DNA. Although there are several other ligands for CB1, these ligands were ruled out for the following reasons. Using a canonical, endogenous ligand, such as anandamide, for receptor-mediated transport poses a safety risk via competition for CB1. Clinical trials with valanafusp, which targets the insulin receptor, have reported hypoglycemia, albeit transient and manageable (146). Furthermore, canonical, endogenous ligands or synthetic compounds, such as rimonabant, would be difficult for gene therapy studies. In gene therapy, the transgene is administered as a DNA and transcribed, translated, and processed into the enzyme. Compounds have to be conjugated to the lysosomal enzyme to have a therapeutic effect. Given the complexity of gene expression and the numerous macromolecules involved, finding a way to conjugate a compound to the enzyme intracellularly did not seem feasible. For that reason, conjugation of the enzyme using a biotin-avidin system to target the CB1 receptor also did not appear feasible.

Among the known pepcans, pepcan-12 was chosen as the ligand for the CB1 receptor for this study based on the following characteristics:

- High affinity for CB1
- Ability to induce internalization of the CB1 receptor
- Information available on how it binds to CB1
- Physiological effects, including knowledge of adverse effects
- Relative selectivity for CB1

Each of these characteristics are detailed below.

One reason why pepcan-12 was chosen as the ligand is because it has a higher affinity for CB1 receptors than other pepcans. A seminal paper by Bauer et al. identified and characterized several pepcans (260). An equilibrium binding

assay compared pepcans' abilities to displace radiolabeled, synthetic compounds that have low nanomolar affinities for human CB1 receptors (260). Pepcan-12, pepcan-14, pepcan-15, pepcan-17, and pepcan-20 were chosen in that study because they were present in murine brain, hamster brain, murine plasma, and human plasma (260). CHO cells expressing human CB1 were co-incubated with 1 μM of a pepcan (pepcan-12, pepcan-14, pepcan-15, pepcan-17, or pepcan-20) and 0.5 nM of [^{3}H]CP55,940 or 2.5 nM of [^{3}H]WIN55,212-2 (260). Pepcan-12, pepcan-14, then pepcan-20, in the listed order, caused moderate-to-low displacement of radioligands (260). Pepcan-15 and pepcan-17 did not demonstrate displacement (260).

Pepcan-12 induces the internalization of CB1 receptors, supporting its potential to mediate receptor-mediated endocytosis. Internalization of CB1 has been measured in studies as the % reduction of CB1 expression at the surface. One study reported that pepcan-12 caused a 21% reduction of CB1 expression at the surface (260). A second study reported an approximately 50% reduction of CB1 surface expression (262). In both studies, the co-administration of SR141716, a CB1 antagonist that inhibits the internalization of CB1, and pepcan-12 resulted in normal CB1 expression (260, 262, 263). Information about how CB1 agonists induce internalization may provide further insight into pepcan-12's mechanism. After binding to agonists (WIN55,212-2, CP55,940, or HU210), CB1 was internalized after 20 minutes using clathrin-coated pits (263). This internalization of CB1 required its 460-463 amino acids at the C terminal but not the G protein α_1, α_0, and α_s subunits (263).

The N-terminal of pepcan-12 is important for binding to CB1. Pepcan-12 conjugates that had a fluorescein at the N-terminal had weaker binding to CB1 receptors than conjugates at the C-terminal (260). Another study showed that the five amino acids of pepcan-9's N-terminal were needed for CB1 recognition (**PVNFK**FLSH) (264). Pepcan-12 has also been reported to be a negative allosteric modulator of CB1 (260).

Given CB1's role in the endocannabinoid system, the physiological effects of pepcan-12 were an important safety consideration. An intraperitoneal injection of 10 μmol of pepcan-12 once daily for 14 days decreased food consumption in rats, although total body weight was not affected (265). Administration of pepcan-12 intracerebroventricularly restored impaired memory functions in Alzheimer's mice (266). Because pepcan-12 could have similar physiological effects as other pepcans, I also considered adverse effects caused by other pepcans. Pepcan-9 causes dose-dependent hypotensive effects in mice, but hypotension was mild and transient (267). Pepcans have also caused antinociceptive and hypothermic effects (decreased body temperature by -1.75 °C) in rodents (268). Based on previous reports, pepcans appeared to have anorexigenic, antinociceptive, hypotensive, and hypothermic effects, but these effects seemed to be manageable. Furthermore, while it is important to be aware of the potential adverse effects, these were not guaranteed to be caused by the fusion enzyme. The function of a 12 amino acid peptide would likely be altered when the peptide is attached to a large enzyme like iduronidase.

Adverse effects can also be caused by a ligand non-selectively binding to receptors, potentially resulting in a fusion enzyme's off-target effects. In addition to CB1 receptors, pepcan-12 can bind to CB2 receptors (260). Therefore, a fusion enzyme could exhibit off-target effects from binding to CB2 receptors. However, pepcan-12 did not bind to other receptors that are activated by endocannabinoids, specifically transient receptor potential cation channel subfamily V member 1 (TRPV1) and G protein-coupled receptor 55 (GPR55) (260). Pepcan-12 also did not cross-react with other physiologically important receptors, such as μ-opioid, Δ-opioid, α2-adrenergic, β2-adrenergic, or angiotensin II type 1 (AT1) receptors (262).

4.1.3 MPS I as the Disease Model

MPS I was chosen as the initial disease model because iduronidase has a simple protein structure and has more published information on its use as a fusion enzyme, ERT, and gene therapy. More information on MPS' pathology, clinical progression, and murine models is also available compared to other lysosomal diseases. Therefore, the MPS I was chosen as the initial disease model because of the reduced likelihood of having unknown confounding factors. Once a strategy to increase uptake of iduronidase was identified and optimized, the eventual goal was to apply it to a lysosomal disease without a therapy, such as GM1-gangliosidosis.

4.1.4 Selection of Linkers

Linkers are sequences that join two protein domains together. The term linker is used interchangeably with the term spacer. Spacers are sequences that separate two protein domains. Directly fusing two domains may impair gene expression, protein folding, and the activity of enzymes (269). Thus, a linker's/spacer's purpose is to join two domains together on the same polypeptide strand but separate the domains far enough to preserve the protein's processing and function.

A DNA sequence of a linker was used to physically attach the pepcan sequence to the *IDUA* sequence. The choice of the linker was based primarily on one that would not decrease the activity of iduronidase. The second preference for a linker was that it would be a short enough sequence to fit into AAV in future studies.

Previous studies with fusion lysosomal enzymes used varying linkers. Some linkers may have been a byproduct of plasmid cloning because the amino acids did not fit the traditional sequences of linkers. One study used a DNA sequence that encoded for six amino acids between the 5' of *IDUA* and 3' of

murine transferrin (270). The resulting fusion enzyme had a 15% decrease in activity levels (270). Another study used a linker to join iduronidase to a ligand for apolipoprotein E (271). In that study, *IDUA* was followed by a human myc tag, a DNA sequence encoding for the five amino acid sequence IDILE, then the receptor-binding domain of apolipoprotein E (271). This linker appeared to preserve the activity levels of iduronidase, but the linker was located in the C terminal end of iduronidase.

I chose two linkers for this study, which are denoted as Linker S and Linker T. Linker S contained the 45 bp DNA sequence GGGGGAGGCGGGAGCGGGGGAGGCGGGAGCGGGGGAGGCGGGAGC, which can be abbreviated as (GGGGGAGGCGGGAGC)3. Linker S is translated into the 15 amino acid sequence Gly-Gly-Gly-Gly-Ser-Gly-Gly-Gly-Gly-Ser-Gly-Gly-Gly-Gly-Ser, which can be abbreviated as (Gly-Gly-Gly-Gly-Ser)3 or (GGGGS)3. The (GGGGS)n motif is commonly used for linkers in fusion enzyme studies (269). The small size of glycine allows for interaction between domains or increased spatial separation of domains (269). This linker has been used in non-lysosomal enzymes and proteins (269). A similar linker, L(GGGGS)4, was used to fuse five cell-penetrating peptides to the C terminal of the aryl sulfamidase, a lysosomal enzyme (272)

Linker T contained the 15 bp DNA sequence GGCGGCGGCGGAACGGGA, which is translated into the six amino acid sequence Gly-Gly-Gly-Gly-Thr-Gly or GGGGTG. Linker T has been studied in a different lysosomal disease, MPS VII (186).

Pepcan-12 and linkers were encoded immediately downstream of iduronidase's signal sequence at the N terminal. Multiple studies have shown that pepcan-12's N terminal is important for binding to CB1 (260, 264). Therefore, the final fusion enzyme needed to have a pepcan-12 with a free N terminal, which would only be possible if the pepcan-12 was encoded on the N terminal of iduronidase. Literature and database searches were performed to determine if disrupting iduronidase's N terminal would affect its activity. No structural or

functional domains were reported in either the N or C terminal of iduronidase, except for the signal sequence at the N terminal (48, 251, 273).

4.1.5 Dose Rationale

A dose of 50 µg of plasmid was chosen in this study. Ideally, the dose would have been based on the levels of the fusion enzyme that is needed to saturate the target receptor (243). However, there was insufficient published literature on the quantification of CB1 receptor levels on the BBB in mice and humans. Moreover, there was insufficient information from studies on the levels of iduronidase enzymes, either physical levels or activity levels, that are produced from plasmids. The relationship between the dose of gene therapy and the resulting enzyme levels reported in other studies was difficult to extrapolate to this study because previous studies used different constructs for gene therapy (i.e., plasmid vs AAV, different promoters, different genes) and/or only one dose was studied. Therefore, a commonly used dose for hydrodynamic injections of plasmids was chosen. This dose of 50 µg of plasmid has been used previously in the Whitley lab and other labs (270, 271, 274). This dose had been shown to cause the highest expression levels for *IDUA*. That is, doses past 50 µg did not increase the activity levels of iduronidase. The 50 µg represents the maximum effective dose in this study because the highest activity levels of iduronidase would maximize the number of bound receptors and transport into the CNS.

4.2 Methods

4.2.1 Experimental Design

The overall experimental design is shown in Figure 10.

Figure 10: Experimental Design for Testing Fusion Idurondase Enzymes

A)

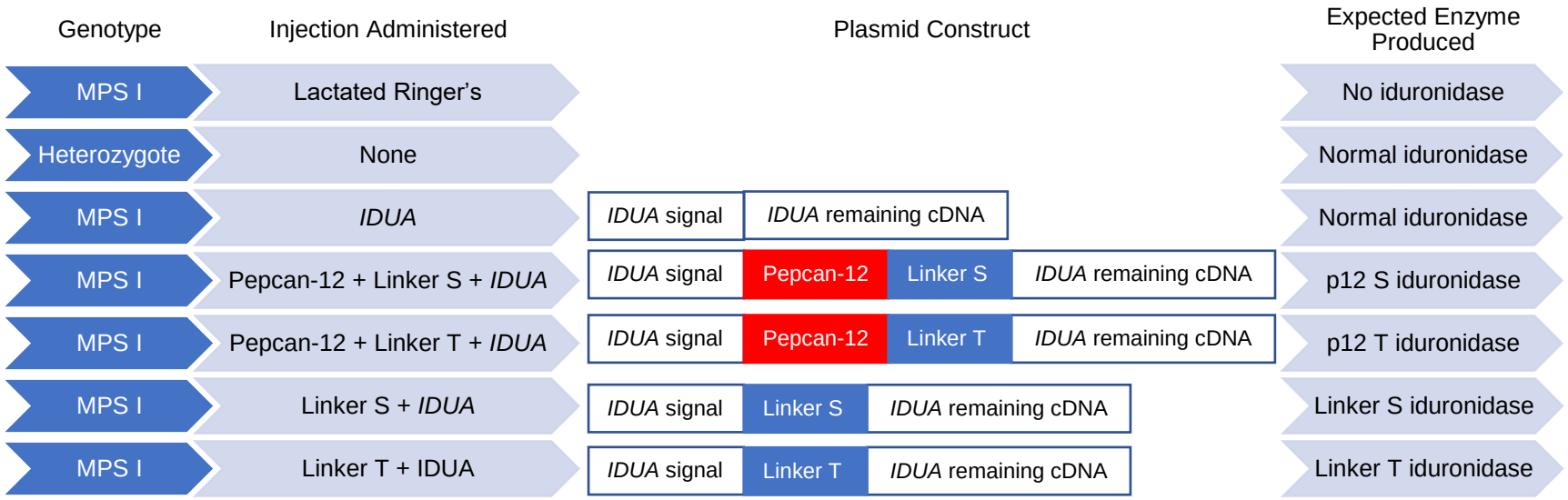

B)

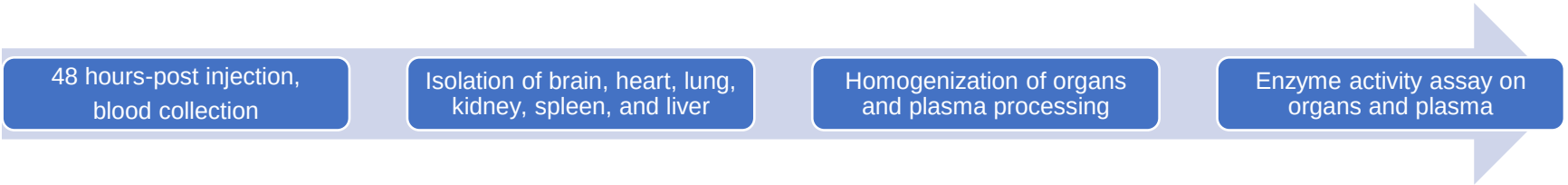

A) Pepcan-12 is the ligand for the CB1 receptor. Mice injected with Lactated Ringer's (LR) are negative controls. Heterozygotes are positive controls. Mice injected with IDUA are a control group for the supraphysiological enzyme activity levels produced by hydrodynamic injection of plasmids. Mice injected with linker + IDUA serve as control groups to determine if linkers affect the enzyme activity. The size of the domains are not drawn to scale and are as follows: IDUA signal (57 bp), pepcan-12 (36 bp), Linker S (45 bp), Linker T (18 bp), IDUA remaining cDNA (1905 bp). B) The experimental steps after injection are shown.

4.2.2 Plasmid Cloning

A third-generation lentiviral transfer plasmid was used as the backbone. This plasmid contained a human α1-antitrypsin (hAAT) promoter and the hepatic control region of human apolipoprotein E (HCR-apoE) to drive the expression of the transgene. The hAAT promoter causes liver-specific expression of transgenes, and HCR-apoE enhances the expression (274, 275). The plasmid contained a codon-optimized sequence of human *IDUA* that has been used previously (236, 276).

The cDNA sequence for pepcan-12 was obtained from the human *HBA1* gene, which encodes for the α chain of hemoglobin (277-279). In humans, the *HBA2* gene also encodes for the α chain of hemoglobin (278). In mice, there is only one gene, *Hba-a1*, which encodes for the α chain of hemoglobin (279). The region of nucleotides that encoded for pepcan-12 was identical among *HBA1*, *HBA2*, and *Hba-a1* (280). The DNA sequence for pepcan-12 was cgggtggacccggtcaacttcaagctcctaagccac. The DNA sequence for linkers was codon-optimized for humans using the Codon Optimization Tool from Integrated DNA Technologies (281).

The cDNA constructs from plasmids are shown in Figure 10. The sequences for pepcan-12+Linker S or pepcan-12+Linker T were inserted directly downstream of *IDUA*'s signal sequence. Constructs were cloned by ligation of the polymerase chain reaction (PCR)-synthesized insert using the primers between EcoRI/BlpI sites. The pepcan-12+Linker S+*IDUA* and pepcan-12+Linker T+*IDUA* plasmids used the cloning primers ctcctgacaggttggtgtacagtgaattcatgc and tggggaacagctgccggatctgctgagcgacg. The Linker S+*IDUA* and Linker T+*IDUA* plasmids were generated by cloning out the pepcan-12 sequences. Linker S+*IDUA* plasmid used the cloning primers cagtgaattcatgcggcccctgcggcctagagccgccctgctggctctcctggcttctctgctggccGGGGGA GGCGGGAGCGGGGGAGGCGGGA and tggggaacagctgccggatctgctgagcgacg. Linker T+*IDUA* used the cloning primers

cagtgaattcatgcggcccctgcggcctagagccgccctgctggctctcctggcttctctgctggccGGCGGC GGCGGAACGGGAgctccccctg and tggggaacagctgccggatctgctgagcgacg. The inserts were sequenced by the primers: AGCCCTGCCCTGAGACTG and ATTGTACTAACCTTCTTCTCTTTC. Plasmid cloning and sequencing was performed by the Custom Cloning Division within the Emory Integrated Genomics Core.

4.2.3 Hydrodynamic Injection

Hydrodynamic delivery is a commonly used technique for gene delivery in pre-clinical studies with rodents, and its principles are described in this paragraph (282). A DNA solution that is 8 to 10% of the mouse's weight is administered over five to seven seconds as an intravenous injection, typically using the tail vein (282). The DNA solution travels from the tail vein to the inferior vena cava (282). The high volume of DNA solution in the heart increases the cardiac preload, induces cardiac congestion, and causes retrograde blood flow to the liver (282, 283). The high volume of DNA solution causes a hydrodynamic force that separates the endothelial cells in the liver's vessels (282, 283). The blood vessel's disrupted endothelial layer allows the DNA to reach and transfect hepatocytes (282, 283). The liver is the major site for transgene expression, though minor expression has been detected in the heart, lung, spleen, and kidney (274). In rodents, the cardiac preload rapidly normalizes due to their high heart rate (283). In humans, the rapid increase of cardiac preload poses safety risks, limiting the clinical translatability of hydrodynamic gene delivery (282, 283).

Mice were housed in specific pathogen-free conditions. All protocols involving animals were approved by the University of Minnesota Institutional Animal Use and Care (IACUC) committee. All mice were C57BL/6. The plasmid mixture was prepared by mixing 50 µg of plasmids with a volume of Lactated Ringer's (LR) Injection, United States Pharmacopeia (USP), needed to achieve a total volume that is 10% of the mouse's body weight. For example, a mouse

weighing 20 g corresponds to 2 mL of the plasmid mixture. The maximum volume of the plasmid mixture was 2.7 mL.

Mice were lightly sedated with ketamine/butorphanol/acepromazine cocktail. The sedative cocktail was prepared by UMN's Research Animal Resources (RAR) as follows: 4.5 ml of 0.9% Sodium Chloride Injection, USP, 0.4 ml of 100 mg/ml ketamine, 0.05 ml of 1 mg/ml butorphanol, and 0.05 ml of 10 mg/ml acepromazine maleate injection were mixed to a final volume of 5 mL. Mice were administered 20 µL of the sedative cocktail intraperitoneally 30 minutes before hydrodynamic injection. The plasmid mixture was injected intravenously through the tail vein using a 27G butterfly needle.

4.2.4 Dissection and Sample Processing

Forty-eight hours after hydrodynamic injection, blood and organs were collected. Approximately 200 µL of blood was collected from the submandibular vein. The blood was mixed with 20 µL of 100 units/mL Heparin LockFlush Solution, USP, then centrifuged for ten minutes at 3,000 revolutions per minute (rpm). The translucent layer corresponding to the plasma was transferred to a new tube and stored at -80°C.

Mice were euthanized with CO_2 asphyxiation. Cardiac perfusion was performed with approximately 35 mL of Phosphate-Buffered Saline (PBS) (Corning® ref 21-040-CV). The brain, heart, lung, liver, kidney, and spleen were dissected and snap frozen on dry ice. Samples were stored at -80°C.

Organs were mechanically homogenized with either a rotor-stator (Kinematica Polytron® CH-6010 Kriens-lu PT 10/35) or bead impact (Next Advance Bullet Blender® Storm). In both methods, 1 mL of PBS (Corning® ref 21-040-CV) was added to the organ. After mechanical homogenization, 11 µL of 10% Triton in PBS (Triton X-100 Sigma T8787) was added. After ten minutes, samples were centrifuged at 13.3 rpm for 15 minutes. The supernatant was transferred to a new tube and stored at -80°C.

4.2.5 Enzyme Activity Assay

The enzyme activity assay for iduronidase was performed as previously described but with a different stopping buffer (284). Briefly, a 0.4 M formate buffer was prepared by mixing 4.45 mL of formic acid (Sigma F0507), 6.8 g of sodium formate (Sigma S2140), 4.5 g of sodium chloride (Sigma 567440), and sufficient distilled water for a total volume of 500 mL. The 0.4 M formate buffer was adjusted to a pH of 3.5 with 0.4 M formic acid and 0.4 M sodium formate. Standards for the enzyme activity assay were created using 4-methylumbelliferone (Sigma M1381). The stopping buffer was 0.15 M glycine-NaOH buffer, pH 10 (Glycine Calbiochem Sigma 3570; NaOH Sigma S0899).

Samples were diluted with the formate buffer when needed. Then, 25 µL of sample was mixed with 25 µL of 360 µM of 4-methylumbelliferyl α-L-iduronide (Glycosynth 44076) in a 96-well polymerase chain reaction (PCR) plate (GeneMate Non-Skirted, VWR 490003-750). On the same plate, 25 µL of standards were added to different wells. The plate was incubated at 37°C for 30 minutes on a thermocycler (Applied Biosystems). The reaction was stopped by adding 200 µL of glycine-NaOH buffer. Then, 200 µL of the mixture was transferred to a black 96-well plate with round bottoms (Corning® 3792). The fluorescence was read at 365 nm excitation and 450 nm emission on a plate reader (BioTek Synergy™ Mx Microplate reader).

For tissue samples, the total protein levels were quantified using a modified Bradford assay. The Pierce™ protein assay was performed as described by the manufacturer (Pierce™ 660-nm Protein Assay Reagent ThermoFisher 22660). Preformulated standards of Bovine Albumin Fraction V in 0.9% NaCl were used (ThermoFisher 23208). Absorbance was read on a clear 96-well plate (Sarstedt 82.1582) at 660 nm.

Samples were ran in triplicate for the enzyme activity assay and the protein assay.

4.2.6 Statistical Analysis

In the initial analysis, the enzyme activity levels of all the experimental groups were compared. However, it became clear that the hydrodynamic injection of plasmids caused supraphysiological enzyme activities in the plasma and organs, except the brain.

For enzyme activity levels in the brain, all experimental groups were compared. The enzyme activity levels in the brain were natural log transformed, and a Welch one-way ANOVA test followed by Dunnett's T3 multiple comparisons test was performed using GraphPad Prism version 9.2.0 for Windows, GraphPad Software, San Diego, California USA, www.graphpad.com. A Welch ANOVA was chosen over ordinary ANOVA because of unequal variances among groups. A Dunnett's T3 multiple comparisons test was chosen because the sample size in each group was less than 50.

For the enzyme activity levels in the plasma and remaining organs, only the plasmid-treated groups were compared statistically to conserve power. Data were natural log-transformed, and an ordinary one-way ANOVA followed by Tukey's multiple comparisons test was performed using GraphPad Prism version 9.2.0 for Windows, GraphPad Software, San Diego, California USA, www.graphpad.com. The enzyme activity levels for the Lactated Ringer's and heterozygote groups are still shown on the graphs for contextual purposes.

A Pearson's correlation test was performed for age at injection and enzyme activity levels in the heart. A second Pearson's correlation test was performed for the age of injection and enzyme activity levels in the plasma. Pearson's correlation tests were performed using GraphPad Prism version 9.2.0 for Windows, GraphPad Software, San Diego, California USA, www.graphpad.com

4.3 Results

4.3.1 Age and Gender of Mice

There were a total of 64 mice in this study (Table 3). The mean age of mice at injection was 14.2 weeks and ranged between 6.3 weeks and 24.1 weeks. Generally, the age at injection was similar across groups, with two noticeable differences. Mice that were injected with Lactated Ringer's were older than the rest of the groups. Mice that administered Linker T+*IDUA* were on average four weeks younger than mice administered *IDUA*. Genders were balanced across groups, except in Pepcan-12+Linker S+*IDUA* and Pepcan-12+Linker T+*IDUA* groups, which had a greater number of females.

Table 3: Age and Gender of Mice in Experiment

Group	**Mean age at injection in weeks (minimum and maximum age)**	**Number of females**	**Number of males**	**Total number of mice**
Lactated Ringer's	17.3 (6.3-24.1)	5	5	10
IDUA	14.9 (10.0-18.1)	4	4	8
Pepcan-12+ Linker S+*IDUA*	13.2 (6.3-16.9)	6	3	9
Pepcan-12+ Linker T+*IDUA*	13.8 (6.3-18.0)	7	4	11
Linker S+*IDUA*	12.4 (11.1-18.1)	5	4	9
Linker T+*IDUA*	11.0 (10.6-11.1)	3	2	5
Heterozygotes	15.1 (8.1-18.3)	6	6	12

4.3.2 Enzyme Activity Levels in the Organs and Plasma

In the brain, there was a statistically significant difference in enzyme activity levels among groups ($F=41.12$, $p<0.0001$). All plasmid-treated groups had statistically significantly higher enzyme activity than the LR group (Figure 11, Appendix Table 3). However, all plasmid-treated groups had statistically significantly lower enzyme activity in the brain than the heterozygous group. These statistically significant differences are not shown in Figure 11 for ease of viewing, and these details are reported in Appendix Table 3. Moreover, there were no statistically significant differences between the plasmid-treated groups.

Figure 11: Enzyme Activity Levels in the Brain

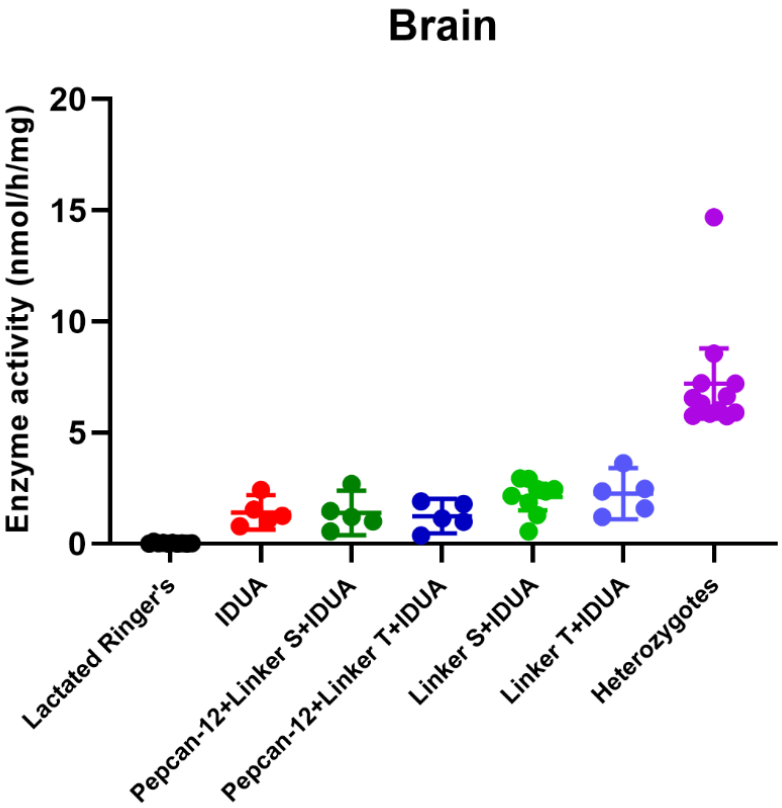

The mean and 95% confidence intervals for each group are shown. Each symbol represents one mouse (n=10 mice in LR, n=5 in IDUA, n=5 in pepcan-12+Linker S+IDUA, n=5 in pepcan-12+Linker T+IDUA, n=9 in Linker S+IDUA, n=5 in Linker T+IDUA, n=12 heterozygotes). For the brain, there are fewer mice in the plasmid-treated groups than the LR or heterozygous groups because of the cross-contamination from liver samples in the rotor-stator homogenization method.

In the heart, there was a statistically significant difference in enzyme activity levels among plasmid-treated groups (F=3.344, p=0.0196). Mice treated with pepcan-12+Linker T+*IDUA* had statistically significantly higher enzyme activity in the heart than mice treated with *IDUA* (Figure 12). Intriguingly, mice treated with Linker T+*IDUA* also had statistically significantly higher enzyme activity in the heart than mice treated with *IDUA*. The results for all comparisons between plasmid-treated groups are reported in Appendix Table 4.

Figure 12: Enzyme Activity Levels in the Heart

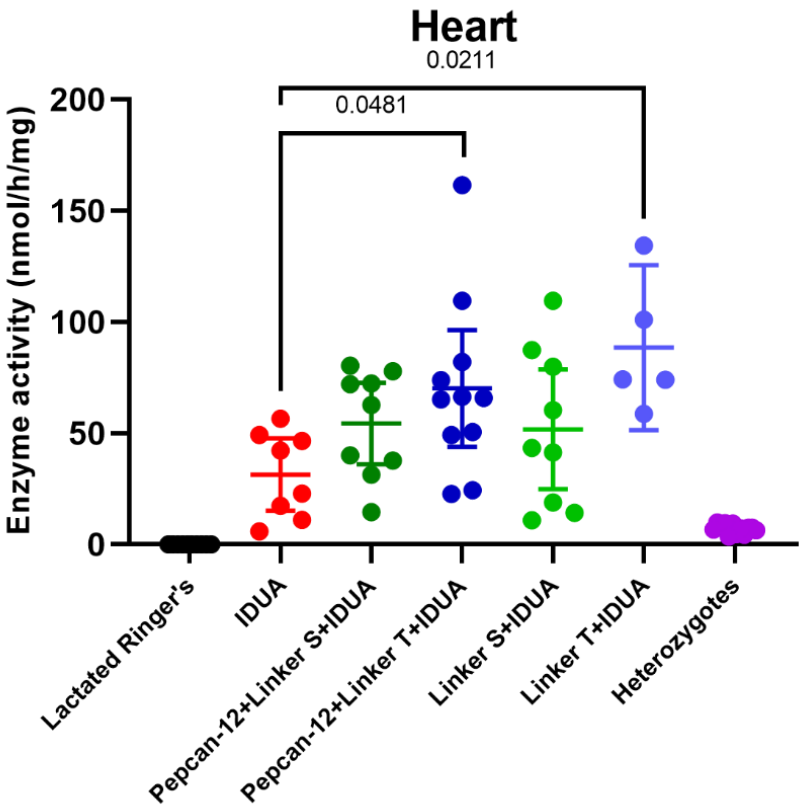

The mean and 95% confidence intervals for each group are shown. Each symbol represents one mouse (n=10 mice in LR, n=8 in IDUA, n=9 in pepcan-12+Linker S+IDUA, n=11 in pepcan-12+Linker T+IDUA, n=9 in Linker S+IDUA, n=5 in Linker T+IDUA, n=12 heterozygotes).

In the lungs, there were no statistically significant differences in enzyme activity levels among the plasmid-treated groups (F=2.630, p=0.0594) (Figure 13). Therefore, a multiple comparison test was not performed. The failure to detect a significant difference may have been due to the low number of lung samples, as the lungs were added on in later studies.

Figure 13: Enzyme Activity Levels in the Lung

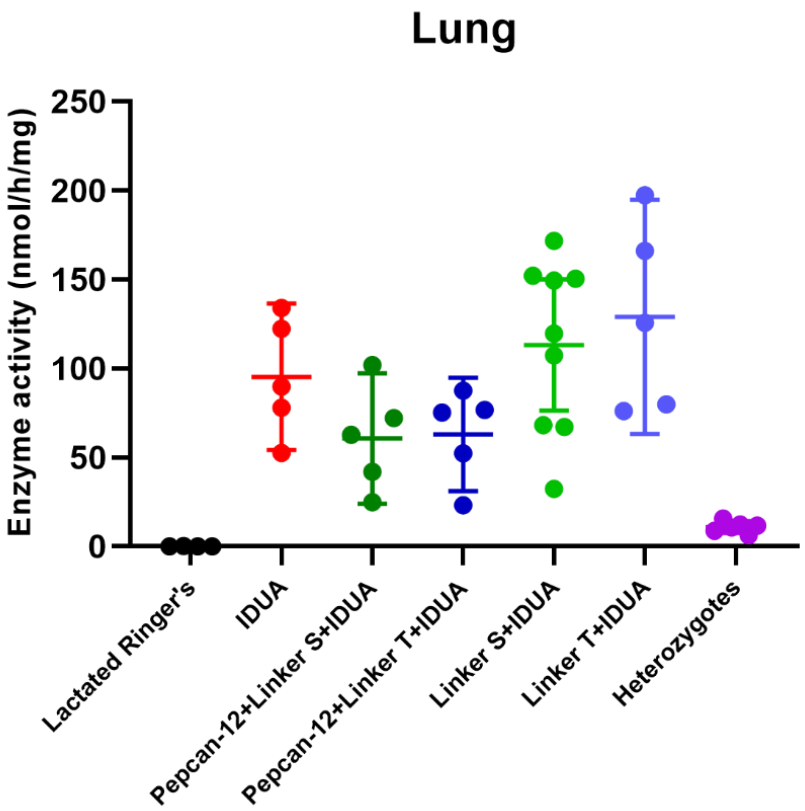

The mean and 95% confidence intervals for each group are shown. Each symbol represents one mouse (n=4 mice in LR, n=5 in IDUA, n=5 in pepcan-12+Linker S+IDUA, n=5 in pepcan-12+Linker T+IDUA, n=9 in Linker S+IDUA, n=5 in Linker T+IDUA, n=6 heterozygotes).

In the liver, there was a statistically significant difference in enzyme activity levels among plasmid-treated groups (F=2.692, p=0.0458) (Figure 14). There were no statistically significant pairwise comparisons (Appendix Table 5). However, mice treated with Linker T+*IDUA* had higher enzyme activity levels than mice treated with pepcan-12+Linker T+*IDUA*, which neared statistical significance (p=0.0547).

Figure 14: Enzyme Activity Levels in the Liver

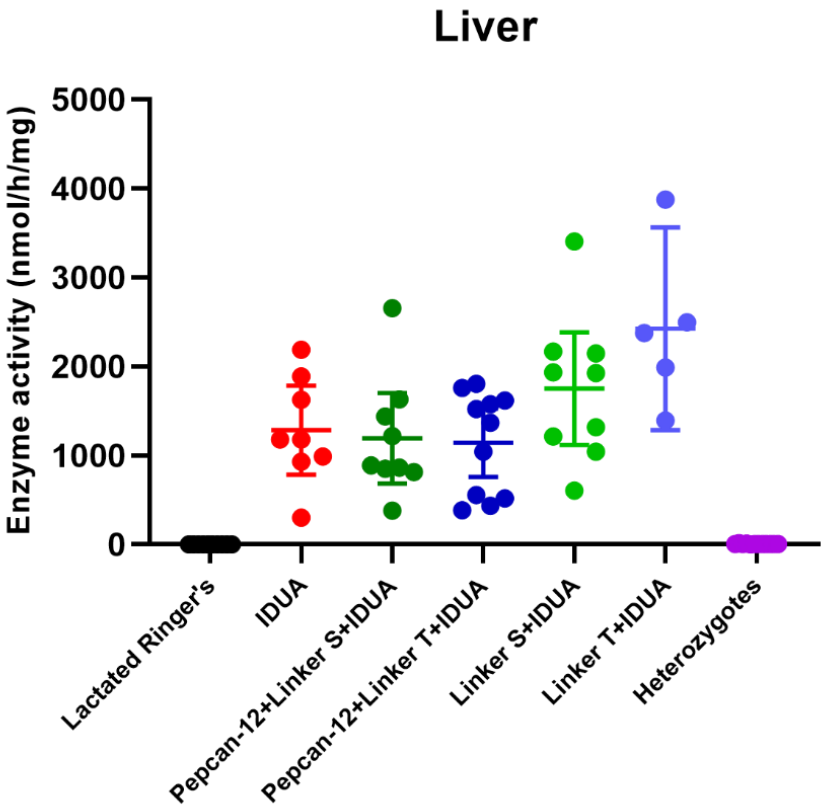

The mean and 95% confidence intervals for each group are shown. Each symbol represents one mouse (n=10 mice in LR, n=8 in IDUA, n=9 in pepcan-12+Linker S+IDUA, n=11 in pepcan-12+Linker T+IDUA, n=9 in Linker S+IDUA, n=5 in Linker T+IDUA, n=12 heterozygotes).

In the spleen, there was a statistically significant difference in enzyme activity levels among plasmid-treated groups (F=4.408, p=0.0052) (Figure 15). Mice treated with either the Linker S+*IDUA* or Linker T+*IDUA* had statistically significantly higher enzyme activity than mice treated with pepcan-12+Linker T+*IDUA* (Figure 15). Similarly, mice treated with either the Linker S+*IDUA* or Linker T+*IDUA* had higher enzyme activity than mice treated with pepcan-12+Linker S+*IDUA*, which neared statistical significance (p=0.0671, p=0.0545, respectively) (Appendix Table 6).

Figure 15: Enzyme Activity Levels in the Spleen

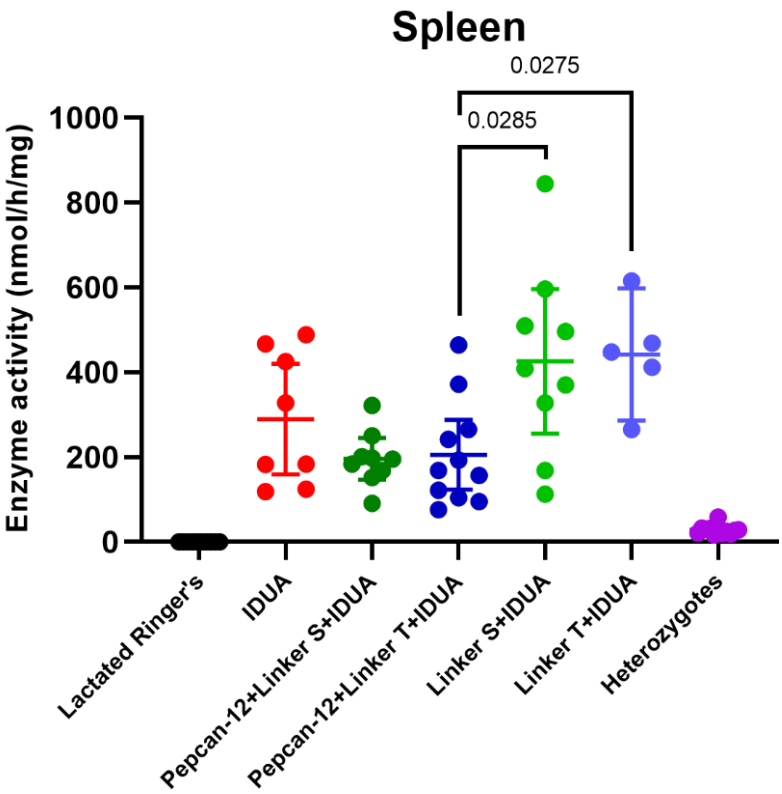

The mean and 95% confidence intervals for each group are shown. Each symbol represents one mouse (n=10 mice in LR, n=8 in IDUA, n=9 in pepcan-12+Linker S+IDUA, n=11 in pepcan-12+Linker T+IDUA, n=9 in Linker S+IDUA, n=5 in Linker T+IDUA, n=12 heterozygotes).

In the kidney, there was a statistically significant difference in enzyme activity levels among the plasmid-treated groups (F=5.594, p=0.0013) (Figure 16). Mice treated with either the Linker S+*IDUA* or Linker T+*IDUA* had statistically significantly higher enzyme activity than mice treated with pepcan-12+Linker S+*IDUA.* Similarly, mice treated with either the Linker S+*IDUA* or Linker T+*IDUA* had statistically significantly higher enzyme activity than mice treated with pepcan-12+Linker S+*IDUA*. The results for all comparisons between plasmid-treated groups are reported in Appendix Table 7.

Figure 16: Enzyme Activity Levels in the Kidney

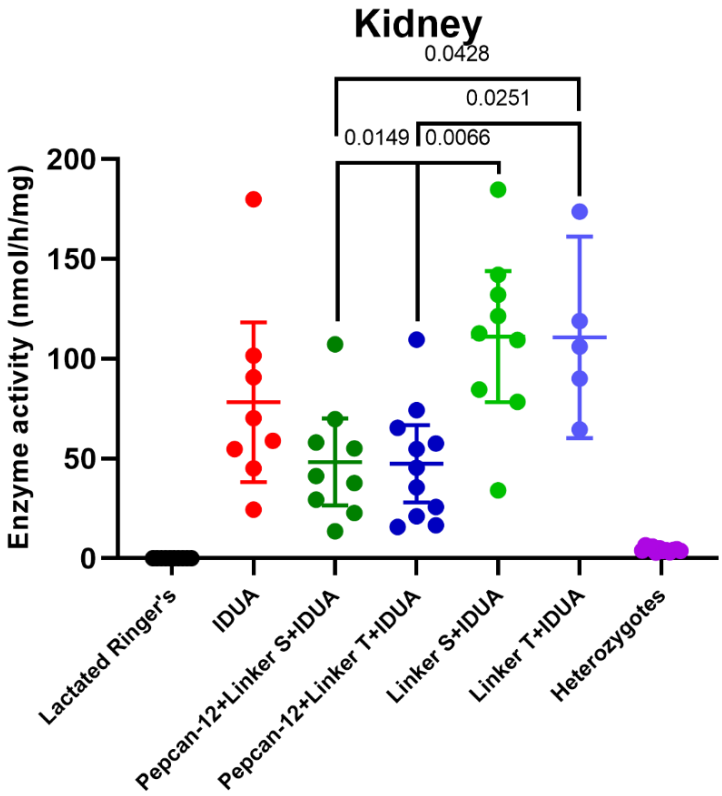

The mean and 95% confidence intervals for each group are shown. Each symbol represents one mouse (n=10 mice in LR, n=8 in IDUA, n=9 in pepcan-12+Linker S+IDUA, n=11 in pepcan-12+Linker T+IDUA, n=9 in Linker S+IDUA, n=5 in Linker T+IDUA, n=12 heterozygotes).

In the plasma, there was a statistically significant difference in enzyme activity levels among plasmid-treated groups (F=7.488, p=0.0002) (Figure 17). Mice treated with either the Linker S+*IDUA* or Linker T+*IDUA* had statistically significantly higher enzyme activity than mice treated with *IDUA*. Mice treated with the Linker S+*IDUA* also had statistically significantly higher enzyme activity than mice treated with pepcan-12+Linker T+*IDUA*. The results for all comparisons between plasmid-treated groups are reported in Appendix Table 8.

Figure 17: Enzyme Activity Levels in the Plasma

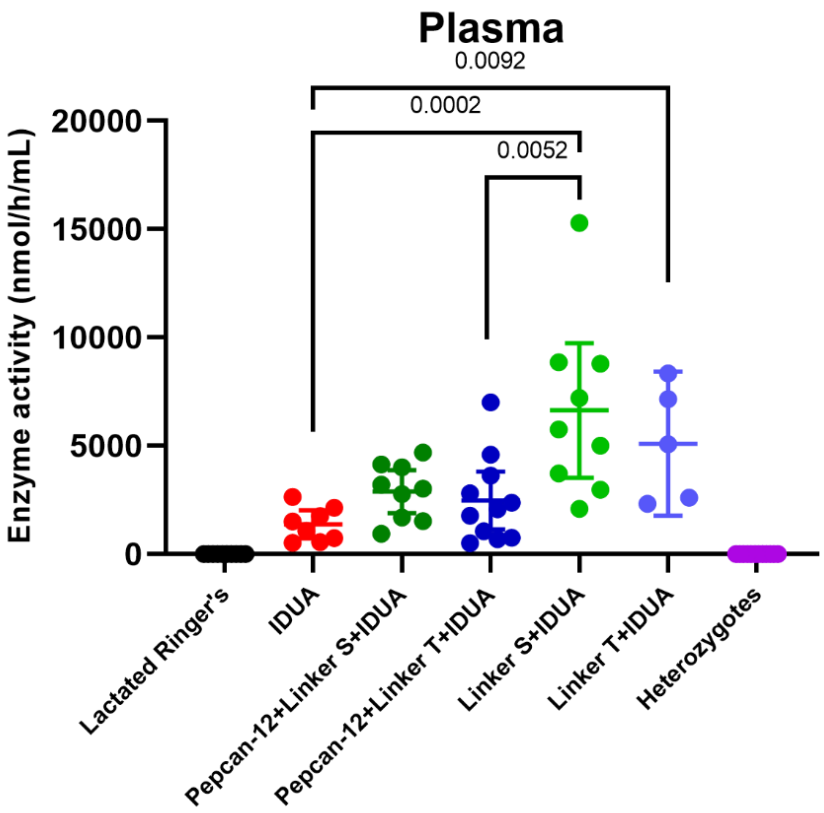

The mean and 95% confidence intervals for each group are shown. Each symbol represents one mouse (n=10 mice in LR, n=8 in IDUA, n=9 in pepcan-12+Linker S+IDUA, n=11 in pepcan-12+Linker T+IDUA, n=9 in Linker S+IDUA, n=5 in Linker T+IDUA, n=12 heterozygotes).

One possibility for the higher activity levels in the Linker S+*IDUA* and Linker T+*IDUA* compared to the other plasmid-treated groups is because of the younger mice in the Linker groups. Age may induce anatomical or physiological changes that impact response to hydrodynamic injections or iduronidase activity. A Pearson's correlation test was performed for plasmid-treated mice with the variables age at injection and enzyme activity levels in the heart. A multiple linear regression was not performed because the small sample sizes relative to the number of variables may have caused overfitting. The heart was used in the correlation test because the heart showed a significant difference between *IDUA* and fusion enzymes. There was no correlation between age at injection and enzyme activity in the heart (r^2=0.01640, p=0.4190) (Figure 18). The plasma was another sample that showed a significant difference between *IDUA* and fusion enzymes. There was no correlation between age at injection and enzyme activity in the plasma (r^2=-0.04050, p=0.2013) (Figure 19).

Figure 18: Relationship Between Age at Injection and Enzyme Activity Levels in the Heart

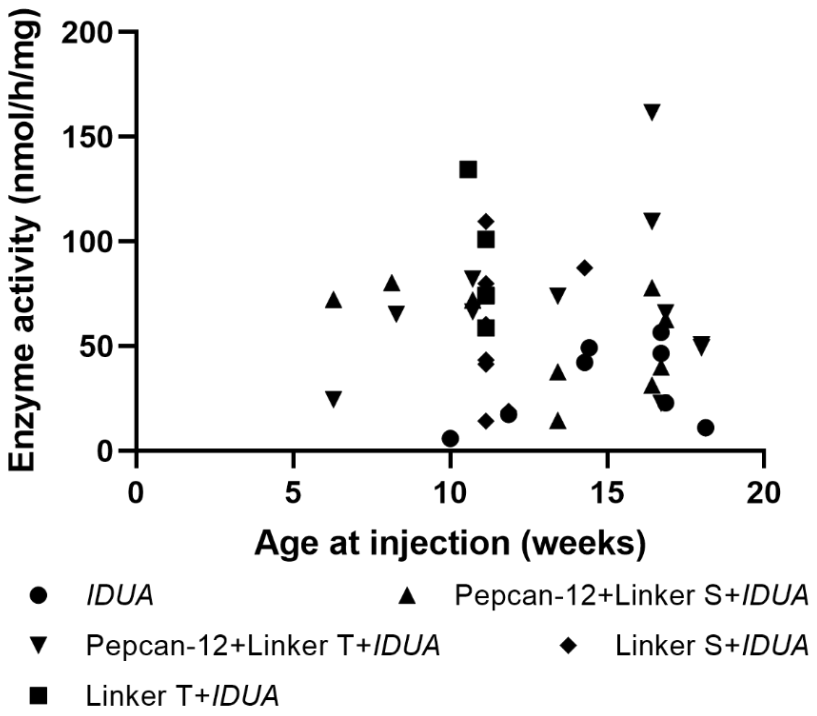

Figure 19: Relationship Between Age at Injection and Enzyme Activity Levels in the Plasma

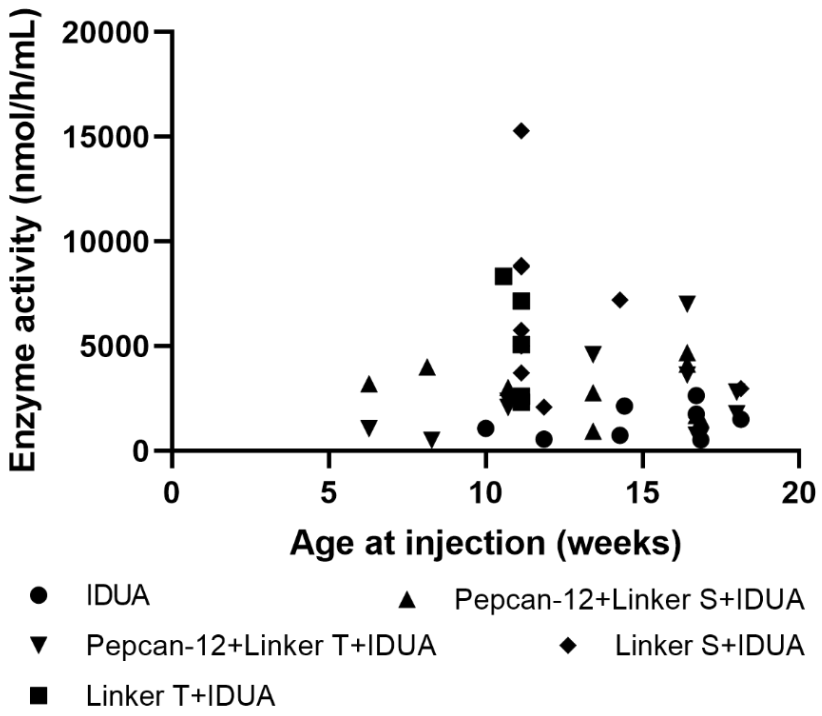

4.4 Discussion

The **objective** of this study was to determine if pepcan-12 can increase the uptake of iduronidase in the brain of MPS I mice. The primary **hypothesis** was that the plasmid encoding pepcan-12 in tandem with *IDUA* would have higher enzyme activity levels in the brain than the plasmid encoding *IDUA*. Based on the results, pepcan-12 did not appear to increase the activity levels of iduronidase in the brain. The heart was the only tissue that showed a difference in enzyme activity levels between *IDUA* alone and a construct containing pepcan-12. Unexpectedly, in the heart, Linker T+*IDUA* also had higher enzyme activity levels than *IDUA* alone. The secondary **hypothesis** was that the linkers would not affect enzyme activity levels. Based on the results, it appears that

Linker T, not pepcan-12, is causing higher enzyme activity levels in the heart. Furthermore, Linker S+*IDUA* and Linker T+*IDUA* had higher enzyme activity levels than *IDUA* alone in the plasma. The higher enzyme activity levels in the linker groups could not be explained by the age or gender of mice. The potential explanations for increased enzyme activities in fusion enzymes are discussed in Section 4.4.1.

4.4.1 Potential Mechanisms for Higher Enzyme Activity Levels in Fusion Enzymes

Several possible explanations why the linkers caused higher iduronidase activity levels have been explored. The nucleic acid sequence of linkers may increase the gene expression of *IDUA*, indirectly increasing enzyme activity. The addition of linkers may have introduced a protein domain or motif, which could have increased enzyme activity directly or through protein-protein interaction. Each of these possibilities is discussed below, with a focus on Linker T.

While the linkers contain guanine-rich nucleic acid sequences, the linkers are unlikely to increase gene expression by forming a G-quadruplex. G-quadruplexes are three-dimensional structures with the consensus sequence of $G_{\geq 3}N_xG_{\geq 3}N_xG_{\geq 3}N_xG_{\geq 3}$ in which x denotes the number of nucleotides in loops (285). The function of G-quadruplexes is an active area of research. Previously published literature focus on G-quadruplexes' roles in telomeres or genome instability, which are not applicable to plasmids (285). Additionally, the mechanisms that G-quadruplexes use to regulate gene expression appear to primarily repress transcription and translation (285). G-quadruplexes could theoretically upregulate transcription by displacing an inhibitory transcription factor. Furthermore, the Quadruplex forming G-rich Sequence (QGRS) mapper did not predict a putative G-rich sequence that could form a G-quadruplex in Linker T+*IDUA*, under a maximum QGRS length of 30 and a minimum G-group size of 3 (286).

The linkers are unlikely to increase gene expression by containing an alternative start codon and allowing translation of multiple new open reading frames because linkers were encoded downstream of *IDUA*'s signal sequence. The signal sequence ensures the proper processing of an enzyme, thereby impacting enzyme activity. If the linkers contained an alternative start codon, the signal sequence would be absent in those nascent proteins. The lack of a signal peptide would cause improper processing of iduronidase, resulting in lower enzyme activity. Furthermore, two programs did not detect any open reading frames that began in Linker T (287, 288). Open reading frames were searched using the National Center for Biotechnology Information (NCBI) Open Reading Frame (ORF) program and SnapGene using the minimal open reading frame length of 30 nucleotides and alternative initiation codons (287, 288).

The addition of Linker T within the *IDUA* sequence may have created a protein domain or motif that altered the enzyme activity. The sequences of iduronidase and Linker T iduronidase were compared in various databases of protein domains and motifs. Database searches did not detect a new protein domain or motif on Linker T iduronidase. MOTIF did not detect new protein domains or motifs using the Pfam database and NCBI Conserved Domain Database (289-291). PROSITE detected two N-myristoylation sites on Linker T+*IDUA* (292). These N-myristolyation sites were also detected on pepcan-12+Linker T+*IDUA* (292). However, N-myristoylation sites are common in many protein sequences (292). Linker T sequences did not fit the known signal peptides in lysosomal enzymes (293, 294).

The glycine residues in the linkers are likely increasing flexibility in the fusion iduronidase enzymes. The linkers contained Gly, Ser, and Thr, which are all small amino acids. These small amino acids allow the linkers to be flexible and allow mobility between functional domains (269). Additionally, Ser and Thr are polar and can form hydrogen bonds with water or the peptide backbone (295). A review of naturally occurring linkers by Argos stated, “pentapeptides with only Gly, Ser and Thr would make the best general linkers as these residues

occur most often in and are strongly preferred by natural linkers" (295). The described linker is very similar to Linker T. A more recent review also found Thr to be preferred in naturally occurring linkers but not Gly or Ser (296).

In addition to the types of amino acids present, the length of the linker also affects the production and activity of fusion enzymes (269, 297). Given the highly similar amino acid residues in Linker S and Linker T, the shorter length of Linker T is the most likely explanation for the differences seen in their corresponding fusion iduronidase enzymes. The review by Argos suggests that five amino acids are the best length (295). However, other studies suggest that longer linkers, such as 20 or 34 amino acids, have higher enzyme activities than shorter linkers (295, 297, 298). Therefore, there is no consensus on the optimal length of linkers, and the optimal length is likely determined by a complex combination of the domain's properties, linker's properties, and experimental conditions (269). This dissertation's study suggests that shorter flexible linkers at the N terminal of iduronidase cause higher enzyme activity than longer linkers. Longer linkers may decrease enzyme activity by interfering with the sorting and processing of fusion iduronidase proteins.

Linker T has been studied in a different lysosomal enzyme, β-glucuronidase (186). In that study, the fusion enzyme was generated from a plasmid construct that contained *GUSB* + Linker T + Fc domain in human IgG (186). That is, Linker T was used to join the C terminal of β-glucuronidase to the Fc component of IgG. The fusion β-glucuronidase and the normal β-glucuronidase were administered intravenously into MPS VII mice, and the enzyme activity levels were measured in the plasma at several timepoints up to one hour post-injection (186). The fusion β-glucuronidase had a longer half-life, estimated with enzyme activity levels, than the normal β-glucuronidase (186). More specifically, the time it took to see a 50% decrease in the enzyme activity was estimated to be 36 minutes and 1.7 minutes post-injection for the fusion β-glucuronidase and the normal β-glucuronidase, respectively (186). The fusion β-glucuronidase and normal β-glucuronidase were also administered to MPS VII

mice who were deficient in mannose receptors (MR) (186). In the double mutant mice (MPS VII$^{-/-}$ MR$^{-/-}$), the time it took to see a 50% decrease in the enzyme activity was estimated to be 72 minutes and 19 minutes post-injection for the fusion β-glucuronidase and the normal β-glucuronidase, respectively (186). Moreover, fusion β-glucuronidase levels were higher than the normal β-glucuronidase in the brain, heart, lung, liver, spleen, kidney, and eyes of newborn pups from moms treated during pregnancy (186). One explanation for these results is that the Fc region on the fusion β-glucuronidase enables recycling of the enzyme. It is also possible that Linker T is contributing to the prolonged activity of the fusion β-glucuronidase in the plasma. It is difficult to discern whether the prolonged enzyme activity is due to Linker T or Fc domain because the normal β-glucuronidase did not contain Linker T.

By using databases and literature, the most probable explanation is that the flexible glycine residues are increasing the stability or activity of the fusion enzymes. This may be at the protein sorting step, given that the linkers are located immediately downstream of the signal sequence. The flexible linkers may form a favorable interaction between the *IDUA* signal sequence and the proteins involved in sorting and processing.

4.4.2 Study Significance

The significance of this study was the identification of fusion iduronidase enzymes that have higher activity than the normal iduronidase. The linkers can be used in fusion enzymes encoded for gene therapy or administered directly as ERT, enabling multiple types of therapies. These findings can advance the development of therapies for patients with MPS I and other lysosomal diseases.

Fusion iduronidase enzymes containing a Linker T could alleviate cardiovascular complications and may have greater cardiovascular improvements than existing therapies for MPS. The cardiovascular disorders in MPS are detailed in Section 1.2.4. Briefly, approximately 60 to 100% of patients

with MPS exhibit cardiovascular disease, and cardiovascular disease has a higher prevalence in patients with MPS I, MPS II, and MPS VI (100, 103-109). HCT and ERT can alleviate some CV manifestations but do not improve cardiac valvular thickening, left-sided valvular regurgitation, or left-sided valvular stenosis (100, 126, 132-136). HCT and ERT cannot access poorly vascular sites such as the cardiac valves (100). Approximately 60 to 90% of patients with MPS exhibit a cardiac valve abnormality (100, 105, 107). Thus, there is an unmet medical need for therapies that can alleviate cardiac valve disorders in patients with MPS. In this study, hearts were homogenized, so future studies will aim to characterize the specific benefits on cardiac valves.

Furthermore, the linkers may increase the uptake of other lysosomal enzymes into organs. Linker T iduronidase had higher activity levels in the heart and plasma. It is possible that Linker T stabilizes the enzyme's activity in the plasma, resulting in greater uptake into the heart. The longer a lysosomal enzyme persists in the circulation, the greater its chance of interacting with the M6P receptors or other extracellular receptors that mediate organ uptake. However, an enzyme's longer residence time in the circulatory system can decrease its activity due to blood's relatively high pH compared to the lysosome's (14). Because ineffective enzymes can enter the organs, the levels of active enzymes in the plasma and organs should be quantified. Previous studies in lysosomal diseases suggest that prolonged activity levels of enzymes in the plasma, represented as a longer $t_{1/2}$ using enzyme activity, can increase the uptake of enzymes into organs (166, 185, 186). Therefore, these linkers may prolong the activity levels in the plasma in other lysosomal enzymes, which can increase the uptake of enzymes into organs.

It is uncertain why pepcan-12 did not increase enzyme activity levels in the brain at 48 hours. However, it is still notable that activity levels for fusion enzymes were comparable to the native iduronidase enzyme in the CNS. Future studies with other pepcans would better characterize the CB1 receptor's ability to mediate the transport of biological therapies into the CNS.

4.4.3 Study Strengths and Considerations for Future Studies

One strength of this study was the extensive use of control groups. Most studies with fusion enzymes report the untreated mutants as a negative control group and heterozygotes as a positive control group. Few studies have administered the normal enzyme as an additional control group. Even fewer studies have administered the enzyme containing only the linker as a control group. One rationale for why studies omit the linker control group is that there is no need for a linker if there is no ligand. Other reasons for omitting linker control groups from studies are decreased cost, reduced sample size requirement, faster completion, and a more straightforward study design and analysis. In rare cases, there may be strong, extensive scientific evidence that the linker does not affect the enzyme's structure and activity. Having extensive control groups is not always feasible. For example, certain disease models cause mice to breed poorly, so adding another control group could delay the study for several months. On the other hand, when feasible to do so, having thorough control groups may yield unexpected results like in this study. The serendipitous nature of this study is similar to 2-hydroxypropyl-β-cyclodextrin, which is currently in clinical trials for Niemann-Pick disease type C1 (299, 300). This compound was initially used as a vehicle for a different drug for Niemann-Pick disease type C1, as cyclodextrin is commonly used in drug formulations (299, 300).

Another strength of this study was increasing the clinical translatability of results from hydrodynamic injections. Hydrodynamic injections are commonly used to study gene therapy in pre-clinical studies. Hydrodynamic delivery causes high expression of transgenes by inducing cardiac overload. Mice can quickly recover from cardiac overload because of their heart rate of 500 beats per minute. Humans have a much slower heart rate, so hydrodynamic injections would pose a significant safety risk. In this study, the clinical translatability of hydrodynamic injections was improved by the inclusion of the experimental group

injected with *IDUA* plasmids. Without the *IDUA* plasmid group, the enzyme activities from the fusion constructs would be compared to the heterozygotes and untreated mutants. The overwhelmingly high enzyme activity levels in the fusion constructs may misleadingly suggest that this is due to the fusion enzymes. In reality, the hydrodynamic delivery of plasmids was the cause of the supraphysiological levels of enzyme activity. In this study, the main negative control group was the *IDUA* plasmid group. The fusion enzymes demonstrated higher activities compared to normal iduronidase in near identical experimental conditions.

Future experiments at the cellular level could elucidate information on the mechanism. Even though database searches did not detect a new protein domain or motif, fusion enzymes could still interact with other proteins to alter their activity. A future study on protein-protein interaction could be performed using co-immunoprecipitation followed by mass spectrometry. The proteins that interact with iduronidase could then be compared to proteins that interact with fusion enzymes to detect novel protein-protein interactions.

A long-term assessment of safety and efficacy would substantiate the therapeutic role of these fusion enzymes. In this study, enzyme activity levels were assessed after 48 hours. A more comprehensive study on the long-term safety and efficacy would be carried out in the future as follows. The transgene from the plasmid constructs will be cloned and packaged into an AAV vector. AAV vectors allow for the long-term expression of transgenes. AAV vectors were not used in this study because AAV is considerably more expensive than plasmids because of AAV's complex manufacturing. In the long-term study, there would be three groups of mice: untreated MPS I mutants, MPS I mutants treated with AAV encoding Linker T+*IDUA*, and heterozygotes. Ideally, there would be a fourth group, MPS I mutants treated with AAV encoding *IDUA*, but this may not be feasible given the high cost of AAV. AAV would be administered intravenously to neonates through the facial vein. Morbidity and mortality would be observed daily. Plasma samples would be collected every two weeks to monitor enzyme

activity levels. Behavioral testing would be performed at six months of age when MPS I mice begin to exhibit symptoms (236). Shortly after behavioral testing, the brain, heart, lung, liver, kidney, spleen, and plasma would be collected. The enzyme activity levels in these organs and plasma would be quantified using an enzyme activity assay. Enzyme levels in the organs can be visualized using immunohistochemistry. Improvements in the cardiac valves and the CV system could be assessed using previously described methods (114, 118). The levels of glycosaminoglycans could be quantified using a Blyscan Kit (301-304).

CHAPTER 5: PHARMACOKINETIC ANALYSIS OF IDURONIDASE AND A FUSION IDURONIDASE ENZYME ENCODED IN GENE THERAPY

5.1 Introduction

In the previous chapter, I developed fusion iduronidase enzymes that had higher activity levels than the normal iduronidase. Linker T iduronidase had higher activity levels than the normal iduronidase in the plasma and the cardiac tissue at 48 hours post-injection. One potential mechanism for these results is that Linker T stabilizes the enzyme's activity in the plasma, resulting in greater uptake into the heart. This proposed mechanism is partially based on the well-established knowledge of cross-correction and the role of M6P receptors in lysosomal enzymes. The longer a lysosomal enzyme persists in the circulation, the greater chance it has of interacting with the M6P receptors or other extracellular receptors that mediate organ uptake. On the other hand, prolonged enzyme levels in the circulatory system can diminish enzymatic activity due to blood's relatively high pH compared to the lysosome's, resulting in ineffective enzymes entering organs (14). Previous studies in lysosomal diseases suggest that prolonged activity levels of enzymes in the plasma, represented as a longer $t_{1/2}$ using enzyme activity, can increase the uptake of enzymes into organs (166, 185, 186). However, these methods to calculate the $t_{1/2}$ of activity were not well described.

A formal pharmacokinetic analysis using enzyme activity could elucidate mechanistic information on Linker T. Linker T's effects on enzyme activity, such as stabilization in the plasma, may be reflected in pharmacokinetic parameters such as the area under the curve (AUC) or half-life. If Linker T can stabilize the activity of iduronidase in the plasma, this finding could be applied to multiple lysosomal diseases by investigating other lysosomal enzymes' entry into organs. Lysosomal enzymes can be conjugated to the peptide form of Linker T or encoded alongside Linker T, facilitating ERT and gene therapy studies, respectively.

The **objective** of this study was to perform a pharmacokinetic analysis of iduronidase and Linker T iduronidase, which were both delivered as gene

therapies. The **hypothesis** was that Linker T iduronidase would have a higher AUC or longer half-life using enzyme activity than the normal iduronidase in the plasma. This study performs a pharmacokinetic analysis on a traditionally pharmacodynamic outcome (i.e., enzyme activity in gene therapy). This approach utilizes enzyme activity levels, one of the most important parameters for efficacy in gene therapy. This approach generates pharmacokinetic parameters that need to be interpreted in the context of gene therapy. Therefore, I integrate my scientific knowledge of gene therapy, lysosomal diseases, and pharmacokinetics to propose how different biological processes are reflected in time-enzyme activity curves and pharmacokinetic parameters.

5.1.1 Selection of Linker T Iduronidase

The Linker T iduronidase, which is encoded by Linker T+*IDUA*, was chosen out of the four fusion iduronidase enzymes tested in earlier experiments because Linker T+*IDUA* had a statistically significantly higher enzyme activity than the normal iduronidase enzyme in more organs and plasma than the other fusion iduronidase enzymes. Pepcan-12 + Linker T+*IDUA* and Linker S+*IDUA* each had a significantly higher enzyme activity than the normal enzyme in one location in the body.

5.1.2 Selection of Plasma and Liver

The plasma and liver were chosen as the sites of interest in the body. The liver is the site of enzyme production in this study because of the liver-specific hAAT promoter in the plasmids, as mentioned in Section 4.2.2. The plasma was chosen because of the mechanism of cross-correction in lysosomal enzymes, described in Section 1.2.

5.1.3 Rationale for Performing Pharmacokinetic Analysis on a Time Curve of Enzyme Activity

One of this study's goals was to assess the potential of lysosomal enzymes for uptake into the organs. The most well-known mechanism in lysosomal enzymes is mediated by extracellular receptors on organs, namely the M6P receptor.

One way to increase the uptake of enzymes into organs is to increase the amount of the enzyme, such as increasing the dose in ERT. Initially, adding more enzymes would increase the number of bound receptors. However, once all the receptors are occupied, adding additional enzymes has no benefit. This is because, in receptor-mediated transport, the uptake of an enzyme into a cell is limited by the number of available receptors on the cell's surface. Furthermore, high doses of ERT or gene therapy are challenging and expensive to produce and can increase the risk of immune responses.

Another way to enhance the uptake of enzymes into organs is to increase the number of receptors on the cell surface. For example, adrenaline has been reported to increase the expression of M6P receptors, but repeated administration of adrenaline poses clear safety risks (305). Mechanisms that affect the receptor's expression may have a greater risk of off-target effects. Increasing the expression of the M6P receptor would affect the transport of multiple different lysosomal enzymes.

Increasing the exposure of receptors to an enzyme, similar to the concept of AUC, may be another way to increase the uptake of enzymes into organs. If all the receptors on a cell's surface are already occupied, the freely circulating enzyme must wait for a free receptor to enter organs. Increasing the duration of an enzyme's circulation improves its chance of interacting with free receptors. One way to characterize the duration of an enzyme's circulation is to measure its half-life in the plasma. However, a long residence time in the blood can diminish the enzyme's activity, because of the blood's high pH relative to the lysosome,

resulting in ineffective enzymes entering organs (14). Previous studies have suggested that prolonged levels of enzyme activity in the plasma, quantified as $t_{1/2}$ of enzyme activity, can increase the uptake into organs in lysosomal diseases (166, 185, 186). However, the methods to quantify changes in enzyme activity levels over time are not well-described in these studies (185-188). There are no conversion factors, equations, no reference to a PK program, and the $t_{1/2}$ was reported when a 50% decrease in activity was not seen in graphs (185-188).

The half-life, and other parameters that reflect changes in a therapy over time in the body, are routinely quantified in the field of pharmacokinetics. Moreover, the PK field has rigorous, standardized, and reproducible methods for quantification that are used in the drug approval process. However, PK studies are challenging in gene therapy because gene therapy studies use different units that are not readily convertible. Furthermore, the classic absorption, distribution, metabolism, and elimination processes have yet to be adapted for biological therapies. Section 2.4 discusses the gap between the fields of lysosomal diseases/gene therapy and PK/PD in more detail.

In this study, I aimed to integrate the emphasis of efficacy from the field of lysosomal diseases/gene therapy with the rigorous, reproducible methods from the field of PK. Therefore, the activity levels of enzymes were chosen for pharmacokinetic analysis because enzyme activity is more predictive of efficacy than the physical levels of enzymes. An alternative method of performing PK analysis would be to link the physical levels of the enzyme to the activity levels. However, since plasmids encoding the enzymes were administered, this would require measuring and analyzing data of both DNA and physical enzyme levels at several points. Future studies will be aimed at creating comprehensive PKPD models for gene therapy using DNA levels, physical levels of enzymes, enzyme activity levels, and substrate levels.

5.1.4 Selection of Replicate Sampling

Replicate sampling was chosen in this study. There are three potential sampling strategies in pre-clinical PK studies: replicate sampling, staggered sampling, and serial sampling (306). Each of these sampling strategies is discussed below, followed by the rationale for choosing replicate sampling in this study.

In replicate sampling, each animal is used for one timepoint. For example, a mouse is used for 0.5 hours post-injection and no other timepoints. The test article is administered, animals are euthanized at their timepoint, and plasma and organs are collected. Replicate sampling is also referred to as discrete, endpoint, or terminal sampling (306). Since each animal is assessed at one timepoint, the concentration-time curve cannot be constructed in each animal, resulting in a sparse dataset. Instead, a composite concentration-time profile is formed by pooling data from multiple animals (306). Analysis requires specialized population pharmacokinetics modeling tools because the conventional determination of pharmacokinetic parameters for individuals cannot be performed (306). An advantage of replicate sampling is that large sample volumes can be collected (306). Replicate sampling may be necessary for sample types that require euthanasia of animals, e.g., whole organs. The main disadvantage of replicate sampling is the high number of animals needed in the study (306).

In staggered sampling, each animal contributes to multiple timepoints but not all timepoints. For example, one mouse has samples taken at 0.5 hour, 4 hour, and 24 hours; another mouse has samples taken at 1 hour, 8 hour, and 48 hours. Similar to sparse sampling, the sparse dataset requires specialized population pharmacokinetics modeling tools (306). An advantage of staggered sampling is that fewer animals are required than replicate sampling (306). One unique advantage of staggered sampling is that it allows for flexibility in study design, similar to adaptive randomization in clinical trials. Animals can be reallocated from timepoints with low inter-animal variability to timepoints with high

inter-animal variability, resulting in more precise parameter estimates without increasing the total number of animals needed (306).

In serial sampling, each animal contributes to all the timepoints. For example, one nonhuman primate has blood samples taken from 0.5 hours to 7 days. The intensive sampling allows concentration-time curves to be constructed in each animal (306). Thus, conventional pharmacokinetic modeling tools such as regression analysis can be performed (306). One advantage of serial sampling is the lower number of animals needed (306). A disadvantage of serial sampling is that the volume of samples is limited because each sample removes a portion of the injected dose.

In this study, replicate sampling was chosen because future experiments would assess the enzyme activity in organs. This would require obtaining organs at multiple timepoints, and obtaining organs is a terminal procedure. Furthermore, staggered sampling and serial sampling may alter enzyme levels in the plasma, potentially decreasing uptake into organs. Additionally, staggered sampling or serial sampling would have required fluid replacement to comply with UMN RAR guidelines for multiple blood draws in rodents. Fluid replacement would have decreased the concentration of enzymes in the plasma, decreasing uptake into organs.

5.1.5 Selection of Timepoints, Number of Timepoints, and Number of Mice

To generate a time profile of enzyme activity levels, several timepoints were needed: early timepoints to capture the ascending phase, timepoints near the approximate peak of activity, and multiple late timepoints to capture the descending phase activity. As this was the initial pharmacokinetic study of Linker T iduronidase, there was no known data on its $t_{1/2}$ or C_{max} of activity to guide the study design. Therefore, information from other studies was used to select the timepoints.

Although there is a recombinant form of iduronidase approved as ERT, laronidase, the half-life of laronidase was not used in this study design. Clinical studies of laronidase report its mean elimination $t_{1/2}$ to be either 0.3 to 1.9 hours or 1.5 to 3.6 hours in the plasma, depending on patients' ages (307). Two pre-clinical studies of laronidase in MPS I canines reported biphasic clearance in the plasma with even shorter half-lives (307). In the first study, one canine received 0.1 mg/kg on three consecutive days and had a "presumed distribution phase ($t_{1/2\ \alpha}$=0.9 minutes) and a slow clearance phase ($t_{1/2\ \beta}$=18.9 minutes)" (307). In the second pre-clinical study, two canines received a weekly intravenous infusion of 2 mg/kg for ten weeks (307). "At week 2, the initial decline in concentration was very rapid with α t½ = 0.61 and 0.94 minutes; the second, terminal phase was slower with β t ½ = 59.5 and 84.9 minutes. At week 10, the concentration declined monophasically with terminal half-lives of 66.2 and 23.8 minutes, respectively, in the two dogs... The reasons for these changes are not known" (307). Laronidase's $t_{1/2}$ may have been calculated using physical enzyme levels (307). Additionally, $t_{1/2}$ of laronidase appeared too short for approximating Linker T iduronidase because Linker T iduronidase had high activity levels in the plasma at 48 hours. This can be explained by their considerably different method of delivery. More specifically, laronidase is infused intravenously as an enzyme. In contrast, Linker T iduronidase is delivered as a plasmid which requires certain biological processes to occur before its activity levels can be detected in the plasma, such as cell transfection, gene expression, post-translational modification, and distribution from the liver to the plasma. Therefore, enzymes administered as gene therapies would have delayed time courses than ERT, therefore a PK study for Linker T duronidase would require later timepoints than the ones used for laronidase.

While there are several gene therapy studies for MPS I, there were challenges in using these studies to design a pharmacokinetic study. In studies that measured enzyme activity levels in the plasma at multiple timepoints, gene therapy constructs were intended for life-long expression such as AAV or

lentivirus (183, 236, 271, 276, 308). In contrast, gene therapy constructs with plasmids, such as the one used in this study, are expected to have short-term expression. However, MPS I studies with plasmids only assessed activity levels at one timepoint (270, 271). Furthermore, gene therapy studies used different promoters, transgenes, and doses, which could also affect the pharmacokinetic profile.

The timepoints chosen in this study were based on a previous study by Liu et al. that had the most similar study design. These timepoints were adapted using suggestions on pre-clinical PK studies (274, 306, 309). In the study by Liu et al., plasmids were hydrodynamically injected and enzyme levels were measured over time in mice (274). Mice were hydrodynamically injected with 10 µg of a plasmid encoding the gene for the luciferase enzyme under either the hAAT promoter or cytomegalovirus (CMV) promoter (274). The luciferase levels were then measured at the timepoints of 2, 4, 8, 24, 72, and 144 hours in the heart, lung, liver, kidney, and spleen (274). The luciferase levels are reported as physical levels, which were derived from measuring the luciferase enzyme activity (274). Luciferase levels were detected as early as 2 hours, peaked at around 8 hours, and declined afterward (274). The decline in the rate of luciferase levels varied among organs (274). At 144 hours, luciferase levels in the heart, lung, kidney, and spleen were at the background level. In contrast, the liver still had detectable luciferase levels (274). Similar patterns were seen in both promoters (274).

In this study, the timepoints of 0.5, 1, 2, 4, 8, 12, 24, 48, 72, 96, and 168 hours post-injection were chosen. In Liu et al. transgene expression occurred before 2 hours post-injection (274). Therefore, the 0.5 hour and 1 hour post-injection times were included in this study. The earliest timepoint, 0.5 hour, was based on the workflow time needed for dissections. A 12 hour post-injection was included in this study to better characterize when the enzyme levels peaked. The 48, 96, and 168 hours post-injection were included in this study to characterize

the elimination phase. At 168 hours, the enzyme activity levels were expected to be undetectable in the plasma and non-liver organs.

Three to four mice were allotted to each timepoint. Three to five mice per timepoint was recommended in a review for pre-clinical PK studies (306). Having five mice per timepoint was considered, but the number of animals per timepoint needs to be balanced with the number of timepoints to maintain the study's feasibility. Since this was the first PK study for Linker T iduronidase, data from more timepoints would be more helpful than more mice per timepoint. This is because data from more timepoints can be used to refine timepoints in future PK studies. Four mice were randomized to each timepoint, with the expectation that there would be three to four mice per timepoint.

5.2 Methods

5.2.1 Experimental Design

Table 4 summarizes the design for the pharmacokinetics study and outlines this study's differences from the study with iduronidase and Linker T iduronidase.

Table 4: The Pharmacokinetic Study Design and its Differences from the Previous Study with Iduronidase and Linker T Iduronidase

Study Design	**Previous Fusion Enzyme Study**	**Pharmacokinetic Study**
Plasmid/ Enzyme Tested	*IDUA*, Pepcan-12 + Linker S + *IDUA*, Pepcan-12 + Linker T + *IDUA,* Linker S + *IDUA,* Linker T + *IDUA*	*IDUA*, Linker T+ *IDUA*
Time of Sample Collection	One timepoint (48 hours post-injection)	Multiple timepoints (0.5, 1, 2, 4, 8, 12, 24, 48, 72, 96, and 168 hours post-injection)*
Blood Collection	Live mice, blood collection from facial vein	Euthanized mice, blood collected using cardiac puncture
Sample Processing	Organs were homogenized using either rotor-stator or bullet blender	Organs were homogenized using only bullet blender
Quantification of Activity Levels of Iduronidase Enzyme (Fusion and normal iduronidase)	Assessed in brain, heart, lung, liver, spleen, kidney, and plasma	Assessed in the liver and plasma
Quantification of Physical Levels of Iduronidase Enzyme (Fusion and normal iduronidase)	Not assessed	Assessed in the liver using ELISA
Statistical Methods	One-way ANOVA, Pearson's correlation	PK analysis, Pearson's correlation

**For MPS I mice treated with Lactated Ringer's or heterozygotes, blood and organs were not collected at all timepoints*

5.2.2 Dose

A dose of 50 µg of plasmid was used in this study, the same dose used in the previous study with iduronidase and Linker T iduronidase. The dose remained the same for two reasons. The first reason was to maintain consistency between the two studies. Different doses may have resulted in differences in the enzyme activity kinetics. The second reason was that a different study using hydrodynamic injections saw that doses greater than 25 µg of plasmids did not increase the transgene's protein levels in the heart, liver, spleen, and lung when measured 8 hours post-injection (274). The dose of plasmids that causes saturation of gene expression in the kidneys was not clear because the kidneys still exhibited an increase in gene expression at the highest dose tested, which was 25 µg (274).

5.2.3 Quantification of Physical Levels of Enzymes using ELISA

An ELISA was used to quantify the physical level of normal iduronidase and Linker T iduronidase present in liver samples. The general principle of a sandwich ELISA is described below, followed by the rationale for the ELISA chosen in this study.

The general principles of an indirect sandwich ELISA are as follows. In ELISA, antibodies are used to detect the presence of an antigen, typically a protein antigen. There are four types of ELISA: direct, indirect, sandwich, and competitive. Antibodies that are specific for the antigen are attached to a solid phase, typically a microplate (310). Commercially available ELISA kits may perform this step and provide plates that are pre-coated with an antibody. Samples are added, and the antigens present in the samples bind to the coated antibodies (310). Unbound antigens are washed away (310). A second set of antibodies are added, which will be called biotin-conjugated antibodies. These antibodies are also specific for the antigen but are conjugated to a molecule,

such as biotin (310). These biotin-conjugated antibodies bind to the antigen, and the antigen is now sandwiched between two antibodies. Unbound biotin-conjugated antibodies are washed away (310). A third set of antibodies are added, for example, horseradish peroxidase (HRP)-conjugated antibodies. These antibodies are conjugated to avidin and an enzyme that catalyzes a detectable reaction like HRP. The HRP-conjugated antibodies bind to the biotin-conjugated antibodies via a biotin-avidin interaction. These HRP-conjugated antibodies are washed away (310). Then a chromogenic substrate for the enzyme is added, such as 3,3',5,5'-tetramethylbenzidine (TMB) for the HRP enzyme. A colorimetric reaction occurs, the reaction is stopped, and the change in color can be quantified using a spectrophotometer (310).

In this study, a commercially available kit for human iduronidase was used for sandwich ELISA (abx253700, Abbexa®) (311). This ELISA kit was chosen over other commercially available assays because both sets of antigen-specific antibodies did not recognize near the N-terminal of iduronidase. The antigen-specific antibodies recognized the 100 to 306 amino acid residues of UniProt P35475 (273). This allowed the kit to be used for both normal iduronidase and Linker T iduronidase. Furthermore, this kit was compatible with plasma and tissue homogenates (311). The kit had a sensitivity of 0.1 ng/mL and a range of 0.156 ng/mL and 10 ng/mL (311).

Liver samples from mice treated with *IDUA* and Linker T+*IDUA* were used for ELISA. Livers were homogenized as described in Section 4.2.4. One mouse from each plasmid-treated group was assessed at the 0.5, 1, 2, 4, 8, and 12 hours post-injection. Two mice from each plasmid-treated group were assessed at 24, 48, 96, and 168 hours post-injection.

ELISA was performed per the manufacturer’s instructions which is described in this paragraph (abx253700, Abbexa®) (311). The kit components and samples were equilibrated to room temperature (18-25 °C) (311). Standards and samples were measured in duplicate (311). A 100 µL of each standard,

control, and sample were added into the appropriate wells (311). The plate was sealed with a cover and incubated for 1 hour at 37°C (311). The cover was removed, and the liquid was discarded (311). A 100 µl of the Detection Reagent A working solution was added to each well (311). The plate was sealed with a cover and incubated for 1 hour at 37°C (311). The cover was removed, and the solution was discarded (311). The plates were washed three times with 1X Wash Buffer (311). A 100 µL of Detection Reagent B working solution was added to each well, sealed, and incubated at 37°C for 30 minutes (311). The solution was discarded, and plates were washed five times with wash buffer (311). A 90 µl of TMB Substrate was added into each well (311). Plates were sealed with a cover and incubated at 37°C for 10 to 20 minutes while avoiding exposure to light (311). A 50 µL of Stop Solution was added to each well (311). The plate was read at 450 nm immediately afterward (311). The optical density at 450 nm were averaged for the control wells and subtracted from the average optical density at 450 nm for each of the reference standard and sample (311). The standard curve was plotted with the concentration of each standard solution on the X axis and the relative optical density at 450 nm for the reference standard solution on the Y axis (311). The concentration of iduronidase in the samples were interpolated from the standard curve (311).

5.2.4 Pharmacokinetic Analysis Using Noncompartmental Analysis

A noncompartmental analysis (NCA) of enzyme activity levels in the plasma and liver was performed for mice treated with *IDUA* and Linker T+*IDUA.* NCA was performed using Phoenix® 64 (Phoenix 64, Build 8.3.3.33, Certara L.P., 100 Overlook Center, Suite 101, Princeton, NJ 08540 USA). The below quantification limit (BQL) was inputted for samples with fluorescence readings less than twice the “blank” wells. The lower limit of quantification (LLOQ) was substituted for BQL for the conditions before T_{max}, after T_{max}, and the first

consecutive after T_{max}. The LLOQ value for enzyme activity in plasma was 0.93 nmol/h/mL, which was calculated from “blank” wells. The LLOQ value for enzyme activity in the liver was 2.20 nmol/h/mg, which was calculated from “blank” wells in the enzyme activity assay and Pierce protein assay.

For the therapeutic response settings, a lower boundary was set, which was the average levels from heterozygous mice. The lower boundary represented the minimum enzyme activity needed for efficacy and thus minimum effective concentration (MEC). The lower boundary of 6.10 nmol/h/mL for enzyme activity in the plasma. The lower boundary was 3.89 nmol/h/mg for enzyme activity in the liver.

The NCA model type of plasma (200-202) was chosen for the enzyme activity in the plasma and the liver. Nominal timepoints and uniform weighting were used because of sparse sampling. In sparse sampling, the NCA object takes the mean concentration value for each unique time value for data and calculates the mean concentration curve of the data. The mean concentration curve is used to calculate the parameters. A dose of 50 µg was entered, but this value did not affect the pharmacokinetic parameters chosen in this study. The following pharmacokinetic parameters were calculated: T_{max} of activity, C_{max} of activity, Lambda_z (reported as k_e of activity), HL_Lambda_z (reported as $t_{1/2}$ of activity or half-life of enzyme activity), AUC_{last} (reported as $AUC_{0\text{-}168\ hours}$ of activity), AUCINF (AUC from time of dosing extrapolated to infinity based on last observed concentration; reported as $AUC_{0\text{-}\infty}$ of activity), TimeHigh (reported as $Time_{above\ MEC}$ of activity), AUCHigh (reported as $AUC_{above\ MEC}$ of activity).

A linear trapezoidal-linear extrapolation method was used to calculate the AUC of enzyme activity in the plasma and the liver. A linear-linear method was chosen because Bailer’s method, with modifications described by Phoenix, was planned to compare the AUC of activity between enzymes (312-314). Bailer’s method allows testing of equality in AUCs in study designs that use destructive measurements, and Bailer’s method relies on AUCs calculated by linear

trapezoidal rules (312). The AUC of activity's mean and standard error of the mean was obtained from Phoenix. Phoenix calculates the AUC's standard error of the mean using Bailer's method with modifications from Nedelman and Jia's 1998 publication and Holder's 2001 published comment (312-314). The AUC of activity's mean and standard error of the mean were then entered into GraphPad to perform an unpaired, two-tailed t-test to compare the AUC of activity between enzymes.

To calculate k_e and $t_{1/2}$ of enzyme activity levels in the plasma, 24 to 168 hours were used to calculate a slope. The rationale for choosing the 24 to 168 hours is discussed in Section 5.4.1.1. From k_e of activity, $t_{1/2}$ of activity was calculated using the equation $t_{1/2}$ of activity = 0.693*k_e of activity. The k_e and $t_{1/2}$ of activity using only the 96 and 168 hours were also calculated. The timepoints of 96 and 168 hours were chosen because Linker T+*IDUA* appeared to be going through a different phase at 48 hours and to maintain consistency with *IDUA.* The rationale for calculating $t_{1/2}$ for two different time ranges are included in the discussion.

Graphs were generated with GraphPad Prism version 9.2.0 for Windows, GraphPad Software, San Diego, California USA, www.graphpad.com.

5.2.5 Non-Pharmacokinetic Statistical Analysis

Pearson's correlation test was performed for the enzyme's physical levels in the liver and the enzyme's activity levels in the liver for mice treated with *IDUA* and Linker T+*IDUA*. Pearson's correlation tests were performed using GraphPad Prism version 9.2.0 for Windows, GraphPad Software, San Diego, California USA, www.graphpad.com.

5.3 Results

5.3.1 Age and Gender of Mice at Each Timepoint

There was a total of 79 mice in this study, including the four mice injected with Lactated Ringer's and four heterozygotes. The age, gender, and number of plasmid-treated mice at each timepoint are shown in Table 5. At each timepoint, there were three to four mice in each plasmid-treated group. In general, age and gender were balanced with the following exceptions. Mice in the 0.5 hour and 1 hour timepoints were approximately two weeks older than other timepoints. Mice in the Linker T+*IDUA* group were approximately two weeks older than the *IDUA* group at the 2 hours and 8 hours timepoints. The *IDUA* group at 1 hour had a higher percentage of females, and the Linker T+*IDUA* group at 96 hours had a higher percentage of males. The four mice in the Lactated Ringer's group had a mean age of 7.6 weeks and were 50% female. The four mice in the heterozygous group had a mean age of 9.5 weeks and were 50% female.

Table 5: Age, Gender, and Total Number of Plasmid-Treated Mice at Each Timepoint

	Mean age at sample collection in weeks		**Percent of females**		**Total number of mice**	
Time post-injection (hours)	**IDUA**	**Linker T + IDUA**	**IDUA**	**Linker T + IDUA**	**IDUA**	**Linker T + IDUA**
0.5	10.9	11.1	50%	33.3%	4	3
1	10.9	11.2	75%	66.7%	4	3
2	8.4	10.2	50%	33.3%	4	3
4	7.9	8.6	33.3%	66.7%	3	3
8	8.1	10.1	50%	66.7%	4	3
12	7.6	7.9	50%	66.7%	4	3
24	8.6	8.0	66.7%	50%	3	4
48	7.9	9.2	50%	33.3%	4	3
96	8.8	8.7	50%	25%	4	4
168	9.4	9.5	25%	50%	4	4
All timepoints	8.9	9.4	50%	48.5%	38	33

5.3.2 Physical Levels of Enzymes Over Time in the Liver

The physical levels of iduronidase and Linker T iduronidase in the liver appeared similar from 8 to 168 hours post-injection (Figure 20). Only timepoints from 8 to 168 hours post-injection were shown in the figure because earlier timepoints had absorbance readings outside the standard curve.

Figure 20: Physical Levels of Enzymes in the Liver Over Time

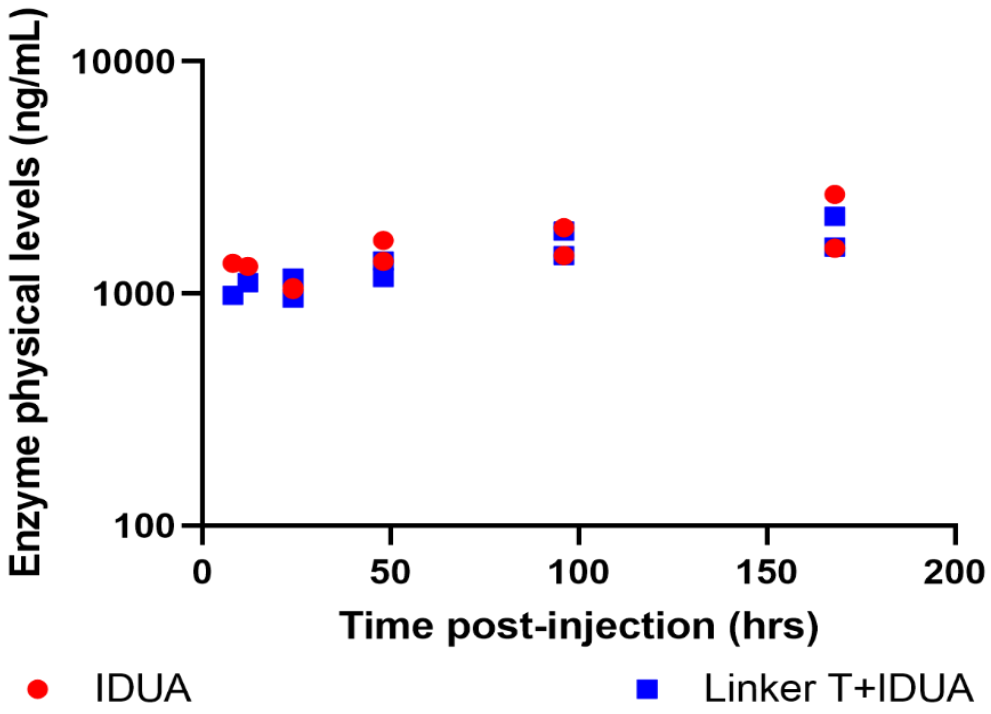

Each symbol represents one mouse. The physical levels of enzymes in the liver were measured using ELISA.

The enzyme's physical levels in the liver were compared to its activity levels in the liver (Figure 21). There was no correlation between the enzyme's physical levels in the liver and its activity levels in the liver for either the *IDUA* or Linker T+*IDUA* group (*IDUA* r^2=0.05341, p=0.5206; Linker T+*IDUA* r^2=0.01666, p=0.7223).

Figure 21: Relationship of Physical Levels of Enzymes in the Liver and Enzyme Activity Levels of Enzymes in the Liver

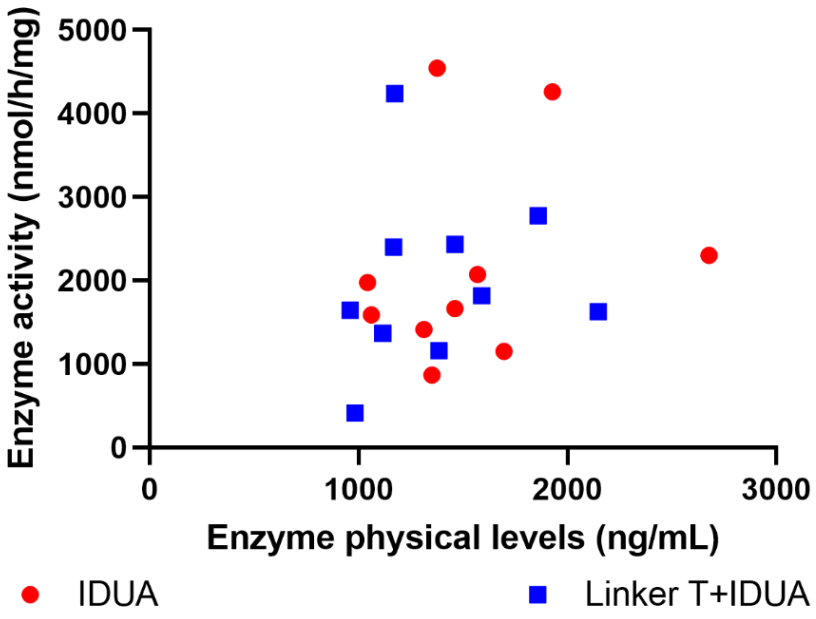

Each symbol represents one mouse. Timepoints from 8 hours to 168 hours post-injection were used for analysis because earlier timepoints yielded absorbance readings outside the standard curve.

5.3.3 Enzyme Activity Levels Over Time in the Liver

The iduronidase and Linker T iduronidase activity levels in the liver were similar over time (Figure 22). The parameters from the pharmacokinetics analysis

are presented in Table 6. Both enzymes had no detectable activity levels until 4 hours post-injection. Both enzymes' activities peaked at 48 hours and were steady afterward. Both enzymes had high activity levels at 168 hours post-injection. The AUC of activity was similar between the two enzymes ($p=0.6372$). The k_e and half-life of activity could not be calculated because there were no negative slopes.

Figure 22: Enzyme Activity Levels Over Time in Liver

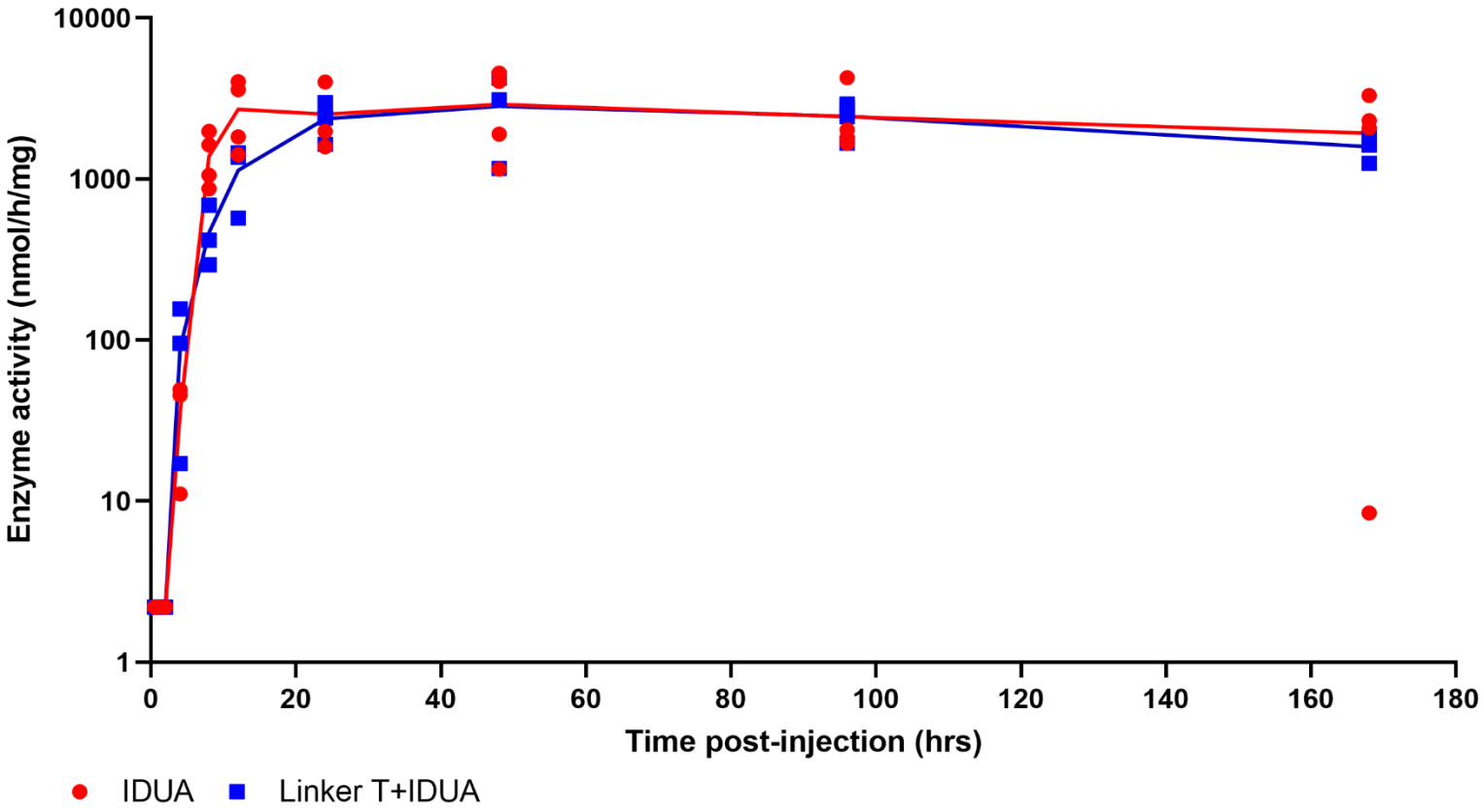

Each symbol represents one mouse. The line is the mean enzyme activity for a timepoint. Standard deviation bars are not shown in the figure because each timepoint had three to four mice per group. The LLOQ value was 2.198 nmol/h/mg.

Table 6: Pharmacokinetics of Enzyme Activity Levels in the Liver

Treatment	T_{max} (hr)	C_{max} (nmol/h/mg)	$AUC_{0\text{-}168\ hours}$ (hr*nmol/h/mg)	$Time_{above\ MEC}$ (hr)	$AUC_{above\ MEC}$ (hr*nmol/h/mg)
IDUA	48	2908.25	393168.77	165.90	392518.95
Linker T + IDUA	48	2835.88	360217.10	165.96	359567.22
			p=0.6372		

Pharmacokinetic analysis was performed using enzyme activity levels.

5.3.4 Enzyme Activity Levels Over Time in the Plasma

In the plasma, Linker T iduronidase had higher activity than iduronidase from 24 to 168 hours post-injection. The enzyme activity levels in the plasma over time are shown in Figure 23, and the exact values are in Table 8. The pharmacokinetic analysis is shown in Table 8. Both enzymes had no detectable enzyme activity levels until 4 hours post-injection. Iduronidase activity peaked at 8 hours, and Linker T iduronidase activity peaked at 12 hours. Iduronidase had a higher peak activity level than Linker T iduronidase. Beginning at 12 hours post-injection, a clear separation between the two enzymes' activity levels can be seen. Linker T iduronidase had a smaller decline (less negative slope) between 12 and 48 hours post-injection. Between 96 and 168 hours post-injection, Linker T iduronidase and iduronidase had similar declines (parallel slopes). When half-lives of activity were calculated using the 24 and 168 hours, the half-lives of activity were similar between enzymes. However, the Linker T iduronidase had a two-fold higher AUC of activity than the normal iduronidase, which was statistically significant ($p=0.0034$). The MEC of activity was defined as the enzyme activity level in heterozygotes. $\text{Time}_{\text{above MEC}}$ of activity were similar between the two enzymes, but the Linker T iduronidase had a two-fold higher $\text{AUC}_{\text{above MEC}}$ of activity.

Figure 23: Enzyme Activity Levels Over Time in Plasma

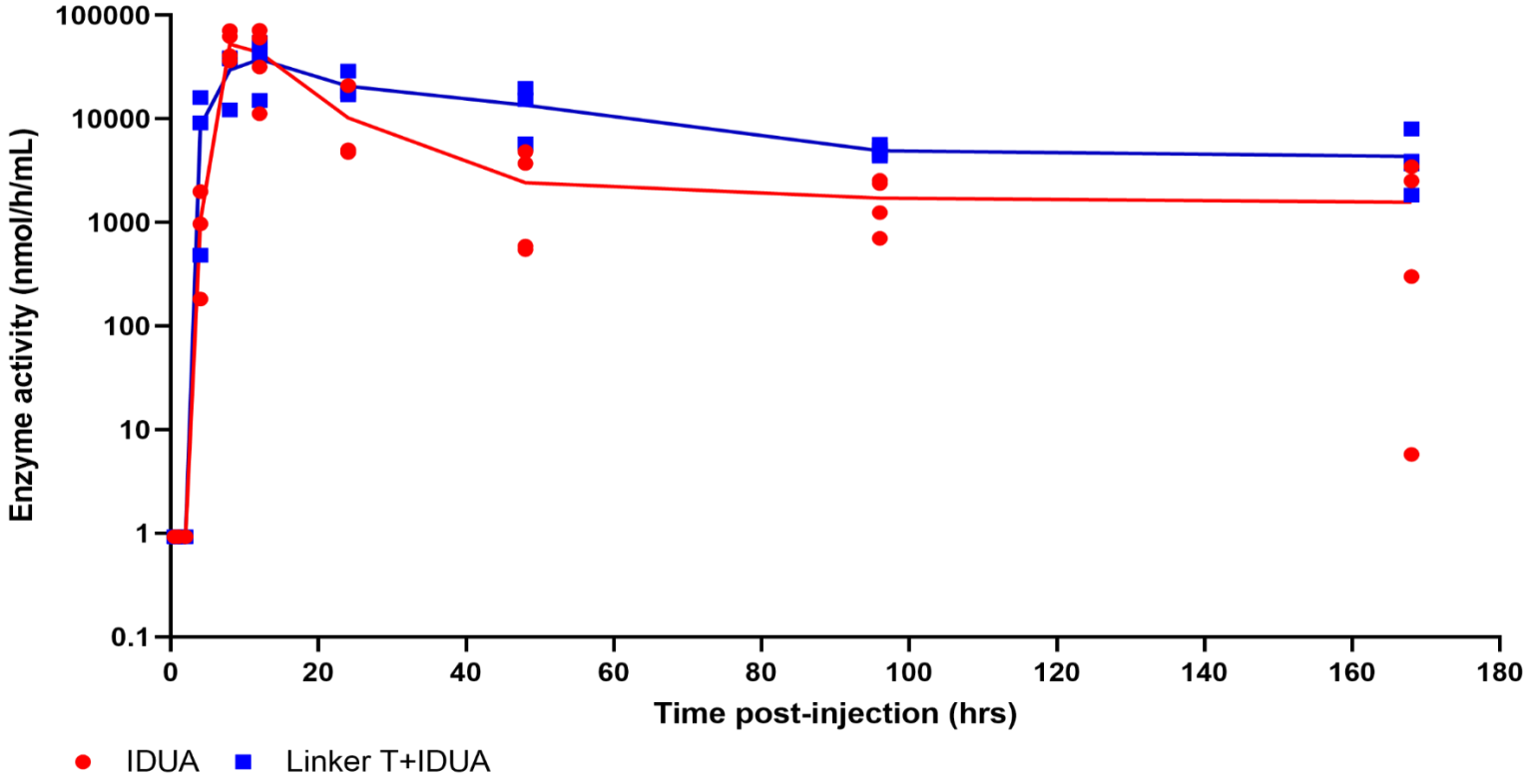

Each symbol represents one mouse. The line is the mean enzyme activity. Standard deviation bars are not shown in the figure because each timepoint had three to four mice per group. Standard deviations are in Table 6. The LLOQ value was 0.926 nmol/h/mL.

Table 7: Enzyme Activity Levels Over Time in the Plasma (Exact Values)

	Plasmid			
	IDUA		Linker T + IDUA	
Time post-injection (hours)	**Mean (nmol/h/mL)**	**SD**	**Mean (nmol/h/mL)**	**SD**
0.5	0.93	0	0.93	0
1	0.93	0	0.93	0
2	0.93	0	0.93	0
4	1046.56	903.01	8581.39	7833.05
8	52717.78	16902.84	29718.45	15147.67
12	43831.24	27506.93	37624.96	20421.59
24	10226.86	9274.89	20645.78	5564.81
48	2423.87	2188.68	13620.37	7142.28
96	1716.07	888.09	4941.72	583.67
168	1571.69	1686.65	4356.35	2602.53

The mean and standard deviation (SD) values of the enzyme activity levels in the plasma are reported. The LLOQ value was 0.926 nmol/h/mL.

Table 8: Pharmacokinetics of Enzyme Activity Levels in the Plasma

Treatment	T_{max} (hr)	C_{max} (nmol/h/mL)	k_e (1/hr)	$t_{1/2}$ (hr)	$AUC_{0\text{-}168\ hours}$ (hr*nmol/h/mL)	$AUC_{0\text{-}\approx}$ (hr*nmol/h/mL)	$Time_{above\ MEC}$ (hr)	$AUC_{above\ MEC}$ (hr*nmol/h/mL)
IDUA	8	52717.78	0.0105	66.03	995551.23	1145347.65	165.99	994537.88
Linker T + IDUA	12	37624.96	0.0110	63.10	1760909.40	2157474.36	166.00	1759896.02
					p=0.0034			

*Pharmacokinetics analysis was performed using enzyme activity levels. This table reports the k_e, $t_{1/2}$, and $AUC_{0\text{-}\approx}$ using 24 to 168 hours. When only the 96 and 168 hours are used, the k_e was 0.00122 1/hr for IDUA and 0.00175 1/hr for Linker T+IDUA. The $t_{1/2}$ using only 96 and 168 hours was 567.83 hr for IDUA and 395.83 hr Linker T+IDUA. The $AUC_{0\text{-}\approx}$ using 96 and 168 hours are 2283093.03 and 4248687.12 hr*nmol/h/mL for IDUA and Linker T+IDUA, respectively.*

5.4 Discussion

The **objective** of this study was to perform a pharmacokinetic analysis of iduronidase and Linker T iduronidase that were delivered as gene therapies. The **hypothesis** was that Linker T iduronidase would have a higher AUC or longer half-life of enzyme activity than the normal iduronidase in the plasma. The Linker T iduronidase had a two-fold higher AUC of activity in the plasma than the normal iduronidase. The Linker T iduronidase and iduronidase had similar half-lives of activity when estimated with the 24 to 168 hours, as well as the 96 to 168 hours, because NCA was used for a biphasic process. In the next section, I provide reinterpretations of these traditional PK parameters in the context of gene therapy by integrating my scientific knowledge of PK, gene therapy, and lysosomal diseases.

5.4.1 Integration of Principles from Pharmacokinetics and Gene Therapy

In this study, I performed a PK analysis directly on enzyme activity levels after gene therapy was administered. In this section, I interpreted the PK parameters generated from this approach by integrating concepts from PK, gene therapy, and lysosomal diseases. I also adapt some of the traditional PK processes of absorption, distribution, metabolism, and elimination for gene therapy. The following three figures show a time course profile for a part of the body that is important in gene therapy: site of gene expression (Figure 24), circulatory system (Figure 25), and the desired site of action (Figure 26). Hypothetical data was used for Figure 24, Figure 25, and Figure 26 to discuss parameters that could not be quantified using NCA, such as k_a. Furthermore, certain phases worthy of discussion did not occur in this study, such as the descending phase in the liver. Importantly, the interpretation of these PK phases and parameters will vary greatly with respect to the body's site.

Figure 24: Application of Pharmacokinetic Principles to Gene Therapy in the Host Organ

Time Profile in a "Host" Organ Expressing the Gene Therapy (E.g., Liver)

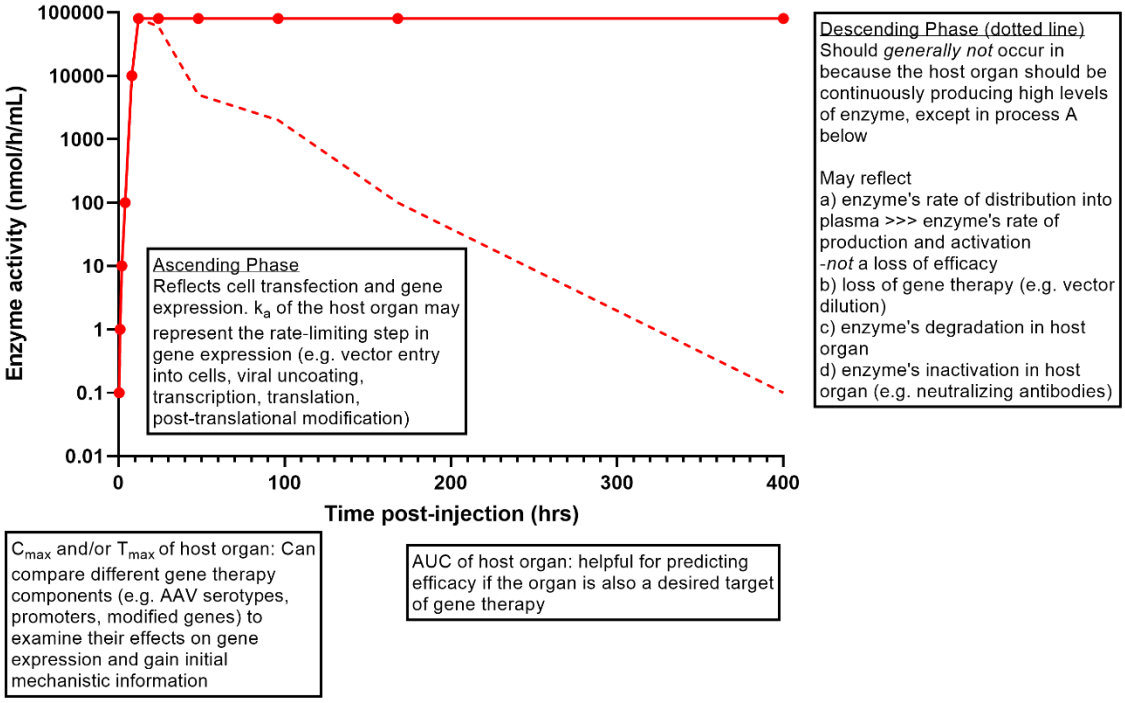

In Figure 24, the host organ is the site of gene expression. The site of transgene expression is primarily dictated by the promoter. In this study, the liver was the host organ because the hAAT promoter was used. If a ubiquitous promoter like CMV is used, there are multiple host organs. The host organ may also be the desired site of action, such as the liver in this study. In these instances, the AUC of activity in the host organ may be helpful to predict long-term efficacy. In general, pharmacokinetic parameters of the host organ may be helpful for supplementing mechanistic information gained from cellular-level studies, such as intracellular kinetics.

Figure 25: Application of Pharmacokinetic Principles to Gene Therapy in the Circulatory System

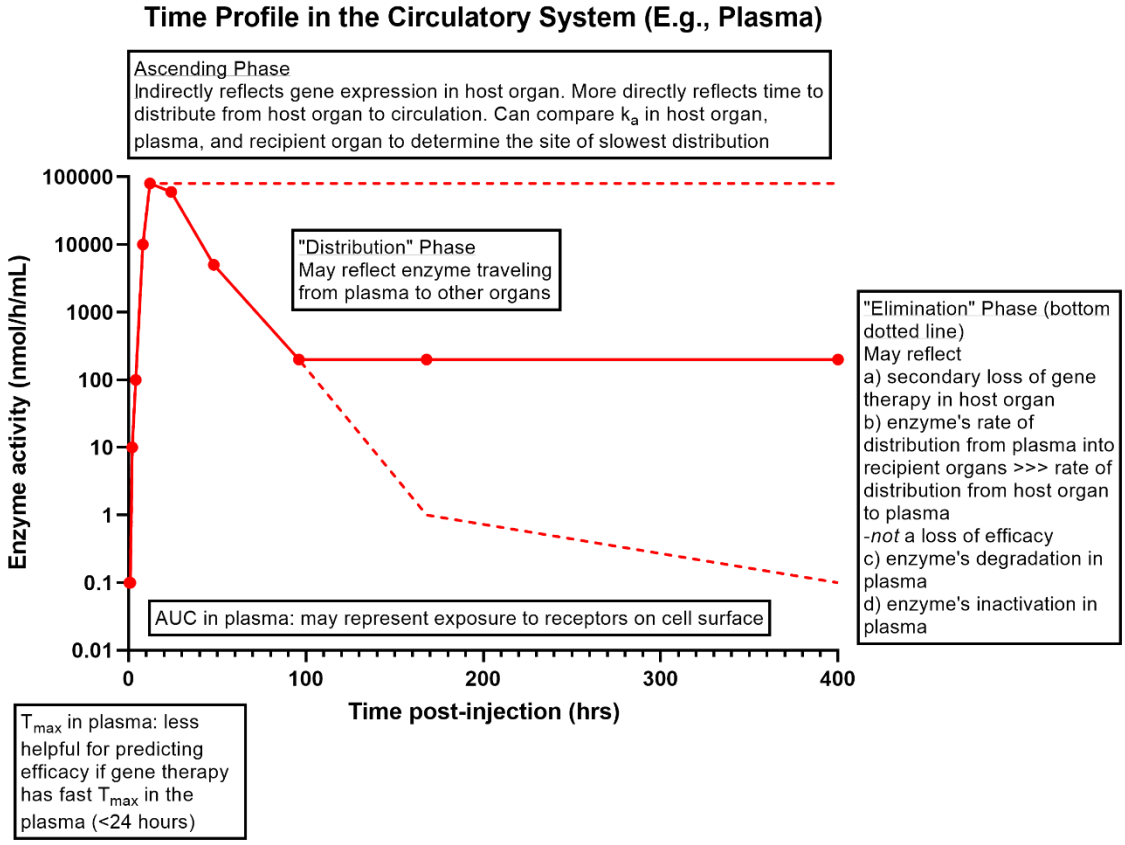

Lysosomal enzymes can distribute from the host organ to the desired site of action using the circulatory system (Figure 25). Enzyme activity levels in the circulatory system can be measured from the serum or plasma samples, which are common in clinical and pre-clinical studies in lysosomal diseases, respectively. The pharmacokinetic parameters and different phases in the plasma indirectly reflect the changes in the host organ. For example, if the gene therapy is degraded in the liver, this would cause a downstream decrease in enzyme activity levels in the plasma. Additionally, the descending phase in the plasma may also reflect degradation and/or inactivation of the enzyme in the recipient organ through target-mediated drug disposition (197).

In previous studies in lysosomal diseases or gene therapy, a decline in enzyme activity levels in the plasma has been interpreted as diminished therapeutic efficacy (185, 189). However, pharmacokinetic profiles of multicompartmental therapies, like gene therapy, would be expected to have a descending phase in the plasma because it requires distribution into organs to have a therapeutic effect. Further declines in activity levels in the plasma, like an "elimination phase," may even be theoretically possible, if the enzyme's rate of distribution from the plasma into recipient organs is much faster than the rate of distribution from the host to plasma. Therefore, a descending phase in the plasma per se would not necessarily indicate a loss of therapeutic efficacy.

In pharmacokinetics, the AUC represents the body's total exposure to the drug. Therefore, the AUC of activity in the plasma may reflect the receptors' exposure to the enzyme. For lysosomal enzymes, this may include the M6P receptor that has a well-known function of transporting enzymes from the circulatory system and into organs. However, the interpretation of AUC must be carefully considered in the context of other data. On the one hand, a high AUC in the plasma can be caused by biological processes that enhance efficacy. For example, a linker that stabilizes the enzyme's activity may cause higher activity levels in the plasma for a longer period of time, increasing the AUC of plasma activity. On the other hand, a high AUC in the plasma can also be caused by biological processes that diminish efficacy. For example, a high AUC of plasma activity can be caused by decreased uptake of enzymes into organs, which diminishes efficacy. In the next section, I will discuss the biological processes that can impact the AUC of plasma activity in the context of Linker T Iduronidase.

5.4.1.1 Interpretation of Linker T Iduronidase's Higher AUC of Enzyme Activity in the Plasma

In this study, the Linker T iduronidase had a two-fold higher AUC of activity in the plasma than the normal iduronidase. In general terms, AUC is impacted by the amount of drug and the clearance of the drug. AUC has the general equation of AUC = Dose / Clearance. When we consider AUC in the context of gene therapy and enzyme activity, multiple biological processes can impact AUC. These processes are divided as factors that would increase "dose" and factors that would decrease the "clearance." These biological factors and their possibilities of occurring in Linker T iduronidase are discussed below.

Biological processes that correspond to the concept of a higher effective "dose" of Linker T iduronidase in the plasma, which would ultimately cause a higher AUC of plasma activity

- Higher production of the enzyme in the liver (e.g., greater transfection efficiency or higher gene expression in the liver)
    - Unlikely to occur in Linker T iduronidase because both Linker T iduronidase and iduronidase had similar physical levels in the liver
- Increase in enzyme activity specifically in the liver (e.g., post-translational modification in hepatocytes)
    - Unlikely to occur for Linker T iduronidase because both enzymes had similar activity levels in the liver
- Higher distribution of an enzyme from the liver to the plasma
    - Possible explanation for Linker T iduronidase's mechanism. Assuming all other factors are the same between the enzymes in the plasma and other organs, a higher distribution from the liver to the plasma should theoretically cause downstream higher activity levels in at least some organs. One supporting evidence is that

Linker T iduronidase had higher activity levels than the native iduronidase in the heart at 48 hours in Chapter 4.

- Increase in enzyme activity, specifically in the plasma
    - It is uncertain whether this occurs in Linker T iduronidase. This explanation/mechanism is consistent with the results from this chapter and Chapter 4. In the pharmacokinetic study, both enzymes have similar activity levels over time in the liver, and Linker T iduronidase has higher activity levels in the plasma. Similarly, in Chapter 4, both enzymes had similar activity levels in the liver, and Linker T iduronidase had higher activity levels in the plasma. However, there is currently no known biological process that would increase a lysosomal enzyme's activity level in the plasma without affecting its levels in the host organ (e.g., liver). One theoretical possibility might be a change in protein folding, possibly from the blood's pH. However, this or other biological processes that increase the activity of Linker T iduronidase in the plasma would have to offset the decreased activity caused by the relatively high pH in the blood.
- Production of enzyme from non-liver organs
    - Unlikely explanation for Linker T iduronidase's mechanism. Theoretically, a higher activity could be seen in the plasma and not the liver, if there was higher production of enzymes from non-liver organs. This explanation seems unlikely in this study because both enzymes were expressed from the liver-specific hAAT promoter (188, 274, 275, 315). The hAAT promoter causes a 1000-fold higher expression of the luciferase gene in the liver compared to other organs (e.g., heart, kidney, spleen) (274, 315). Additionally, the time profiles of luciferase levels in non-liver organs exhibit ascending and descending phases that appear parallel to the liver's (274). Although these results are for luciferase and not a lysosomal

enzyme, the liver-specificity of the hAAT promoter is harder to ascertain from studies with lysosomal enzymes due to cross-correction.

Biological processes that correspond to the concept of a lower effective "clearance" of Linker T iduronidase in the plasma, which would ultimately cause a higher AUC of plasma activity

- Decreased uptake of enzyme into organs (Note: would correspond to lower efficacy)
    - Unlikely to occur in Linker T iduronidase because Chapter 4's results showed Linker T iduronidase had higher activity levels than iduronidase in the heart at 48 hours post-injection. Furthermore, other organs had similar activity levels of Linker T iduronidase and iduronidase at 48 hours.
- Decreased elimination and/or decreased inactivation of enzyme in the plasma
    - Likely explanation for Linker T iduronidase's mechanism. Decreased inactivation would be seen as sustained activity of Linker T iduronidase in the plasma (e.g., less negative slope). Figure 23 shows a biexponential profile in both enzymes. Linker T iduronidase had a smaller decline (less negative slope) between 12 and 48 hours post-injection. Between 96 and 168 hours post-injection, Linker T iduronidase and iduronidase had similar declines (parallel slopes). Decreased elimination should be reflected as a higher $t_{1/2}$ of activity. However, in this study, enzymes had similar calculated $t_{1/2}$ of activity, because NCA was applied to a biphasic profile, and later timepoints are needed to capture the terminal elimination phase. NCA and $t_{1/2}$ of activity are discussed further in the next paragraph.

NCA calculates one $t_{1/2}$, and the biological processes reflected in this $t_{1/2}$ of activity depend on the chosen timepoints. Based on the shape of the curves in Figure 23, distribution appears to predominate between approximately 24 to 48 hours post-injection, and elimination between 96 and 168 hours. One purpose of measuring enzyme activity levels in the plasma is to associate it with distribution into organs (i.e., the desired sites of action). Therefore, using the 24 to 168 hours to calculate the $t_{1/2}$ of activity would provide some information about the distribution of enzymes from the plasma to recipient organs. If 24 to 168 hours were used to calculate one $t_{1/2}$ of activity, this $t_{1/2}$ would combine information about the distribution and elimination processes. This $t_{1/2}$ of activity from NCA would describe how the activity disappears from the plasma but would not be specific for the elimination process. Using 24 to 168 hours, the $t_{1/2}$ of activity was 66.06 hours in iduronidase and 63.10 hours in Linker T iduronidase. If 96 to 168 hours were used to calculate one $t_{1/2}$ of activity, this $t_{1/2}$ of activity would reflect more of the elimination process. However, only two timepoints are used to calculate $t_{1/2}$ of activity which can cause imprecisions in the slope estimate. When using 96 to 168 hours, the $t_{1/2}$ of activity was 567.83 hours in iduronidase and 395.83 hours in Linker T iduronidase. These estimates of the terminal $t_{1/2}$ would be refined with later timepoints and analysis with compartmental models.

Figure 26: Application of Pharmacokinetic Principles to Gene Therapy in the Recipient Organ

Time Profile in a "Recipient" Organ with Enzymatic Uptake (E.g., Brain or Heart)

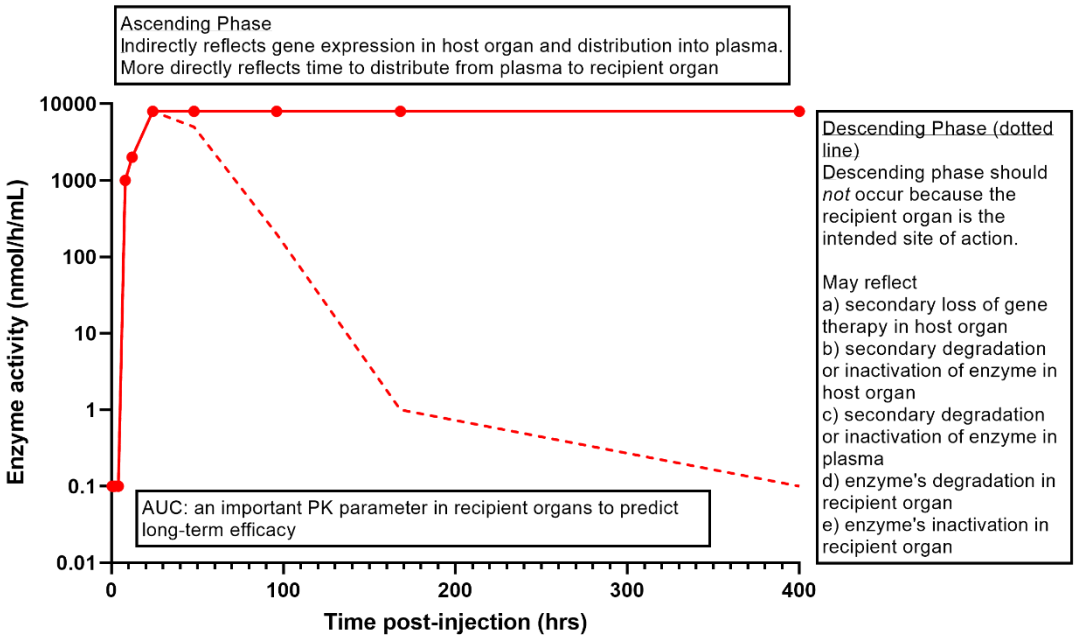

In Figure 26, the recipient organ(s) are the desired sites of action, i.e., the organs that need enzymes for therapeutic effect. The brain and heart would be examples of recipient organs in this study. If the host organ is also a desired site of action, the PK processes should be interpreted from the host organ example in Figure 24. Compared to the plasma, the AUC of activity in the target organ has a more straightforward relationship with efficacy.

5.4.1.2 Important Considerations for Integrating Pharmacokinetic and Gene Therapy Principles

One important consideration is that distribution and elimination can occur during the ascending phase. The presence of an ascending phase means that the rate of biological processes that increase enzyme activity (e.g., gene

expression) is greater than the rate of processes that decrease enzyme activity (e.g., distribution and elimination). Conversely, processes that increase the rate of enzyme activity (e.g., gene expression) can occur during the descending phase. This principle from pharmacokinetics is why a descending phase in the host organ may not necessarily correspond to inefficacy. A descending phase could occur if the enzyme's rate of distribution into the circulatory system is far greater than the rate of processes that increase enzyme activity (e.g., gene expression).

Some traditionally important PK parameters, namely clearance and volume of distribution, are not included because of the yet uncertain interpretation using enzyme activity. Additionally, some PK parameters were not included because can vary depending on the dose entered, which is difficult to define for gene therapy, because the dose of gene therapy uses different units than enzyme activity. Furthermore, these figures and concepts assume that there is no flip-flop kinetics.

Application of pharmacokinetic principles to gene-editing therapies, such as CRISPR-Cas9 systems, would be more complex than the traditional gene replacement therapies. Gene replacement therapies, such as plasmids or AAV alone, add a correct copy of a gene into the cell's genome or outside the genome as an episome. In contrast, gene-editing therapies correct the mutated gene in the genome. One potential advantage of gene-editing therapies is that efficacy may be sustained in rapidly dividing cells or in pediatric patients as they age. Gene-editing systems have more components than gene replacement therapies which need to be considered when applying pharmacokinetic principles. For example, the ascending phase in the host organ would also be impacted by co-transfection rates, expression of Cas9, and efficiency of gene-editing. The complexity of gene-editing will likely be exhibited as a greater variation between individuals in time-course profiles. In a study by the Hackett group, mice that were treated with a gene therapy that required two components (e.g., transposon

and transposase) exhibited greater variation in enzyme activity levels in the plasma compared to mice treated with one-component gene therapy (e.g., transposon) (188).

Another important note is that these PK parameters examine the total level of enzymatic activity within a body compartment. Changes in enzyme activity using PK analysis are different than changes in enzyme activity reported in other molecular studies of enzymes (e.g., Michaelis-Menten kinetics). For example, $t_{1/2}$ of activity and $1/2V_{max}$ are not interchangeable. The $t_{1/2}$ of activity provides a broader picture of the enzyme activity that is more clinically translatable than $1/2V_{max}$.

5.4.2 Study Significance

In this study, I developed a novel approach by performing pharmacokinetic analysis on enzyme activity, which would traditionally be a pharmacodynamic outcome in gene therapy. This approach combines the rigorous, reproducible quantitative methods from pharmacokinetics with a clinically and scientifically important parameter in gene therapy. Moreover, I demonstrate how biological and mechanistic information from gene therapy can be gained by integrating my knowledge from the fields of PK, gene therapy, and lysosomal diseases.

This dissertation's study differs from previous studies in two ways. First, this study performs a formal pharmacokinetic analysis directly on enzyme activity levels in gene therapy. More specifically, I use a PK program to conduct noncompartmental analysis and calculate multiple PK parameters. In contrast, previous studies in lysosomal diseases have reported $t_{1/2}$ using enzyme activity but did not perform a formal pharmacokinetic analysis (185-188). That is, these studies have estimated one or two PK parameters, namely $t_{1/2}$ measured with enzyme activity, and the methods for these estimations were not well described

(185-188). Section 2.4.1 discusses these studies in detail. Most of the graphs from these studies showed a biphasic profile in the plasma, similar to my study (185-188). In this study, estimating the $t_{1/2}$ of activity in biphasic profiles was limited by NCA. Therefore, estimations of $t_{1/2}$ of activity would be improved with more advanced methods, such as compartmental modeling. Another novelty of this study is that a formal pharmacokinetic analysis occurs in gene therapy. The current standard of performing pharmacokinetic analysis for gene therapy only utilizes the DNA levels of the vector, which can limit its application for efficacy. The challenges in using traditional PK or PKPD approaches for gene therapy are discussed in Section 2.4.2. One study by the Hackett group reported $t_{1/2}$ of enzyme activity in the plasma from gene therapy but did not describe how it was calculated (188). The work in my dissertation differs by performing a formal pharmacokinetic analysis of enzyme activity in the plasma and the liver.

Using this approach, I discovered that Linker T iduronidase had a markedly two-fold higher AUC of activity in the plasma than the normal iduronidase. In traditional pharmacokinetics, the AUC represents the total drug exposure over time. Therefore, the plasma was exposed to 100% higher enzyme activity from Linker T iduronidase than the normal iduronidase. The AUC of activity in the plasma could also represent exposure to receptors, including the M6P receptors that mediate uptake of lysosomal enzymes into organs. Therefore, adding Linker T to other lysosomal enzymes could increase their uptake into organs, representing therapeutic benefits in multiple lysosomal diseases. Furthermore, Linker T iduronidase's higher AUC of plasma activity is not caused by a higher production of enzyme in the liver because the physical levels of Linker T iduronidase and iduronidase were similar in the liver. This is an important consideration for ERT, because if Linker T iduronidase's AUC of plasma activity was caused by a higher production of enzyme, that is, higher physical levels of enzyme, then higher doses of Linker T iduronidase would be needed as ERT to achieve the same therapeutic effect.

I elucidated the potential mechanisms of Linker T iduronidase by combining my scientific knowledge from the fields of PK, gene therapy, and lysosomal diseases. When considering the data so far, there are three possible explanations for Linker T iduronidase's high AUC of activity in the plasma. First, Linker T may cause a higher distribution from the liver to the plasma. For example, the Linker T may cause a higher number of enzymes to be secreted after protein sorting. This mechanism would be beneficial if Linker T iduronidase was delivered as gene therapy. Compared to the same dose of gene therapy encoding iduronidase, a gene therapy encoding Linker T iduronidase can cause more enzymes to circulate and ultimately taken up into organs. Therefore, this would decrease the time and cost to manufacture high doses of gene therapy and reduce the risk of immune responses to viral vectors from gene therapy (316). The second explanation for Linker T iduronidase's higher AUC of plasma activity is that Linker T increases the activity of an enzyme specifically in the plasma. While this explanation fits with the data, there is currently no known biological explanation, aside from a theoretical change in protein folding from the blood's pH. Nevertheless, this mechanism would still confer an advantage to Linker T iduronidase because a lower dose, either as ERT or gene therapy, could be administered to achieve a similar therapeutic effect iduronidase. A third explanation for Linker T iduronidase's higher AUC of plasma activity is that Linker T causes decreased elimination and/or decreased inactivation of enzymes. Linker T's stabilization of an enzyme's activity in the plasma could be investigated in other lysosomal diseases, as other lysosomal enzymes with prolonged plasma activity levels had higher uptake into organs (185). Therefore, Linker T could improve therapeutic outcomes as ERT and gene therapies in several lysosomal diseases. Investigating other doses would provide more information on Linker T's potential for clinical benefit.

5.4.3 Study Strengths and Considerations for Future Studies

The strengths of this study are discussed in Section 5.4.2, which discusses the study's significance.

This study used NCA on a biphasic profile, which was discussed in Section 5.4.1.1. Future studies with compartmental analysis and later timepoints would improve the estimation of the terminal $t_{1/2}$ of activity in the plasma. A common challenge in designing pilot pharmacokinetic studies is the selection of timepoints (306). Section 5.1.5 discusses the rationale for the timepoints chosen in this study. Estimation of $t_{1/2}$ of activity from previously published studies was challenging because of different study designs and gene therapy constructs. In this study, ten timepoints were assessed, but there were still high enzyme activity levels in the liver and plasma at the last timepoint of 168 hours. In a study by Liu et al., which also hydrodynamically injected plasmids with the hAAT promoter, there were no detectable luciferase levels in non-liver organs at 144 hours (274). Therefore, I did not expect the plasma to have high activity levels at 168 hours in my study. The results from these two studies are probably due to differences in the dose and transgene. Future studies with later timepoints will refine the characterization of PK parameters.

Investigating a range of doses with a long-term expression vector like AAV would provide additional information on the clinical benefit of Linker T iduronidase. Testing different doses of Linker T iduronidase and seeing if PK parameters, such as the AUC of activity, show linear or nonlinear changes would further characterize this fusion enzyme and its clinical importance. Additionally, data on enzyme activity levels in other organs and substrate levels in organs could substantiate that Linker T iduronidase is more efficacious than normal iduronidase. Future studies will measure enzyme activity in other organs as part of comprehensive PKPD models of gene therapy. The DNA levels of plasmid in the liver will be quantified using quantitative polymerase chain reaction (qPCR),

(317). A traditional PK analysis could then occur, and this PK will be linked to the physical levels of enzymes in the liver. The physical levels of enzymes in the liver will be linked to enzyme activity in the liver. This, in turn, will be linked to enzyme activity in the plasma and enzyme activity in other organs. Therefore, comprehensive PKPD models of gene therapy will be generated. PKPD models and simulations can provide more precise estimates of the changes in gene therapy over time to yield deeper mechanistic information. These PKPD models and simulations can serve as tools to improve the success rate of gene therapy, aiding in therapeutic development.

CHAPTER 6: CONCLUSION

The **overall objective** of this dissertation is to improve the delivery of therapeutics to targeted tissues in lysosomal diseases. To accomplish this objective, three main studies were performed.

6.1 Validation of Chitotriosidase as a CNS Biomarker for Gangliosidoses

There is an unmet need for surrogate endpoints or biomarkers that can predict long-term clinical benefit from gene therapy for lysosomal diseases. Furthermore, a biomarker that can distinguish among disease phenotypes would allow earlier diagnosis of phenotypes, which would improve clinical trial enrichment and be synergistic with newborn screening. Neuroinflammation is an important pathological process in lysosomal diseases. A biomarker that reliably reflects neuroinflammation would have the potential to be a valuable tool for diagnosing disease phenotypes, monitoring disease progression, and assessing response to therapies for lysosomal diseases.

CSF chitotriosidase was investigated as a probable surrogate endpoint for clinical trials with gene therapy. The **first objective** was to validate chitotriosidase levels for important clinical outcomes in patients with lysosomal diseases. This study has shown that CSF and serum chitotriosidase may serve as a candidate biomarker for select lysosomal diseases with a CNS pathology. Specifically, CSF chitotriosidase levels were higher in the most severe infantile forms of the gangliosidoses compared to the attenuated juvenile and adult/late-onset forms. CSF chitotriosidase was associated with neurocognitive declines and may reflect disease progression in gangliosidoses. The **second objective** was to assess chitotriosidase's ability to detect effective gene therapy in murine models of lysosomal diseases. Chitotriosidase levels appear to be useful in murine models for MPS I, as there was a significant difference among the untreated, gene therapy treated, and heterozygous mice. The utility of chitotriosidase levels in murine models of GM1-gangliosidosis and Sandhoff

disease is uncertain. Future studies with more mice and at various disease stages would further elucidate chitotriosidase's response to gene therapies with respect to disease progression and in different lysosomal diseases. Other future studies would involve sequencing the *chit1* gene to determine if carriers have lower chitotriosidase levels. Another future study would be to directly quantify the elevations in serum and CSF chitotriosidase levels seen in lysosomal diseases compared to other conditions such as Alzheimer's disease and cerebral adrenoleukodystrophy.

These results motivate the use of CSF chitotriosidase to measure the therapeutic effect and response to gene therapy in clinical trials for lysosomal diseases. Chitotriosidase is a probable surrogate endpoint that is supported by strong mechanistic rationale and a clinically validated biomarker. CSF chitotriosidase may also be a valuable tool for clinical trial enrichment by objectively differentiating among the phenotypes of a lysosomal disease. As a potential biomarker for neurological improvement, CSF chitotriosidase can aid in the development of therapies that target the CNS.

6.2 Investigation of Iduronidase Enzymes Linked to Pepcan to Improve Delivery to Targeted Tissues

There is an unmet need for therapies that are safe and effective for neurological disorders in lysosomal diseases. The **objective** of this study was to determine if pepcan-12 can increase the uptake of iduronidase in the brain of MPS I mice. Pepcan-12 is a ligand for the CB1 receptor that is highly expressed in the CNS. The primary **hypothesis** was that the plasmid encoding pepcan-12 in tandem with *IDUA* would cause higher enzyme activity in the brain than the plasmid encoding *IDUA* alone. The secondary **hypothesis** was that the linkers would not affect the enzyme activity of iduronidase. The purpose of the linkers was to link the pepcan-12 ligand with the iduronidase enzyme. In the brain, enzyme activities were similar between fusion enzymes and normal iduronidase.

Unexpectedly, the fusion enzymes had higher activities than the normal iduronidase in the heart and plasma, which appears to be due to the linkers. These results are valuable in developing ERT and gene therapies with increased uptake into organs. The addition of these linkers to enzymes may improve cardiovascular outcomes in MPS I and other lysosomal diseases. These fusion enzymes' therapeutic potential would be substantiated with future studies assessing long-term safety and efficacy. Furthermore, these linkers can be investigated in ERT or gene therapies for other lysosomal diseases, particularly diseases without treatments.

6.3 Pharmacokinetic Analysis of Iduronidase and a Fusion Iduronidase Enzyme Encoded in Gene Therapy

In the previous study, I developed a fusion enzyme, Linker T iduronidase, that had higher activity levels than iduronidase in the plasma and heart. I initially sought to investigate the mechanism of Linker T iduronidase using pharmacokinetic analysis. However, I realized there was a gap between the fields of lysosomal diseases/gene therapy and pharmacokinetics/ pharmacodynamics.

The fields of lysosomal diseases and gene therapy emphasize pharmacodynamic outcomes (e.g., enzyme activity levels in ERT or gene therapy). However, the methods to quantify changes in enzyme activity levels over time were not well described. Previous studies have proposed that one mechanism to improve the delivery of lysosomal enzymes into organs is to increase the enzyme's half-life in the plasma (166, 185, 186). These studies estimated half-life using enzyme activity levels but did not mention any conversion factors, equations, or PK programs, and the $t_{1/2}$ was reported when a 50% decrease in activity was not seen in graphs. Furthermore, PK parameters

and time-course profiles of enzyme activity levels have been interpreted differently in the field of lysosomal diseases.

The field of pharmacokinetics routinely characterizes the $t_{1/2}$ and other changes in a therapy over time in the body. Moreover, the pharmacokinetic field has rigorous, reproducible, standardized quantification methods that play integral roles in the drug approval process. However, traditional pharmacokinetic approaches are challenging for gene therapy. Gene therapy studies use different units, which hinders the use of PK equations. Furthermore, the PK processes of absorption, distribution, metabolism, and elimination are well-characterized for small molecular drugs but have yet to be adapted for biological therapies.

To begin to build a bridge between the fields of lysosomal disease/gene therapy and PK/PD, the **objective** of this study was to perform a pharmacokinetic analysis of iduronidase and Linker T iduronidase, which were both delivered as gene therapies. I aimed to develop an approach that would combine the emphasis on efficacy from the lysosomal diseases/gene therapy fields with the rigorous, reproducible, quantitative methods from the PK field. The **hypothesis** was that Linker T iduronidase would have a higher AUC or longer half-life using enzyme activity than the normal iduronidase in the plasma. This study used a novel approach by performing a pharmacokinetics analysis on a traditionally pharmacodynamic outcome (e.g., enzyme activity in gene therapy). Using this approach, the Linker T iduronidase had a two-fold higher AUC of activity in the plasma than the normal iduronidase.

I interpreted the PK parameters generated from this approach and elucidated the potential mechanisms of Linker T, by integrating my knowledge from the fields of PK, gene therapy, and lysosomal diseases. Linker T iduronidase's higher AUC of activity in the plasma could not be due to a higher production of enzymes. The liver-specific promoter causes the synthesis of enzymes only in the liver, and both enzymes had similar physical levels over time in the liver. This suggests that Linker T iduronidase has some distinct property

that confers stabilization of activity in the plasma. Although the time-enzyme activity levels in the plasma graphs showed a smaller decline for Linker T iduronidase, the calculated half-lives using NCA were similar for both enzymes. A future study with longer timepoints and compartmental analysis would better characterize Linker T iduronidase's half-life. Future studies with PKPD models and simulations of gene therapy will yield more precise mechanistic information to improve the success rate of gene therapy. In this study, I integrated concepts from pharmacokinetics and gene therapy to provide ways for researchers to investigate biological and mechanistic information about their gene therapy, advancing ERT and gene therapies for multiple lysosomal diseases.

6.4 Summary

In summary, these findings improve the therapeutics for lysosomal diseases through the validation of a biomarker for neurological function and the creation of a novel lysosomal fusion enzyme that has improved activity in the heart and plasma. Finally, I describe a novel approach using pharmacokinetic analysis to provide biological and mechanistic insights on gene therapy.

BIBLIOGRAPHY

1. Fuller M, Meikle PJ, Hopwood JJ. Epidemiology of lysosomal storage diseases: an overview. In: Mehta A, Beck M, Sunder-Plassmann G, editors. Fabry Disease: Perspectives from 5 Years of FOS. Oxford: Oxford PharmaGenesis. Copyright © 2006, Oxford PharmaGenesis™. 2006.
2. Neuronal ceroid lipofuscinosis. Genetic and Rare Disease Information Center. National Center for Advancing Translational Sciences. National Institute of Health. Updated February 1 2021. https://rarediseases.info.nih.gov/diseases/10739/neuronal-ceroid-lipofuscinosis#ref_9561.
3. Jarnes Utz JR, Kim S, King K, Ziegler R, Schema L, Redtree ES, Whitley CB. Infantile gangliosidoses: Mapping a timeline of clinical changes. Molecular genetics and metabolism. 2017;121(2):170-9.
4. Alroy J, Garganta C, Wiederschain G. Secondary biochemical and morphological consequences in lysosomal storage diseases. Biochemistry (Mosc). 2014;79(7):619-36.
5. Bosch ME, Kielian T. Neuroinflammatory paradigms in lysosomal storage diseases. Frontiers in neuroscience. 2015;9(417).
6. Meikle PJ, Hopwood JJ, Clague AE, Carey WF. Prevalence of lysosomal storage disorders. Jama. 1999;281(3):249-54.
7. Online Mendelian Inheritance in Man, OMIM®. Johns Hopkins University, Baltimore, MD. MIM Number: 606272: CYSTINOSIN; CTNS. Last edited December 11 2017. World Wide Web URL: https://omim.org/entry/606272.
8. Ballabio A, Gieselmann V. Lysosomal disorders: From storage to cellular damage. Biochimica et Biophysica Acta (BBA) - Molecular Cell Research. 2009;1793(4):684-96.
9. Giugliani R, Vairo F, Kubaski F, Poswar F, Riegel M, Baldo G, Saute JA. Neurological manifestations of lysosomal disorders and emerging therapies targeting the CNS. Lancet Child Adolesc Health. 2018;2(1):56-68.
10. Whitley CB. Emerging Trends: State-of-the-Art for Experts. February 2019. WORLDSymposium. Orlando, FL.

11. Vitner EB, Platt FM, Futerman AH. Common and Uncommon Pathogenic Cascades in Lysosomal Storage Diseases*. Journal of Biological Chemistry. 2010;285(27):20423-7.
12. Beck M. Therapy for lysosomal storage disorders. IUBMB Life. 2010;62(1):33-40.
13. Fratantoni JC, Hall CW, Neufeld EF. Hurler and Hunter Syndromes: Mutual Correction of the Defect in Cultured Fibroblasts. Science (New York, NY). 1968;162(3853):570-2.
14. Whitley CB, Ramsay NK, Kersey JH, Krivit W. Bone marrow transplantation for Hurler syndrome: assessment of metabolic correction. Birth Defects Orig Artic Ser. 1986;22(1):7-24.
15. Muenzer J. Overview of the mucopolysaccharidoses. Rheumatology (Oxford). 2011;50 Suppl 5:v4-12.
16. Platt FM, d'Azzo A, Davidson BL, Neufeld EF, Tifft CJ. Lysosomal storage diseases. Nature Reviews Disease Primers. 2018;4(1):27.
17. Wang RY, Bodamer OA, Watson MS, Wilcox WR. Lysosomal storage diseases: diagnostic confirmation and management of presymptomatic individuals. Genetics in medicine : official journal of the American College of Medical Genetics. 2011;13(5):457-84.
18. Brunetti-Pierri N, Scaglia F. GM1 gangliosidosis: Review of clinical, molecular, and therapeutic aspects. Molecular genetics and metabolism. 2008;94(4):391-6.
19. Sinigerska I, Chandler D, Vaghjiani V, Hassanova I, Gooding R, Morrone A, Kremensky I, Kalaydjieva L. Founder mutation causing infantile GM1-gangliosidosis in the Gypsy population. Molecular genetics and metabolism. 2006;88(1):93-5.
20. GLB1 galactosidase beta 1 [Homo sapiens (human)] [Internet]. Bethesda (MD): National Library of Medicine (US), National Center for Biotechnology Information; 2004 – [cited 2021 Oct 30]. Available from: https://www.ncbi.nlm.nih.gov/gene/2720.
21. Morreau H, Galjart NJ, Gillemans N, Willemsen R, van der Horst GT, d'Azzo A. Alternative splicing of beta-galactosidase mRNA generates the classic lysosomal enzyme and a beta-galactosidase-related protein. The Journal of biological chemistry. 1989;264(34):20655-63.
22. UniProtKB - O43318 (M3K7_HUMAN). UniprotKB. Last updated November 13, 2019. Accessed November 25, 2019. https://www.uniprot.org/uniprot/O43318.

23. Hinek A, Wilson SE. Impaired elastogenesis in Hurler disease: dermatan sulfate accumulation linked to deficiency in elastin-binding protein and elastic fiber assembly. The American journal of pathology. 2000;156(3):925-38.
24. UniProtKB - P16278 (BGAL_HUMAN). Universal Protein Resource (UniProt). https://www.uniprot.org/uniprot/P16278.
25. Ohto U, Usui K, Ochi T, Yuki K, Satow Y, Shimizu T. Crystal structure of human beta-galactosidase: structural basis of Gm1 gangliosidosis and morquio B diseases. The Journal of biological chemistry. 2012;287(3):1801-12.
26. D'Azzo A, Hoogeveen A, Reuser AJ, Robinson D, Galjaard H. Molecular defect in combined beta-galactosidase and neuraminidase deficiency in man. Proceedings of the National Academy of Sciences of the United States of America. 1982;79(15):4535-9.
27. Hoogeveen AT, Reuser AJ, Kroos M, Galjaard H. GM1-gangliosidosis. Defective recognition site on beta-galactosidase precursor. The Journal of biological chemistry. 1986;261(13):5702-4.
28. van der Spoel A, Bonten E, d'Azzo A. Processing of lysosomal beta-galactosidase. The C-terminal precursor fragment is an essential domain of the mature enzyme. The Journal of biological chemistry. 2000;275(14):10035-40.
29. HEXA hexosaminidase subunit alpha [Homo sapiens (human)] [Internet]. Bethesda (MD): National Library of Medicine (US), National Center for Biotechnology Information; 2004 – [cited 2021 Oct 30]. Available from: https://www.ncbi.nlm.nih.gov/gene/3073.
30. HEXB hexosaminidase subunit beta [Homo sapiens (human)] [Internet]. Bethesda (MD): National Library of Medicine (US), National Center for Biotechnology Information; 2004 – [cited 2021 Oct 30]. Available from: https://www.ncbi.nlm.nih.gov/gene/3074.
31. GM2A GM2 ganglioside activator [Homo sapiens (human)] [Internet]. Bethesda (MD): National Library of Medicine (US), National Center for Biotechnology Information; 2004 – [cited 2021 Oct 30]. Available from: https://www.ncbi.nlm.nih.gov/gene/2760.
32. Hou Y, Tse R, Mahuran DJ. Direct determination of the substrate specificity of the alpha-active site in heterodimeric beta-hexosaminidase A. Biochemistry. 1996;35(13):3963-9.
33. UniProtKB - P06865 (HEXA_HUMAN). Universal Protein Resource (UniProt). https://www.uniprot.org/uniprot/P06865.

34. Lemieux MJ, Mark BL, Cherney MM, Withers SG, Mahuran DJ, James MNG. Crystallographic structure of human beta-hexosaminidase A: interpretation of Tay-Sachs mutations and loss of GM2 ganglioside hydrolysis. Journal of molecular biology. 2006;359(4):913-29.
35. Bley AE, Giannikopoulos OA, Hayden D, Kubilus K, Tifft CJ, Eichler FS. Natural history of infantile G(M2) gangliosidosis. Pediatrics. 2011;128(5):e1233-41.
36. Regier DS, Proia RL, D'Azzo A, Tifft CJ. The GM1 and GM2 Gangliosidoses: Natural History and Progress toward Therapy. Pediatr Endocrinol Rev. 2016;13 Suppl 1(Suppl 1):663-73.
37. King KE, Kim S, Whitley CB, Jarnes-Utz JR. The juvenile gangliosidoses: A timeline of clinical change. Molecular genetics and metabolism reports. 2020;25:100676.
38. Maegawa GH, Stockley T, Tropak M, Banwell B, Blaser S, Kok F, Giugliani R, Mahuran D, Clarke JT. The natural history of juvenile or subacute GM2 gangliosidosis: 21 new cases and literature review of 134 previously reported. Pediatrics. 2006;118(5):e1550-62.
39. Smith NJ, Winstone AM, Stellitano L, Cox TM, Verity CM. GM2 gangliosidosis in a UK study of children with progressive neurodegeneration: 73 cases reviewed. Dev Med Child Neurol. 2012;54(2):176-82.
40. Kannebley JS, Silveira-Moriyama L, Bastos LO, Steiner CE. Clinical Findings and Natural History in Ten Unrelated Families with Juvenile and Adult GM1 Gangliosidosis. JIMD reports. 2015;24:115-22.
41. Neudorfer O, Kolodny EH. Late-onset Tay-Sachs disease. The Israel Medical Association journal : IMAJ. 2004;6(2):107-11.
42. Frey LC, Ringel SP, Filley CM. The natural history of cognitive dysfunction in late-onset GM2 gangliosidosis. Archives of neurology. 2005;62(6):989-94.
43. Scarpelli M, Tomelleri G, Bertolasi L, Salviati A. Natural history of motor neuron disease in adult onset GM2-gangliosidosis: A case report with 25 years of follow-up. Molecular genetics and metabolism reports. 2014;1:269-72.
44. Puckett Y, Mallorga-Hernández A, Montaño AM. Epidemiology of mucopolysaccharidoses (MPS) in United States: challenges and opportunities. Orphanet Journal of Rare Diseases. 2021;16(1):241.

45. IDUA alpha-L-iduronidase [Homo sapiens (human)] [Internet]. Bethesda (MD): National Library of Medicine (US), National Center for Biotechnology Information; 2004 – [cited 2021 Oct 30]. Available from: https://www.ncbi.nlm.nih.gov/gene/3425.
46. Whitley CB, Gorlin RJ, Krivit W. A nonpathologic allele (IW) for low alpha-L-iduronidase enzyme activity vis-a-vis prenatal diagnosis of Hurler syndrome. Am J Med Genet. 1987;28(1):233-43.
47. Aronovich EL, Pan D, Whitley CB. Molecular genetic defect underlying alpha-L-iduronidase pseudodeficiency. Am J Hum Genet. 1996;58(1):75-85.
48. alpha-L-iduronidase isoform a precursor [Homo sapiens] [Internet]. Bethesda (MD): National Library of Medicine (US), National Center for Biotechnology Information; [1988] - [cited 2021 Oct 15]. Available from: https://www.ncbi.nlm.nih.gov/protein/NP_000194.2.
49. Scott HS, Bunge S, Gal A, Clarke LA, Morris CP, Hopwood JJ. Molecular genetics of mucopolysaccharidosis type I: diagnostic, clinical, and biological implications. Hum Mutat. 1995;6(4):288-302.
50. Muenzer J, Wraith JE, Clarke LA. Mucopolysaccharidosis I: management and treatment guidelines. Pediatrics. 2009;123(1):19-29.
51. Abbott NJ. Blood-brain barrier structure and function and the challenges for CNS drug delivery. J Inherit Metab Dis. 2013;36(3):437-49.
52. Shapiro EG, Jones SA, Escolar ML. Developmental and behavioral aspects of mucopolysaccharidoses with brain manifestations — Neurological signs and symptoms. Molecular genetics and metabolism. 2017;122:1-7.
53. Nestrasil I, Ahmed A, Utz JM, Rudser K, Whitley CB, Jarnes-Utz JR. Distinct progression patterns of brain disease in infantile and juvenile gangliosidoses: Volumetric quantitative MRI study. Molecular genetics and metabolism. 2018;123(2):97-104.
54. van Baarsen KM, Kleinnijenhuis M, Jbabdi S, Sotiropoulos SN, Grotenhuis JA, van Cappellen van Walsum AM. A probabilistic atlas of the cerebellar white matter. Neuroimage. 2016;124(Pt A):724-32.
55. Nestrasil I, Ahmed A, Utz JM, Rudser K, Whitley CB, Jarnes-Utz JR. Distinct progression patterns of brain disease in infantile and juvenile gangliosidoses: Volumetric quantitative MRI study. Molecular genetics and metabolism. 2018;123(2):97-104.

56. Zafeiriou DI, Batzios SP. Brain and spinal MR imaging findings in mucopolysaccharidoses: a review. AJNR American journal of neuroradiology. 2013;34(1):5-13.
57. Nestrasil I, Vedolin L. Quantitative neuroimaging in mucopolysaccharidoses clinical trials. Molecular genetics and metabolism. 2017;122s:17-24.
58. Bigger BW, Begley DJ, Virgintino D, Pshezhetsky AV. Anatomical changes and pathophysiology of the brain in mucopolysaccharidosis disorders. Molecular genetics and metabolism. 2018;125(4):322-31.
59. Davies EH, Seunarine KK, Banks T, Clark CA, Vellodi A. Brain white matter abnormalities in paediatric Gaucher Type I and Type III using diffusion tensor imaging. Journal of Inherited Metabolic Disease. 2011;34(2):549-53.
60. Bava S, Theilmann RJ, Sach M, May SJ, Frank LR, Hesselink JR, Vu D, Trauner DA. Developmental changes in cerebral white matter microstructure in a disorder of lysosomal storage. Cortex. 2010;46(2):206-16.
61. Vogel DG, Malekzadeh MH, Cornford ME, Schneider JA, Shields WD, Vinters HV. Central nervous system involvement in nephropathic cystinosis. J Neuropathol Exp Neurol. 1990;49(6):591-9.
62. Prietsch V, Arnold S, Kraegeloh-Mann I, Kuehr J, Santer R. Severe hypomyelination as the leading neuroradiological sign in a patient with fucosidosis. Neuropediatrics. 2008;39(1):51-4.
63. Morse RP, Kleta R, Alroy J, Gahl WA. Novel form of intermediate salla disease: clinical and neuroimaging features. Journal of child neurology. 2005;20(10):814-6.
64. Pujol J, López-Sala A, Sebastián-Gallés N, Deus J, Cardoner N, Soriano-Mas C, Moreno A, Sans A. Delayed myelination in children with developmental delay detected by volumetric MRI. Neuroimage. 2004;22(2):897-903.
65. Folkerth RD, Alroy J, Bhan I, Kaye EM. Infantile G(M1) gangliosidosis: complete morphology and histochemistry of two autopsy cases, with particular reference to delayed central nervous system myelination. Pediatric and developmental pathology : the official journal of the Society for Pediatric Pathology and the Paediatric Pathology Society. 2000;3(1):73-86.
66. Chen CY, Zimmerman RA, Lee CC, Chen FH, Yuh YS, Hsiao HS. Neuroimaging findings in late infantile GM1 gangliosidosis. AJNR American journal of neuroradiology. 1998;19(9):1628-30.

67. Kroll RA, Pagel MA, Roman-Goldstein S, Barkovich AJ, D'Agostino AN, Neuwelt EA. White matter changes associated with feline GM2 gangliosidosis (Sandhoff disease): correlation of MR findings with pathologic and ultrastructural abnormalities. AJNR American journal of neuroradiology. 1995;16(6):1219-26.
68. Yuksel A, Yalcinkaya C, Islak C, Gunduz E, Seven M. Neuroimaging findings of four patients with Sandhoff disease. Pediatric neurology. 1999;21(2):562-5.
69. Hasegawa D, Tamura S, Nakamoto Y, Matsuki N, Takahashi K, Fujita M, Uchida K, Yamato O. Magnetic resonance findings of the corpus callosum in canine and feline lysosomal storage diseases. PloS one. 2013;8(12):e83455.
70. Andronikou S, Pillay T, Gabuza L, Mahomed N, Naidoo J, Hlabangana LT, du Plessis V, Prabhu SP. Corpus callosum thickness in children: an MR pattern-recognition approach on the midsagittal image. Pediatric Radiology. 2015;45(2):258-72.
71. De Grandis E, Di Rocco M, Pessagno A, Veneselli E, Rossi A. MR Imaging Findings in 2 Cases of Late Infantile GM1 Gangliosidosis. PloS one. 2009;30(7):1325-7.
72. Gururaj A, Sztriha L, Hertecant J, Johansen JG, Georgiou T, Campos Y, Drousiotou A, d'Azzo A. Magnetic resonance imaging findings and novel mutations in GM1 gangliosidosis. Journal of child neurology. 2005;20(1):57-60.
73. Kasama T, Taketomi T. Abnormalities of cerebral lipids in GM1-gangliosidoses, infantile, juvenile, and chronic type. The Japanese journal of experimental medicine. 1986;56(1):1-11.
74. Renard D, Castelnovo G, Campello C, Bouly S, Le Floch A, Thouvenot E, Waconge A, Taieb G. Thalamic Lesions: A Radiological Review. Behavioural Neurology. 2014;2014:154631.
75. Erol I, Alehan F, Pourbagher MA, Canan O, Vefa Yildirim S. Neuroimaging findings in infantile GM1 gangliosidosis. European journal of paediatric neurology : EJPN : official journal of the European Paediatric Neurology Society. 2006;10(5-6):245-8.
76. Vogler C, Levy B, Kyle JW, Sly WS, Williamson J, Whyte MP. Mucopolysaccharidosis VII: postmortem biochemical and pathological findings in a young adult with beta-glucuronidase deficiency. Mod Pathol. 1994;7(1):132-7.
77. Hadfield MG, Ghatak NR, Nakoneczna I, Lippman HR, Myer EC, Constantopoulos G, Bradley RM. Pathologic findings in mucopolysaccharidosis type IIIB (Sanfilippo's sydnrome B). Archives of neurology. 1980;37(10):645-50.

78. Hamano K, Hayashi M, Shioda K, Fukatsu R, Mizutani S. Mechanisms of neurodegeneration in mucopolysaccharidoses II and IIIB: analysis of human brain tissue. Acta Neuropathol. 2008;115(5):547-59.
79. Dekaban AS, Patton VM. Hurler's and Sanfilippo's variants of mucopolysaccharidosis. Cerebral pathology and lipid chemistry. Arch Pathol. 1971;91(5):434-43.
80. Walkley SU, Haskins ME, Shull RM. Alterations in neuron morphology in mucopolysaccharidosis type I. Acta Neuropathologica. 1988;75(6):611-20.
81. Ferrer I, Cusí V, Pineda M, Glofré E, Vila J. Focal dendritic swellings in Purkinje cells in mucopolysaccharidoses types I, II and III. A Golgi and ultrastructural study. Neuropathology and applied neurobiology. 1988;14(4):315-23.
82. Constantopoulos G, Iqbal K, Dekaban AS. Mucopolysaccharidosis Types IH, IS, II and IIIA: Glycosaminoglycans and Lipids of Isolated Brain Cells and Other Fractions from Autopsied Tissues. Journal of neurochemistry. 1980;34(6):1399-411.
83. Kriel RL, Hauser WA, Sung JH, Posalaky Z. Neuroanatomical and electroencephalographic correlations in Sanfilippo syndrome, type A. Archives of neurology. 1978;35(12):838-43.
84. Walkley SU, Siegel DA, Wurzelmann S. Ectopic dendritogenesis and associated synapse formation in swainsonine-induced neuronal storage disease. The Journal of neuroscience : the official journal of the Society for Neuroscience. 1988;8(2):445-57.
85. Siegel DA, Walkley SU. Growth of ectopic dendrites on cortical pyramidal neurons in neuronal storage diseases correlates with abnormal accumulation of GM2 ganglioside. Journal of neurochemistry. 1994;62(5):1852-62.
86. Walkley SU. Pyramidal neurons with ectopic dendrites in storage diseases exhibit increased GM2 ganglioside immunoreactivity. Neuroscience. 1995;68(4):1027-35.
87. Bellettato CM, Scarpa M. Pathophysiology of neuropathic lysosomal storage disorders. J Inherit Metab Dis. 2010;33(4):347-62.
88. Ginhoux F, Lim S, Hoeffel G, Low D, Huber T. Origin and differentiation of microglia. Frontiers in Cellular Neuroscience. 2013;7(45).
89. Campos D, Monaga M. Mucopolysaccharidosis type I: current knowledge on its pathophysiological mechanisms. Metabolic Brain Disease. 2012;27(2):121-9.

90. Thundyil J, Lim KL. DAMPs and neurodegeneration. Ageing Res Rev. 2015;24(Pt A):17-28.
91. Utz JR, Crutcher T, Schneider J, Sorgen P, Whitley CB. Biomarkers of central nervous system inflammation in infantile and juvenile gangliosidoses. Molecular genetics and metabolism. 2015;114(2):274-80.
92. Jeyakumar M, Thomas R, Elliot-Smith E, Smith DA, van der Spoel AC, d'Azzo A, Perry VH, Butters TD, Dwek RA, Platt FM. Central nervous system inflammation is a hallmark of pathogenesis in mouse models of GM1 and GM2 gangliosidosis. Brain : a journal of neurology. 2003;126(Pt 4):974-87.
93. Baudry M, Yao Y, Simmons D, Liu J, Bi X. Postnatal development of inflammation in a murine model of Niemann–Pick type C disease: immunohistochemical observations of microglia and astroglia. Experimental Neurology. 2003;184(2):887-903.
94. Farfel-Becker T, Vitner EB, Futerman AH. Animal models for Gaucher disease research. Disease models & mechanisms. 2011;4(6):746-52.
95. Pontikis CC, Cella CV, Parihar N, Lim MJ, Chakrabarti S, Mitchison HM, Mobley WC, Rezaie P, Pearce DA, Cooper JD. Late onset neurodegeneration in the Cln3-/- mouse model of juvenile neuronal ceroid lipofuscinosis is preceded by low level glial activation. Brain research. 2004;1023(2):231-42.
96. Williams IM, Wallom KL, Smith DA, Al Eisa N, Smith C, Platt FM. Improved neuroprotection using miglustat, curcumin and ibuprofen as a triple combination therapy in Niemann-Pick disease type C1 mice. Neurobiology of disease. 2014;67:9-17.
97. DiRosario J, Divers E, Wang C, Etter J, Charrier A, Jukkola P, Auer H, Best V, Newsom DL, McCarty DM, Fu H. Innate and adaptive immune activation in the brain of MPS IIIB mouse model. Journal of neuroscience research. 2009;87(4):978-90.
98. Archer LD, Langford-Smith KJ, Bigger BW, Fildes JE. Mucopolysaccharide diseases: a complex interplay between neuroinflammation, microglial activation and adaptive immunity. J Inherit Metab Dis. 2014;37(1):1-12.
99. Wilkinson FL, Holley RJ, Langford-Smith KJ, Badrinath S, Liao A, Langford-Smith A, Cooper JD, Jones SA, Wraith JE, Wynn RF, Merry CL, Bigger BW. Neuropathology in mouse models of mucopolysaccharidosis type I, IIIA and IIIB. PloS one. 2012;7(4):e35787.
100. Braunlin EA, Harmatz PR, Scarpa M, Furlanetto B, Kampmann C, Loehr JP, Ponder KP, Roberts WC, Rosenfeld HM, Giugliani R. Cardiac disease in patients with

mucopolysaccharidosis: presentation, diagnosis and management. J Inherit Metab Dis. 2011;34(6):1183-97.
101. Ortiz A, Germain DP, Desnick RJ, Politei J, Mauer M, Burlina A, Eng C, Hopkin RJ, Laney D, Linhart A, Waldek S, Wallace E, Weidemann F, Wilcox WR. Fabry disease revisited: Management and treatment recommendations for adult patients. Molecular genetics and metabolism. 2018;123(4):416-27.
102. Nair V, Belanger EC, Veinot JP. Lysosomal storage disorders affecting the heart: a review. Cardiovascular Pathology. 2019;39:12-24.
103. Chen MR, Lin SP, Hwang HK, Yu CH. Cardiovascular changes in mucopolysaccharidoses in Taiwan. Acta Cardiol. 2005;60(1):51-3.
104. Dangel JH. Cardiovascular changes in children with mucopolysaccharide storage diseases and related disorders--clinical and echocardiographic findings in 64 patients. Eur J Pediatr. 1998;157(7):534-8.
105. Fesslová V, Corti P, Sersale G, Rovelli A, Russo P, Mannarino S, Butera G, Parini R. The natural course and the impact of therapies of cardiac involvement in the mucopolysaccharidoses. Cardiology in the young. 2009;19(2):170-8.
106. Leal GN, de Paula AC, Leone C, Kim CA. Echocardiographic study of paediatric patients with mucopolysaccharidosis. Cardiology in the young. 2010;20(3):254-61.
107. Wippermann CF, Beck M, Schranz D, Huth R, Michel-Behnke I, Jüngst BK. Mitral and aortic regurgitation in 84 patients with mucopolysaccharidoses. Eur J Pediatr. 1995;154(2):98-101.
108. Martins AM, Dualibi AP, Norato D, Takata ET, Santos ES, Valadares ER, Porta G, de Luca G, Moreira G, Pimentel H, Coelho J, Brum JM, Semionato Filho J, Kerstenetzky MS, Guimarães MR, Rojas MV, Aranda PC, Pires RF, Faria RG, Mota RM, Matte U, Guedes ZC. Guidelines for the management of mucopolysaccharidosis type I. The Journal of pediatrics. 2009;155(4 Suppl):S32-46.
109. Pastores GM, Arn P, Beck M, Clarke JT, Guffon N, Kaplan P, Muenzer J, Norato DY, Shapiro E, Thomas J, Viskochil D, Wraith JE. The MPS I registry: design, methodology, and early findings of a global disease registry for monitoring patients with Mucopolysaccharidosis Type I. Molecular genetics and metabolism. 2007;91(1):37-47.
110. Krovetz LJ, Lorincz AE, Schiebler GL. Cardiovascular Manifestations of the Hurler Syndrome: Hemodynamic and Angiocardiographic Observations in 15 Patients. Circulation. 1965;31:132-41.

111. Rigante D, Segni G. Cardiac structural involvement in mucopolysaccharidoses. Cardiology. 2002;98(1-2):18-20.
112. Thomas JA, Beck M, Clarke JT, Cox GF. Childhood onset of Scheie syndrome, the attenuated form of mucopolysaccharidosis I. J Inherit Metab Dis. 2010;33(4):421-7.
113. Braunlin E, Mackey-Bojack S, Panoskaltsis-Mortari A, Berry JM, McElmurry RT, Riddle M, Sun L-Y, Clarke LA, Tolar J, Blazar BR. Cardiac Functional and Histopathologic Findings in Humans and Mice with Mucopolysaccharidosis Type I: Implications for Assessment of Therapeutic Interventions in Hurler Syndrome. Pediatric Research. 2006;59(1):27-32.
114. Liu Y, Xu L, Hennig AK, Kovacs A, Fu A, Chung S, Lee D, Wang B, Herati RS, Mosinger Ogilvie J, Cai SR, Parker Ponder K. Liver-directed neonatal gene therapy prevents cardiac, bone, ear, and eye disease in mucopolysaccharidosis I mice. Mol Ther. 2005;11(1):35-47.
115. Tan EY, Boelens JJ, Jones SA, Wynn RF. Hematopoietic Stem Cell Transplantation in Inborn Errors of Metabolism. Front Pediatr. 2019;7(433).
116. Tan CT, Schaff HV, Miller FA, Jr., Edwards WD, Karnes PS. Valvular heart disease in four patients with Maroteaux-Lamy syndrome. Circulation. 1992;85(1):188-95.
117. Yano S, Moseley K, Pavlova Z. Postmortem studies on a patient with mucopolysaccharidosis type I: histopathological findings after one year of enzyme replacement therapy. J Inherit Metab Dis. 2009;32 Suppl 1:S53-7.
118. Braunlin E, Tolar J, Mackey-Bojack S, Masinde T, Krivit W, Schoen FJ. Clear cells in the atrioventricular valves of infants with severe human mucopolysaccharidosis (Hurler syndrome) are activated valvular interstitial cells. Cardiovascular pathology : the official journal of the Society for Cardiovascular Pathology. 2011;20(5):315-21.
119. Hishitani T, Wakita S, Isoda T, Katori T, Ishizawa A, Okada R. Sudden death in Hunter syndrome caused by complete atrioventricular block. The Journal of pediatrics. 2000;136(2):268-9.
120. Lin HY, Lin SP, Chuang CK, Chen MR, Chen BF, Wraith JE. Mucopolysaccharidosis I under enzyme replacement therapy with laronidase--a mortality case with autopsy report. J Inherit Metab Dis. 2005;28(6):1146-8.
121. Brosius FC, 3rd, Roberts WC. Coronary artery disease in the Hurler syndrome. Qualitative and quantitative analysis of the extent of coronary narrowing at necropsy in six children. The American journal of cardiology. 1981;47(3):649-53.

122. Grande-Allen KJ, Griffin BP, Ratliff NB, Cosgrove DM, Vesely I. Glycosaminoglycan profiles of myxomatous mitral leaflets and chordae parallel the severity of mechanical alterations. J Am Coll Cardiol. 2003;42(2):271-7.
123. Gupta V, Barzilla JE, Mendez JS, Stephens EH, Lee EL, Collard CD, Laucirica R, Weigel PH, Grande-Allen KJ. Abundance and location of proteoglycans and hyaluronan within normal and myxomatous mitral valves. Cardiovascular pathology : the official journal of the Society for Cardiovascular Pathology. 2009;18(4):191-7.
124. Latif N, Sarathchandra P, Taylor PM, Antoniw J, Yacoub MH. Localization and pattern of expression of extracellular matrix components in human heart valves. J Heart Valve Dis. 2005;14(2):218-27.
125. Rentería VG, Ferrans VJ, Roberts WC. The heart in the Hurler syndrome: Gross, histologic and ultrastructural observations in five necropsy cases. The American journal of cardiology. 1976;38(4):487-501.
126. Braunlin EA, Stauffer NR, Peters CH, Bass JL, Berry JM, Hopwood JJ, Krivit W. Usefulness of bone marrow transplantation in the Hurler syndrome. The American journal of cardiology. 2003;92(7):882-6.
127. Gatzoulis MA, Vellodi A, Redington AN. Cardiac involvement in mucopolysaccharidoses: effects of allogeneic bone marrow transplantation. Arch Dis Child. 1995;73(3):259-60.
128. Guffon N, Bertrand Y, Forest I, Fouilhoux A, Froissart R. Bone marrow transplantation in children with Hunter syndrome: outcome after 7 to 17 years. The Journal of pediatrics. 2009;154(5):733-7.
129. Krivit W, Pierpont M, Ayaz K, Tsai M, Ramsay N, Kersey J, Weisdorf S, Sibley R, Snover D, McGovern M. Bone-marrow transplantation in the Maroteaux-Lamy syndrome (mucopolysaccharidosis type VI). Biochemical and clinical status 24 months after transplantation. The New England journal of medicine. 1984;311(25):1606-11.
130. Viñallonga X, Sanz N, Balaguer A, Miro L, Ortega JJ, Casaldaliga J. Hypertrophic cardiomyopathy in mucopolysaccharidoses: regression after bone marrow transplantation. Pediatr Cardiol. 1992;13(2):107-9.
131. Braunlin EA, Rose AG, Hopwood JJ, Candel RD, Krivit W. Coronary artery patency following long-term successful engraftment 14 years after bone marrow transplantation in the Hurler syndrome. The American journal of cardiology. 2001;88(9):1075-7.

132. Yamada Y, Kato K, Sukegawa K, Tomatsu S, Fukuda S, Emura S, Kojima S, Matsuyama T, Sly WS, Kondo N, Orii T. Treatment of MPS VII (Sly disease) by allogeneic BMT in a female with homozygous A619V mutation. Bone Marrow Transplant. 1998;21(6):629-34.
133. Braunlin EA, Berry JM, Whitley CB. Cardiac findings after enzyme replacement therapy for mucopolysaccharidosis type I. The American journal of cardiology. 2006;98(3):416-8.
134. Hirth A, Berg A, Greve G. Successful treatment of severe heart failure in an infant with Hurler syndrome. J Inherit Metab Dis. 2007;30(5):820.
135. Okuyama T, Tanaka A, Suzuki Y, Ida H, Tanaka T, Cox GF, Eto Y, Orii T. Japan Elaprase Treatment (JET) study: idursulfase enzyme replacement therapy in adult patients with attenuated Hunter syndrome (Mucopolysaccharidosis II, MPS II). Molecular genetics and metabolism. 2010;99(1):18-25.
136. Wraith JE, Beck M, Lane R, van der Ploeg A, Shapiro E, Xue Y, Kakkis ED, Guffon N. Enzyme replacement therapy in patients who have mucopolysaccharidosis I and are younger than 5 years: results of a multinational study of recombinant human alpha-L-iduronidase (laronidase). Pediatrics. 2007;120(1):e37-46.
137. McGill JJ, Inwood AC, Coman DJ, Lipke ML, de Lore D, Swiedler SJ, Hopwood JJ. Enzyme replacement therapy for mucopolysaccharidosis VI from 8 weeks of age--a sibling control study. Clin Genet. 2010;77(5):492-8.
138. Gabrielli O, Clarke LA, Bruni S, Coppa GV. Enzyme-replacement therapy in a 5-month-old boy with attenuated presymptomatic MPS I: 5-year follow-up. Pediatrics. 2010;125(1):e183-7.
139. Arn P, Wraith JE, Underhill L. Characterization of surgical procedures in patients with mucopolysaccharidosis type I: findings from the MPS I Registry. The Journal of pediatrics. 2009;154(6):859-64.e3.
140. Deegan PB, Cox TM. Imiglucerase in the treatment of Gaucher disease: a history and perspective. Drug Des Devel Ther. 2012;6:81-106.
141. JCR Pharmaceuticals Announces Approval of IZCARGO® (Pabinafusp Alfa) forTreatment of MPS II (Hunter Syndrome) in Japan. Businesswire. Published March 23, 2021. https://www.businesswire.com/news/home/20210323005577/en/JCR-Pharmaceuticals-Announces-Approval-of-IZCARGO%C2%AE-Pabinafusp-Alfa-for-Treatment-of-MPS-II-Hunter-Syndrome-in-Japan.

142. Kishnani PS, Dickson PI, Muldowney L, Lee JJ, Rosenberg A, Abichandani R, Bluestone JA, Burton BK, Dewey M, Freitas A, Gavin D, Griebel D, Hogan M, Holland S, Tanpaiboon P, Turka LA, Utz JJ, Wang YM, Whitley CB, Kazi ZB, Pariser AR. Immune response to enzyme replacement therapies in lysosomal storage diseases and the role of immune tolerance induction. Molecular genetics and metabolism. 2016;117(2):66-83.
143. Kim S, Whitley CB, Jarnes Utz JR. Correlation between urinary GAG and anti-idursulfase ERT neutralizing antibodies during treatment with NICIT immune tolerance regimen: A case report. Molecular genetics and metabolism. 2017;122(1-2):92-9.
144. Clarke JT, Stoltz JM, Mulcahey MR. Neutral glycosphingolipids of serum lipoproteins in Fabry's disease. Biochimica et biophysica acta. 1976;431(2):317-25.
145. Wraith JE, Clarke LA, Beck M, Kolodny EH, Pastores GM, Muenzer J, Rapoport DM, Berger KI, Swiedler SJ, Kakkis ED, Braakman T, Chadbourne E, Walton-Bowen K, Cox GF. Enzyme replacement therapy for mucopolysaccharidosis I: a randomized, double-blinded, placebo-controlled, multinational study of recombinant human α-L-iduronidase (laronidase). The Journal of pediatrics. 2004;144(5):581-8.
146. Giugliani R, Giugliani L, de Oliveira Poswar F, Donis KC, Corte AD, Schmidt M, Boado RJ, Nestrasil I, Nguyen C, Chen S, Pardridge WM. Neurocognitive and somatic stabilization in pediatric patients with severe Mucopolysaccharidosis Type I after 52 weeks of intravenous brain-penetrating insulin receptor antibody-iduronidase fusion protein (valanafusp alpha): an open label phase 1-2 trial. Orphanet Journal of Rare Diseases. 2018;13(1):110.
147. Shapiro EG, Whitley CB, Eisengart JB. Beneath the floor: re-analysis of neurodevelopmental outcomes in untreated Hurler syndrome. Orphanet Journal of Rare Diseases. 2018;13(1):76.
148. Poe MD, Chagnon SL, Escolar ML. Early treatment is associated with improved cognition in Hurler syndrome. Annals of neurology. 2014;76(5):747-53.
149. Aldenhoven M, Wynn RF, Orchard PJ, O'Meara A, Veys P, Fischer A, Valayannopoulos V, Neven B, Rovelli A, Prasad VK, Tolar J, Allewelt H, Jones SA, Parini R, Renard M, Bordon V, Wulffraat NM, de Koning TJ, Shapiro EG, Kurtzberg J, Boelens JJ. Long-term outcome of Hurler syndrome patients after hematopoietic cell transplantation: an international multicenter study. Blood. 2015;125(13):2164-72.
150. Muenzer J, Beck M, Eng CM, Giugliani R, Harmatz P, Martin R, Ramaswami U, Vellodi A, Wraith JE, Cleary M, Gucsavas-Calikoglu M, Puga AC, Shinawi M, Ulbrich B,

Vijayaraghavan S, Wendt S, Conway AM, Rossi A, Whiteman DA, Kimura A. Long-term, open-labeled extension study of idursulfase in the treatment of Hunter syndrome. Genetics in medicine : official journal of the American College of Medical Genetics. 2011;13(2):95-101.

151. Muenzer J, Wraith JE, Beck M, Giugliani R, Harmatz P, Eng CM, Vellodi A, Martin R, Ramaswami U, Gucsavas-Calikoglu M, Vijayaraghavan S, Wendt S, Puga AC, Ulbrich B, Shinawi M, Cleary M, Piper D, Conway AM, Kimura A. A phase II/III clinical study of enzyme replacement therapy with idursulfase in mucopolysaccharidosis II (Hunter syndrome). Genetics in medicine : official journal of the American College of Medical Genetics. 2006;8(8):465-73.

152. Okuyama T, Eto Y, Sakai N, Nakamura K, Yamamoto T, Yamaoka M, Ikeda T, So S, Tanizawa K, Sonoda H, Sato Y. A Phase 2/3 Trial of Pabinafusp Alfa, IDS Fused with Anti-Human Transferrin Receptor Antibody, Targeting Neurodegeneration in MPS-II. Molecular Therapy. 2021;29(2):671-9.

153. Treiber A, Morand O, Clozel M. The pharmacokinetics and tissue distribution of the glucosylceramide synthase inhibitor miglustat in the rat. Xenobiotica. 2007;37(3):298-314.

154. Shayman JA. The design and clinical development of inhibitors of glycosphingolipid synthesis: will invention be the mother of necessity? Trans Am Clin Climatol Assoc. 2013;124:46-60.

155. Patterson MC, Vecchio D, Prady H, Abel L, Wraith JE. Miglustat for treatment of Niemann-Pick C disease: a randomised controlled study. The Lancet Neurology. 2007;6(9):765-72.

156. Shapiro BE, Pastores GM, Gianutsos J, Luzy C, Kolodny EH. Miglustat in late-onset Tay-Sachs disease: a 12-month, randomized, controlled clinical study with 24 months of extended treatment. Genetics in medicine : official journal of the American College of Medical Genetics. 2009;11(6):425-33.

157. Schiffmann R, Fitzgibbon EJ, Harris C, DeVile C, Davies EH, Abel L, van Schaik IN, Benko W, Timmons M, Ries M, Vellodi A. Randomized, controlled trial of miglustat in Gaucher's disease type 3. Annals of neurology. 2008;64(5):514-22.

158. Guffon N, Bin-Dorel S, Decullier E, Paillet C, Guitton J, Fouilhoux A. Evaluation of Miglustat Treatment in Patients with Type III Mucopolysaccharidosis: A Randomized,

Double-Blind, Placebo-Controlled Study. The Journal of pediatrics. 2011;159(5):838-44.e1.

159. Whitley CB, Belani KG, Chang PN, Summers CG, Blazar BR, Tsai MY, Latchaw RE, Ramsay NK, Kersey JH. Long-term outcome of Hurler syndrome following bone marrow transplantation. Am J Med Genet. 1993;46(2):209-18.

160. Hobbs JR, Hugh-Jones K, Barrett AJ, Byrom N, Chambers D, Henry K, James DC, Lucas CF, Rogers TR, Benson PF, Tansley LR, Patrick AD, Mossman J, Young EP. Reversal of clinical features of Hurler's disease and biochemical improvement after treatment by bone-marrow transplantation. Lancet. 1981;2(8249):709-12.

161. Rare Diseases: Common Issues in Drug Development Guidance for Industry. Food and Drug Administration. Silver Spring, MD. February 2019.

162. New Drug Therapy Approvals 2019. Food and Drug Administration. https://www.fda.gov/drugs/new-drugs-fda-cders-new-molecular-entities-and-new-therapeutic-biological-products/new-drug-therapy-approvals-2019.

163. FAQs About Rare Diseases. Genetic and Rare Disease Information Center. National Center for Advancing Translational Sciences. National Institute of Health. Updated November 30, 2017. https://rarediseases.info.nih.gov/diseases/pages/31/faqs-about-rare-diseases.

164. Subpart C - Designation of an Orphan Drug. Electronic Code of Federal Regulations. Title 21, Chapter 1, Subchapter D, Part 316, Subpart C. May 30, 2019. https://www.ecfr.gov/cgi-bin/retrieveECFR?gp=&SID=718f6fcbc20f2755bd1f5a980eb5eecd&mc=true&n=sp21.5.316.c&r=SUBPART&ty=HTML#se21.5.316_129.

165. Abbott NJ, Patabendige AA, Dolman DE, Yusof SR, Begley DJ. Structure and function of the blood-brain barrier. Neurobiology of disease. 2010;37(1):13-25.

166. Banks WA. From blood-brain barrier to blood-brain interface: new opportunities for CNS drug delivery. Nature reviews Drug discovery. 2016;15(4):275-92.

167. Begley DJ, Pontikis CC, Scarpa M. Lysosomal storage diseases and the blood-brain barrier. Current pharmaceutical design. 2008;14(16):1566-80.

168. Laterra J, Keep R, Betz LA, Goldstein GW. Blood—Brain Barrier. In: Siegel GJ, Agranoff BW, Albers RW, et al., editors. Basic Neurochemistry: Molecular, Cellular and Medical Aspects. 6th edition. Philadelphia: Lippincott-Raven; 1999. Available from: https://www.ncbi.nlm.nih.gov/books/NBK28180/.

169. Gynther M, Laine K, Ropponen J, Leppänen J, Mannila A, Nevalainen T, Savolainen J, Järvinen T, Rautio J. Large neutral amino acid transporter enables brain drug delivery via prodrugs. Journal of medicinal chemistry. 2008;51(4):932-6.
170. Lajoie JM, Shusta EV. Targeting receptor-mediated transport for delivery of biologics across the blood-brain barrier. Annual review of pharmacology and toxicology. 2015;55:613-31.
171. Xie J, Bi Y, Zhang H, Dong S, Teng L, Lee RJ, Yang Z. Cell-Penetrating Peptides in Diagnosis and Treatment of Human Diseases: From Preclinical Research to Clinical Application. Frontiers in pharmacology. 2020;11(697).
172. Schwarze SR, Ho A, Vocero-Akbani A, Dowdy SF. In Vivo Protein Transduction: Delivery of a Biologically Active Protein into the Mouse. Science (New York, NY). 1999;285(5433):1569-72.
173. Hocquemiller M, Giersch L, Audrain M, Parker S, Cartier N. Adeno-Associated Virus-Based Gene Therapy for CNS Diseases. Human gene therapy. 2016;27(7):478-96.
174. Edelmann MJ, Maegawa GHB. CNS-Targeting Therapies for Lysosomal Storage Diseases: Current Advances and Challenges. Front Mol Biosci. 2020;7:559804.
175. Schulz A, Ajayi T, Specchio N, de Los Reyes E, Gissen P, Ballon D, Dyke JP, Cahan H, Slasor P, Jacoby D, Kohlschütter A. Study of Intraventricular Cerliponase Alfa for CLN2 Disease. The New England journal of medicine. 2018;378(20):1898-907.
176. Brinker T, Stopa E, Morrison J, Klinge P. A new look at cerebrospinal fluid circulation. Fluids and barriers of the CNS. 2014;11:10-.
177. Schmitz NS, Krach LE, Coles LD, Schrogie J, Cloyd JC, Kriel RL. Characterizing Baclofen Withdrawal: A National Survey of Physician Experience. Pediatric neurology. 2021;122:106-9.
178. Bottros MM, Christo PJ. Current perspectives on intrathecal drug delivery. J Pain Res. 2014;7:615-26.
179. Keller L-A, Merkel O, Popp A. Intranasal drug delivery: opportunities and toxicologic challenges during drug development. Drug Delivery and Translational Research. 2021.
180. Neurelis. VALTOCO® (diazepam nasal spray). Full prescribing information. San Diego, CA: Neurelis; 2020.

181. UCB. NAYZILAM® (midazolam nasal spray). Full prescribing information. Smyrna, GA: UCB; 2019.
182. AFREZZA® (insulin human) inhalation powder, for oral inhalation use. Full prescribing information. MannKind Corporation, Danbury, CT. 2014.
183. Belur LR, Temme A, Podetz-Pedersen KM, Riedl M, Vulchanova L, Robinson N, Hanson LR, Kozarsky KF, Orchard PJ, Frey WH, 2nd, Low WC, McIvor RS. Intranasal Adeno-Associated Virus Mediated Gene Delivery and Expression of Human Iduronidase in the Central Nervous System: A Noninvasive and Effective Approach for Prevention of Neurologic Disease in Mucopolysaccharidosis Type I. Human gene therapy. 2017;28(7):576-87.
184. Cloyd J, Haut S, Carrazana E, Rabinowicz AL. Overcoming the challenges of developing an intranasal diazepam rescue therapy for the treatment of seizure clusters. Epilepsia. 2021;62(4):846-56.
185. Grubb JH, Vogler C, Levy B, Galvin N, Tan Y, Sly WS. Chemically modified beta-glucuronidase crosses blood-brain barrier and clears neuronal storage in murine mucopolysaccharidosis VII. Proceedings of the National Academy of Sciences of the United States of America. 2008;105(7):2616-21.
186. Grubb JH, Vogler C, Tan Y, Shah GN, MacRae AF, Sly WS. Infused Fc-tagged β-glucuronidase crosses the placenta and produces clearance of storage in utero in mucopolysaccharidosis VII mice. Proc Natl Acad Sci USA. 2008;105(24):8375-80.
187. Sly WS, Vogler C, Grubb JH, Levy B, Galvin N, Tan Y, Nishioka T, Tomatsu S. Enzyme therapy in mannose receptor-null mucopolysaccharidosis VII mice defines roles for the mannose 6-phosphate and mannose receptors. Proceedings of the National Academy of Sciences of the United States of America. 2006;103(41):15172-7.
188. Aronovich EL, Hall BC, Bell JB, McIvor RS, Hackett PB. Quantitative analysis of α-L-iduronidase expression in immunocompetent mice treated with the Sleeping Beauty transposon system. PloS one. 2013;8(10):e78161.
189. Aronovich EL, Bell JB, Belur LR, Gunther R, Koniar B, Erickson DC, Schachern PA, Matise I, McIvor RS, Whitley CB, Hackett PB. Prolonged expression of a lysosomal enzyme in mouse liver after Sleeping Beauty transposon-mediated gene delivery: implications for non-viral gene therapy of mucopolysaccharidoses. The journal of gene medicine. 2007;9(5):403-15.

190. Pardridge WM, Boado RJ, Giugliani R, Schmidt M. Plasma Pharmacokinetics of Valanafusp Alpha, a Human Insulin Receptor Antibody-Iduronidase Fusion Protein, in Patients with Mucopolysaccharidosis Type I. BioDrugs : clinical immunotherapeutics, biopharmaceuticals and gene therapy. 2018;32(2):169-76.
191. Qi Y, McKeever K, Taylor J, Haller C, Song W, Jones SA, Shi J. Pharmacokinetic and Pharmacodynamic Modeling to Optimize the Dose of Vestronidase Alfa, an Enzyme Replacement Therapy for Treatment of Patients with Mucopolysaccharidosis Type VII: Results from Three Trials. Clinical Pharmacokinetics. 2019;58(5):673-83.
192. Boado RJ, Hui EK, Lu JZ, Pardridge WM. IgG-enzyme fusion protein: pharmacokinetics and anti-drug antibody response in rhesus monkeys. Bioconjugate chemistry. 2013;24(1):97-104.
193. Qi Y, Musson DG, Schweighardt B, Tompkins T, Jesaitis L, Shaywitz AJ, Yang K, O'Neill CA. Pharmacokinetic and pharmacodynamic evaluation of elosulfase alfa, an enzyme replacement therapy in patients with Morquio A syndrome. Clinical pharmacokinetics. 2014;53(12):1137-47.
194. Considerations for the Design of Early-Phase Clinical Trials of Cellular and Gene Therapy Products, Guidance for Industry. Food and Drug Administration. Silver Spring, MD. June 2015.
195. Chowdhury EA, Meno-Tetang G, Chang HY, Wu S, Huang HW, Jamier T, Chandran J, Shah DK. Current progress and limitations of AAV mediated delivery of protein therapeutic genes and the importance of developing quantitative pharmacokinetic/pharmacodynamic (PK/PD) models. Adv Drug Deliv Rev. 2021;170:214-37.
196. Parra-Guillén ZP, González-Aseguinolaza G, Berraondo P, Trocóniz IF. Gene Therapy: A Pharmacokinetic/Pharmacodynamic Modelling Overview. Pharmaceutical research. 2010;27(8):1487-97.
197. An G. Concept of Pharmacologic Target-Mediated Drug Disposition in Large-Molecule and Small-Molecule Compounds. Journal of clinical pharmacology. 2020;60(2):149-63.
198. Levy G. Pharmacologic target-mediated drug disposition. Clinical pharmacology and therapeutics. 1994;56(3):248-52.

199. FDA-NIH Biomarker Working Group. BEST (Biomarkers, EndpointS, and other Tools) Resource. 2016. Food and Drug Administration (US): Silver Spring (MD). National Institutes of Health (US): Bethesda (MD).

.

200. Ou L, Kim S, Whitley CB, Jarnes-Utz JR. Genotype-phenotype correlation of gangliosidosis mutations using in silico tools and homology modeling. Molecular genetics and metabolism reports. 2019;20:100495.

201. Ou L, Przybilla MJ, Whitley CB. SAAMP 2.0: An algorithm to predict genotype-phenotype correlation of lysosomal storage diseases. Clin Genet. 2018;93(5):1008-14.

202. Kim S, Whitley CB, Jarnes JR. Chitotriosidase as a biomarker for gangliosidoses. Molecular genetics and metabolism reports. 2021;29:100803.

203. Hollak CE, van Weely S, van Oers MH, Aerts JM. Marked elevation of plasma chitotriosidase activity. A novel hallmark of Gaucher disease. The Journal of clinical investigation. 1994;93(3):1288-92.

204. Renkema GH, Boot RG, Strijland A, Donker-Koopman WE, van den Berg M, Muijsers AO, Aerts JM. Synthesis, sorting, and processing into distinct isoforms of human macrophage chitotriosidase. European journal of biochemistry. 1997;244(2):279-85.

205. van Eijk M, van Roomen CP, Renkema GH, Bussink AP, Andrews L, Blommaart EF, Sugar A, Verhoeven AJ, Boot RG, Aerts JM. Characterization of human phagocyte-derived chitotriosidase, a component of innate immunity. International immunology. 2005;17(11):1505-12.

206. Guo Y, He W, Boer AM, Wevers RA, de Bruijn AM, Groener JE, Hollak CE, Aerts JM, Galjaard H, van Diggelen OP. Elevated plasma chitotriosidase activity in various lysosomal storage disorders. J Inherit Metab Dis. 1995;18(6):717-22.

207. Michelakakis H, Dimitriou E, Labadaridis I. The expanding spectrum of disorders with elevated plasma chitotriosidase activity: an update. J Inherit Metab Dis. 2004;27(5):705-6.

208. Isman F, Hobert JA, Thompson JN, Natowicz MR. Plasma chitotriosidase in lysosomal storage diseases. Clinica chimica acta; international journal of clinical chemistry. 2008;387(1-2):165-7.

209. Elmonem MA, Ramadan DI, Issac MS, Selim LA, Elkateb SM. Blood spot versus plasma chitotriosidase: a systematic clinical comparison. Clinical biochemistry. 2014;47(1-2):38-43.
210. Sheth JJ, Sheth FJ, Oza NJ, Gambhir PS, Dave UP, Shah RC. Plasma chitotriosidase activity in children with lysosomal storage disorders. Indian journal of pediatrics. 2010;77(2):203-5.
211. Aerts JM, Kallemeijn WW, Wegdam W, Joao Ferraz M, van Breemen MJ, Dekker N, Kramer G, Poorthuis BJ, Groener JE, Cox-Brinkman J, Rombach SM, Hollak CE, Linthorst GE, Witte MD, Gold H, van der Marel GA, Overkleeft HS, Boot RG. Biomarkers in the diagnosis of lysosomal storage disorders: proteins, lipids, and inhibodies. J Inherit Metab Dis. 2011;34(3):605-19.
212. Hollak CE, Maas M, Aerts JM. Clinically relevant therapeutic endpoints in type I Gaucher disease. J Inherit Metab Dis. 2001;24 Suppl 2:97-105; discussion 87-8.
213. Genzyme Corporation. Cerezyme-imiglucerase injection, powder, lyophilized, for solution. Human prescription drug label. Last updated 4/2021.
214. Takeda Pharmaceuticals America, Inc. VPRIV- velaglucerase alfa injection, powder, lyophilized, for solution. Human prescription drug label. Last updated 12/15/2020.
215. Pfizer. Elelyso- taliglucerase alfa injection, powder, lyophilized, for solution. Human prescription drug label. Last updated 12/17/2020.
216. Shapiro EG, Nestrasil I, Rudser K, Delaney K, Kovac V, Ahmed A, Yund B, Orchard PJ, Eisengart J, Niklason GR, Raiman J, Mamak E, Cowan MJ, Bailey-Olson M, Harmatz P, Shankar SP, Cagle S, Ali N, Steiner RD, Wozniak J, Lim KO, Whitley CB. Neurocognition across the spectrum of mucopolysaccharidosis type I: Age, severity, and treatment. Molecular genetics and metabolism. 2015;116(1-2):61-8.
217. Jeyakumar M, Butters TD, Dwek RA, Platt FM. Glycosphingolipid lysosomal storage diseases: therapy and pathogenesis. Neuropathology and applied neurobiology. 2002;28(5):343-57.
218. Ou L, Przybilla MJ, Whitley CB. Proteomic analysis of mucopolysaccharidosis I mouse brain with two-dimensional polyacrylamide gel electrophoresis. Molecular genetics and metabolism. 2017;120(1-2):101-10.

219. Ou L, Przybilla MJ, Whitley CB. Metabolomics profiling reveals profound metabolic impairments in mice and patients with Sandhoff disease. Molecular genetics and metabolism. 2019;126(2):151-6.
220. Whitley CB, Jarnes JR. Chitotriosidase as a biomarker for central nervous system inflammation in the gangliosidosis diseases. February 2019. WORLDSymposium. Orlando, FL.
221. Wajner A, Michelin K, Burin MG, Pires RF, Pereira ML, Giugliani R, Coelho JC. Comparison between the biochemical properties of plasma chitotriosidase from normal individuals and from patients with Gaucher disease, GM1-gangliosidosis, Krabbe disease and heterozygotes for Gaucher disease. Clinical biochemistry. 2007;40(5-6):365-9.
222. Arash-Kaps L, Komlosi K, Seegräber M, Diederich S, Paschke E, Amraoui Y, Beblo S, Dieckmann A, Smitka M, Hennermann JB. The Clinical and Molecular Spectrum of GM1 Gangliosidosis. The Journal of pediatrics. 2019;215:152-7.e3.
223. Di Rosa M, Tibullo D, Vecchio M, Nunnari G, Saccone S, Di Raimondo F, Malaguarnera L. Determination of chitinases family during osteoclastogenesis. Bone. 2014;61:55-63.
224. Di Rosa M, Malaguarnera L. Chitinases as Biomarkers in Bone Studies. In: Patel VB, Preedy VR, editors. Biomarkers in Bone Disease. Biomarkers in Disease: Methods, Discoveries and Applications. Dordrecht: Springer Netherlands; 2017. p. 301-27.
225. Stirnemann J, Belmatoug N, Vincent C, Fain O, Fantin B, Mentre F. Bone events and evolution of biologic markers in Gaucher disease before and during treatment. Arthritis research & therapy. 2010;12(4):R156.
226. Raskovalova T, Deegan PB, Mistry PK, Pavlova E, Yang R, Zimran A, Berger J, Bourgne C, Pereira B, Labarere J, Berger MG. Accuracy of chitotriosidase activity and CCL18 concentration in assessing type I Gaucher disease severity. A systematic review with meta-analysis of individual participant data. Haematologica. 2020.
227. Elmonem MA, van den Heuvel LP, Levtchenko EN. Immunomodulatory Effects of Chitotriosidase Enzyme. Enzyme research. 2016;2016:2682680.
228. Varghese AM, Sharma A, Mishra P, Vijayalakshmi K, Harsha HC, Sathyaprabha TN, Bharath SM, Nalini A, Alladi PA, Raju TR. Chitotriosidase - a putative biomarker for sporadic amyotrophic lateral sclerosis. Clinical proteomics. 2013;10(1):19.

229. Malaguarnera L, Di Rosa M, Zambito AM, dell'Ombra N, Di Marco R, Malaguarnera M. Potential role of chitotriosidase gene in nonalcoholic fatty liver disease evolution. The American journal of gastroenterology. 2006;101(9):2060-9.
230. Wada R, Tifft CJ, Proia RL. Microglial activation precedes acute neurodegeneration in Sandhoff disease and is suppressed by bone marrow transplantation. Proceedings of the National Academy of Sciences of the United States of America. 2000;97(20):10954-9.
231. Coskun O, Oter S, Yaman H, Kilic S, Kurt I, Eyigun CP. Evaluating the validity of serum neopterin and chitotriosidase levels in follow-up brucellosis patients. Intern Med. 2010;49(12):1111-8.
232. Tasci C, Tapan S, Ozkaya S, Demirer E, Deniz O, Balkan A, Ozkan M, Inan I, Kurt I, Bilgic H. Efficacy of serum chitotriosidase activity in early treatment of patients with active tuberculosis and a negative sputum smear. Ther Clin Risk Manag. 2012;8:369-72.
233. Artieda M, Cenarro A, Ganan A, Jerico I, Gonzalvo C, Casado JM, Vitoria I, Puzo J, Pocovi M, Civeira F. Serum chitotriosidase activity is increased in subjects with atherosclerosis disease. Arterioscler Thromb Vasc Biol. 2003;23(9):1645-52.
234. Orchard PJ, Lund T, Miller W, Rothman SM, Raymond G, Nascene D, Basso L, Cloyd J, Tolar J. Chitotriosidase as a biomarker of cerebral adrenoleukodystrophy. Journal of neuroinflammation. 2011;8:144.
235. Mattsson N, Tabatabaei S, Johansson P, Hansson O, Andreasson U, Mansson JE, Johansson JO, Olsson B, Wallin A, Svensson J, Blennow K, Zetterberg H. Cerebrospinal fluid microglial markers in Alzheimer's disease: elevated chitotriosidase activity but lack of diagnostic utility. Neuromolecular medicine. 2011;13(2):151-9.
236. Ou L, Przybilla MJ, Ahlat O, Kim S, Overn P, Jarnes J, O'Sullivan MG, Whitley CB. A Highly Efficacious PS Gene Editing System Corrects Metabolic and Neurological Complications of Mucopolysaccharidosis Type I. Mol Ther. 2020;28(6):1442-54.
237. Ou L, Przybilla MJ, Tăbăran AF, Overn P, O'Sullivan MG, Jiang X, Sidhu R, Kell PJ, Ory DS, Whitley CB. A novel gene editing system to treat both Tay-Sachs and Sandhoff diseases. Gene therapy. 2020;27(5):226-36.
238. Przybilla, M. J. Models and Gene Therapy for GM1-Gangliosidosis and Morquio Syndrome Type B. December 2018. University of Minnesota. PhD Dissertation. ProQuest Dissertations and Theses database.

239. Boot RG, Bussink AP, Verhoek M, de Boer PA, Moorman AF, Aerts JM. Marked differences in tissue-specific expression of chitinases in mouse and man. The journal of histochemistry and cytochemistry : official journal of the Histochemistry Society. 2005;53(10):1283-92.
240. Monoszon AA, Cherkanova MS, Duzhak AB, Korolenko TA. Chitotriosidase activity in the blood serum and organs of mice of various strains under the influence of chitin. Bulletin of experimental biology and medicine. 2012;154(1):40-3.
241. Mizukami H, Mi Y, Wada R, Kono M, Yamashita T, Liu Y, Werth N, Sandhoff R, Sandhoff K, Proia RL. Systemic inflammation in glucocerebrosidase-deficient mice with minimal glucosylceramide storage. The Journal of clinical investigation. 2002;109(9):1215-21.
242. Waterston RH, Lindblad-Toh K, Birney E, Rogers J, Abril JF, Agarwal P, Agarwala R, Ainscough R, Alexandersson M, An P, Antonarakis SE, Attwood J, Baertsch R, Bailey J, Barlow K, Beck S, Berry E, Birren B, Bloom T, Bork P, Botcherby M, Bray N, Brent MR, Brown DG, Brown SD, Bult C, Burton J, Butler J, Campbell RD, Carninci P, Cawley S, Chiaromonte F, Chinwalla AT, Church DM, Clamp M, Clee C, Collins FS, Cook LL, Copley RR, Coulson A, Couronne O, Cuff J, Curwen V, Cutts T, Daly M, David R, Davies J, Delehaunty KD, Deri J, Dermitzakis ET, Dewey C, Dickens NJ, Diekhans M, Dodge S, Dubchak I, Dunn DM, Eddy SR, Elnitski L, Emes RD, Eswara P, Eyras E, Felsenfeld A, Fewell GA, Flicek P, Foley K, Frankel WN, Fulton LA, Fulton RS, Furey TS, Gage D, Gibbs RA, Glusman G, Gnerre S, Goldman N, Goodstadt L, Grafham D, Graves TA, Green ED, Gregory S, Guigó R, Guyer M, Hardison RC, Haussler D, Hayashizaki Y, Hillier LW, Hinrichs A, Hlavina W, Holzer T, Hsu F, Hua A, Hubbard T, Hunt A, Jackson I, Jaffe DB, Johnson LS, Jones M, Jones TA, Joy A, Kamal M, Karlsson EK, Karolchik D, Kasprzyk A, Kawai J, Keibler E, Kells C, Kent WJ, Kirby A, Kolbe DL, Korf I, Kucherlapati RS, Kulbokas EJ, Kulp D, Landers T, Leger JP, Leonard S, Letunic I, Levine R, Li J, Li M, Lloyd C, Lucas S, Ma B, Maglott DR, Mardis ER, Matthews L, Mauceli E, Mayer JH, McCarthy M, McCombie WR, McLaren S, McLay K, McPherson JD, Meldrim J, Meredith B, Mesirov JP, Miller W, Miner TL, Mongin E, Montgomery KT, Morgan M, Mott R, Mullikin JC, Muzny DM, Nash WE, Nelson JO, Nhan MN, Nicol R, Ning Z, Nusbaum C, O'Connor MJ, Okazaki Y, Oliver K, Overton-Larty E, Pachter L, Parra G, Pepin KH, Peterson J, Pevzner P, Plumb R, Pohl CS, Poliakov A, Ponce TC, Ponting CP, Potter S, Quail M, Reymond A, Roe BA, Roskin KM,

Rubin EM, Rust AG, Santos R, Sapojnikov V, Schultz B, Schultz J, Schwartz MS, Schwartz S, Scott C, Seaman S, Searle S, Sharpe T, Sheridan A, Shownkeen R, Sims S, Singer JB, Slater G, Smit A, Smith DR, Spencer B, Stabenau A, Stange-Thomann N, Sugnet C, Suyama M, Tesler G, Thompson J, Torrents D, Trevaskis E, Tromp J, Ucla C, Ureta-Vidal A, Vinson JP, Von Niederhausern AC, Wade CM, Wall M, Weber RJ, Weiss RB, Wendl MC, West AP, Wetterstrand K, Wheeler R, Whelan S, Wierzbowski J, Willey D, Williams S, Wilson RK, Winter E, Worley KC, Wyman D, Yang S, Yang SP, Zdobnov EM, Zody MC, Lander ES. Initial sequencing and comparative analysis of the mouse genome. Nature. 2002;420(6915):520-62.

243. Pardridge WM, Kang YS, Buciak JL, Yang J. Human insulin receptor monoclonal antibody undergoes high affinity binding to human brain capillaries in vitro and rapid transcytosis through the blood-brain barrier in vivo in the primate. Pharmaceutical research. 1995;12(6):807-16.

244. Boado RJ, Zhang Y, Zhang Y, Xia CF, Wang Y, Pardridge WM. Genetic engineering of a lysosomal enzyme fusion protein for targeted delivery across the human blood-brain barrier. Biotechnology and bioengineering. 2008;99(2):475-84.

245. Boado RJ, Hui EK, Lu JZ, Zhou QH, Pardridge WM. Reversal of lysosomal storage in brain of adult MPS-I mice with intravenous Trojan horse-iduronidase fusion protein. Molecular pharmaceutics. 2011;8(4):1342-50.

246. Prigent SA, Stanley KK, Siddle K. Identification of epitopes on the human insulin receptor reacting with rabbit polyclonal antisera and mouse monoclonal antibodies. The Journal of biological chemistry. 1990;265(17):9970-7.

247. Battista N, Di Tommaso M, Bari M, Maccarrone M. The endocannabinoid system: an overview. Front Behav Neurosci. 2012;6(9).

248. CNR1 cannabinoid receptor 1 [Homo sapiens (human)] [Internet]. Bethesda (MD): National Library of Medicine (US), National Center for Biotechnology Information; 2004 – [cited 2021 Oct 15]. Available from: https://www.ncbi.nlm.nih.gov/gene/1268.

249. Cnr1 cannabinoid receptor 1 (brain) [Mus musculus (house mouse)] [Internet]. Bethesda (MD): National Library of Medicine (US), National Center for Biotechnology Information; 2004 – [cited 2021 Oct 15]. Available from: https://www.ncbi.nlm.nih.gov/gene/12801.

250. cannabinoid receptor 1 isoform a [Homo sapiens] [Internet]. Bethesda (MD): National Library of Medicine (US), National Center for Biotechnology Information; [1988]

- [cited 2021 Oct 17]. Available from: https://www.ncbi.nlm.nih.gov/protein/NP_001357474.1.

251. The UniProt Consortium. UniProt: the universal protein knowledgebase in 2021. Nucleic Acids Res. 49:D1 (2021).

252. cannabinoid receptor 1 [Mus musculus] [Internet]. Bethesda (MD): National Library of Medicine (US), National Center for Biotechnology Information; [1988] - [cited 2021 Oct 17]. Available from: https://www.ncbi.nlm.nih.gov/protein/NP_001352810.1.

253. Stephen F. Altschul, Thomas L. Madden, Alejandro A. Schäffer, Jinghui Zhang, Zheng Zhang, Webb Miller, and David J. Lipman (1997), "Gapped BLAST and PSI-BLAST: a new generation of protein database search programs", Nucleic Acids Res. 25:3389-3402.

254. Golech SA, McCarron RM, Chen Y, Bembry J, Lenz F, Mechoulam R, Shohami E, Spatz M. Human brain endothelium: coexpression and function of vanilloid and endocannabinoid receptors. Brain research Molecular brain research. 2004;132(1):87-92.

255. Lu TS, Avraham HK, Seng S, Tachado SD, Koziel H, Makriyannis A, Avraham S. Cannabinoids inhibit HIV-1 Gp120-mediated insults in brain microvascular endothelial cells. J Immunol. 2008;181(9):6406-16.

256. Maccarrone M, Fiori A, Bari M, Granata F, Gasperi V, De Stefano ME, Finazzi-Agro A, Strom R. Regulation by cannabinoid receptors of anandamide transport across the blood-brain barrier and through other endothelial cells. Thrombosis and haemostasis. 2006;95(1):117-27.

257. Bénard G, Massa F, Puente N, Lourenço J, Bellocchio L, Soria-Gómez E, Matias I, Delamarre A, Metna-Laurent M, Cannich A, Hebert-Chatelain E, Mulle C, Ortega-Gutiérrez S, Martín-Fontecha M, Klugmann M, Guggenhuber S, Lutz B, Gertsch J, Chaouloff F, López-Rodríguez ML, Grandes P, Rossignol R, Marsicano G. Mitochondrial CB1 receptors regulate neuronal energy metabolism. Nature Neuroscience. 2012;15(4):558-64.

258. Fagerberg L, Hallström BM, Oksvold P, Kampf C, Djureinovic D, Odeberg J, Habuka M, Tahmasebpoor S, Danielsson A, Edlund K, Asplund A, Sjöstedt E, Lundberg E, Szigyarto CA-K, Skogs M, Takanen JO, Berling H, Tegel H, Mulder J, Nilsson P, Schwenk JM, Lindskog C, Danielsson F, Mardinoglu A, Sivertsson A, von Feilitzen K, Forsberg M, Zwahlen M, Olsson I, Navani S, Huss M, Nielsen J, Ponten F, Uhlén M.

Analysis of the human tissue-specific expression by genome-wide integration of transcriptomics and antibody-based proteomics. Mol Cell Proteomics. 2014;13(2):397-406.
259. Rioli V, Gozzo FC, Heimann AS, Linardi A, Krieger JE, Shida CS, Almeida PC, Hyslop S, Eberlin MN, Ferro ESJTJobcV. Novel natural peptide substrates for endopeptidase 24.15, neurolysin, and angiotensin-converting enzyme. The Journal of biological chemistry. 2003(10):8547-55.
260. Bauer M, Chicca A, Tamborrini M, Eisen D, Lerner R, Lutz B, Poetz O, Pluschke G, Gertsch J. Identification and quantification of a new family of peptide endocannabinoids (Pepcans) showing negative allosteric modulation at CB1 receptors. The Journal of biological chemistry. 2012;287(44):36944-67.
261. Bomar MG, Galande AK. Modulation of the cannabinoid receptors by hemopressin peptides. Life Sciences. 2013;92(8):520-4.
262. Gomes I, Grushko JS, Golebiewska U, Hoogendoorn S, Gupta A, Heimann AS, Ferro ES, Scarlata S, Fricker LD, Devi LA. Novel endogenous peptide agonists of cannabinoid receptors. FASEB journal : official publication of the Federation of American Societies for Experimental Biology. 2009;23(9):3020-9.
263. Hsieh C, Brown S, Derleth C, Mackie K. Internalization and recycling of the CB1 cannabinoid receptor. Journal of neurochemistry. 1999;73(2):493-501.
264. Heimann AS, Gomes I, Dale CS, Pagano RL, Gupta A, de Souza LL, Luchessi AD, Castro LM, Giorgi R, Rioli V, Ferro ES, Devi LA. Hemopressin is an inverse agonist of CB1 cannabinoid receptors. Proceedings of the National Academy of Sciences of the United States of America. 2007;104(51):20588-93.
265. Ferrante C, Recinella L, Leone S, Chiavaroli A, Di Nisio C, Martinotti S, Mollica A, Macedonio G, Stefanucci A, Dvorácskó S, Tömböly C, De Petrocellis L, Vacca M, Brunetti L, Orlando G. Anorexigenic effects induced by RVD-hemopressin(α) administration. Pharmacological reports : PR. 2017;69(6):1402-7.
266. Zhang R-s, He Z, Jin W-d, Wang R. Effects of the cannabinoid 1 receptor peptide ligands hemopressin, (m)RVD-hemopressin(α) and (m)VD-hemopressin(α) on memory in novel object and object location recognition tasks in normal young and Aβ1–42-treated mice. Neurobiology of Learning and Memory. 2016;134:264-74.

267. Blais PA, Côté J, Morin J, Larouche A, Gendron G, Fortier A, Regoli D, Neugebauer W, Gobeil F, Jr. Hypotensive effects of hemopressin and bradykinin in rabbits, rats and mice. A comparative study. Peptides. 2005;26(8):1317-22.
268. Han Z-l, Fang Q, Wang Z-l, Li X-h, Li N, Chang X-m, Pan J-x, Tang H-z, Wang R. Antinociceptive Effects of Central Administration of the Endogenous Cannabinoid Receptor Type 1 Agonist VDPVNFKLLSH-OH [(m)VD-hemopressin], an N-Terminally Extended Hemopressin Peptide. Journal of Pharmacology and Experimental Therapeutics. 2014;348(2):316-23.
269. Chen X, Zaro JL, Shen W-C. Fusion protein linkers: property, design and functionality. Advanced drug delivery reviews. 2013;65(10):1357-69.
270. Osborn MJ, McElmurry RT, Peacock B, Tolar J, Blazar BR. Targeting of the CNS in MPS-IH Using a Nonviral Transferrin-α-l-iduronidase Fusion Gene Product. Molecular Therapy. 2008;16(8):1459-66.
271. Wang D, El-Amouri SS, Dai M, Kuan CY, Hui DY, Brady RO, Pan D. Engineering a lysosomal enzyme with a derivative of receptor-binding domain of apoE enables delivery across the blood-brain barrier. Proceedings of the National Academy of Sciences of the United States of America. 2013;110(8):2999-3004.
272. Bockenhoff A, Cramer S, Wolte P, Knieling S, Wohlenberg C, Gieselmann V, Galla HJ, Matzner U. Comparison of five peptide vectors for improved brain delivery of the lysosomal enzyme arylsulfatase A. The Journal of neuroscience : the official journal of the Society for Neuroscience. 2014;34(9):3122-9.
273. UniProtKB - P35475 (IDUA_HUMAN). Universal Protein Resource (UniProt). https://www.uniprot.org/uniprot/P35475.
274. Liu F, Song Y, Liu D. Hydrodynamics-based transfection in animals by systemic administration of plasmid DNA. Gene therapy. 1999;6(7):1258-66.
275. Miao CH, Ohashi K, Patijn GA, Meuse L, Ye X, Thompson AR, Kay MA. Inclusion of the Hepatic Locus Control Region, an Intron, and Untranslated Region Increases and Stabilizes Hepatic Factor IX Gene Expression in Vivo but Not in Vitro. Molecular Therapy. 2000;1(6):522-32.
276. Ou L, Przybilla MJ, Koniar BL, Whitley CB. Elements of lentiviral vector design toward gene therapy for treating mucopolysaccharidosis I. Molecular genetics and metabolism reports. 2016;8:87-93.

277. Homo sapiens hemoglobin subunit alpha 1 (HBA1), mRNA [Internet]. Bethesda (MD): National Library of Medicine (US), National Center for Biotechnology Information; [1988] - [cited 2021 Oct 17]. Available from: https://www.ncbi.nlm.nih.gov/nuccore/NM_000558.5.
278. Homo sapiens hemoglobin subunit alpha 2 (HBA2), mRNA [Internet]. Bethesda (MD): National Library of Medicine (US), National Center for Biotechnology Information; [1988] - [cited 2021 Oct 17]. Available from: https://www.ncbi.nlm.nih.gov/nuccore/1441565460.
279. Mus musculus hemoglobin alpha, adult chain 1 (Hba-a1), mRNA [Internet]. Bethesda (MD): National Library of Medicine (US), National Center for Biotechnology Information; [1988] - [cited 2021 Oct 17]. Available from: https://www.ncbi.nlm.nih.gov/nuccore/NM_008218.
280. Altschul SF, Gish W, Miller W, Myers EW, Lipman DJ. Basic local alignment search tool. J Mol Biol. 1990;215(3):403-10.
281. https://www.idtdna.com/CodonOpt COTIDTCO.
282. Suda T, Liu D. Hydrodynamic Gene Delivery: Its Principles and Applications. Molecular Therapy. 2007;15(12):2063-9.
283. Sendra L, Herrero MJ, Aliño SF. Translational Advances of Hydrofection by Hydrodynamic Injection. Genes. 2018;9(3).
284. Ou L, Herzog TL, Wilmot CM, Whitley CB. Standardization of α-L-iduronidase enzyme assay with Michaelis–Menten kinetics. Molecular genetics and metabolism. 2014;111(2):113-5.
285. Varshney D, Spiegel J, Zyner K, Tannahill D, Balasubramanian S. The regulation and functions of DNA and RNA G-quadruplexes. Nature Reviews Molecular Cell Biology. 2020;21(8):459-74.
286. QGRS Mapper: a web-based server for predicting G-quadruplexes in nucleotide sequences. Oleg Kikin, Lawrence D'Antonio and Paramjeet S Bagga. Nucleic Acids Research 2006 July; 34 (Web Server issue):W676-W682.
287. ORFfinder [Internet]. Bethesda (MD): National Library of Medicine (US), National Center for Biotechnology Information; 2021 – [cited 2021 Oct 17]. Available from: https://www.ncbi.nlm.nih.gov/orffinder/.
288. SnapGene® software (from Insightful Science; available at snapgene.com).
289. https://www.genome.jp/tools/motif/ MSKUBCAO.

290. Bateman A, Birney E, Cerruti L, Durbin R, Etwiller L, Eddy SR, Griffiths-Jones S, Howe KL, Marshall M, Sonnhammer EL. The Pfam protein families database. Nucleic acids research. 2002;30(1):276-80.
291. Lu S, Wang J, Chitsaz F, Derbyshire MK, Geer RC, Gonzales NR, Gwadz M, Hurwitz DI, Marchler GH, Song JS, Thanki N, Yamashita RA, Yang M, Zhang D, Zheng C, Lanczycki CJ, Marchler-Bauer A. CDD/SPARCLE: the conserved domain database in 2020. Nucleic acids research. 2020;48(D1):D265-d8.
292. https://prosite.expasy.org/ PSSIoBAO.
293. Braulke T, Bonifacino JS. Sorting of lysosomal proteins. Biochimica et Biophysica Acta (BBA) - Molecular Cell Research. 2009;1793(4):605-14.
294. Staudt C, Puissant E, Boonen M. Subcellular Trafficking of Mammalian Lysosomal Proteins: An Extended View. International journal of molecular sciences. 2016;18(1):47.
295. Argos P. An investigation of oligopeptides linking domains in protein tertiary structures and possible candidates for general gene fusion. Journal of Molecular Biology. 1990;211(4):943-58.
296. George RA, Heringa J. An analysis of protein domain linkers: their classification and role in protein folding. Protein Eng. 2002;15(11):871-9.
297. McCormick AL, Thomas MS, Heath AW. Immunization with an interferon-gamma-gp120 fusion protein induces enhanced immune responses to human immunodeficiency virus gp120. The Journal of infectious diseases. 2001;184(11):1423-30.
298. Bergeron LM, Gomez L, Whitehead TA, Clark DS. Self-renaturing enzymes: design of an enzyme-chaperone chimera as a new approach to enzyme stabilization. Biotechnology and bioengineering. 2009;102(5):1316-22.
299. Ory DS, Ottinger EA, Farhat NY, King KA, Jiang X, Weissfeld L, Berry-Kravis E, Davidson CD, Bianconi S, Keener LA, Rao R, Soldatos A, Sidhu R, Walters KA, Xu X, Thurm A, Solomon B, Pavan WJ, Machielse BN, Kao M, Silber SA, McKew JC, Brewer CC, Vite CH, Walkley SU, Austin CP, Porter FD. Intrathecal 2-hydroxypropyl-β-cyclodextrin decreases neurological disease progression in Niemann-Pick disease, type C1: a non-randomised, open-label, phase 1-2 trial. Lancet. 2017;390(10104):1758-68.
300. Liu B. Therapeutic potential of cyclodextrins in the treatment of Niemann-Pick type C disease. Clin Lipidol. 2012;7(3):289-301.

301. Method for the Detection of Mucopolysaccharide Disease (Serial No. 194,553) submitted May 13, 1988; continuation-in-part (Serial No. 07/297,051) submitted January 16, 1989; amendment, Method for the detection of mucopolysaccharide storage disease, continuation-in-part (Serial No. 07/297,051) submitted May 29, 1991; patent allowed, November, 1993; patent application (Serial No. 07/806,833) Method for the Detection of Mucopolysaccharide Storage Diseases issued on May 10, 1994 as U.S. Patent No. 5,310,646.

302. Whitley CB, Ridnour MD, Draper KA, Dutton CM, Neglia JP. Diagnostic test for mucopolysaccharidosis. I. Direct method for quantifying excessive urinary glycosaminoglycan excretion. Clinical chemistry. 1989;35(3):374-9.

303. Whitley CB, Draper KA, Dutton CM, Brown PA, Severson SL, France LA. Diagnostic test for mucopolysaccharidosis. II. Rapid quantification of glycosaminoglycan in urine samples collected on a paper matrix. Clinical chemistry. 1989;35(10):2074-81.

304. Whitley CB, Spielmann RC, Herro G, Teragawa SS. Urinary glycosaminoglycan excretion quantified by an automated semimicro method in specimens conveniently transported from around the globe. Molecular genetics and metabolism. 2002;75(1):56-64.

305. Urayama A, Grubb JH, Banks WA, Sly WS. Epinephrine enhances lysosomal enzyme delivery across the blood brain barrier by up-regulation of the mannose 6-phosphate receptor. Proceedings of the National Academy of Sciences of the United States of America. 2007;104(31):12873-8.

306. Valic MS, Halim M, Schimmer P, Zheng G. Guidelines for the experimental design of pharmacokinetic studies with nanomaterials in preclinical animal models. Journal of controlled release : official journal of the Controlled Release Society. 2020;323:83-101.

307. Product Monograph: Aldurazyme(R) laronidase. Genzyme Canada, a division of Sanofi-Aventis Canada Inc. Mississauga, ON. https://products.sanofi.ca/en/aldurazyme-en.pdf.

308. El-Amouri SS, Dai M, Han JF, Brady RO, Pan D. Normalization and improvement of CNS deficits in mice with Hurler syndrome after long-term peripheral delivery of BBB-targeted iduronidase. Mol Ther. 2014;22(12):2028-37.

309. ICH S12 Guideline. Nonclinical Biodstribution Consdierations for Gene Therapy Products. Draft Version. Accessed Oct 27 2021. https://www.fda.gov/media/152123/download.

310. Systems in ELISA. The ELISA Guidebook. Totowa, NJ: Humana Press; 2009. p. 9-42.

311. Human Alpha-L-iduronidase (IDUA) ELISA Kit. Catalog number abx253700. 2021. Abbexa LTD C, UK. https://www.abbexa.com/human-alpha-l-iduronidase-elisa-kit.

312. Bailer AJ. Testing for the equality of area under the curves when using destructive measurement techniques. J Pharmacokinet Biopharm. 1988;16(3):303-9.

313. Nedelman JR, Jia X. An extension of Satterthwaite's approximation applied to pharmacokinetics. J Biopharm Stat. 1998;8(2):317-28.

314. Holder DJ. Comments on Nedelman and Jia's extension of Satterthwaite's approximation applied to pharmacokinetics. J Biopharm Stat. 2001;11(1-2):75-9.

315. Dalsgaard T, Cecchi CR, Askou AL, Bak RO, Andersen PO, Hougaard D, Jensen TG, Dagnæs-Hansen F, Mikkelsen JG, Corydon TJ, Aagaard L. Improved Lentiviral Gene Delivery to Mouse Liver by Hydrodynamic Vector Injection through Tail Vein. Mol Ther Nucleic Acids. 2018;12:672-83.

316. Mingozzi F, High KA. Immune responses to AAV vectors: overcoming barriers to successful gene therapy. Blood. 2013;122(1):23-36.

317. Becker K, Pan D, Whitley CB. Real-time quantitative polymerase chain reaction to assess gene transfer. Human gene therapy. 1999;10(15):2559-66.

APPENDIX

Appendix Table 1: Comparison of Average Chitotriosidase Levels in the CSF Between Different Lysosomal Diseases and Disease Phenotypes

Disease Phenotype Comparisons		p-value
Gaucher I	GM1, infantile	0.0003***
Gaucher I	GM1, juvenile	0.8167
Gaucher I	GM1, late-infantile	0.0004***
Gaucher I	MPS IS	0.8759
Gaucher I	MPS II, attenuated	1
Gaucher I	MPS IIIA	0.9981
Gaucher I	MSD	0.9998
Gaucher I	Sandhoff, infantile	0.1616
Gaucher I	Tay-Sachs, late-onset	0.9969
Gaucher I	Tay-Sachs, infantile	<0.0001****
Gaucher I	Tay-Sachs, juvenile	0.0622
GM1, infantile	GM1, juvenile	0.1704
GM1, infantile	GM1, late-infantile	1
GM1, infantile	MPS IS	<.0001****
GM1, infantile	MPS II, attenuated	0.0001****
GM1, infantile	MPS IIIA	<.0001****
GM1, infantile	MSD	0.005**
GM1, infantile	Sandhoff, infantile	0.3447
GM1, infantile	Tay-Sachs, late-onset	<.0001****
GM1, infantile	Tay-Sachs, infantile	0.9996
GM1, infantile	Tay-Sachs, juvenile	0.341
GM1, juvenile	GM1, late-infantile	0.1944
GM1, juvenile	MPS IS	0.0209*
GM1, juvenile	MPS II, attenuated	0.6151
GM1, juvenile	MPS IIIA	0.9515
GM1, juvenile	MSD	0.9948
GM1, juvenile	Sandhoff, infantile	0.9986
GM1, juvenile	Tay-Sachs, late-onset	0.9865
GM1, juvenile	Tay-Sachs, infantile	0.0925
GM1, juvenile	Tay-Sachs, juvenile	0.984
GM1, late-infantile	MPS IS	<.0001****

GM1, late-infantile	MPS II, attenuated	0.0001****
GM1, late-infantile	MPS IIIA	<.0001****
GM1, late-infantile	MSD	0.0064**
GM1, late-infantile	Sandhoff, infantile	0.4022
GM1, late-infantile	Tay-Sachs, late-onset	<.0001****
GM1, late-infantile	Tay-Sachs, infantile	0.9997
GM1, late-infantile	Tay-Sachs, juvenile	0.417
MPS IS	MPS II, attenuated	0.9808
MPS IS	MPS IIIA	0.0075**
MPS IS	MSD	0.3465
MPS IS	Sandhoff, infantile	<.0001****
MPS IS	Tay-Sachs, late-onset	0.0265*
MPS IS	Tay-Sachs, infantile	<.0001****
MPS IS	Tay-Sachs, juvenile	<.0001****
MPS II, attenuated	MPS IIIA	0.9603
MPS II, attenuated	MSD	0.9947
MPS II, attenuated	Sandhoff, infantile	0.0697
MPS II, attenuated	Tay-Sachs, late-onset	0.9557
MPS II, attenuated	Tay-Sachs, infantile	<.0001****
MPS II, attenuated	Tay-Sachs, juvenile	0.0226*
MPS IIIA	MSD	1
MPS IIIA	Sandhoff, infantile	0.0822
MPS IIIA	Tay-Sachs, late-onset	1
MPS IIIA	Tay-Sachs, infantile	<.0001****
MPS IIIA	Tay-Sachs, juvenile	0.0072**
MSD	Sandhoff, infantile	0.6089
MSD	Tay-Sachs, late-onset	1
MSD	Tay-Sachs, infantile	0.0024**
MSD	Tay-Sachs, juvenile	0.366
Sandhoff, infantile	Tay-Sachs, late-onset	0.2568
Sandhoff, infantile	Tay-Sachs, infantile	0.1776
Sandhoff, infantile	Tay-Sachs, juvenile	1
Tay-Sachs, late-onset	Tay-Sachs, infantile	<.0001****
Tay-Sachs, late-onset	Tay-Sachs, juvenile	0.0615

Tay-Sachs, infantile	Tay-Sachs, juvenile	0.1622

*A one-way ANOVA was performed with disease phenotype and chitotriosidase levels in the CSF. Neuronopathic phenotype of Gaucher disease was excluded from analysis because the exact phenotype of Gaucher was uncertain (i.e., type 2 vs type 3). Multiple comparisons were adjusted using Tukey's method. Gaucher I = Gaucher disease type I. MPS = mucopolysaccharidosis. MPS IS = MPS I Scheie. MPS IIIA = MPS III type A. MSD = multiple sulfatase deficiency. * p <0.5. ** p<.01. *** p<.001. ****p<.0001.*

Appendix Table 2: Comparison of Average Chitotriosidase Levels in the Serum Between Different Lysosomal Diseases and Phenotypes

Disease Phenotype Comparisons		p-value
Gaucher I	GM1, infantile	0.9868
Gaucher I	GM1, juvenile	0.0016***
Gaucher I	GM1, late-infantile	0.3498
Gaucher I	MPS IH	<.0001****
Gaucher I	MPS IS	<.0001****
Gaucher I	MPS II, attenuated	<.0001****
Gaucher I	MPS IIIA	<.0001****
Gaucher I	MPS IVA	0.4582
Gaucher I	Sandhoff, infantile	0.0001****
Gaucher I	Tay-Sachs, late-onset	0.0001****
Gaucher I	Tay-Sachs, infantile	<.0001****
Gaucher I	Tay-Sachs, juvenile	<.0001****
GM1, infantile	GM1, juvenile	0.0252*
GM1, infantile	GM1, late-infantile	0.9696
GM1, infantile	MPS IH	0.0002***
GM1, infantile	MPS IS	<.0001****
GM1, infantile	MPS II, attenuated	<.0001****
GM1, infantile	MPS IIIA	<.0001****
GM1, infantile	MPS IVA	0.8031
GM1, infantile	Sandhoff, infantile	0.0007***
GM1, infantile	Tay-Sachs, late-onset	0.0012**
GM1, infantile	Tay-Sachs, infantile	<.0001****
GM1, infantile	Tay-Sachs, juvenile	<.0001****
GM1, juvenile	GM1, late-infantile	0.3462
GM1, juvenile	MPS IH	0.0876
GM1, juvenile	MPS IS	<.0001****
GM1, juvenile	MPS II, attenuated	0.0273*
GM1, juvenile	MPS IIIA	0.0393*
GM1, juvenile	MPS IVA	1
GM1, juvenile	Sandhoff, infantile	0.5838
GM1, juvenile	Tay-Sachs, late-onset	0.9842

GM1, juvenile	Tay-Sachs, infantile	0.0603
GM1, juvenile	Tay-Sachs, juvenile	0.207
GM1, late-infantile	MPS IH	0.0015**
GM1, late-infantile	MPS IS	<.0001****
GM1, late-infantile	MPS II, attenuated	0.0003***
GM1, late-infantile	MPS IIIA	<.0001****
GM1, late-infantile	MPS IVA	0.9815
GM1, late-infantile	Sandhoff, infantile	0.0085**
GM1, late-infantile	Tay-Sachs, late-onset	0.0264*
GM1, late-infantile	Tay-Sachs, infantile	<.0001****
GM1, late-infantile	Tay-Sachs, juvenile	0.0001****
MPS IH	MPS IS	1
MPS IH	MPS II, attenuated	1
MPS IH	MPS IIIA	0.9404
MPS IH	MPS IVA	0.453
MPS IH	Sandhoff, infantile	0.9748
MPS IH	Tay-Sachs, late-onset	0.4759
MPS IH	Tay-Sachs, infantile	0.9013
MPS IH	Tay-Sachs, juvenile	0.9565
MPS IS	MPS II, attenuated	1
MPS IS	MPS IIIA	0.1424
MPS IS	MPS IVA	0.1025
MPS IS	Sandhoff, infantile	0.6765
MPS IS	Tay-Sachs, late-onset	0.0087**
MPS IS	Tay-Sachs, infantile	0.0736
MPS IS	Tay-Sachs, juvenile	0.3625
MPS II, attenuated	MPS IIIA	0.736
MPS II, attenuated	MPS IVA	0.2572
MPS II, attenuated	Sandhoff, infantile	0.8632
MPS II, attenuated	Tay-Sachs, late-onset	0.2314
MPS II, attenuated	Tay-Sachs, infantile	0.6547
MPS II, attenuated	Tay-Sachs, juvenile	0.7912
MPS IIIA	MPS IVA	0.8914
MPS IIIA	Sandhoff, infantile	1

MPS IIIA	Tay-Sachs, late-onset	0.8819
MPS IIIA	Tay-Sachs, infantile	1
MPS IIIA	Tay-Sachs, juvenile	1
MPS IVA	Sandhoff, infantile	0.9687
MPS IVA	Tay-Sachs, late-onset	1
MPS IVA	Tay-Sachs, infantile	0.9284
MPS IVA	Tay-Sachs, juvenile	0.9319
Sandhoff, infantile	Tay-Sachs, late-onset	0.9952
Sandhoff, infantile	Tay-Sachs, infantile	1
Sandhoff, infantile	Tay-Sachs, juvenile	1
Tay-Sachs, late-onset	Tay-Sachs, infantile	0.9416
Tay-Sachs, late-onset	Tay-Sachs, juvenile	0.9667
Tay-Sachs, infantile	Tay-Sachs, juvenile	1

*A one-way ANOVA was performed with disease phenotype and chitotriosidase levels in the serum. Neuronopathic phenotype of Gaucher disease was excluded from analysis because the exact phenotype of Gaucher was uncertain (i.e., type 2 vs type 3). Multiple comparisons were adjusted using Tukey's method. Gaucher I = Gaucher type I. MPS = mucopolysaccharidosis. MPS IH = MPS I Hurler. MPS IS = MPS I Scheie. MPS IIIA = MPS III type A. MPS IVA = MPS IV type A. * p <0.5. ** p<.01. *** p<.001. ****p<.0001.*

Appendix Table 3: Pairwise Test Results for Enzyme Activity in the Brain

Dunnett's T3 multiple comparisons test	Mean Diff.	95.00% CI of diff.	Summary	Adjusted P Value
Lactated Ringer's vs. IDUA	-5.482	-9.428 to -1.537	**	0.0024
Lactated Ringer's vs. Pepcan-12+Linker S+IDUA	-5.408	-9.422 to -1.393	**	0.003
Lactated Ringer's vs. Pepcan-12+Linker T+IDUA	-5.285	-9.240 to -1.330	**	0.0029
Lactated Ringer's vs. Linker S+IDUA	-5.86	-9.794 to -1.926	**	0.0014
Lactated Ringer's vs. Linker T+IDUA	-5.951	-9.897 to -2.005	**	0.0012
Lactated Ringer's vs. Heterozygotes	-7.144	-11.14 to -3.144	***	0.0004
IDUA vs. Pepcan-12+Linker S+IDUA	0.07436	-1.470 to 1.619	ns	>0.9999
IDUA vs. Pepcan-12+Linker T+IDUA	0.1974	-1.491 to 1.886	ns	>0.9999
IDUA vs. Linker S+IDUA	-0.3776	-1.484 to 0.7283	ns	0.9148
IDUA vs. Linker T+IDUA	-0.4686	-1.702 to 0.7642	ns	0.7747
IDUA vs. Heterozygotes	-1.662	-2.828 to -0.4956	**	0.0052
Pepcan-12+Linker S+IDUA vs. Pepcan-12+Linker T+IDUA	0.1231	-1.668 to 1.914	ns	>0.9999
Pepcan-12+Linker S+IDUA vs. Linker S+IDUA	-0.452	-1.883 to 0.9786	ns	0.9104
Pepcan-12+Linker S+IDUA vs. Linker T+IDUA	-0.543	-2.088 to 1.002	ns	0.796
Pepcan-12+Linker S+IDUA vs. Heterozygotes	-1.736	-3.265 to -0.2073	*	0.0144
Pepcan-12+Linker T+IDUA vs. Linker S+IDUA	-0.575	-2.228 to 1.078	ns	0.8046
Pepcan-12+Linker T+IDUA vs. Linker T+IDUA	-0.6661	-2.355 to 1.023	ns	0.6848
Pepcan-12+Linker T+IDUA vs. Heterozygotes	-1.859	-3.587 to -0.1320	*	0.0182
Linker S+IDUA vs. Linker T+IDUA	-0.09101	-1.198 to 1.016	ns	>0.9999
Linker S+IDUA vs. Heterozygotes	-1.284	-2.084 to -0.4845	***	0.0006
Linker T+IDUA vs. Heterozygotes	-1.193	-2.361 to -0.02530	*	0.0228

Appendix Table 4: Pairwise Test Results for Enzyme Activity in the Heart

Tukey's multiple comparisons test	Mean Diff.	95% CI of diff.	Summary	Adjusted P Value
IDUA vs. Pepcan-12+Linker S+IDUA	-0.6647	-1.597 to 0.2679	ns	0.2662
IDUA vs. Pepcan-12+Linker T+IDUA	-0.8971	-1.789 to -0.005284	*	0.0481
IDUA vs. Linker S+IDUA	-0.47	-1.403 to 0.4626	ns	0.6035
IDUA vs. Linker T+IDUA	-1.229	-2.324 to -0.1351	*	0.0211
Pepcan-12+Linker S+IDUA vs. Pepcan-12+Linker T+IDUA	-0.2324	-1.095 to 0.6303	ns	0.937
Pepcan-12+Linker S+IDUA vs. Linker S+IDUA	0.1947	-0.7101 to 1.099	ns	0.9715
Pepcan-12+Linker S+IDUA vs. Linker T+IDUA	-0.5646	-1.635 to 0.5060	ns	0.5615
Pepcan-12+Linker T+IDUA vs. Linker S+IDUA	0.4271	-0.4356 to 1.290	ns	0.6195
Pepcan-12+Linker T+IDUA vs. Linker T+IDUA	-0.3322	-1.367 to 0.7030	ns	0.8874
Linker S+IDUA vs. Linker T+IDUA	-0.7593	-1.830 to 0.3113	ns	0.2707

Appendix Table 5: Pairwise Test Results for Enzyme Activity in the Liver

Tukey's multiple comparisons test	Mean Diff.	95% CI of diff.	Summary	Adjusted P Value
IDUA vs. Pepcan-12+Linker S+IDUA	0.07098	-0.7013 to 0.8432	ns	0.9989
IDUA vs. Pepcan-12+Linker T+IDUA	0.1344	-0.6040 to 0.8729	ns	0.9846
IDUA vs. Linker S+IDUA	-0.3348	-1.107 to 0.4375	ns	0.7267
IDUA vs. Linker T+IDUA	-0.7111	-1.617 to 0.1949	ns	0.1844
Pepcan-12+Linker S+IDUA vs. Pepcan-12+Linker T+IDUA	0.06346	-0.6509 to 0.7778	ns	0.999
Pepcan-12+Linker S+IDUA vs. Linker S+IDUA	-0.4058	-1.155 to 0.3434	ns	0.5361
Pepcan-12+Linker S+IDUA vs. Linker T+IDUA	-0.7821	-1.669 to 0.1044	ns	0.1058
Pepcan-12+Linker T+IDUA vs. Linker S+IDUA	-0.4692	-1.184 to 0.2451	ns	0.344
Pepcan-12+Linker T+IDUA vs. Linker T+IDUA	-0.8456	-1.703 to 0.01163	ns	0.0547
Linker S+IDUA vs. Linker T+IDUA	-0.3763	-1.263 to 0.5101	ns	0.7416

Appendix Table 6: Pairwise Test Results for Enzyme Activity in the Spleen

Tukey's multiple comparisons test	Mean Diff.	95% CI of diff.	Summary	Adjusted P Value
IDUA vs. Pepcan-12+Linker S+IDUA	0.2977	-0.4327 to 1.028	ns	0.769
IDUA vs. Pepcan-12+Linker T+IDUA	0.3512	-0.3472 to 1.050	ns	0.6056
IDUA vs. Linker S+IDUA	-0.3793	-1.110 to 0.3511	ns	0.5761
IDUA vs. Linker T+IDUA	-0.5298	-1.387 to 0.3271	ns	0.4043
Pepcan-12+Linker S+IDUA vs. Pepcan-12+Linker T+IDUA	0.05353	-0.6221 to 0.7291	ns	0.9994
Pepcan-12+Linker S+IDUA vs. Linker S+IDUA	-0.6769	-1.385 to 0.03164	ns	0.0671
Pepcan-12+Linker S+IDUA vs. Linker T+IDUA	-0.8275	-1.666 to 0.01090	ns	0.0545
Pepcan-12+Linker T+IDUA vs. Linker S+IDUA	-0.7305	-1.406 to -0.05486	*	0.0285
Pepcan-12+Linker T+IDUA vs. Linker T+IDUA	-0.881	-1.692 to -0.07030	*	0.0275
Linker S+IDUA vs. Linker T+IDUA	-0.1506	-0.9890 to 0.6878	ns	0.9853

Appendix Table 7: Pairwise Test Results for Enzyme Activity in the Kidney

Tukey's multiple comparisons test	Mean Diff.	95% CI of diff.	Summary	Adjusted P Value
IDUA vs. Pepcan-12+Linker S+IDUA	0.4893	-0.3082 to 1.287	ns	0.412
IDUA vs. Pepcan-12+Linker T+IDUA	0.5258	-0.2368 to 1.288	ns	0.2971
IDUA vs. Linker S+IDUA	-0.4161	-1.214 to 0.3814	ns	0.5716
IDUA vs. Linker T+IDUA	-0.4472	-1.383 to 0.4884	ns	0.6499
Pepcan-12+Linker S+IDUA vs. Pepcan-12+Linker T+IDUA	0.03649	-0.7012 to 0.7742	ns	>0.9999
Pepcan-12+Linker S+IDUA vs. Linker S+IDUA	-0.9054	-1.679 to -0.1318	*	0.0149
Pepcan-12+Linker S+IDUA vs. Linker T+IDUA	-0.9365	-1.852 to -0.02111	*	0.0428
Pepcan-12+Linker T+IDUA vs. Linker S+IDUA	-0.9419	-1.680 to -0.2043	**	0.0066
Pepcan-12+Linker T+IDUA vs. Linker T+IDUA	-0.973	-1.858 to -0.08782	*	0.0251
Linker S+IDUA vs. Linker T+IDUA	-0.03109	-0.9465 to 0.8843	ns	>0.9999

Appendix Table 8: Pairwise Test Results for Enzyme Activity in the Plasma

Tukey's multiple comparisons test	Mean Diff.	95% CI of diff.	Summary	Adjusted P Value
IDUA vs. Pepcan-12+Linker S+IDUA	-0.7917	-1.721 to 0.1373	ns	0.1265
IDUA vs. Pepcan-12+Linker T+IDUA	-0.4493	-1.338 to 0.4391	ns	0.6004
IDUA vs. Linker S+IDUA	-1.573	-2.502 to -0.6436	***	0.0002
IDUA vs. Linker T+IDUA	-1.345	-2.435 to -0.2554	**	0.0092
Pepcan-12+Linker S+IDUA vs. Pepcan-12+Linker T+IDUA	0.3424	-0.5170 to 1.202	ns	0.7832
Pepcan-12+Linker S+IDUA vs. Linker S+IDUA	-0.7809	-1.682 to 0.1204	ns	0.1163
Pepcan-12+Linker S+IDUA vs. Linker T+IDUA	-0.5536	-1.620 to 0.5128	ns	0.5763
Pepcan-12+Linker T+IDUA vs. Linker S+IDUA	-1.123	-1.983 to -0.2639	**	0.0052
Pepcan-12+Linker T+IDUA vs. Linker T+IDUA	-0.896	-1.927 to 0.1352	ns	0.1147
Linker S+IDUA vs. Linker T+IDUA	0.2273	-0.8391 to 1.294	ns	0.9725